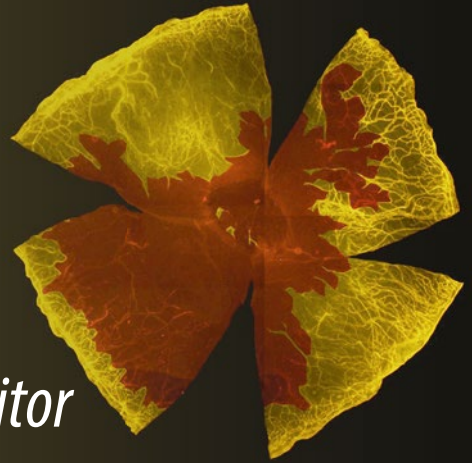


Methods in
Molecular Biology 1609

Springer Protocols



Sanjoy K. Bhattacharya *Editor*

Lipidomics

Methods and Protocols

EXTRAS ONLINE

 Humana Press

METHODS IN MOLECULAR BIOLOGY

Series Editor
John M. Walker
School of Life and Medical Sciences
University of Hertfordshire
Hatfield, Hertfordshire, AL10 9AB, UK

For further volumes:
<http://www.springer.com/series/7651>

Lipidomics

Methods and Protocols

Edited by

Sanjoy K. Bhattacharya

University of Miami, Miami, FL, USA

Editor

Sanjoy K. Bhattacharya
University of Miami
Miami, FL, USA

ISSN 1064-3745 ISSN 1940-6029 (electronic)
Methods in Molecular Biology
ISBN 978-1-4939-6995-1 ISBN 978-1-4939-6996-8 (eBook)
DOI 10.1007/978-1-4939-6996-8

Library of Congress Control Number: 2017939352

© Springer Science+Business Media LLC 2017

This work is subject to copyright. All rights are reserved by the Publisher, whether the whole or part of the material is concerned, specifically the rights of translation, reprinting, reuse of illustrations, recitation, broadcasting, reproduction on microfilms or in any other physical way, and transmission or information storage and retrieval, electronic adaptation, computer software, or by similar or dissimilar methodology now known or hereafter developed.

The use of general descriptive names, registered names, trademarks, service marks, etc. in this publication does not imply, even in the absence of a specific statement, that such names are exempt from the relevant protective laws and regulations and therefore free for general use.

The publisher, the authors and the editors are safe to assume that the advice and information in this book are believed to be true and accurate at the date of publication. Neither the publisher nor the authors or the editors give a warranty, express or implied, with respect to the material contained herein or for any errors or omissions that may have been made. The publisher remains neutral with regard to jurisdictional claims in published maps and institutional affiliations.

Printed on acid-free paper

This Humana Press imprint is published by Springer Nature
The registered company is Springer Science+Business Media LLC
The registered company address is: 233 Spring Street, New York, NY 10013, U.S.A.

Preface

The history of lipids spans almost four centuries, ever since Techenius Otto suggested the presence of acidic compound in fat in 1673 (fatty acids: Otto found that the alkali is neutralized by animal fat in the process of making soap). Lipids are the biomolecules that provide boundary to cells. They are also highly efficient signaling molecules. Every fragment generated from a lipid can be used for differential signaling in a living cell. Indeed, all major journals with biological chemistry mandate have a dedicated section for lipid biochemistry and signaling. Despite a rich history of lipid research that includes perspectives from fundamental biology and synthetic organic chemistry, the lipids are not a dominant theme in most biological laboratories. Only about a 10th or less of the laboratories engaged in biomedical research focus on lipid biochemistry. This is also partly due to the lack of easily available reagents and otherwise due to the lack of awareness about tools, techniques, and knowledge of protocols. For example, antibodies to most lipids are neither available nor could be easily generated. However, in the last five years alone, there have been tremendous advancements in lipid identification and quantification methods. This includes major advancements in mass spectrometric and bioinformatic methods towards identification and quantification of lipids. There have also been tremendous advancements in other techniques as well as in generating mice models with specific alterations in lipid metabolizing enzymes. A wealth of clones of different enzymes and lipid handling proteins also have been accumulated over a number of years. This book presents an account of areas of utility, techniques, and bioinformatic advancements. We expect this issue of the *Methods in Molecular Biology* series to be useful to Biochemists, Molecular Biologists, and Neuroscientists with interest in Neurology, Ophthalmology, and Vision Science as well as Mass spectrometrists with interest in disease discovery. This issue includes protocols for lipid isolation for extractive as well as imaging mass spectrometry. The latter helps in localization of lipids in tissues and is expected to address issues such as pathologic deposits and fluorescence in correct cellular layers within the tissue. The protocols also include isolation of specific membranes and specialized fractionation of subcellular compartments. A number of different high-throughput mass spectrometric approaches, databases, and bioinformatic analyses methods are included in protocols. These protocols have been complemented by utilization of methods in specific problems from fractionated organelles, cells to whole organism. A few protocols have dealt with computational and functional analysis of lipid metabolizing enzymes while others about their interaction with proteins including an electrochemical method. It is hoped that these protocols will come handy in the investigation of biological questions in many biomedical research laboratories in ensuing future.

Miami, FL, USA

Sanjoy K. Bhattacharya

Contents

<i>Preface</i>	<i>v</i>
<i>Contributors</i>	<i>ix</i>
1 Lipid Sample Preparation for Biomedical Research <i>Ravin Sajnani and Katyayini Aribindi</i>	1
2 Lipid Extraction Techniques for Stable Isotope Analysis and Ecological Assays <i>Kyle H. Elliott, James D. Roth, and Kevin Crook</i>	9
3 Isolation of Lipid Raft Proteins from CD133+ Cancer Stem Cells <i>Vineet K. Gupta and Sulagna Banerjee</i>	25
4 Isolation of Neuronal Synaptic Membranes by Sucrose Gradient Centrifugation <i>Blake R. Hopiavuori, Dustin R. Masser, Joseph L. Wilkerson, Richard S. Brush, Nawajes A. Mandal, Robert E. Anderson, and Willard M. Freeman</i>	33
5 Sample Preparation and Analysis for Imaging Mass Spectrometry <i>Genea Edwards, Annia Mesa, Robert I. Vazquez-Padron, Jane-Marie Kowalski, and Sanjoy K. Bhattacharya</i>	43
6 Direct Measurement of Free and Esterified Cholesterol Mass in Differentiated Human Podocytes: A TLC and Enzymatic Assay-Based Method <i>Christopher E. Pedigo, Sandra M. Merscher, and Alessia Fornoni</i>	51
7 High-Performance Chromatographic Separation of Cerebrosides <i>Renaud Sicard and Ralf Landgraf</i>	57
8 Lipid Identification by Untargeted Tandem Mass Spectrometry Coupled with Ultra-High-Pressure Liquid Chromatography <i>Gabriel B. Gugiu</i>	65
9 Utility of Moderate and High-Resolution Mass Spectrometry for Class-Specific Lipid Identification and Quantification. <i>Maria del Carmen Piqueras</i>	83
10 A Robust Lipidomics Workflow for Mammalian Cells, Plasma, and Tissue Using Liquid-Chromatography High-Resolution Tandem Mass Spectrometry <i>Candice Z. Ulmer, Rainey E. Patterson, Jeremy P. Koelmel, Timothy J. Garrett, and Richard A. Yost</i>	91
11 Combined Use of MALDI-TOF Mass Spectrometry and ³¹ P NMR Spectroscopy for Analysis of Phospholipids <i>Jenny Schröter, Yulia Popkova, Rosmarie Süß, and Jürgen Schiller</i>	107

12	Global Monitoring of the Mammalian Lipidome by Quantitative Shotgun Lipidomics	123
	<i>Inger Ødum Nielsen, Kenji Maeda, and Mesut Bilgin</i>	
13	Bioinformatics Pertinent to Lipid Analysis in Biological Samples	141
	<i>Justin Ma, Ulises Arbelo, Yenifer Guerra, Katyayani Aribindi, Sanjoy K. Bhattacharya, and Daniel Pelaez</i>	
14	LC-MS-Based Lipidomics and Automated Identification of Lipids Using the LipidBlast In-Silico MS/MS Library.	149
	<i>Tomas Cajka and Oliver Fiehn</i>	
15	Single-Step Capture and Targeted Metabolomics of Alkyl-Quinolones in Outer Membrane Vesicles of <i>Pseudomonas aeruginosa</i>	171
	<i>Pallavi Lahiri and Dipankar Ghosh</i>	
16	Analysis of Fatty Acid and Cholesterol Content from Detergent-Resistant and Detergent-Free Membrane Microdomains	185
	<i>Mark E. McClellan and Michael H. Elliott</i>	
17	Computational Functional Analysis of Lipid Metabolic Enzymes	195
	<i>Carolina Bagnato, Arjen Ten Have, María B. Prados, and María V. Beligni</i>	
18	Isoprenylation of Monomeric GTPases in Human Trabecular Meshwork Cells	217
	<i>Evan B. Stubbs Jr.</i>	
19	Purification and Validation of Lipid Transfer Proteins	231
	<i>Matti A. Kjellberg, Anders P.E. Backman, Anna Möuts, and Peter Mattjus</i>	
20	Incorporation of Artificial Lipid-Anchored Proteins into Cultured Mammalian Cells	241
	<i>Rania Leventis and John R. Silvius</i>	
21	Sonication-Based Basic Protocol for Liposome Synthesis	255
	<i>Roberto Mendez and Santanu Banerjee</i>	
22	On Electrochemical Methods for Determination of Protein-Lipid Interaction	261
	<i>Zhiping Hu and Yanli Mao</i>	
23	Angiogenesis Model of Cornea to Understand the Role of Sphingosine 1-Phosphate	267
	<i>Joseph L. Wilkerson and Nawajes A. Mandal</i>	
	<i>Index</i>	277

Contributors

- ROBERT E. ANDERSON • *Oklahoma Center for Neuroscience, University of Oklahoma Health Sciences Center, Oklahoma City, OK, USA; Department of Ophthalmology, Dean McGee Eye Institute, University of Oklahoma Health Sciences Center, Oklahoma City, OK, USA; Department of Cell Biology, University of Oklahoma Health Sciences Center, Oklahoma City, OK, USA*
- ULISES ARBELO • *Bascom Palmer Eye Institute, University of Miami, Miami, FL, USA*
- KATYAYINI ARIBINDI • *Bascom Palmer Eye Institute, University of Miami, Miami, FL, USA*
- ANDERS P.E. BACKMAN • *Department of Biochemistry, Faculty of Science and Engineering, Åbo Akademi University, Turku, Finland*
- CAROLINA BAGNATO • *Instituto de Energía y Desarrollo Sustentable – Comisión Nacional de Energía Atómica, Centro Atómico Bariloche, S.C. de Bariloche, Río Negro, Argentina*
- SANTANU BANERJEE • *Division of Surgical Oncology, Department of Surgery, Sylvester Comprehensive Cancer Center, Miller School of Medicine, University of Miami, Miami, FL, USA*
- SULAGNA BANERJEE • *Division of Surgical Oncology, Department of Surgery, Miller School of Medicine, University of Miami, Miami, FL, USA*
- MARÍA V. BELIGNI • *Instituto de Investigaciones Biológicas (IIB-CONICET-UNMdP), Facultad de Ciencias Exactas y Naturales, Universidad Nacional de Mar del Plata, Mar del Plata, Argentina*
- SANJOY K. BHATTACHARYA • *Bascom Palmer Eye Institute, University of Miami, Miami, FL, USA; Department of Biochemistry and Molecular Biology, University of Miami, Miami, FL, USA*
- MESUT BILGIN • *Cell Death and Metabolism Unit, Center for Autophagy, Recycling and Disease, Danish Cancer Society Research Center, Copenhagen, Denmark*
- RICHARD S. BRUSH • *Department of Ophthalmology, Dean McGee Eye Institute, University of Oklahoma Health Sciences Center, Oklahoma City, OK, USA*
- TOMAS CAJKA • *UC Davis Genome Center—Metabolomics, University of California-Davis, Davis, CA, USA*
- KEVIN CROOK • *Department of Biological Sciences, University of Manitoba, Winnipeg, Manitoba, Canada*
- GENEA EDWARDS • *Bascom Palmer Eye Institute, University of Miami, Miami, FL, USA; Department of Biochemistry and Molecular Biology, University of Miami, Miami, FL, USA*
- KYLE H. ELLIOTT • *Department of Natural Resource Sciences, McGill University, Ste. Anne-de-Bellevue, Quebec, Canada*
- MICHAEL H. ELLIOTT • *Department of Ophthalmology, Dean McGee Eye Institute, University of Oklahoma Health Sciences Center, Oklahoma City, OK, USA; Department of Physiology, University of Oklahoma Health Sciences Center, Oklahoma City, OK, USA; Oklahoma Center for Neuroscience, University of Oklahoma Health Sciences Center, Oklahoma City, OK, USA*

- OLIVER FIEHN • *UC Davis Genome Center—Metabolomics, University of California-Davis, Davis, CA, USA; Biochemistry Department, King Abdulaziz University, Jeddah, Saudi Arabia*
- ALESSIA FORNONI • *Division of Nephrology and Hypertension and Peggy and Harold Katz Drug Discovery Center, Miller School of Medicine, University of Miami, Miami, FL, USA*
- WILLARD M. FREEMAN • *Oklahoma Center for Neuroscience, University of Oklahoma Health Sciences Center, Oklahoma City, OK, USA; Department of Physiology, University of Oklahoma Health Sciences Center, Oklahoma City, OK, USA; Reynolds Oklahoma Center on Aging, University of Oklahoma Health Sciences Center, Oklahoma City, OK, USA*
- TIMOTHY J. GARRETT • *Department of Pathology, Immunology and Laboratory Medicine, College of Medicine, University of Florida, Gainesville, FL, USA*
- DIPANKAR GHOSH • *Special Center for Molecular Medicine, Jawaharlal Nehru University, New Delhi, India*
- YENIFER GUERRA • *Orbital Vision Research Center, Bascom Palmer Eye Institute, University of Miami, Miami, FL, USA*
- GABRIEL B. GUGIU • *Beckman Research Institute of the City of Hope, Duarte, CA, USA*
- VINEET K. GUPTA • *Division of Surgical Oncology, Department of Surgery, University of Miami, Miami, FL, USA*
- ARJEN TEN HAVE • *Instituto de Investigaciones Biológicas (IIB-CONICET-UNMdP), Facultad de Ciencias Exactas y Naturales, Universidad Nacional de Mar del Plata, Mar del Plata, Argentina*
- BLAKE R. HOPIAVUORI • *Oklahoma Center for Neuroscience, University of Oklahoma Health Sciences Center, Oklahoma City, OK, USA; Department of Ophthalmology, Dean McGee Eye Institute, University of Oklahoma Health Sciences Center, Oklahoma City, OK, USA*
- ZHIPING HU • *School of Physics and Electronics, Henan University, Kaifeng, China*
- MATTI A. KJELLBERG • *Biochemistry, Faculty of Science and Engineering, Åbo Akademi University, Turku, Finland*
- JEREMY KOELMEL • *Department of Chemistry, University of Florida, Gainesville, FL, USA*
- PAUL KOWALSKI • *Bruker Daltonics Inc., Billerica, MA, USA*
- PALLAVI LAHIRI • *Special Center for Molecular Medicine, Jawaharlal Nehru University, New Delhi, India*
- RALF LANDGRAF • *Department of Biochemistry and Molecular Biology, Sylvester Comprehensive Cancer Center, Miller School of Medicine, University of Miami, Miami, FL, USA*
- RANIA LEVENTIS • *Department of Biochemistry, McGill University, Montreal, Quebec, Canada*
- JUSTIN MA • *Bascom Palmer Eye Institute, University of Miami, Miami, FL, USA*
- KENJI MAEDA • *Cell Death and metabolism Unit, Center for Autophagy, Recycling and Disease, Danish Cancer Society Research Center, Copenhagen, Denmark*
- NAWAJES A. MANDAL • *Department of Cell Biology, University of Oklahoma Health Sciences Center, Oklahoma City, OK, USA; Dean McGee Eye Institute, Oklahoma City, OK, USA; Department of Ophthalmology, University of Tennessee Health Sciences Center, Memphis, TN, USA; Department of Anatomy and Neurobiology, University of Tennessee Health Sciences Center, Memphis, TN, USA*
- YANLI MAO • *School of Physics and Electronics, Henan University, Kaifeng, China*

- DUSTIN R. MASSER • *Department of Physiology, University of Oklahoma Health Sciences Center, Oklahoma City, OK, USA; Reynolds Oklahoma Center on Aging, University of Oklahoma Health Sciences Center, Oklahoma City, OK, USA*
- PETER MATTJUS • *Department of Biochemistry, Åbo Akademi University, Turku, Finland*
- MARK E. MCCLELLAN • *Department of Ophthalmology, Dean McGee Eye Institute, University of Oklahoma Health Sciences Center, Oklahoma City, OK, USA*
- ROBERTO MENDEZ • *Division of Surgical Oncology, Department of Surgery, Sylvester Comprehensive Cancer Center, Miller School of Medicine, University of Miami, Miami, FL, USA*
- SANDRA M. MERSCHER • *Division of Nephrology and Hypertension and Peggy and Harold Katz Drug Discovery Center, Miller School of Medicine, University of Miami, Miami, FL, USA*
- ANNIA MESA • *Department of Surgery and Vascular Biology Institute, University of Miami, Miami, FL, USA*
- ANNA MÖUTS • *Department of Biochemistry, Faculty of Science and Engineering, Åbo Akademi University, Turku, Finland*
- INGER ØDUM NIELSEN • *Cell Death and Metabolism Unit, Center for Autophagy, Recycling and Disease, Danish Cancer Society Research Center, Copenhagen, Denmark*
- RAINEY PATTERSON • *Department of Chemistry, University of Florida, Gainesville, FL, USA*
- CHRISTOPHER E. PEDIGO • *Division of Nephrology and Hypertension and Peggy and Harold Katz Drug Discovery Center, Miller School of Medicine, University of Miami, Miami, FL, USA*
- DANIEL PELAEZ • *Orbital Vision Research Center, Bascom Palmer Eye Institute, University of Miami, Miami, FL, USA*
- MARIA DEL CARMEN PIQUERAS • *Bascom Palmer Eye Institute, University of Miami, Miami, FL, USA*
- YULIA POPKOVA • *Institute of Medical Physics and Biophysics, University of Leipzig, Leipzig, Germany*
- MARÍA B. PRADOS • *Instituto de Energía y Desarrollo Sustentable - Comisión Nacional de Energía Atómica, Centro Atómico Bariloche, S. C. de Bariloche, Río Negro, Argentina*
- JAMES D. ROTH • *Department of Biological Sciences, University of Manitoba, Winnipeg, Manitoba, Canada*
- RAVIN SAJNANI • *Bascom Palmer Eye Institute, University of Miami, Miami, FL, USA*
- JÜRGEN SCHILLER • *Institute of Medical Physics and Biophysics, University of Leipzig, Leipzig, Germany*
- JENNY SCHRÖTER • *Institute of Medical Physics and Biophysics, University of Leipzig, Leipzig, Germany*
- RENAUD SICARD • *Department of Biochemistry and Molecular Biology, Sylvester Comprehensive Cancer Center, Miller School of Medicine, University of Miami, Miami, FL, USA*
- JOHN R. SILVIUS • *Department of Biochemistry, McGill University, Montréal, Quebec, Canada; McIntyre Medical Sciences, Montréal, QC, Canada*
- EVAN B. STUBBS JR. • *Research Service, Department of Veterans Affairs, Edward Hines Jr. VA Hospital, Hines, IL, USA; Department of Ophthalmology, Stritch School of Medicine, Loyola University Chicago, Maywood, IL, USA*
- ROSMARIE SÜSS • *Institute of Medical Physics and Biophysics, University of Leipzig, Leipzig, Germany*

CANDICE Z. ULMER • *Department of Chemistry, University of Florida, Gainesville, FL, USA*

ROBERT I. VAZQUEZ-PADRON • *Department of Surgery and Vascular Biology Institute, University of Miami, Miami, FL, USA*

JOSEPH L. WILKERSON • *Department of Ophthalmology, Dean McGee Eye Institute, University of Oklahoma Health Sciences Center, Oklahoma City, OK, USA;*
Department of Cell Biology, University of Oklahoma Health Sciences Center, Oklahoma City, OK, USA

RICHARD A. YOST • *Department of Chemistry, University of Florida, Gainesville, FL, USA*

Chapter 1

Lipid Sample Preparation for Biomedical Research

Ravin Sajnani and Katyayini Aribindi

Abstract

We describe here a step-by-step protocol for extraction of lipids from tissue/cell samples for biomedical research. The protocol described here works well for biological samples that contain lipids, which are less than 2% of weight compared to total wet weight of tissue or cells. The protocols described here are suitable and incremental modification of previously published protocols. These protocols have been developed based on our experience with different tissues and cells, and yield estimates determined using class-specific mass spectrometry either using direct infusion or after chromatographic separation.

Key words Lipid sample, Lipid extraction, Bligh and Dyer method, Protein quantification, Bradford assay

1 Introduction

Lipid extraction allows for the identification and characterization of lipid species even in tissues with a traditionally low lipid yield. Lipids are normally extracted using one of three common methods: Folch, methyl tertiary-butyl ether (MtBE), and Bligh and Dyer. The Folch method is considered the gold standard of lipid extraction, regardless of lipid yield [1], but is considered time consuming to perform [2, 3]. The MtBE lipid extraction protocol was found to be a suitable substitute for rapid lipid extraction for high-throughput mass spectrometric analyses [2], and was considered superior to the Bligh and Dyer method. However, in low lipid yield tissues as in the eye (<2% lipid composition), the Bligh and Dyer method is as effective and rapid as the Folch and MtBE lipid extraction protocols, respectively [3]. We describe here the Bligh and Dyer method with suitable modifications for low lipid yield ocular tissues. Modifications include using an appropriate synthetic standard for recovery purposes, while simultaneously reducing contamination for mass spectrometric analyses and minimizing oxidation of lipids for increased accuracy of identification and quantification [4–6]. Up to 99% recovery of synthetic standards

can be obtained from this method [4–6]. To normalize the lipid amount in ocular tissues, we determine the protein concentration using a Bradford assay if the protein concentration is determinable [7, 8] or PHAST gel densitometry protein quantification if the protein yield is similarly low to the lipid yield [9, 10].

2 Materials

Prepare all solutions using LC–MS grade quality unless otherwise specified. Avoid polyethylene glycol (PEG) contamination as much as possible. It is ubiquitous in solvents, plastic materials, dish wash soap. Use glass and Eppendorf brand microcentrifuge tubes as much as possible. Avoid autoclaved materials as the sterilization techniques increase contamination in the mass spectrometer during analysis. Use Thermo Scientific Finntip sterile pipette tips for all aspects of lipid extraction for contamination reduction, they do not need to be autoclaved and are not made of PEG.

2.1 Tissue Preparation

1. Eppendorf Tubes 1.5 mL: tissue storage in $-80\text{ }^{\circ}\text{C}$ until ready for extraction.
2. Scissors sterilized with 70% ethanol to mince tissues.
3. Parafilm: use for wrapping tubes to prevent loss of tissue sample during tissue preparation phase.
4. Liquid nitrogen: store in insulating styrofoam bucket. Prepare freshly at every round of lipid extraction.
5. $40\text{ }^{\circ}\text{C}$ bath: prepare freshly at every round of lipid extraction.
6. Argon gas: use frequently during tissue preparation phase every time tubes are opened to displace atmospheric air with a nonreacting gas to prevent lipid oxidation. Store the tank in a cool, dry place on the ground at room temperature (*see Note 1*).

2.2 Lipid Extraction

1. Handheld homogenizer or Vortex machine: sterilize tips for homogenizer with 70% ethanol, and use to mix tissues and solutions further.
2. Small vortex machine suitable for 1.5 mL tubes.
3. Amber glass vials with caps 12 mL for solution storage: use to store LC–MS grade solutions and protect for oxidation and reactions caused by light (*see Note 2*).
4. External standard, e.g., PC (12:0/13:0) (Avanti Lipids: LM-1000) for recovery purposes.
5. Extraction solution: methanol:chloroform (1:1) with 10 mM butylated hydroxytoluene (BHT): all LC–MS grade solvents, store at room temperature, prepare freshly during each round of extraction (*see Note 3*).

6. Aqueous phase solution: LC–MS grade methanol.
7. Organic phase solution: LC–MS grade chloroform.
8. Antioxidant: butylated hydroxytoluene.
9. Centrifuge: place in cold room at 4 °C.
10. Speed vacuum: at room temperature, no heat added.
11. Argon gas: Use frequently during lipid extraction every time the tubes containing lipids are opened to displace atmospheric air with a nonreacting gas to prevent lipid oxidation. Store tank in cool, dry place on the ground at room temperature.
12. Protein Buffer: sodium dodecyl sulfate (SDS) and HPLC water.
13. Protein Quantification Standard: Bovine Serum Albumin analytical standard 200 mg/mL.

2.3 Protein Quantification

1. ELISA 96-well plate.
2. BSA standard: 0.1 µg/µL concentration.
3. Bradford protein assay reagent.
4. Aqueous phase of samples.
5. Prepare standard according to Bradford et al. [7].

3 Methods

3.1 Tissue Preparation

1. Mince the tissue with scissors sterilized with 70% ethanol for at least 1 min. Flush with argon gas before closing the cap of tube to prevent lipid oxidation.
2. Wrap tubes containing weighed tissue samples in parafilm, so the tube cap cannot open during the preparation phase.
3. Using long tweezers, place tubes in liquid nitrogen for 10 min.
4. Transfer tubes to heated water bath of 40 °C for 10 min.
5. Repeat four more times. The process of a hot bath and liquid nitrogen will flash freeze and melt the samples, thus facilitating breaking the phospholipid bilayer cell membrane and allowing for lipids to be more easily solubilized in the organic phase.

3.2 Lipid Extraction

1. Add 5 mL of LC–MS grade chloroform and 5 mL of LC–MS grade methanol into an amber 12 mL glass vial for a 1:1 (v/v) solution (*see Note 4*).
2. Measure 220.36 mg of BHT in 10 mL of LC–MS grade water. Take 1 µL of that solution and add it to the previous solution of 10 mL of LC–MS grade methanol:chloroform (1:1) for a final concentration of 10 µM BHT in methanol:chloroform (1:1).
3. Keep the tubes containing lipid samples in ice buckets.

4. Flush lipid samples with argon gas frequently to prevent lipid oxidation.
5. Sterilize handheld homogenizer tip with 70% ethanol.
6. In order to ensure extraction efficiency, an external standard, e.g., 10 pmol of PC (12:0/13:0) can be premixed with sample prior to lipid extraction (*see Note 5*).
7. Add 500 μL of the methanol:chloroform (1:1) with 10 μM BHT into the tubes containing samples. Homogenize for 2 min. Flush with argon gas afterward. Keep the sample in an ice bucket for as much as possible.
8. Add 300 μL of pure LC-MS grade chloroform to the sample. Homogenize for another 2 min. Flush with argon gas. Keep the sample in an ice bucket for as much as possible.
9. Optional: vortex for 30 s.
10. Flush samples in argon gas before centrifugation.
11. Centrifuge samples at 13,000 RPM ($11,337\times g$) for 15 min. When centrifugation is completed, there should be three layers: the superior aqueous layer, the middle tissue layer, and the inferior organic layer. The lipids are contained in the organic layer.
12. In four separate tubes, evenly split the organic layer. For the solution above, there is a total of 550 μL of chloroform, so add 135 μL of the organic layer in each of the tubes. These are the lipid aliquots. Because ocular tissue has a low lipid yield, four aliquots of trabecular meshwork lipids allow for detectable amounts, and keep mass spectrometer clean from excess lipids. For brain, liver, or other tissues where lipid yield is expected to be high, we recommend using either the Folch or MtBE method of lipid extraction and increasing the number of aliquots as keep the mass spectrometer analyses clean as possible (*see Note 6*).
13. Flush each aliquot with argon gas.
14. Speed-vac with no heat to vaporize the remaining chloroform in the organic layer, until lipid samples are completely dry.
15. Flush with argon gas (*see Note 7*).
16. Store at $-80\text{ }^{\circ}\text{C}$ until mass spectrometric analysis (*see Note 8*).

3.3 Protein Quantification

1. Speed-vac the tubes with the sample containing the aqueous layer and the remaining tissue until the tissue is barely moist. You may use the temperature up to $30\text{ }^{\circ}\text{C}$ if desired, however, be careful that the tissue is not burned from staying too long in the heated Speed-Vac.
2. Store at $-80\text{ }^{\circ}\text{C}$ until ready for protein quantification.
3. Use 0.05% SDS as a buffer for protein extraction. To make: Add 25 μL of sodium dodecyl sulfate to 49.975 mL of HPLC water for a 0.05% SDS solution.

4. Keep tubes with samples in ice bucket as much as possible in the protein extraction phase.
5. Add 400 μL of 0.05% SDS buffer to samples with tissue.
6. Homogenize with handheld homogenizer with tips sterilized in 70% ethanol for 2 min.
7. Vortex for 2 min.
8. Centrifuge for 13,000 RPM ($11,337\times g$) for 15 min.
9. Separate the supernatant or the top aqueous phase containing the proteins into different tubes.
10. Speed-vac to less than 50 μL with optional heat up to 30 $^{\circ}\text{C}$. Because ocular tissues are small and have a low protein yield when compared to other common biological samples, our protein samples needed to be concentrated further, down to 15–20 μL at times for protein quantification to be done correctly.
11. Add 0.5 μL of BSA and add to 999.5 μL of HPLC water to create a 0.1 $\mu\text{g}/\mu\text{L}$ BSA standard solution.
12. Take a 96 ELISA well-plate and label the wells appropriately with at least three separate readings *per* sample or standard.
13. Dilute the protein reagent assay 1:10 with distilled water. We make 50 mL of protein reagent solution stock at a time, and store in the 4 $^{\circ}\text{C}$ freezer by diluting 5 mL of reagent with 45 mL of distilled water.
14. By Bradford method [7, 8], a protein standard should encompass concentrations from 0 to above the highest protein concentration contained in one of the samples to successfully extrapolate the protein concentration of samples. Because if the low protein concentration is expected in ocular tissues, we use 0, 1, 2, 4, 6, and 8 $\mu\text{g}/\mu\text{L}$ BSA concentrations as a standard.
15. To make the 1 $\mu\text{g}/\mu\text{L}$ standard: add 0.4 μL of BSA standard into 399.6 μL of diluted protein reagent in a tube. This solution now has a concentration of 1 $\mu\text{g}/\mu\text{L}$. For the 2 $\mu\text{g}/\mu\text{L}$ standard: add 0.8 μL of BSA standard into 399.2 μL of the protein reagent. For the 4 $\mu\text{g}/\mu\text{L}$ standard: add 1.6 μL of BSA standard into 398.4 μL of the protein reagent. For the 6 $\mu\text{g}/\mu\text{L}$ standard: add 2.4 μL of BSA standard into 397.6 μL of protein reagent. For the 8 $\mu\text{g}/\mu\text{L}$ standard: add 3.2 μL of BSA standard into 396.8 μL of protein reagent in a tube.
16. Add to each of the three wells designated as the 0 $\mu\text{g}/\mu\text{L}$, 100 μL of the protein reagent alone.
17. Add to three wells, 100 μL of the 1 $\mu\text{g}/\mu\text{L}$ standard each. Add to three more wells, 100 μL of the 2 $\mu\text{g}/\mu\text{L}$ standard each. Repeat for the 4 $\mu\text{g}/\mu\text{L}$ standard, the 6 $\mu\text{g}/\mu\text{L}$ standard, and the 8 $\mu\text{g}/\mu\text{L}$ standard.

18. Add 99 μL of the protein assay reagent into three wells. Add 1 μL of the protein sample (the supernatant that has been concentrated by speed-vac and stored at $-80\text{ }^{\circ}\text{C}$) to each of the three wells for a total volume of 100 μL .
19. Repeat **step 18** for each of the samples.
20. Repeating the absorbance three times will provide maximum accuracy and precision of both the standard and the subsequent protein concentration of the samples.
21. Obtain the absorbance using instrumentation available (*see Note 9*).
22. Create a curve with the concentration of the standards on the x -axis and the corresponding absorbance on the y -axis.
23. Calculate the concentrations of the protein samples.
24. Multiply the concentrations in $\mu\text{g}/\mu\text{L}$ by the total number of μL for each supernatant. This is the total μg of protein in each sample, and the normalization for the total amount of lipids obtained from the mass spectrometric analysis, i.e., lipid amounts are expressed as pmol of lipid/ μg protein.
25. For even lower protein amounts unable to detect using a Bradford method, we recommend the use of the PHAST gel densitometry with a BSA standard for protein quantification [10].

4 Notes

1. The argon gas is best administered through a tube taped to the cut-off tip of a 20–200 μL pipette. Be sure not to increase the pressure too high so as to cause spillage of tube contents.
2. Use glass when handling tissues if they need to be dissected or separated from other biological specimens further to avoid contaminants by PEGs and other plastics.
3. Butylated hydroxytoluene is an antioxidant used to prevent lipid peroxidation.
4. The chloroform is a volatile solution, and fumes can be toxic. We advise to wear a mask to decrease chloroform fume exposure.
5. Any internal standard can be used, so long as it is synthetic in nature to ensure the only source of the standard is the standard itself, and can therefore allow for accurate calculation of recovery.
6. If the lipid extraction is being done on fluid tissues, i.e., ocular aqueous humor, cerebrospinal fluid, joint aspirate, the three layers after centrifuging, i.e., the superior aqueous layer, the middle tissue layer, and the lower organic layer may not be apparent. We found that adding 100 μL of LC-MS grade water and after

homogenization, vortex, and centrifugation of the sample, the three layers become more apparent. We would caution you not to contaminate the lipid aliquots by overestimating the amount of organic layer as it may increase contamination from proteins or tissue particles in the mass spectrometric analysis.

7. Argon gas should be used frequently to prevent lipid oxidation from the reactive species in the atmospheric air. Because argon gas is both a noble gas and heavier than atmospheric air, it will both displace the reactive species, and not react with the lipids. A good rule of thumb is to flush with argon gas every time the tube containing lipids is opened to prevent lipid oxidation to the maximum amount.
8. Samples should not be stored in liquid at -80°C for long periods of time (>12 h). We have found that storing lipids in solution and freezing them increased lipid degradation and have resulted in inaccurate spectra.
9. Protein concentration through the Bradford method can be done with whatever instrumentation is most convenient.

References

1. Folch J, Lees M, Sloane Stanley GH (1957) A simple method for the isolation and purification of total lipides from animal tissues. *J Biol Chem* 226(1):497–509
2. Matyash V, Liebisch G, Kurzchalia TV, Shevchenko A, Schwudke D (2008) Lipid extraction by methyl-tert-butyl ether for high-throughput lipidomics. *J Lipid Res* 49(5):1137–1146. doi:[10.1194/jlr.D700041-JLR200](https://doi.org/10.1194/jlr.D700041-JLR200)
3. Iverson SJ, Lang SL, Cooper MH (2001) Comparison of the Bligh and Dyer and Folch methods for total lipid determination in a broad range of marine tissue. *Lipids* 36(11):1283–1287
4. Aribindi K, Guerra Y, Lee RK, Bhattacharya SK (2013) Comparative phospholipid profiles of control and glaucomatous human trabecular meshwork. *Invest Ophthalmol Vis Sci* 54(4):3037–3044. doi:[10.1167/iovs.12-10517](https://doi.org/10.1167/iovs.12-10517)
5. Edwards G, Aribindi K, Guerra Y, Lee RK, Bhattacharya SK (2014) Phospholipid profiles of control and glaucomatous human aqueous humor. *Biochimie* 101:232–247. doi:[10.1016/j.biochi.2014.01.020](https://doi.org/10.1016/j.biochi.2014.01.020)
6. Aribindi K, Guerra Y, Piqueras Mdel C, Banta JT, Lee RK, Bhattacharya SK (2013) Cholesterol and glycosphingolipids of human trabecular meshwork and aqueous humor: comparative profiles from control and glaucomatous donors. *Curr Eye Res* 38(10):1017–1026. doi:[10.3109/02713683.2013.803123](https://doi.org/10.3109/02713683.2013.803123)
7. Bradford MM (1976) A rapid and sensitive method for the quantitation of microgram quantities of protein utilizing the principle of protein-dye binding. *Anal Biochem* 72:248–254
8. Zor T, Selinger Z (1996) Linearization of the Bradford protein assay increases its sensitivity: theoretical and experimental studies. *Anal Biochem* 236(2):302–308. doi:[10.1006/abio.1996.0171](https://doi.org/10.1006/abio.1996.0171)
9. Vincent SG, Cunningham PR, Stephens NL, Halayko AJ, Fisher JT (1997) Quantitative densitometry of proteins stained with coomassie blue using a Hewlett Packard scanjet scanner and Scanplot software. *Electrophoresis* 18(1):67–71. doi:[10.1002/elps.1150180114](https://doi.org/10.1002/elps.1150180114)
10. van Eijk HG, van Noort WL (1992) The analysis of human serum transferrins with the PhastSystem: quantitation of microheterogeneity. *Electrophoresis* 13(6):354–358

Lipid Extraction Techniques for Stable Isotope Analysis and Ecological Assays

Kyle H. Elliott, James D. Roth, and Kevin Crook

Abstract

Lipid extraction is an important component of many ecological and ecotoxicological measurements. For instance, percent lipid is often used as a measure of body condition, under the assumption that those individuals with higher lipid reserves are healthier. Likewise, lipids are depleted in ^{13}C compared with protein, and it is consequently a routine to remove lipids prior to measuring carbon isotopes in ecological studies so that variation in lipid content does not obscure variation in diet. We provide detailed methods for two different protocols for lipid extraction: Soxhlet apparatus and manual distillation. We also provide methods for polar and nonpolar solvents. Neutral (nonpolar) solvents remove some lipids but few non-lipid compounds, whereas polar solvents remove most lipids but also many non-lipid compounds. We discuss each of the methods and provide guidelines for best practices. We recommend that, for stable isotope analysis, researchers test for a relationship between the change in carbon stable isotope ratio and the amount of lipid extracted to see if the degree of extraction has an impact on isotope ratios. Stable isotope analysis is widely used by ecologists, and we provide a detailed methodology that minimizes known biases.

Key words Lipid extraction, Stable isotope analysis, Polar lipids, Neutral lipids, Soxhlet apparatus, Ecophysiology, Ecotoxicology, Diet reconstruction

1 Introduction

Stable isotope analysis (SIA) can be used to determine what constitutes a consumer's diet [1–3]. As a consumer digests its food, the nutrients are assimilated into the consumer's tissues. Atoms from the food are absorbed in the gut and used for metabolism and repair in all tissues in the consumer's body; thus, if the ratio of heavy to light isotope (e.g., $^{13}\text{C}:^{12}\text{C}$) is different for different prey items, one can deduce what proportion of each prey was eaten by the consumer. In particular, stable isotope ratios are often used to disentangle variation in contaminant levels associated with diet

Electronic supplementary material: The online version of this chapter (doi:[10.1007/978-1-4939-6996-8_2](https://doi.org/10.1007/978-1-4939-6996-8_2)) contains supplementary material, which is available to authorized users.

from variation associated with environmental factors [4–6]. A continuous-flow stable isotope mass spectrometer measures the weight of heavy and light isotopes of different elements from various tissues relative to a standard reference material, resulting in the stable isotope ratio of that individual [2, 3]. Different types of tissues grow at different rates and during different times of year, so different types of tissues can be used to get diet information from different time periods [2, 3].

^{13}C is depleted in lipids compared to proteins and variation in lipid content can confound interpretation of diet [7–10]. To estimate stable isotope ratios in proteins, it is therefore necessary to chemically extract lipids from samples before measuring stable isotope ratios, or to algebraically account for such effects for most consumer tissues [11–20].

Several methods have been used to chemically extract lipids from tissues. The most common method uses chloroform–methanol as a solvent [21, 22]. However, sometimes petroleum ether, hexane, and ethyl acetate/alcohol are used as alternative solvents [6, 23]. As both chloroform–methanol and ethyl acetate are more polar than petroleum ether or hexane, those compounds extract a greater proportion of polar compounds, including proteins, than petroleum ether or hexane [23–25]. In particular, nonpolar solvents (e.g., hexane, petroleum ether) only remove neutral lipids while polar solvents (e.g., chloroform–methanol) also remove structural lipids, such as phospholipids. As a result, stable isotope values on tissue extracted with polar solvents tend to be more enriched in ^{13}C and ^{15}N than tissue extracted with nonpolar solvents [23, 25].

Here, we provide a detailed protocol for preparing tissues for stable isotope analysis. We provide only the methods up to the point of weighing and encapsulation. Samples are then sent to a stable isotope laboratory for the measurement of stable isotope ratios using an isotope ratio mass spectrometer. Various tissues can be used for stable isotope analysis, and we provide representative methods for muscle and hair. Most soft tissues (i.e., eggs, liver, other internal organs) can be treated virtually identically to muscle. Feathers can be treated very similar to hair. Most tissues can be prepared with minor modification to these methods.

We focus on the lipid extraction step. Apart from stable isotope analysis, lipid extraction is widely used to measure lipid content (*see Note 1*). Percent lipid is often used as an index of body condition, under the assumption that fatter individuals are healthier, and our process could also be used to measure body condition. Percent lipid is also used to normalize lipophilic contaminant concentrations, as tissues that have higher lipids are likely to be more contaminated with lipophilic contaminants (e.g., PCBs, DDE, etc.). For each of those applications, Subheading 3.2 or 3.3 can be used to estimate lipid content. The lipid extraction technique (Subheading 3.2 or 3.3) can be used in many ecological applications where lipid content is desired. For instance, such a procedure

can be used to measure lipid content for contaminants analyses or to measure body condition. Regardless, the Soxhlet apparatus is preferable to manual washing because it automates the procedure and improves reproducibility.

The solvent used clearly impacts carbon and nitrogen stable isotope ratios (*see Note 2*). Nonpolar solvents (e.g., petroleum ether, hexane) extract only the neutral lipids that store energy while polar solvents (e.g., chloroform-methanol) extract structural lipids, such as phospholipids, as well as neutral lipids. In most cases, the simplest matrix possible is desired, to minimize variation associated with matrix composition. In that case, the chloroform:methanol method is likely preferable, as it completely extracts all lipids. However, lipid extraction also alters nitrogen isotope ratios because amino acids bound to phospholipids on cell membranes, and other lipids are usually naturally depleted in ^{15}N [26]. Thus, accurate measurement of $\delta^{15}\text{N}$ requires a separate analysis of nonextracted tissue. As an alternative to chemical lipid extraction, it is possible to account for lipid content using the carbon to nitrogen ratio. Such algebraic approximations have nearly five times as much error as the chemical lipid extraction outlined in this protocol [20].

We provide a detailed, reproducible methodology for preparation of samples for stable isotope analysis, including lipid extraction. With minor modification, our protocol can be used for most tissues. The carbonaceous exoskeleton of arthropods and some other invertebrates must be removed using acid hydrolysis because calcium carbonate is enriched in ^{13}C , causing similar issues as lipids [27]. Likewise, the removal of collagen from bone requires additional work and various washing techniques can be applied to feathers to remove preen oils [28, 29]. However, our methods work well for most tissues.

2 Materials

1. Disposable 2 mL microcentrifuge tubes along with permanent markers to write on the tubes and fiberboard storage boxes and dividers to store tubes, and kimwipes for cleaning.
2. Benchtop freeze dryer, standard lab oven with electronic control, drying chamber, and desiccator cabinet.
3. Vacuum pump with pump oil.
4. Soxhlet apparatus with Allihn condenser.
5. Standard orbital shaker and centrifuge rotary evaporator.
6. Glass microfiber filters (55 mm).
7. High performance cellulose extraction thimble (1 mm wall, 10 × 50 mm).
8. Multi extraction mantles—6 recess, heating only, 250 mL.

9. Hook connector, 3-prong dual adjustment clamp.
10. Refrigerated bath circulator.
11. Microbalance (e.g., 5.1 g × 1.0 µg).
12. Petroleum ether or chloroform (99%) and methanol.
13. Clear PVS tubing 5/16''–50''.
14. 30 mm jar forceps.
15. 20 mL glass screw thread scintillation vials.
16. Tin capsules 5 × 9 mm.
17. Flat-bottom plates with lids.

3 Methods

3.1 *Subsampling Tissue*

1. The protocol described here is specifically for muscle, but can be used with little alteration for any other soft tissue, such as egg contents, plasma, blood, liver, pancreas, stomach, or any other internal organs. Digestive tract contents would need to be emptied and rinsed prior to any analysis. Liquids (e.g., plasma, blood) are typically freeze-dried prior to any analysis, to simplify homogenization. Subsampling of liquids would occur with a pipette following vortexing.
2. General sanitation. Preparing samples for stable isotope analysis requires certain steps to be followed to ensure that accurate results are obtained. Cross contamination is a serious concern when preparing samples. Samples are measured in micrograms, so contaminants that might be negligible to other procedures can be highly influential to our results. To prevent contamination, clean gloves should be worn at all times when working with samples, to protect both the sample and the researcher. In this protocol, we use a 70% ethanol (alcohol) solution to clean and disinfect our tools, the counter, other surfaces, our gloves, etc. Before working with each sample, the workspace and tools should be wiped with a Kimwipe and ethanol. Do not forget to put everything away, especially samples, which may become contaminated or start to decompose. Tools should be washed with soap and water and dried or left to dry (on the rack) before being put away. Make certain to create an accurate labeling method so that each sample can be uniquely identified throughout the process.
3. Subsampling from muscles. Tools and supplies needed for sampling include gloves, cutting board, scalpel or knife, micro-centrifuge tubes and boxes, forceps, fine point marker, kimwipes, and ethanol. In our lab, muscle samples are often provided as pieces of frozen meat in a small container or bag, usually far more sample than is needed for stable isotope

analysis. Begin by cutting the sample into small (approximately grape-sized) pieces with either a scalpel or a knife. Try to include only lean, red muscle, with as little fat and connective tissue as possible. This may be difficult depending on the quality of the sample, so patience and attention to detail are required. The sample run for stable isotope analysis should consist of a 2 mL micro-centrifuge tube filled about half way with muscle. The tube should be labeled with a fine point marker on the lid and side with the sample ID number. Use forceps to pack the sample into the tube; avoid leaving air pockets underneath the sample, as they may expand and force the sample out of the tube during freeze-drying (next step). Once filled, these tubes should be placed in a micro-centrifuge box to help avoid confusion should the samples come out in the freeze dryer. Leave an empty space between tubes in the micro-centrifuge box to prevent contamination if a sample is forced out of its tube (covering the tube with parafilm with perforations should further ensure that) during freeze-drying. Additional samples can be archived for future use or otherwise disposed appropriately.

4. Freeze-drying. Prior to stable isotope analysis, samples must be dried to remove all traces of water from the sample and prevent decomposition during storage. Freeze-drying is the preferred method for muscle samples or other soft tissues, but hair, feathers, or plant samples can be dried in a drying oven. Samples should be frozen before using the freeze dryer, as any liquid material may foam and expand, causing cross-contamination with neighboring samples. Ensure that all tube lids are open so the vacuum reaches the sample. If necessary, several boxes of samples can be stacked on top of each other. Grease the seals with silicon to create a strong seal. Ensure that the air valve is closed, and that the plastic end cap is inserted into the end of the rubber drain hose attached to the bottom of the dryer. Turn the dryer on. Samples typically need at least 48 h of freeze-drying to completely remove moisture and will not be affected by freeze-drying for longer than is necessary. The freeze dryer can be left running overnight or over the weekend. Once the samples have had at least 48 h in the dryer, end the freeze-drying. Very slowly open the valve on the top to allow air into the dome. It will be possible to hear the air rushing in. Once the air can no longer be heard, take the samples out. Leave the dome off so moisture from the freezer coils does not condense on the inside. Take the end cap out of the drain hose to allow the liquid to drain. Once the frost on the freezer coils has melted, use paper towels to dry the inside of the freeze dryer. The samples are now completely dehydrated and no longer need to be kept frozen, and can be stored in a desiccator cabinet.

3.2 Lipid Extraction by Soxhlet Apparatus

1. The soxhlet apparatus is commonly used in chemistry applications for dissolving soluble substances from a solid matrix. Freeze-drying has removed all the water from the sample, but not the lipids (oils and fats). The Soxhlet removes lipids by bathing the sample in a solvent that will dissolve and remove lipids from the sample (e.g., petroleum ether or chloroform). A heater under each of the Soxhlet extractors boils the solvent, and the vapors rise and condense in the top section, which is cooled by water. The freshly distilled solvent drips down from the condenser to saturate the samples in the extractor, and when the solvent level rises high enough, it fills a siphon and drains back into the reservoir to be boiled again. Thus the samples are constantly bathed in fresh solvent, while the lipids become concentrated in the bottom reservoir. The Soxhlet apparatus should be set up in a fume hood, in case any solvent escapes past the condensers. Before starting, the following tools are needed: gloves, a set of cellulose thimbles in their beakers, the corresponding data sheet, a pencil, a mortar and pestle, 55 mm glass microfiber filter papers, Kimwipes, and ethanol.
2. Identifying thimbles. Each sample will be placed in a cellulose thimble, and each extractor holds a set number of thimbles; in our extractor it is six 10 × 50 mm thimbles. We use notches in the top of each thimble to identify individual samples, which correspond to a sample ID number indicated on the data sheet. Thus, a set of six notched thimbles is needed for each extractor.
3. Breaking up the sample. Crushing the dried sample with mortar and pestle for a few seconds will break up connective tissue in muscle, make the sample easier to wrap in the filter paper, and allow the solvent to penetrate more easily. Take the sample out of the micro-centrifuge tube and put it into the mortar. Crush the sample with the pestle for a few seconds. Ideally the sample will break into small pieces, but some will not come apart as easily. This should not matter, as long as the sample can still be made to fit into the thimble later. Some samples may appear greasy or even wet, most likely because the sample might have excessive fat content; proceed with Soxhlet preparation like any other sample.
4. Addition to filter paper. To prevent bits of cellulose shed from the thimbles from contaminating the samples, each sample will be wrapped in glass microfiber filter paper. Dump the sample out of the mortar onto a filter paper. Carefully wrap the sample in the filter paper by folding over each end and rolling it up like a burrito. There may be more sample than can fit in a single filter paper without ripping it, but one paper will hold plenty for stable isotope analysis. Before inserting the sample, check the thimble for large pieces of paper or sample that may be

stuck in the bottom, remove any such pieces, then slide the rolled paper into the thimble. Forceps may be needed to insert the paper completely. Be careful not to rip the filter paper. If a rip occurs, throw the paper out and rewrap the sample in a new paper. Clean everything with ethanol and a Kimwipe. Make sure the mortar is dry before adding a new sample.

5. Preparing the Soxhlet. To remove neutral lipids a nonpolar solvent such as petroleum ether or hexane can be used. To remove all lipids (including phospholipids and structural lipids) a polar solvent must be used, such as chloroform/methanol. However, the latter will also remove a small amount of non-lipid material. Check the solvent level in the flask. The volume of solvent in the flask should be three to four times the volume of the extractor chamber (usually about half full), with a few boiling chips in the bottom of the flask. The solvent can be reused for multiple extractions and slowly turns yellow as more lipid becomes dissolved in it and eventually will need to be replaced (we keep a waste ether jug stored in a flammables cabinet). The boiling chips can be reused, so try not to dump them out of the flask. Petroleum ether and other solvents are toxic and the fumes are highly flammable, so when adding new solvent to the flask only pour it under the fume hood and be careful not to get it on exposed skin. Use a glass funnel to avoid spills. Fit the Soxhlet sections back together and clamp them back into place. Fill the other extractors in the same manner. Leave each empty beaker beside the tube that contains the corresponding thimbles, and leave the data sheet under the fume hood with the samples to avoid confusion about what is in the Soxhlet.
6. Loading the Soxhlet. Once all samples have been prepared, or all 36 thimbles are full (for a 6-heater unit), begin loading them into the Soxhlet. First unscrew the clamp at the top and carefully slide the condenser (the top section) up and out of the extractor (the middle section), then retighten the clamp to hold the condenser in place. Slide the extractor out of the flask (the bottom section). Use long forceps to slide the six thimbles from one beaker into the extractor, all the way to the bottom. If they are stacked on top of each other they will not become fully immersed in the solvent and the Soxhlet will not be effective. Make sure the thimbles are not blocking the siphon as this will not allow the solvent to drain back into the flask.
7. Starting the Soxhlet. Before turning on the Soxhlet heater, check the water level in the recirculating chiller by taking the hatch off the top. It should be full right to the very top. Add more water if necessary. If the water runs out while running, the coolant will fail and the Soxhlet will boil dry. Turn on the chiller pump. Use the buttons to navigate the screen menu. Adjust the temperature to 10°. High humidity sometimes

causes water to condense inside the Soxhlet, which interferes with the solvent draining. Under these conditions a higher water temperature may help avoid this moisture condensation, but may slow the rate at which the solvent condenses.

8. Extraction in the Soxhlet. Once the water reaches the desired temperature, turn on each of the heaters under the flask holding the solvent (at a setting of approximately 4.5 on our unit). Check the Soxhlet after a little while to ensure that the solvent is at a slow, steady boil and that it is draining properly. Don't forget to close the fume hood to its operational level. Samples need at least 8 h in the Soxhlet. It can be left running overnight, but not for longer than 24 h or the solvent may boil dry.
9. Removal from Soxhlet. After running, turn off the Soxhlet heaters and remove the samples, placing them back into their appropriate beakers with the long forceps. Place the beakers with the samples into the drying oven set at 60 °C for at least 48 h. Keep the data sheet with the samples in the oven to avoid losing it.

3.3 Lipid Extraction with a Shaker (If a Soxhlet Apparatus is Not Available, Lipid Extraction Must be Performed Manually)

1. Weighing the sample. Add freeze-dried and broken up tissue (Subheading 2, steps 1 and 2) to a sample tube labeled with the sample ID number. Weigh the tube before and after the sample is added.
2. Extraction. Add the solvent to the sample tubes, typically chloroform/methanol (2/1), which is known as Folch's reagent. The final volume of the solvent should be 20 times the tissue sample (50 mg of dried tissue in 1 mL of solvent mixture). Place the box of sample tubes on a shaker and agitate the whole mixture at room temperature for 15–20 min.
3. Centrifugation. After shaking, centrifuge the samples for 3 min to separate the sample tissue from the solvent. After centrifugation, pour out the solvent and repeat Subheading 3.2. This extraction step should be repeated three times.
4. Evaporation. Evaporate the samples under vacuum in a rotary evaporator for 45 min or under a nitrogen stream if the volume is low. Reweigh the sample (the difference in weight will provide the lipid content of the original sample).

3.4 Unpacking and Homogenization

1. Once the samples have dried, they must be removed from the thimbles or sample tubes and prepared for weighing. Before a sample can be weighed, it must be reduced to a fine powder. The following items will be needed: gloves, forceps, a stainless-steel dissection probe, vials (such as scintillation vials), a black permanent marker, Kimwipes, and ethanol.
2. Label the vial with the sample ID number on the lid and also on the sides of the vial (written twice, 90° apart to reduce the

chance of smudging both labels by pinching between thumb and forefinger). If lipids were extracted using the shaker method, place the sample in the vial and proceed to **step 3.5**. If using the Soxhlet method, continue with **step 3.3**.

3. Carefully remove the sample from the thimble. Be gentle, as the filter paper will be very delicate and can rip easily. Check the thimble to make sure no sample or large chunks of filter paper remain in the bottom. Put the thimble back in the correct beaker.
4. Unwrap the filter paper, empty the sample into the vial, and discard the filter paper. If small pieces of filter paper become stuck to the sample, try to remove these with forceps. It may not be possible to remove all traces of paper, while this is not ideal, it is acceptable since the glass microfiber filter paper contains no nitrogen or carbon that will affect the measured stable isotope ratios (although it could affect the sample weight, which would affect %C and %N estimates).
5. Use the blunt handle end of the probe to homogenize the sample inside the vial. Be careful not to use too much force as the glass vials are prone to breaking. If the vial breaks, transfer the sample into a new vial, and carefully remove all traces of broken glass from the sample. Pounding or grinding the sample should reduce some of the sample into a fine powder, which is what is weighed out and prepared for final analysis. Only a very small amount of powder is needed; even a thin coating on the bottom of the vial should be enough. Notice that the majority of the sample will not become powder. Although this is mainly due to connective tissue, the sample must be broken down as much as possible. The point of homogenizing (crushing) the sample is to have a representative subsample when weighed.
6. Tighten the lid on the vial and place it back in the tray. Clean the workspace and utensils with ethanol and Kimwipes before moving on to other samples.

3.5 Weighing

1. A precise amount of sample must be weighed out on the microbalance and carefully packaged in tin capsules for mass spectrometer analysis. This final step of sample preparation demands a great deal of precision, any mistake at this stage is almost guaranteed to affect the accuracy of the final results. Proper sterilization and cleanliness of workspace and materials are particularly important to avoid contamination. The microbalance is a delicate and expensive instrument. It must be handled carefully; even a vibration in the table may affect the reading. After weighing and wrapping, the samples are sent to a laboratory for analysis using a mass spectrometer. The results are typically emailed back. The following equipment is needed:

gloves, one or two sets of forceps, a well plate, tin capsules, a stable isotope submission spreadsheet, a pencil, a red marker, Kimwipes, and ethanol.

2. Turn the Microbalance on. The balance will probably need to be calibrated when turned on and after every few hours of operation. If the calibration light flashes while weighing a sample, finish weighing it before starting calibration. Touch the tab to begin calibration. Calibration is automatic and usually takes 2 or 3 min. Once finished, press *back* on the screen to return to weighing the sample.
3. Open the balance door. Using forceps carefully place a tin capsule on the raised center tray. Try to place it as close to the center as possible, where the measurement will be the most accurate. Close the balance door to prevent drafts from interfering with the measurement (Yes—slight air drafts in the room can affect the weight of the sample). The weight displayed on the screen will fluctuate first, but it will settle on a weight after a few seconds. In general, it has not settled until *mg* appears after the weight, and it may still change after. Once it has stopped fluctuating, press the *tare* button to zero the weight. From now on, it will display the weight of the sample in the capsule only, not the capsule itself. Every capsule will have a different weight, so it is crucial to tare the balance with each new capsule.
4. Open the door and remove the capsule. Close the door afterward to prevent powder from entering the balance because it may affect the weight or contaminate the sample. Stand the capsule on the sterilized lab bench to add sample. The forceps can be used to gently open the rim of the capsule more. The capsules are made of pure tin so that it does not contaminate the sample. They are very thin and very fragile, so be careful not to crush or tear them. If the tin is torn, discard the capsule and begin again.
5. Very carefully use the forceps to take some of the powdery sample out of the vial and place it in the capsule. Very little is needed (usually 0.4–0.6 mg for muscle, but consult the lab where the stable isotope ratios will be measured). Only add the fine powder, not chunks of sample as these chunks may not be pure tissue (or may over-represent a certain period). When enough sample is in the capsule, open the balance door and place the capsule in the center of the tray like before. Be careful not to spill. If the sample is stuck to the forceps or the outside of the capsule, it should be gently wiped off with a Kimwipe before entering the balance. Different tissues will have different weight windows. If the weight is below this window, the sample may not be detectable by the mass spectrometer, and if it is higher, it may go off the calibrated scale.

6. If the weight is not correct, then add or remove sample. Be very careful when removing the sample, as the point of the forceps can easily tear the bottom of the capsule. If this happens, throw the capsule away and restart.
7. Once the correct weight is obtained, roll or squeeze the capsule into a tight ball or cube using two pairs of forceps or gloved fingers. It is sometimes easiest to crimp the end closed with forceps before rolling to prevent the sample coming out while rolling. The ball or cube should be as small as possible with no cracks, protrusions, or angular edges as these may become caught in the mass spectrometer's autosampler.
8. Place the ball back in the balance, close the door, and record the final weight in the data sheet. The weight will likely be slightly different than the weight previously measured, and it may even fall outside of the target window (typically 0.4–0.6 mg for muscle, but it will depend on the lab). If it is within 0.005 mg of the window, it is usually considered an acceptable error. If it is off by more than 0.005 mg then throw it away and restart (aim for 0.5 mg when weighing muscle).
9. Open the well plate and place the ball into the well indicated by the data sheet. Make sure to replace the plate lid to keep powder and other contaminants out. Use the marker to make a small red dot on the lid of the vial to indicate that this sample has been completed, as it is difficult to tell otherwise.
10. Be sure to wipe down all workspaces and utensils (including hands) before moving on to the next sample. If powder or spilled sample is on the central tray of the microbalance, wipe it off with a Kimwipe. The glass door can be removed by lifting straight up, make sure to line up the notch in the bottom of the door with the peg on the balance when replacing it.
11. Once finished weighing samples, tape the plate lid closed at all four sides, label the tray, and put the plate in the desiccator for storage. Be sure to close the door before turning the microbalance off.

3.6 Processing Hair Samples

1. Most mammals have two types of hairs: guard hair (overhairs), which grow from primary follicles, and underfur (underhairs), which grow from secondary follicles. These hair types often grow at different times of year, so they can be separated to provide more specific dietary information. Guard hair is long, thick, and straight, like the bristles on a paint brush, while underfur is short, thin and may be curly like a cotton ball. We also collect an archive sample containing both types. The following items are needed: gloves, coin envelopes, vials (such as scintillation vials), scissors, a black marker, petri dishes, one or two pairs of forceps, a moustache comb, Kimwipes, and ethanol.

The steps here are specifically for hair, but can be adopted equally well for other external tissues, such as modified scales or feathers. In the case of feathers, they should be washed with detergent and then chloroform-methanol to remove preen oil and other contaminants that would reflect current diet rather than diet when the feather was grown [26].

2. Labeling sample. Label one vial with the sample ID number followed by GH for guard hair, and the other with the ID plus UF for underfur. Label them on the lid and twice on the side. Cut a chunk of hair off a sample as close to the skin as possible. Place it in a petri dish to help contain the hair. The guard hair should stick up above the underfur. Pinch the top of the guard hair between fingers and run the mustache comb, or a set of forceps through the fur. After a few passes, only guard hair will be left in the hand. By the same token the hair that gets caught in the comb will be mostly underfur. A few stray guard hairs may need to be removed one by one.
3. The hair needs to be washed to remove any traces of blood, dirt, feces, or other contaminants. In addition to the tools previously listed, dish soap, a beaker, and a fine mesh tea strainer will also be needed. Use about a tablespoon of dish soap to make some soapy water in a large beaker. Pour about half a vial full of soapy water into the scintillation vial containing the hair. Close the lid and shake the sample vigorously for no less than 1 min. It is optimal to shake multiple samples at the same time to speed the process up.
4. Rinse the sample. Dump the sample into a tea strainer. Rinse out the inside of the vial and lid under high pressure water. Rinse the hair in the strainer under high pressure water. Use the forceps to lift the hair above the strainer and rinse the hair thoroughly. In the past, we have had problems with soap residue being left on the vial or sample, which can confound the stable isotope results. It is vital to rinse the vial, lid, and sample very thoroughly. Once the samples are rinsed, put it back in the appropriate vial and repeat the process, so each sample gets washed and rinsed **twice**. After the second rinse, put the sample back in its vial and place it in the drying oven (place the lid next to the vial in the oven). Let the sample dry for 48 h.
5. Homogenizing. A representative sample of the hair is needed, so the hair needs to be reduced to a powder or very small sections before it can be weighed.
6. Method one: Scissors. Scissors may be used for small numbers of samples, or samples with very little tissue. Simply use a pair of scissors to cut up a hair sample in its scintillation vial. Scissors that pivot at the neck of the vial when the tips reach the bottom are the ideal size. The hair needs to be cut into very small

pieces, preferably into a powder consistency. Static may cause sample to stick to the scissors and vial when humidity is low. It may be necessary to stop homogenizing and come back to finish a sample later when the static has dissipated.

7. Method two: Ball mill. The ball mill is a much more efficient way of homogenizing large numbers of hair samples with adequate sample weight. Samples are placed in a stainless-steel grinding jar with a ball bearing. The mill shakes the cylinder very rapidly and the ball bearing grinds the sample into powder. In addition to the earlier tools, before a spatula, paper towels, Kimwipes, and ethanol are needed. The ball mill runs two samples at once, so a second person speeds up this step.
8. There are several different sizes of cylinders for the ball mill; use the two largest sizes. The ball mill runs grinding jars at once, and it is very important to keep it balanced. Always run two jars of the same size at once, even if one jar is run empty. There are also different sizes of ball bearings; use the largest size.
9. Turn the mill on. Dials control the frequency and duration of shaking. Frequency should be set to 30 Hz and duration depends on the amount of sample, but 2 min is standard.
10. Place the sample inside a jar with a ball bearing and close the lid as tightly as possible. Larger samples should be placed in the larger jars. Make sure someone knows which sample is in which jar as the jars themselves are not labeled. Securely fasten a jar in each clamp and tighten them as much as possible to ensure that the jars do not come out while milling. Close the plastic door to contain the jars. The mill will not run with the door open. Press the start button to begin homogenizing.
11. Once the milling is complete, take the jars out and open them. They may be difficult to open, so use the scoopula as a prying implement. The sample should be reduced to powder, and if not, it may need more time in the mill. Scoop the sample out and place in the correct vial. Some time may be needed to scrape sample off the inside of the jar to get enough. Running a second set of jars while working with this set will allow speed up workflow.
12. Clean the cylinders out with water and dry them with Kimwipes before putting a new sample in. Be sure that the cylinders are clear of all sample residue and other contaminants. Clean the workspace and turn off the mill.
13. Weighing. Follow the same procedure (**step 5**) as weighing muscle samples, except the weight window may be different.

4 Notes

1. Typically, the sample can be weighed before and after lipid extraction (Subheadings 2 or 3). In that case, the difference in weight is the weight of lipids. For stable isotope analysis, the laboratory will report the weight of carbon and nitrogen in the sample, and the stable isotope ratio relative to a standard ($\delta^{13}\text{C}$ or $\delta^{15}\text{N}$). Lipid extraction typically alters both carbon and nitrogen stable isotope ratios. As the alteration in the nitrogen stable isotope ratio is unrelated to lipid content, it is usually ideal to run two sets of samples: one with lipid extraction for $\delta^{13}\text{C}$ and one without lipid extraction for $\delta^{15}\text{N}$.
2. The type of solvent impacts lipid extraction (Fig. 1). Neutral solvents, such as petroleum ether or hexane, do not extract all polar lipids. Consequently, they do not increase $\delta^{13}\text{C}$ or decrease the C:N ratio as much as polar solvents. In contrast, polar solvents, such as chloroform:methanol, extract more lipids, including polar lipids. However, they also remove a greater proportion of non-lipid compounds.

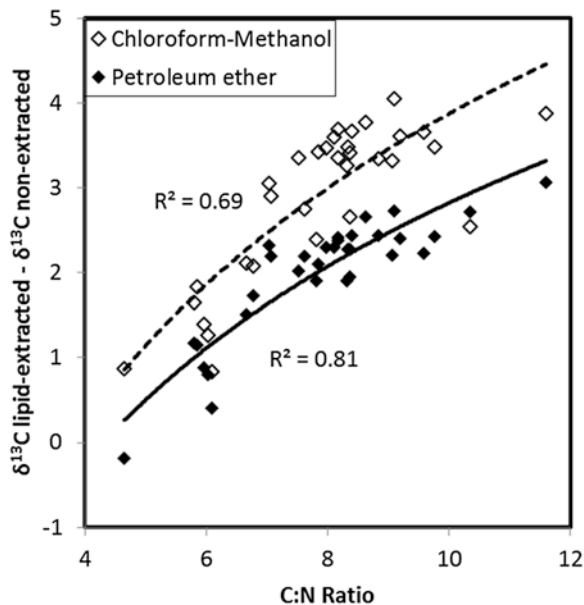


Fig. 1 The change in carbon stable isotope ratio following lipid extraction using petroleum ether as a solvent and using chloroform:methanol as a solvent. *Filled symbols* are for petroleum ether while *unfilled symbols* are for chloroform:methanol

Acknowledgments

The protocol is based on a text developed by I. Burrton and D. Mocker. Funding for sample preparation equipment was provided by the Canada Foundation for Innovation.

References

1. Hussey NE, Macneil MA, McMeans BC, Olin JA, Dudley SF, Cliff G, Wintner SP, Fennessy ST, Fisk AT (2014) Rescaling the trophic structure of marine food webs. *Ecol Lett* 17(2):239–250. doi:10.1111/ele.12226
2. Inger R, Bearhop S (2008) Applications of stable isotope analyses to avian ecology. *Ibis* 150(3):447–461. doi:10.1111/j.1474-919X.2008.00839.x
3. Rubenstein DR, Hobson KA (2004) From birds to butterflies: animal movement patterns and stable isotopes. *Trends Ecol Evol* 19(5):256–263. doi:10.1016/j.tree.2004.03.017
4. Braune BM, Gaston AJ, Hobson KA, Gilchrist HG, Mallory ML (2014) Changes in food web structure alter trends of mercury uptake at two seabird colonies in the Canadian Arctic. *Environ Sci Technol* 48(22):13246–13252. doi:10.1021/es5036249
5. Braune BM, Gaston AJ, Hobson KA, Grant Gilchrist H, Mallory ML (2015) Changes in trophic position affect rates of contaminant decline at two seabird colonies in the Canadian Arctic. *Ecotoxicol Environ Saf* 115:7–13. doi:10.1016/j.ecoenv.2015.01.027
6. Elliott JE, Elliott KH (2013) Environmental science. Tracking marine pollution. *Science* 340(6132):556–558. doi:10.1126/science.1235197
7. DeNiro MJ, Epstein S (1977) Mechanism of carbon isotope fractionation associated with lipid synthesis. *Science* 197(4300):261–263
8. Oppel S, Federer RN, O'Brien DM, Powell AN, Hollmén TE (2010) Effects of lipid extraction on stable isotope ratios in Avian egg yolk: is arithmetic correction a reliable alternative? *The Auk* 127(1):72–78. doi:10.1525/auk.2009.09153
9. Post DM, Layman CA, Arrington DA, Takimoto G, Quattrochi J, Montana CG (2007) Getting to the fat of the matter: models, methods and assumptions for dealing with lipids in stable isotope analyses. *Oecologia* 152(1):179–189. doi:10.1007/s00442-006-0630-x
10. Ricca MA, Miles AK, Anthony RG, Deng X, Hung SSO (2007) Effect of lipid extraction on analyses of stable carbon and stable nitrogen isotopes in coastal organisms of the Aleutian archipelago. *Can J Zool* 85(1):40–48. doi:10.1139/z06-187
11. Hussey NE, Olin JA, Kinney MJ, McMeans BC, Fisk AT (2012) Lipid extraction effects on stable isotope values ($\delta^{13}\text{C}$ and $\delta^{15}\text{N}$) of elasmobranch muscle tissue. *J Exp Mar Biol Ecol* 434–435:7–15. doi:10.1016/j.jembe.2012.07.012
12. Kaufman TJ, Pajuelo M, Bjørndal KA, Bolten AB, Pfaller JB, Williams KL, Vander Zanden HB (2014) Mother-egg stable isotope conversions and effects of lipid extraction and ethanol preservation on loggerhead eggs. *Conserv Physiol* 2(1):cou049. doi:10.1093/conphys/cou049
13. Kojadinovic J, Richard P, Le Corre M, Cosson RP, Bustamante P (2008) Effects of lipid extraction on $\delta^{13}\text{C}$ and $\delta^{15}\text{N}$ values in seabird muscle, liver and feathers. *Waterbirds* 31(2):169–178. doi:10.1675/1524-4695(2008)31[169:EOL EOC]2.0.CO;2
14. Lesage V, Morin Y, Rioux È, Pomerleau C, Ferguson SH, Pelletier É (2010) Stable isotopes and trace elements as indicators of diet and habitat use in cetaceans: predicting errors related to preservation, lipid extraction, and lipid normalization. *Mar Ecol Prog Ser* 419:249–265
15. Logan JM, Jardine TD, Miller TJ, Bunn SE, Cunjak RA, Lutcavage ME (2008) Lipid corrections in carbon and nitrogen stable isotope analyses: comparison of chemical extraction and modelling methods. *J Anim Ecol* 77(4):838–846. doi:10.1111/j.1365-2656.2008.01394.x
16. Sotiropoulos MA, Tonn WM, Wassenaar LI (2004) Effects of lipid extraction on stable carbon and nitrogen isotope analyses of fish tissues: potential consequences for food web studies. *Ecol Freshw Fish* 13(3):155–160. doi:10.1111/j.1600-0633.2004.00056.x
17. Sweeting CJ, Polunin NV, Jennings S (2004) Tissue and fixative dependent shifts of $\delta^{13}\text{C}$ and $\delta^{15}\text{N}$ in preserved ecological material. *Rapid Commun Mass Spectrom* 18(21):2587–2592. doi:10.1002/rcm.1661

18. Sweeting CJ, Polunin NV, Jennings S (2006) Effects of chemical lipid extraction and arithmetic lipid correction on stable isotope ratios of fish tissues. *Rapid Commun Mass Spectrom* 20(4):595–601. doi:[10.1002/rcm.2347](https://doi.org/10.1002/rcm.2347)
19. Tarroux A, Ehrlich D, Lecomte N, Jardine TD, Bêty J, Berteaux D (2010) Sensitivity of stable isotope mixing models to variation in isotopic ratios: evaluating consequences of lipid extraction. *Methods Ecol Evol* 1(3):231–241. doi:[10.1111/j.2041-210X.2010.00033.x](https://doi.org/10.1111/j.2041-210X.2010.00033.x)
20. Yurkowski DJ, Hussey NE, Semeniuk C, Ferguson SH, Fisk AT (2015) Effects of lipid extraction and the utility of lipid normalization models on $\delta^{13}\text{C}$ and $\delta^{15}\text{N}$ values in Arctic marine mammal tissues. *Polar Biol* 38(2):131–143. doi:[10.1007/s00300-014-1571-1](https://doi.org/10.1007/s00300-014-1571-1)
21. Blich EG, Dyer WJ (1959) A rapid method of total lipid extraction and purification. *Can J Biochem Physiol* 37(8):911–917. doi:[10.1139/o59-099](https://doi.org/10.1139/o59-099)
22. Folch J, Lees M, Sloane Stanley GH (1957) A simple method for the isolation and purification of total lipides from animal tissues. *J Biol Chem* 226(1):497–509
23. Elliott KH, Elliott JE (2016) Lipid extraction techniques for stable isotope analysis of bird eggs: chloroform–methanol leads to more enriched ^{13}C values than extraction via petroleum ether. *J Exp Mar Biol Ecol* 474:54–57. doi:[10.1016/j.jembe.2015.09.017](https://doi.org/10.1016/j.jembe.2015.09.017)
24. Dobush GR, Ankney CD, Krementz DG (1985) The effect of apparatus, extraction time, and solvent type on lipid extractions of snow geese. *Can J Zool* 63(8):1917–1920. doi:[10.1139/z85-285](https://doi.org/10.1139/z85-285)
25. Logan JM, Lutcavage ME (2008) A comparison of carbon and nitrogen stable isotope ratios of fish tissues following lipid extractions with non-polar and traditional chloroform/methanol solvent systems. *Rapid Commun Mass Spectrom* 22(7):1081–1086. doi:[10.1002/rcm.3471](https://doi.org/10.1002/rcm.3471)
26. Schlacher TA, Connolly RM (2014) Effects of acid treatment on carbon and nitrogen stable isotope ratios in ecological samples: a review and synthesis. *Methods Ecol Evol* 5(6):541–550. doi:[10.1111/2041-210X.12183](https://doi.org/10.1111/2041-210X.12183)
27. Lee-Thorp JA, Sealy JC, Van Der Merwe NJ (1989) Stable carbon isotope ratio differences between bone collagen and bone apatite, and their relationship to diet. *J Archaeol Sci* 16:585–599
28. Paritte JM, Kelly JF (2009) Effect of cleaning regime on stable-isotope ratios of feathers in Japanese Quail (*Coturnix Japonica*). *The Auk* 126(1):165–174. doi:[10.1525/auk.2009.07187](https://doi.org/10.1525/auk.2009.07187)
29. Svensson E, Schouten S, Hopmans EC, Middelburg JJ, Sinninghe Damste JS (2016) Factors controlling the stable nitrogen isotopic composition ($\delta^{15}\text{N}$) of lipids in marine animals. *PLoS One* 11(1):e0146321. doi:[10.1371/journal.pone.0146321](https://doi.org/10.1371/journal.pone.0146321)

Isolation of Lipid Raft Proteins from CD133+ Cancer Stem Cells

Vineet K. Gupta and Sulagna Banerjee

Abstract

Pancreatic cancer cells expressing the surface markers CD133 have been widely reported as cancer stem cells and mainly responsible for tumor recurrence and chemoresistance in pancreatic cancer. In spite of its role as a stem cell marker in pancreatic cancer, its function remains elusive. CD133 (also known as prominin-1) is a pentaspan glycoprotein predominantly localized in lipid rafts, specialized membrane microdomains enriched in crucial signaling proteins. Coexistence of CD133 with these signaling proteins can modulate various signaling pathways that might be responsible for aggressive phenotype of CD133+ cells. This chapter describes a detailed protocol to isolate lipid rafts from CD133+ tumor initiating cells. Purified lipid rafts can be investigated further for protein or lipid composition by mass spectrometry that can shed some light on functional role of CD133 protein in these cancer stem cells.

Key words CD133, Lipid rafts, Tumor Initiating Cells, Pancreatic cancer, Cancer stem cells

1 Introduction

Pancreatic cancer is the third most common cancer-related cause of death in the United States, with 50,000 patients being detected each year and almost as many succumbing to the disease. The major reasons for poor survival are chemoresistance and tumor recurrence. Both these phenomena have been attributed to a specialized population of cells within the tumor, the *tumor initiating cells* or *cancer stem cells*. Over the years many markers have been associated with the pancreatic tumor initiating cells [1–5]. One such marker, CD133, is known to be consistent in giving rise to tumors from a very low number of cells in multiple animal models of this disease [4, 6]. Structurally, CD133 is a cholesterol-interacting pentaspan membrane protein concentrated in plasma membrane protrusions [7, 8]. Its unique distribution suggests CD133 may be involved in membrane organization [8]. This idea is supported by the fact that loss of CD133 from the plasma membrane of human retinal cells causes retinal degeneration, possibly

due to impaired generation of evaginations and/or impaired conversion of evaginations to disks [9].

Topologically, CD133 is located in cholesterol-containing lipid rafts in membrane microdomains, where it is involved in mediating signaling cascades [10, 11]. Lipid rafts are small platforms, composed of sphingolipids and cholesterol in the outer exoplasmic leaflet, connected to phospholipids and cholesterol in the inner cytoplasmic leaflet of the lipid bilayer. These assemblies are fluid but more ordered and tightly packed than the surrounding bilayer. The difference in packing is due to the saturation of the hydrocarbon chains in raft sphingolipids and phospholipids as compared with the unsaturated state of fatty acids of phospholipids in the liquid-disordered phase. The organization of the lipid rafts is considered to play a significant role in regulating EMT (epithelial mesenchymal transition) which is a hallmark of metastasis. Concomitant with the acquisition of an aggressive phenotype, the EMT is marked by a profound rewiring of the cell signaling programs that affect a multitude of pathways [12, 13]. Many pathways are activated by extracellular ligands or receptors located at the plasma membrane (PM), suggesting that changes in the properties of the PM may facilitate the wholesale signaling network rearrangements associated with an EMT. Supporting this possibility, the lipid compositions of cells in epithelial or mesenchymal states have been shown to be distinct [14] and useful in distinguishing cells with an EMT phenotype [15]. Further, alterations in the fluidity of the plasma membrane, e.g., by modulating cholesterol content, can induce or inhibit an EMT [16].

The function of CD133 is even less clear in the context of cancer. Despite its ubiquitous presence on CSCs from various solid tumors, it is unknown whether the intracellular signaling downstream of CD133 contributes to the maintenance of cellular stemness. Clinically, strong CD133 expression correlates with chemo/radio-resistance and a poor prognosis [17].

Interestingly, expression of CD133 has been closely correlated with metastasis and aggressive biology of tumors [6]. Tumors having high expression of CD133 are known to metastasize more than those with lower CD133+ population. Thus, it is of utmost importance to understand the structural association of CD133 in the lipid rafts of the plasma membrane, in order to evaluate the function of this critical TIC marker in pancreatic cancer. In this article, we outline the protocol for isolation of lipid rafts from CD133+ cells from pancreatic tumors. Following isolation, the lipid rafts can be analyzed further by proteomics or lipidomics methods to evaluate the composition of these membrane structures. A complete understanding of the protein and lipid components is required to elucidate the function of this protein and how it may be involved in invasion metastasis and chemoresistance.

2 Materials

1. Primary tumor from patients, spontaneous pancreatic cancer mouse model (KRas^{G12D} TP53^{R172H} Pdx^{Cre}).
2. RPMI 1640 medium, Fetal bovine serum (FBS).
3. Phosphate Buffered Saline.
4. Collagenase IV (Worthington Biochemicals).
5. MACS column (Miltenyi Biotech).
6. Anti-CD133 microbeads (human) or anti-CD133/PROM1 microbeads (mouse).
7. Anti-CD133 antibody.
8. OptiPrep (Sigma Aldrich).
9. Isolation Buffer (IB): 150 mM NaCl, 5 mM dithiothreitol (DTT), 5 mM EDTA, 25 mM Tris-HCl, pH 7.4 supplemented with a cocktail of protease inhibitors.
10. Triton X-100.
11. Ultracentrifuge with any small volume (approx. 10–13 mL) swinging bucket rotor (e.g., Beckman SW41Ti or equivalent).
12. Syringe with metal cannula (for underlayering) or Pasteur pipette (for overlaying).
13. 40-micron nylon mesh, electric pipettor.
14. Dot-blot apparatus.

3 Methods

3.1 Preparation of Single Cell Suspension

1. To generate single cell suspension, cut xenograft tumors from mice or primary human tumors into small pieces with sterile scissors in RPMI medium, and then mince the tissue mechanically with scissors or scalpel until the pieces are 1 mm in size (able to be pipetted without difficulty using 10 mL pipettes). Wash the tissue with RPMI twice, centrifuge samples, and discard the solution.
2. Resuspend the minced tissue in 20–30 mL RPMI in a 50 mL centrifuge tube depending on the amount of tissue. Large amounts of tissue may require additional tubes.
3. Digest minced tissue by adding ultrapure collagenase IV in medium at a final concentration of 200 units/mL.
4. Incubate the sample at 37 °C with shaking at a speed of 120 RPM for 1.5 h for first step enzymatic dissociation.

5. Pipette the sample for 3 min using a 25 mL pipette to mechanically dissociate the sample and put it back to 37 °C incubation.
6. Further mechanically dissociate the sample every 15–20 min by pipetting with a 10 or 5 mL pipette until whole tumor is dissociated.
7. Add RPMI to a total volume of 50 mL and spin down at 800 RPM for 5 min.
8. Discard the supernatant and resuspend the samples with RPMI containing 2% FBS.
9. Filter through a 40-micron nylon mesh to eliminate clumps and debris.
10. Wash cells with RPMI/2% FBS twice to remove enzyme solution. Resuspend cells in RPMI/2% FBS and perform a cell count. Cells are ready for sorting (*see Note 1*).

3.2 MACS Sorting

1. Prepare MACS mini/midi column by washing them with RPMI/2% FBS while attached to magnetic stand.
2. While the column is being washed add anti-CD133 microbeads to single cell suspension of tumor cells (human origin) or anti-Prom1 microbeads to cells of murine origin.
3. Incubate cells on ice for 20 min.
4. Add cell-microbeads mix to column attached to magnetic stand.
5. Collected flow through in a 15 mL tube (this is CD133– cells. Once purity has been determined, this fraction can be discarded).
6. Wash column with RPMI/2% FBS and pool with flow-through to remove traces of CD133– cells.
7. Remove column from magnetic stand and place on 15 mL tube. Elute CD133+ cells using RPMI/2% FBS (this is CD133+ fraction).
8. Analyze 50 µL of elute of CD133+ cells and CD133– cells by flow cytometry (using anti-CD133-PE antibody to confirm purity).

3.3 Cell Lysis

1. Wash CD133+ cell pellet from the tumor (~10–12 million cells from the above mentioned tumor size) twice with PBS (five times the cell pellet volume).
2. Add 0.8 mL of ice-cold 0.1% Triton X-100 IB to the cell pellet (*see Note 2*).
3. Use an automatic pipet to resuspend cell pellet and vortex briefly for 10 s (*see Note 3*).
4. Pass solution through a 23 G needle using a 5 mL syringe 20 times (*see Note 4*).
5. Centrifuge lysed cells in solution for 10 min at $112 \times g$ at 4 °C.
6. Carefully retrieve post nuclear supernatant from pellet of cell debris (*see Note 5*).

3.4 Density Gradient

The density gradient is made of five layers of OptiPrep with different concentrations: 35, 30, 25, 20, and 0%. The lower layer (35% OptiPrep) contains the cell lysate (*see* Table 1). Work with pre-cooled Lysis Buffer, OptiPrep (60% w/v), OptiPrep gradient layers, and 2 mL microcentrifuge tubes.

1. Prepare the five solutions that will form the OptiPrep gradient layers according to Table 1. Mix each one well by vortexing. Keep the prepared solutions on ice (*see* Note 6).
2. Put 2 mL of gradient layer 1 (35% OptiPrep containing the cell lysate) at the bottom of the precooled ultracentrifuge tube.
3. Place each OptiPrep gradient layer over the other in order (*see* Fig. 1) using a Pasteur pipette. It is recommended to use an electric pipettor. Gradient is visible to the naked eye.
4. Spin the density gradient in ultracentrifuge at $200,000 \times g$ for 4 h at 4 °C.
5. Take the tubes carefully out of the ultracentrifuge and put them on ice.

Table 1
Preparation of OptiPrep density gradient layers

Gradient layer	Final OptiPrep (%)	Cell lysate (vol)	IB (mL)	OptiPrep (mL)	Total volume (mL)
1 (bottom)	35	0.84	0	1.16	2
2	30	–	1	1	2
3	25	–	1.16	0.84	2
4	20	–	1.3	0.7	2
5 (top)	0	–	1	0	1

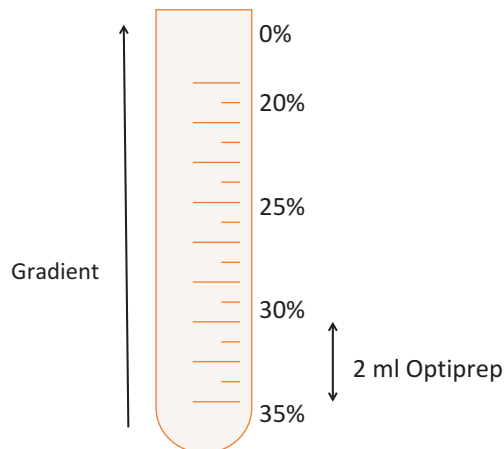


Fig. 1 Demonstration of setting up an OptiPrep gradient for lipid raft isolation

6. Mark nine microcentrifuge tubes from 1 to 9. Tube number 1 will be used for the lowest % of the gradient (the top fraction of the ultracentrifuge tube).
7. CD133 lipid rafts are recovered as a fine dense band at the border of 20 and 30% (w/v) OptiPrep layers after ultracentrifugation at $\sim 200,000 \times g$ for 4 h. Proteins that are part of the rafts or bound to these structures are present in the rafts enriched fraction.

3.5 Fractions Collection

1. Mark a line on a Pasteur pipette to indicate a 1 mL volume. Connect the pipette to an electric pipettor.
2. Carefully collect 1 mL fractions from top to bottom of the ultracentrifuge tube and transfer each fraction to a marked microcentrifuge tube. The number of total collected fractions can vary between 7 and 9. Number the topmost fraction 1 and so on.
3. Keep the fractions on ice for later use.
4. Fractions can be stored in $-80\text{ }^{\circ}\text{C}$ for up to 6 months.

3.6 Gradient Fraction Analysis

1. Perform dot-blot with 2–3 μL of each gradient fraction as well as original lysate on nitrocellulose membrane.
2. Hybridize with CD133 antibody to detect fraction containing lipid raft.

4 Notes

1. Digestion of a 1 cm^3 xenograft tumor will typically result in 10–20 million cells. Excess cells may be frozen for future use by placing cells in a solution of FBS with 10% DMSO.
2. Lipid rafts have a unique feature of relative resistance to solubilization in an ice-cold TRITON X-100 solution. This feature is used for their isolation. Since the procedure is highly temperature dependent, the work should be performed in the cold room. Note that at $8\text{ }^{\circ}\text{C}$ the Caveolae/Rafts proteins may already be soluble in the TRITON X-100 solution and will not float up in the gradient.
3. Solution should appear homogeneous with no clumps of cells in solution.
4. Drawing solution into the syringe and then forcing it out counts as 2 \times .
5. Cell debris pellet will be soft and longer spin time may be needed (up to 20 min). Do NOT spin at any higher speed or membrane lipids will be lost.
6. In order to create an OptiPrep layer, which contains precisely 35% OptiPrep, the volume of cell lysate in tube number 1 should be exactly 0.84 mL.

References

1. Bednar F, Simeone DM (2009) Pancreatic cancer stem cells and relevance to cancer treatments. *J Cell Biochem* 107(1):40–45. doi:[10.1002/jcb.22093](https://doi.org/10.1002/jcb.22093)
2. Bhagwandin VJ, Shay JW (2009) Pancreatic cancer stem cells: fact or fiction? *Biochim Biophys Acta* 1792(4):248–259. doi:[10.1016/j.bbadis.2009.02.007](https://doi.org/10.1016/j.bbadis.2009.02.007)
3. Donahue TR, Dawson DW (2011) Nodal/Activin signaling: a novel target for pancreatic cancer stem cell therapy. *Cell Stem Cell* 9(5):383–384. doi:[10.1016/j.stem.2011.10.006](https://doi.org/10.1016/j.stem.2011.10.006)
4. Hermann PC, Huber SL, Herrler T, Aicher A, Ellwart JW, Guba M, Bruns CJ, Heeschen C (2007) Distinct populations of cancer stem cells determine tumor growth and metastatic activity in human pancreatic cancer. *Cell Stem Cell* 1(3):313–323. doi:[10.1016/j.stem.2007.06.002](https://doi.org/10.1016/j.stem.2007.06.002)
5. Li C, Heidt DG, Dalerba P, Burant CF, Zhang L, Adsay V, Wicha M, Clarke MF, Simeone DM (2007) Identification of pancreatic cancer stem cells. *Cancer Res* 67(3):1030–1037. doi:[10.1158/0008-5472.can-06-2030](https://doi.org/10.1158/0008-5472.can-06-2030)
6. Banerjee S, Nomura A, Sangwan V, Chugh R, Dudeja V, Vickers S, Saluja AK (2014) CD133+ tumor initiating cells (TIC) in a syngenic murine model of pancreatic cancer respond to Minnelide. *Clin Cancer Res* doi:[10.1158/1078-0432.CCR-13-2947](https://doi.org/10.1158/1078-0432.CCR-13-2947)
7. Corbeil D, Marzesco AM, Wilsch-Brauninger M, Huttner WB (2010) The intriguing links between prominin-1 (CD133), cholesterol-based membrane microdomains, remodeling of apical plasma membrane protrusions, extracellular membrane particles, and (neuro)epithelial cell differentiation. *FEBS Lett* 584(9):1659–1664. doi:[10.1016/j.febslet.2010.01.050](https://doi.org/10.1016/j.febslet.2010.01.050)
8. Marzesco AM (2013) Prominin-1-containing membrane vesicles: origins, formation, and utility. *Adv Exp Med Biol* 777:41–54. doi:[10.1007/978-1-4614-5894-4_3](https://doi.org/10.1007/978-1-4614-5894-4_3)
9. Maw MA, Corbeil D, Koch J, Hellwig A, Wilson-Wheeler JC, Bridges RJ, Kumaramanickavel G, John S, Nancarrow D, Roper K, Weigmann A, Huttner WB, Denton MJ (2000) A frameshift mutation in prominin (mouse)-like 1 causes human retinal degeneration. *Hum Mol Genet* 9(1):27–34
10. Roper K, Corbeil D, Huttner WB (2000) Retention of prominin in microvilli reveals distinct cholesterol-based lipid micro-domains in the apical plasma membrane. *Nat Cell Biol* 2(9):582–592. doi:[10.1038/35023524](https://doi.org/10.1038/35023524)
11. Giebel B, Corbeil D, Beckmann J, Hohn J, Freund D, Giesen K, Fischer J, Kogler G, Wernet P (2004) Segregation of lipid raft markers including CD133 in polarized human hematopoietic stem and progenitor cells. *Blood* 104(8):2332–2338. doi:[10.1182/blood-2004-02-0511](https://doi.org/10.1182/blood-2004-02-0511)
12. McCaffrey LM, Macara IG (2011) Epithelial organization, cell polarity and tumorigenesis. *Trends Cell Biol* 21(12):727–735. doi:[10.1016/j.tcb.2011.06.005](https://doi.org/10.1016/j.tcb.2011.06.005)
13. Martin-Belmonte F, Perez-Moreno M (2012) Epithelial cell polarity, stem cells and cancer. *Nat Rev Cancer* 12(1):23–38. doi:[10.1038/nrc3169](https://doi.org/10.1038/nrc3169)
14. Bose R, Wrana JL (2006) Regulation of Par6 by extracellular signals. *Curr Opin Cell Biol* 18(2):206–212. doi:[10.1016/j.ceb.2006.02.005](https://doi.org/10.1016/j.ceb.2006.02.005)
15. Gomez-Lopez S, Lerner RG, Petritsch C (2014) Asymmetric cell division of stem and progenitor cells during homeostasis and cancer. *Cell Mol Life Sci* 71(4):575–597. doi:[10.1007/s00018-013-1386-1](https://doi.org/10.1007/s00018-013-1386-1)
16. Lathia JD, Hitomi M, Gallagher J, Gadani SP, Adkins J, Vasanji A, Liu L, Eyler CE, Heddleston JM, Wu Q, Minhas S, Soeda A, Hoepfner DJ, Ravin R, McKay RD, McLendon RE, Corbeil D, Chenn A, Hjelmeland AB, Park DM, Rich JN (2011) Distribution of CD133 reveals glioma stem cells self-renew through symmetric and asymmetric cell divisions. *Cell Death Dis* 2:e200. doi:[10.1038/cddis.2011.80](https://doi.org/10.1038/cddis.2011.80)
17. Su YJ, Lin WH, Chang YW, Wei KC, Liang CL, Chen SC, Lee JL (2015) Polarized cell migration induces cancer type-specific CD133/integrin/Src/Akt/GSK3beta/beta-catenin signaling required for maintenance of cancer stem cell properties. *Oncotarget* 6(35):38029–38045. doi:[10.18632/oncotarget.5703](https://doi.org/10.18632/oncotarget.5703)

Isolation of Neuronal Synaptic Membranes by Sucrose Gradient Centrifugation

Blake R. Hopiavuori, Dustin R. Masser, Joseph L. Wilkerson, Richard S. Brush, Nawajes A. Mandal, Robert E. Anderson, and Willard M. Freeman

Abstract

Sucrose gradient centrifugation is a very useful technique for isolating specific membrane types based on their size and density. This is especially useful for detecting fatty acids and lipid molecules that are targeted to specialized membranes. Without fractionation, these types of molecules could be below the levels of detection after being diluted out by the more abundant lipid molecules with a more ubiquitous distribution throughout the various cell membranes. Isolation of specific membrane types where these lipids are concentrated allows for their detection and analysis. We describe herein our synaptic membrane isolation protocol that produces excellent yield and clear resolution of five major membrane fractions from a starting neural tissue homogenate: P1 (Nuclear), P2 (Cytoskeletal), P3 (Neurosynaptosomal), PSD (Post-synaptic Densities), and SV (Synaptic Vesicle).

Key words Sucrose gradient centrifugation, Membrane fractionation, Neuronal lipids, Synaptic membrane isolation, Neurosynaptosome isolation

1 Introduction

Sucrose gradient centrifugation has been used by biochemists spanning the last several decades. It is an excellent approach for isolating specialized lipid membranes based on their size and density. The most common variations of this method are performed with either a continuous or discontinuous gradient of various sucrose densities, depending on the application. Discontinuous sucrose gradients allowed the isolation of rod photoreceptor outer segments for characterization of the rod photopigment, rhodopsin, and many other specialized membrane proteins [1], as well as the large lipid component of these membranes [2]. Redburn and Thomas first described isolation of large (ribbon) and small (conventional) synapses from rabbit retina [3]. Our group used a

modified version of Redburn's protocol to resolve these large and small synapses from outer segments in bovine retina to show for the first time, the presence of very-long chain (>26C) polyunsaturated fatty acids in the synapses of the neural retina [4, 5]. Herein, we describe a protocol for the isolation of five major membrane fractions with clear resolution from a starting homogenate of neural tissue that uses a single density of 0.32 M sucrose and applies varying degrees of centrifugal force on each supernatant to spin down each subsequent fraction; a method that produces excellent resolution and enrichment of synaptic membranes (Fig. 1). This is a modification to the published work of VanGuilder et al., 2008 and 2010, in which this type of sucrose gradient centrifugation was successfully used to isolate neurosynaptosomes from diabetic rat retina and from aged rat hippocampus, respectively, for transcriptomic and proteomic analysis [6, 7]. As the fields of lipid biochemistry and neuroscience continue to interact, these types of

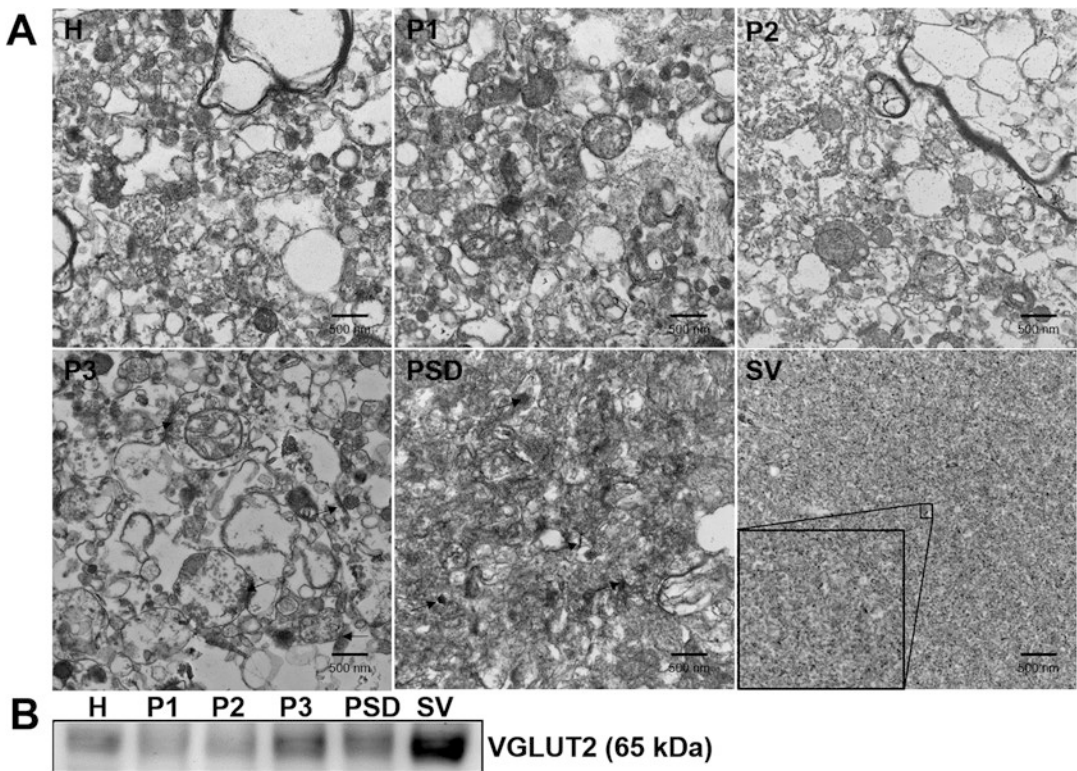


Fig. 1 Synaptic membrane isolation from fresh baboon hippocampus. (a) Representative electron micrographs of all five fractions (P1, P2, P3, PSD, SV) plus the starting hippocampal homogenate (H). (b) Western blot immuno-labeling for the synaptic vesicle-associated protein VGLUT2 shows dramatic enrichment in the synaptic vesicle membrane fraction (SV) compared to the original starting homogenate and compared to the P3 neurosynaptosomal fraction (15 μ g of protein is loaded in each well, rabbit anti-VGLUT2 (Dcf68) 1:4000 was used followed by ECL anti-rabbit secondary 1:2000 for detection)

techniques will be paramount in identifying new lipid molecules that, like docosahexaenoic acid and arachidonic acid, are playing multifaceted roles in the central nervous system.

2 Materials

Prepare all solutions fresh the day before use with ultrapure water (u.p.H₂O). Store at 4 °C (unless indicated otherwise). Follow all waste disposal regulations when disposing of waste materials.

2.1 Solutions

1. 0.32 M Sucrose/4 mM HEPES (300 mL): 32.86 g Sucrose, 0.285 g HEPES, 3 mL 100 mM Na₃VO₄ (tyrosine phosphatase inhibitor; see below for making sodium orthovanadate), pH to 7.4 with either HCl or NaOH as required, make to 300 mL with u.p.H₂O.
2. Lysis buffer (15 mL): 0.09 g HEPES, 0.3 mL 0.05 M EDTA (Ca²⁺ chelator), 0.088 g NaCl, 1.5 mL 10 mM DTT (sulfhydryl reducing agent), 0.031 g NaF (phosphoserine and phosphothreonine phosphatase inhibitor), 150 μL Tween 20 (mild detergent), 150 μL 100 mM Na₃VO₄, 2 Roche complete EDTA-free protease inhibitor tablets, pH to 7.4 with either HCl or NaOH as required, make to 15 mL with u.p.H₂O.
3. Lysis Water (20 mL): 20 mL u.p.H₂O, 2 Roche complete EDTA-free protease inhibitor tablets.
4. Post-Synaptic Density (PSD) Resuspension Buffer (15 mL): 75 μL 10% Triton-X 100 (mild detergent), 30 μL EDTA, 0.179 g HEPES, 2 Roche complete EDTA-free protease inhibitor tablets, pH to 7.4 with either HCl or NaOH as required, make to 15 mL with u.p.H₂O.
5. HEPES-NaOH (pH 7.4) to stop Lysis (1 M): 0.19 g HEPES in 800 μL u.p.H₂O, pH with NaOH to 7.4, make to 1 mL with u.p.H₂O.
6. 1 M Tris-HCl (pH 7.4) (1 L): 121.14 g Tris base in 800 mL u.p.H₂O, pH to 7.4 with HCl, make to 1 L with u.p.H₂O.
7. Wash Buffer (pH 7.4) (900 mL): 6 mL 1 M Tris-HCl (pH 7.4), 45 mL 2 M NaCl (prepared fresh), 1.8 mL 0.5 M EDTA, pH to 7.4 with HCl or NaOH, make to 900 mL with u.p.H₂O.
8. Prepare a 100 mM solution of Na₃VO₄ (10 mL): adjust pH to 10.0 with NaOH, boil until solution is colorless, allow to cool to room temp, repeat **steps 1–3** until solution remains colorless and pH is stable at 10.0, aliquot in 1 mL volumes and store at -20 °C, thaw on ice on day of use.

2.2 Equipment

1. Centrifuge: Beckman Coulter Optima L-80 XP Ultracentrifuge.
2. Rotors: Beckman SW 60 Ti swing-bucket rotor, SW 32 Ti swing-bucket rotor.

3. Swing-buckets: SW 32 Ti (50 mL), SW 32.1 Ti (17 mL), SW 60 Ti (4 mL).
4. Centrifuge Tubes: Beckman, Thinwall, Ultra-Clear centrifuge tube 4, 17, or 50 mL (Catalog #344062, 344061, 344058).

3 Methods

As a general rule, 1 mL of buffer is used per 15–20 mg wet weight of tissue and this is considered **one volume unit** (*see Notes 1 and 2*). Always keep samples on ice, and prechill centrifuge and all rotors to 4 °C before beginning. Euthanize rodents in accordance with your institutional guidelines for animal care and use, keeping in mind that CO₂ and Halothane will rapidly change the structural and functional integrity of neural membranes [8–11]. Our mice are euthanized by cervical dislocation followed by decapitation, rats are euthanized by decapitation. Our baboon brains were obtained post-mortem on ice from the Department of Comparative Medicine Primate Research Facility, University of Oklahoma Health Sciences Center, hippocampus was dissected and processed using this protocol. Due to the larger mass, the hippocampus from each hemisphere was cut into three equal volumes and each of the six pieces were processed in separate tubes before recombining like-samples at the very end before wash and resuspension (Fig. 1). Perform all brain dissections on a cold aluminum plate on ice, use a dissecting microscope to remove white matter, as the myelin will disrupt the purity of the fractionation. Avoid attempting this fractionation protocol on whole brain as there is a dramatic loss in the quality of fraction resolution.

3.1 Isolation Steps

1. Place dissected tissue in one volume of ice-cold 0.32 M Sucrose/4 mM HEPES buffer in a Beckman, Thinwall, Ultra-Clear centrifuge tube 4 mL, 17 mL, or 50 mL, depending on tissue weight (1 volume = approx. 1 mL buffer per 15–20 mg tissue wet weight) (*see Notes 1 and 2*).
2. Incubate on ice for 20 min (allow tissue to sink to the bottom). Pour off buffer and replace it with one volume of ice-cold 0.32 M Sucrose/4 mM HEPES buffer and incubate on ice for another 20 min.
3. Invert tube two to three times and incubate on ice for another 10 min.
4. After tissue settled to the bottom of the tube, replace buffer with one volume of fresh ice-cold 0.32 M Sucrose/4 mM HEPES buffer and repeat **step 3**.
5. Replace the buffer with one volume of fresh ice-cold 0.32 M Sucrose/4 mM HEPES buffer and pour into homogenizer. Be sure to leave enough room in the tube to accommodate the homogenization pestle.

- (a) With a motorized dounce pestle, keeping the samples on ice (speed setting = 1+, use slow, up, and down motion), to homogenize tissue using the full range of motion available and holding for ~3 s at the bottom of the tube (5–10 times).
- (b) With a glass teflon hand homogenizer, keeping the samples on ice, tissue is homogenized with 10–15 slow, even, up and down strokes until the tissue has become homogenous; apply pressure and twist pestle back and forth at the bottom of each stroke to better break up the tissue.

* See **Note 3** before continuing.

6. Transfer back to the Beckman ultracentrifuge tube and place them in the prechilled rotor, making sure that all tubes are balanced by weight (we use the following combination of Beckman swinging bucket rotors: SW 28.1, SW 32.0 Ti, SW 32.1 Ti, SW 60 Ti).
7. *Spin 1* (**RCF = 200 × g**) (*see Note 4* re: RCF) at **4 °C** for **10 min** to isolate the **P1 nuclear fraction** (this is a very low-speed spin, so be careful not to resuspend the pellet while removing the supernatant).
8. Place P1 pellet on ice and transfer supernatant to a new Beckman ultracentrifuge tube and balance by weight for the next spin.
9. *Spin 2* (**RCF = 800 × g**) at **4 °C** for **12 min** to isolate the **P2 cytoskeletal fraction**.
10. Place P2 pellet on ice and transfer supernatant to a new Beckman ultracentrifuge tube and balance by weight for the next spin.
11. *Spin 3* (**RCF = 25,000 × g**) at **4 °C** for **14 min** to isolate the **P3 neurosynaptosomal fraction**.
12. *Spin 4*: Discard the supernatant from your P3 pellet (myelin, microsomes, etc.) or keep for analysis if desired. Wash the P3 pellet in a fresh volume of ice-cold 0.32 M Sucrose/4 mM HEPES buffer, balance by weight, and spin again at **RCF = 25,000 × g** at **4 °C** for **12 min**, discard this supernatant.

STOP: At this stage you have isolated your neurosynaptosomes and can stop here if you do not need to perform the further fractionation required to isolate PSDs and SVs; you may keep the final supernatant from your P3 spin (myelin, microsomes, etc.) for analysis, or discard and place your P3 pellet on ice. *See* Subheading **3.2** for final wash protocol for all pellets [**OR**] if you require enrichment of PSD and/or SVs, then continue to **step 13**.

* *See Note 3* before continuing. Your P3 pellet is now your new starting material.

13. Lyse P3 pellet by resuspending in 3.6 mL ice-cold Lysis Water + 0.4 mL ice-cold 0.32 M Sucrose/4 mM HEPES buffer (*see Note 5*) and after transferring to homogenization tube, homogenize by either method (a) or method (b) using only 3–5 strokes this time.
14. Rapidly add 37.5 μ L of the ice-cold HEPES-NaOH (pH 7.4) buffer and incubate for 30 min on ice to stop lysis.
15. *Spin 5*: balance tubes by weight and spin again to pellet at **RCF = 25,000 $\times g$** at 4 °C for **20 min**.
16. Transfer the supernatant from *Spin 5* to a new tube and set on ice for later (SVs fraction isolation).
17. Resuspend the pellet from *Spin 5* in 3 mL PSD Resuspension Buffer and balance tubes by weight for the next spin.
18. *Spin 6* (**RCF = 32,000 $\times g$**) at 4 °C for **20 min** to isolate the **PSD post-synaptic density fraction**. Place this pellet on ice until ready to begin final wash protocol. Discard supernatant (myelin, microsomes, etc.) or keep for analysis if desired.
19. Take the supernatant from *Spin 5* that you set aside earlier and balance tubes by weight for the next spin with a pre-combined 3.6 mL Lysis Water + 0.4 mL 0.32 M Sucrose/4 mM HEPES solution.
20. *Spin 7* (**RCF = 165,000 $\times g$**) at 4 °C for **120 min** to isolate the **SV synaptic vesicle fraction in the pellet**. Discard supernatant or store for analysis if desired.

3.2 Wash and Storage Steps

1. Resuspend all pellets (P1 through SV) that have been kept on ice until now in one volume each of ice-cold Wash Buffer. Do the same for your starting homogenates as well (H alone or H and P3 if you continued all the way through to SV isolation); dilute with Wash Buffer to remove sucrose.
2. Balance tubes by weight. If there is more than one tube for each fraction for the same biological replicate, now is the time to combine them before moving on (*see Note 6*).
3. *Spin 8* (**RCF = 25,000 $\times g$**) at 4 °C for **20 min** to remove all excess sucrose. For washing **SV use RCF = 160,000 $\times g$** . Discard supernatants.
4. Resuspend final pellets in an appropriate volume of Wash Buffer + one Roach protease inhibitor tab (P.I.) per 10 mL of Wash Buffer (*see Note 7*). Base the volume used on the size of the pellet; SVs will usually require the smallest volume and P1/P2 the largest (typically the range falls between 100 and 900 μ L). This will depend on the amount of starting material, yield obtained, and end-point experiments. We set aside

a portion of this final suspension for membrane lysis and protein isolation for western blotting and use the rest for various lipidomic analyses.

5. Transfer into cryo-vials and snap-freeze in liquid nitrogen and store at -80°C until ready for lipidomic and proteomic analyses.

4 Notes

1. The volume unit can be adjusted if needed, lowering the tissue weight closer to 10–15 mg per mL may improve separation. Remember that in some cases the tissue may be too large to combine all of the tissue from the same biological replicate into one ultracentrifuge tube. If this happens, the tissue can be blocked into more appropriate sizes and processed in more than one tube within the same centrifuge. In this case, at the very end, be sure to combine like fractions from the same biological replicate before doing your final wash spin to save yourself time and to improve your final yield.
2. Always keep an accurate account of your working volumes. The scale of the experiment can vary dramatically when comparing the volumes needed to isolate synaptosomes from baboon hippocampus vs. that of a mouse, so plan accordingly and think through each step so that you do not get caught with either too large or too small a volume.
3. **Always remember to set aside your starting material.** It is not sufficient to use dissected but un-fractionated tissue as a representation of what you started with. You should set aside an aliquot of your starting homogenate (H) before you proceed to *Spin 1* and again from your P3 pellet as a new starting material before lysing for PSD and SV isolation. These aliquots will remain homogenous on ice during the experiment and will be spun down later during the wash phase into a pellet for resuspension and snap-freezing.
4. Note that RCF is equal to the gravitational force and for each rotor that you plan to use you will need to calculate the RPMs that correspond to the RCF values reported here. Be sure to balance tubes (by weight) that will oppose each other in your rotor. We perform all fractionation with swinging bucket rotors as they seem to produce a better yield with better resolution than the fixed-angle rotors.
5. Note that in **step 13**, 4 mL is being added in total to each P3 starting pellet (3.6 mL of Lysis Water + 0.4 mL of 0.32 M Sucrose/4 mM HEPES). We use these volumes because our centrifuge tubes for the SW 60 Ti only hold a volume of 4 mL, if you are able to achieve $160,000 \times g$ with tubes of a larger volume, simply increase the total volume while keeping the

ratio between the two buffers the same. Be sure that protease inhibitors are present in your Lysis Water. Be careful not to over-homogenize here, do not use more than five complete strokes with either method of homogenization.

6. Washing will require several spins to work through all of the samples depending on how many systems you are able to use at once, your number of replicates, and how many fractions you have generated.
7. When resuspending your final pellets for snap-freezing, remember that it is always easier to dilute your sample further than it is to concentrate it down so, if in doubt, stick to the smaller side when choosing your resuspension volumes.

Acknowledgments

Heather VanGuilder Starkey for sharing her isolation protocols with us. Nicolas Bazan for sending us the rabbit anti-VGLUT2 antibody (Dcf68) cloned by his laboratory.

This work was supported by the following grants:

EY024520, EY021716 to WMF

EY023202 to DRM

NS090117, EY004149, EY000871, and EY021725 (P30 Vision Core Grant) to REA

NS089358 to BRH

EY022071, EY025256, to NAM

Foundation Fighting Blindness to REA and NAM

Unrestricted grant from Research to Prevent Blindness, Inc.

References

1. Krebs A, Villa C, Edwards PC, Schertler GF (1998) Characterisation of an improved two-dimensional p22121 crystal from bovine rhodopsin. *J Mol Biol* 282(5):991–1003. doi:[10.1006/jmbi.1998.2070](https://doi.org/10.1006/jmbi.1998.2070)
2. Anderson RE, Maude MB (1970) Phospholipids of bovine outer segments. *Biochemistry* 9(18):3624–3628
3. Redburn DA, Thomas TN (1979) Isolation of synaptosomal fractions from rabbit retina. *J Neurosci Methods* 1(3):235–242
4. Bennett LD, Hopiavuori BR, Brush RS, Chan M, Van Hook MJ, Thoreson WB, Anderson RE (2014) Examination of VLC-PUFA-deficient photoreceptor terminals. *Invest Ophthalmol Vis Sci* 55(7):4063–4072. doi:[10.1167/iovs.14-13997](https://doi.org/10.1167/iovs.14-13997)
5. Hopiavuori BR, Bennett LD, Brush RS, Van Hook MJ, Thoreson WB, Anderson RE (2016) Very long-chain fatty acids support synaptic structure and function in the mammalian retina. *OCL* 23(1):D113
6. VanGuilder HD, Brucklacher RM, Patel K, Ellis RW, Freeman WM, Barber AJ (2008) Diabetes downregulates presynaptic proteins and reduces basal synapsin I phosphorylation in rat retina. *Eur J Neurosci* 28(1):1–11. doi:[10.1111/j.1460-9568.2008.06322.x](https://doi.org/10.1111/j.1460-9568.2008.06322.x)
7. VanGuilder HD, Yan H, Farley JA, Sonntag WE, Freeman WM (2010) Aging alters the expression of neurotransmission-regulating proteins in the hippocampal synaptosome. *J Neurochem* 113(6):1577–1588. doi:[10.1111/j.1471-4159.2010.06719.x](https://doi.org/10.1111/j.1471-4159.2010.06719.x)

8. Angus DW, Baker JA, Mason R, Martin IJ (2008) The potential influence of CO₂, as an agent for euthanasia, on the pharmacokinetics of basic compounds in rodents. *Drug Metab Dispos* 36(2):375–379. doi:[10.1124/dmd.107.018879](https://doi.org/10.1124/dmd.107.018879)
9. Martoft L, Stodkilde-Jorgensen H, Forslid A, Pedersen HD, Jorgensen PF (2003) CO₂ induced acute respiratory acidosis and brain tissue intracellular pH: a ³¹P NMR study in swine. *Lab Anim* 37(3):241–248. doi:[10.1258/002367703766453092](https://doi.org/10.1258/002367703766453092)
10. Mikulec AA, Pittson S, Amagasu SM, Monroe FA, MacIver MB (1998) Halothane depresses action potential conduction in hippocampal axons. *Brain Res* 796(1–2):231–238
11. Silva JH, Gomez MV, Silva JH, Guatimosim C, Gomez RS (2008) Halothane induces vesicular and carrier-mediated release of [³H]serotonin from rat brain cortical slices. *Neurochem Int* 52(6):1240–1246. doi:[10.1016/j.neuint.2008.01.004](https://doi.org/10.1016/j.neuint.2008.01.004)

Sample Preparation and Analysis for Imaging Mass Spectrometry

Genea Edwards, Annia Mesa, Robert I. Vazquez-Padron, Jane-Marie Kowalski, and Sanjoy K. Bhattacharya

Abstract

Imaging mass spectrometry (IMS) is a novel quantitative technique used to investigate diverse biomolecules in tissue sections. Specifically, IMS uses analytical separation of mass spectrometry to determine the spatial distribution of certain lipids and/or proteins located directly on biological sections from a single tissue sample. Typically, IMS is combined with histological analysis to reveal additional distribution details of characterized biomolecules including cell type and/or subcellular localization. In this chapter, we describe the use of Matrix-Assisted Laser Desorption/Ionization (MALDI) Time-Of-Flight/Time-Of-Flight (TOF/TOF) to analyze various cholesterol and phosphatidylcholine species in atherosclerotic plaque of murine heart aortic valves. In particular, we detail animals used, tissue collection, preparation, matrix application, spectra acquisition for generating a color-coded image based on IMS spectral characteristics.

Key words Imaging mass spectrometry (IMS), Matrix-assisted laser desorption ionization (MALDI), Time-of-flight (TOF), Metabolite, Biomarker

1 Introduction

Imaging mass spectrometry (IMS) is a growing analytical technique for studying the frequency, localization, and distribution of biomolecules and their metabolites at the cellular levels in any sectioned tissue sample [1]. Prior to IMS, autoradiography (ARG) was the first molecular imaging technique used for the localization of radioactivity in biological specimens [2]. This technique, based on the analysis of the specific binding of radiolabeled compounds, is limited by some technical problems, which mainly affect both the type of compounds or biological substances that can be detected and the image resolution [3]. IMS, on the other hand, is capable of label-free and multiplex analyses of hundreds of unknown compounds in a given sample.

During IMS studies, sample preparation is a critical first step for obtaining quality, reproducible spectra; therefore, the tissue must be quickly preserved to reduce the molecular degradation process [4]. Likewise, contamination during sample harvesting and processing is a point of major concern given the high sensitivity of IMS. Consequently, tools and solutions used to harvest and process the tissue should be carefully evaluated a priori sample collection to minimize its contamination. In case solutions are required for harvesting and/or processing the tissue, appropriate controls should be included in the experimental design to correct for noise (aka contamination) that will show in the IMS spectra.

MALDI TOF/TOF is the most widely used soft ionization method for IMS in which the flight time of the ion from the source to the detector is correlated to the mass-to-charge ratio (m/z) of the ion. There are several factors that improve the quality of the MALDI spectra including choice of matrix and selection of solvent [5]. In any case, the mass of the lipid of interest is key in determining the preferred method of analysis. In this chapter, we describe step by step a novel protocol to study lipid species distribution in the atherosclerotic plaque of aortic valves from mice on high fat diet. These steps include tissue collection, preparation, matrix application, spectra acquisition, and confirmation of analytes. These methods can be adapted for a given system.

2 Materials

2.1 *Animals, Diet, and Tissue Collection*

1. Eight to ten weeks old apolipoprotein E-deficient (ApoE^{-/-}) female mice (Jackson Laboratory, Bar Harbor, USA).
2. High-fat diet.
3. Isoflurane.
4. Modified OCT medium (mOCT): 5 g Polyvinyl alcohol 6-98, PVA, to a final concentration of 10% (w/v), 50 mL Hank's balanced salt solution, HBSS, 4 mL Polypropylene glycol, PPG 2000, to a final concentration of 8% (w/v), 50 mg Sodium azide, NaN₃, to a final concentration of 0.1% (w/v).

2.2 *Tissue Preparation*

1. Liquid nitrogen.
2. Cryotome.
3. New, fine sectioning brushes.
4. Indium tin oxide (ITO)-coated glass slides (Bruker Daltonik, Bremen, Germany).
5. Nitrogen gas.
6. Flatbed scanner.
7. Hematoxylin & Eosin stain.

8. Home-built sublimation chamber.
9. Hot plate.

2.3 MALDI Mass Spectrometer Hardware and Software

1. UltrafleXtreme MALDI TOF/TOF (Bruker Daltonik, Bremen, Germany).
2. FlexImaging ver. 4.1 software (Bruker Daltonik, Bremen, Germany).

2.4 Matrix and Standard Solutions

1. 2,5-Dihydroxybenzoic acid, DHB: 300 mg for sublimation and 20 mg/mL in methanol for standard spotting.
2. Clozapine standard: 50% Acetonitrile in ultrapure water, 0.1% Trifluoroacetic acid, TFA to a concentration of 300 pmol/ μ L.
3. Caffeine standard: 50% Acetonitrile in ultrapure water, 0.1% TFA to a concentration of 300 pmol/ μ L.
4. Lyophilized peptide standard (Bruker Daltonics, Bremen, Germany): 50% Acetonitrile in ultrapure water, 0.1% TFA for a final concentration of 5 pmol/ μ L for each peptide.
5. Ovine wool cholesterol standard (386.7; catalog no. 700000) (Avanti Polar Lipids Inc., Alabaster, AL): methanol, 20 mg/mL DHB.
6. Phosphatidylcholine standard (649.9; catalog no. 850340) (Avanti Polar Lipids Inc., Alabaster, AL): methanol, 20 mg/mL DHB.

3 Methods

3.1 Animals, Diet, and Tissue Collection

1. Eight to ten weeks old apolipoprotein E-deficient (ApoE^{-/-}) mice [6] ($n = 4$) are fed at libitum high fat diet to induce atherosclerosis development.
2. Following 12 weeks of high-fat diet [7], animals are exsanguinated under anesthesia by drawing total blood from abdominal aorta (*see Note 1*).
3. Mice hearts are harvested after inducing animal euthanasia by over-inhalation of isoflurane.
4. Unflushed hearts are immediately frozen in liquid nitrogen and kept at -80 °C until time of sectioning (*see Note 2*).
5. Tissue may also be embedded in mOCT if embedding must be done for small tissue to provide support for sectioning (*see Note 3*) [3].
6. Prepare mOCT by adding 5 g of PVA 6-98 to 50 ml to make a 10% PVA 6-98 solution.
7. Solution is microwaved and then stir to dissolve the PVA 6-98 into solution.

8. Once the solution has cooled to room temperature add 4 mL of PPG 2000 and 50 mg of sodium azide (NaN_3).
9. Cover and store at room temperature.

3.2 Tissue Preparation

1. A cryotome set at 10 μm thickness is used for tissue sectioning of the heart aortic valves at an optimal temperature between $-20\text{ }^\circ\text{C}$ and $-27\text{ }^\circ\text{C}$.
2. Sections are positioned on ITO-coated glass slides with a fine bristle brush and kept at $-80\text{ }^\circ\text{C}$ until needed for IMS and/or additional analyses (*see Note 4*).
3. Slides with tissue sections are removed from $-80\text{ }^\circ\text{C}$ and dehydrated by immediately placing in a Nitrogen box with a continuous sweeping gas flow for 20 min to remove moisture.
4. A 2400 Dots per Inch (DPI) digital picture of the tissue section is captured using a flatbed scanner (*see Note 5*).
5. Hematoxylin & Eosin (H&E) staining may also be performed on a consecutive section of the same tissue to later superimpose against the IMS-derived color-coded image.

3.3 Matrix Application

1. A home-built sublimation chamber configured with a vacuum pump, cold trap, hot plate, and glass chamber depicted in Fig. 1 is used to deposit matrix onto the tissue.

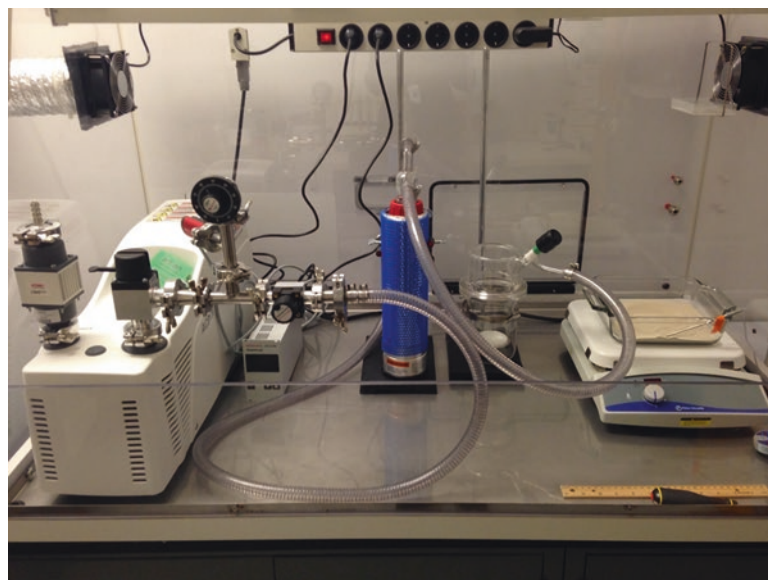


Fig. 1 Home-built sublimation chamber configured with a vacuum pump, cold trap, hot plate, and glass chamber

2. The tissue section is taped to the bottom of the chamber, to be suspended approx. 2 inches above a uniform layer of dry DHB matrix crystals.
3. Adjust vacuum pressure to 50 mTorr, while the hot plate is adjusted to reach a temperature of 150 °C.
4. Once pressure and temperature are stabilized, place the sublimation chamber onto the hot plate filled with sand to help distribute the heat transfer.
5. Deposit DHB matrix onto tissue section by means of sublimation.
6. Sublimation is allowed to take place for a total time of 7 min (*see Note 6*).

3.4 Analysis

1. An UltrafleXtreme MALDI TOF/TOF is used to acquire the molecular images.
2. The instrument is operated in reflector mode to generate positive ions covering a mass range of 300–1000 atomic mass units (amu).
3. Mix DHB matrix with peptide standard, caffeine, clozapine at a volume ratio of (9:1:1:1) respectively.
4. Hand spot 1 μL of mixture on a stainless-steel MALDI plate and allow to air dry.
5. Perform external mass calibration prior to initiating the imaging experiment.
6. The ion source accelerating voltage is set at 20 kV, ion source 2 voltage is 17.8 kV, lens voltage is 7.0 kV, and the delayed extraction time is 120 ns.
7. Operate the smartbeam II laser above threshold, at a repetition of 2000 Hz, accumulating 100 shots at every pixel.
8. Set the laser beam diameter to 10 μm and set pixel step size to 10 μm , in order to uniformly ablate the entire tissue surface (*see Note 7*).
9. Dilute ovine wool cholesterol and a phosphatidylcholine standards and co-mix with DHB matrix (*see Note 8*).
10. Hand spot 1 μL of standard on a stainless-steel MALDI plate and allow to air dry.
11. Select an intense pixel from the MS analysis (*see Note 9*).
12. Manual acquisition is performed utilizing an ion gate (+/-2 Da window) to isolate the target analytes from surrounding signals (*see Note 10*).
13. FlexImaging ver. 4.1 software is used to set up the analysis, as well as post process the results.

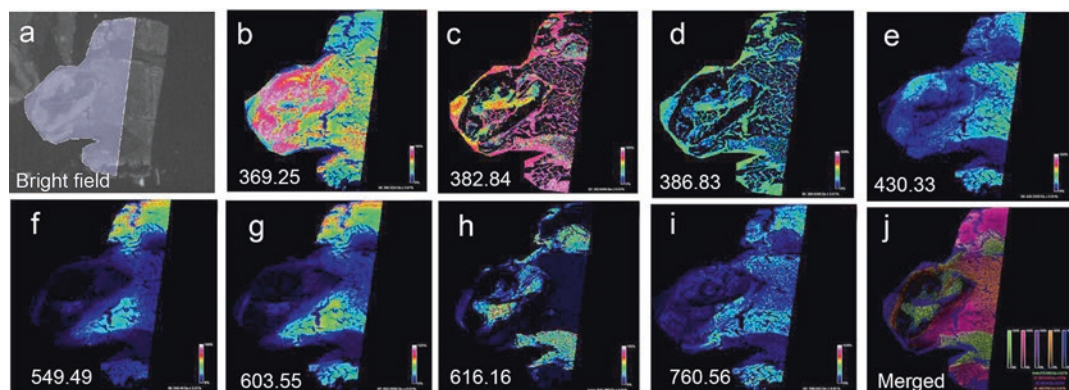


Fig. 2 Imaging mass spectrometry of mouse vein with plaque on a Bruker UltrafleXtreme instrument. **(a)** The bright field image with lasered area indicated by white boundary. **(b–g)** Images of different species of cholesterol/lipid as indicated by different mass by charge ratios (m/z 369.25 to 603.55). **(h)** Heme (m/z 616.16). **(i)** Image of a phosphatidylcholine (m/z 760.56) and **(j)** Merged image of **(d–h)** each using a different pseudo-color

14. Activate normalization of spectra by using the Root Mean Square (RMS) algorithm.
15. Select a desired m/z from the averaged spectrum window to display single ion images (*see Note 11*).
16. To display multiple single ions by selecting those of interest (*see Note 12*).

As shown in Fig. 2, we have analyzed mouse arteries with a plaque for various cholesterol and phosphatidylcholine species. In Fig. 2a, a bright field image with imaged area is shown. In Fig. 2b, we have identified the presence of cholesterol species 369.25 specifically in the plaque but not in the wall of the artery. All other species of cholesterol (Fig. 2b–g) do not show their presence in the plaque. The species with $m/z=369.25$ was characterized using MS/MS analysis confirming its identity as cholesterol.

In Fig. 3a, we present the spectra of parent and fragment ion for phosphatidylcholine. This spectra was generated from MS/MS analyses of ions (m/z 760.56) as depicted in image of Fig. 2i. The fragmentation of phosphatidylcholine was performed in positive ion mode with 7.5 KV collision energy and other well-established parameters. Under these conditions released choline fragment manifests with an m/z 184.07, which is a diagnostic fragment for PCs (Fig. 3b).

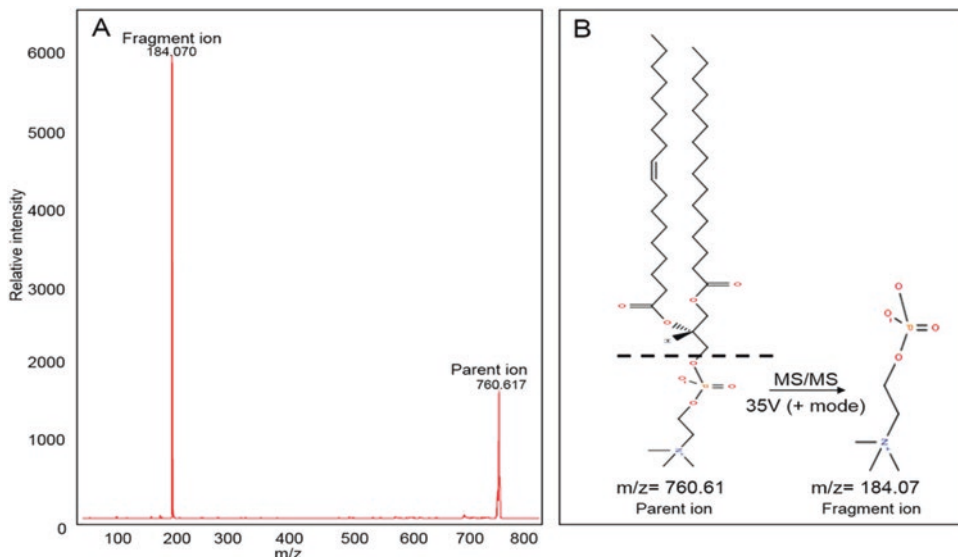


Fig. 3 A parent ion MS/MS spectra at a collision energy of 7.5 KV in positive ion mode to be identified parent phosphatidylcholine (PC) species. (a) The fragment of 184.07 is present in the spectra. (b) Illustration of the fragmentation of the PC parent ion in positive ion mode with a collision energy of 7.5 KV to generate fragment ion (m/z 184.07). The parent ion is consistent with PC(16:0/18:1(9Z)) and was verified with a spotting of a PC standard on the same slide

4 Notes

1. Removal of blood before collecting vascular tissues is desired to minimize nonspecific signal during subsequent IMS analyses on tissue of interest.
2. Due to the tissue size, optimal cutting temperature (OCT) compound was not utilized and should not be utilized in IMS analysis as it has been found to reduce ion formation and the quality of the mass spectra.
3. Embedding in mOCT compatible with IMS may be done.
4. Brand new brushes should be used while sectioning giving that brushes employed in sectioning tissues embedding in parafilm or OCT will contaminate the samples to be submitted for IMS analysis.
5. This high-resolution picture of the tissue section will aid in acquisition setup and facilitate co-registration of the obtained molecular image with the digital picture.
6. A total of 10.2 mg of matrix is deposited on the ITO slide when completed.
7. TOF/TOF mode is used to confirm anticipated intact molecular weights.

8. Standards are used to obtain a reference for molecular weight information for the parent ion and MS/MS fragment ions.
9. On tissue TOF/TOF analyses are performed from known high abundant locations on the tissue, as determined from prior MS analysis of the same tissue section. The instrument XY motors proceed to that corresponding location on the tissue, thus allowing TOF/TOF acquisition to take place.
10. The presence of cholesterol and phosphatidylcholine lipids can now be confirmed.
11. This case is $\pm 0.01\%$.
12. This can be useful when displaying colocalized molecular analytes.

References

1. Chughtai K, Heeren RM (2010) Mass spectrometric imaging for biomedical tissue analysis. *Chem Rev* 110(5):3237–3277. doi:[10.1021/cr100012c](https://doi.org/10.1021/cr100012c)
2. Solon EG, Schweitzer A, Stoeckli M, Prideaux B (2010) Autoradiography, MALDI-MS, and SIMS-MS imaging in pharmaceutical discovery and development. *AAPS J* 12(1):11–26. doi:[10.1208/s12248-009-9158-4](https://doi.org/10.1208/s12248-009-9158-4)
3. Berry KA, Li B, Reynolds SD, Barkley RM, Gijon MA, Hankin JA, Henson PM, Murphy RC (2011) MALDI imaging MS of phospholipids in the mouse lung. *J Lipid Res* 52(8):1551–1560. doi:[10.1194/jlr.M015750](https://doi.org/10.1194/jlr.M015750)
4. Norris JL, Caprioli RM (2013) Analysis of tissue specimens by matrix-assisted laser desorption/ionization imaging mass spectrometry in biological and clinical research. *Chem Rev* 113(4):2309–2342. doi:[10.1021/cr3004295](https://doi.org/10.1021/cr3004295)
5. Le CH, Han J, Borchers CH (2013) Dithranol as a matrix for matrix assisted laser desorption/ionization imaging on a fourier transform ion cyclotron resonance mass spectrometer. *J Vis Exp* 81:e50733. doi:[10.3791/50733](https://doi.org/10.3791/50733)
6. Meir KS, Leitersdorf E (2004) Atherosclerosis in the apolipoprotein-E-deficient mouse: a decade of progress. *Arterioscler Thromb Vasc Biol* 24(6):1006–1014. doi:[10.1161/01.ATV.0000128849.12617.f4](https://doi.org/10.1161/01.ATV.0000128849.12617.f4)
7. Jawien J, Nastalek P, Korbut R (2004) Mouse models of experimental atherosclerosis. *J Physiol Pharmacol* 55(3):503–517

Direct Measurement of Free and Esterified Cholesterol Mass in Differentiated Human Podocytes: A TLC and Enzymatic Assay-Based Method

Christopher E. Pedigo, Sandra M. Merscher, and Alessia Fornoni

Abstract

Esterified cholesterol content is often lower than free cholesterol content in biological systems and thus the determination of the esterified cholesterol content of cells is often challenging. Traditional methods use enzymatic assays in which an indirect measurement of the esterified cholesterol content is obtained by subtracting the measurements of the free from the total cholesterol content. However, this approach fails in the case where the total cholesterol content of cells is unchanged while the ratio of free to esterified cholesterol changes such that total and free cholesterol content are very similar and thus the difference may fall within the background noise of the enzymatic assay. To overcome this challenge, we here describe a method that utilizes a TLC-based technique to isolate esterified cholesterol. Isolated esterified cholesterol can then be measured using traditional enzymatic methods. Therefore, this method provides a practical and more sensitive assay to measure esterified cholesterol content in cellular extracts.

Key words Esterified cholesterol content, Esterified cholesterol mass, Podocyte cholesterol, Cellular cholesterol

1 Introduction

In order to further our understanding of the influence of altered cholesterol metabolism on cellular function, sensitive methods are necessary for the detection and quantification of the cholesterol content of cells. The observation that the esterified cholesterol content of cells is often much lower than the free cholesterol renders the determination of the esterified cholesterol content often challenging. Currently, esterified cholesterol analysis is achieved in various ways including: (a) radiolabeled methods [1], (b) mass spectrometry-based methods [2], or (c) enzymatic assays [3, 4]. Established methods detecting esterified cholesterol were developed in the 1930s [5] and because variable and discrepant results were reported using these methods, the need for more sensitive methods remained. Progress was made that dramatically increased

the sensitivity when compared to the original methods by including saponification steps. This step is still utilized in some current methods especially those requiring mass spectrometry analysis [6]. Later, the development of enzymatic methods utilizing the difference between free and total cholesterol for the determination of esterified cholesterol was developed in tissue extracts [4]. Further enhancement of the sensitivity of these methods was achieved by the introduction of fluorescent probes such as Amplex Red Reagent [3]. While each method is not without limitations as reviewed elsewhere [7, 8], either requiring expensive specialized equipment or being hampered by the lack of sensitivity, the development of *hybrid methods*, similarly to the one described here, allows for a more sensitive detection of the esterified cholesterol content in cells where esterified cholesterol accounts for less than 10% of the total cholesterol. The method presented here requires the isolation of total cholesterol, followed by a TLC-based separation of esterified cholesterol. Esterified cholesterol is then converted to free cholesterol by an enzymatic reaction and the cholesterol content is measured using the sensitive Amplex Red-based cholesterol determination method.

2 Materials

2.1 Lipid Extraction

1. 10× PBS: weigh 800 g NaCl, 20 g KCl, 144 g $\text{Na}_2\text{HPO}_4 \cdot 2\text{H}_2\text{O}$, 24 g KH_2PO_4 up to 8 L of deionized water. Adjust pH with HCl to 6.8. Store at room temperature.
2. 1× PBS: add 100 mL of 10× PBS to 900 mL of deionized water. Store at room temperature.
3. Extraction Solution: Hexane:Isopropanol (3:2, v/v). Add 30 mL of hexane to 20 mL of isopropanol. Store at room temperature.

2.2 Protein Assay

1. Lysis Buffer: 0.1% SDS in 0.1 M NaOH. Add 500 μL of 10% SDS to 45 mL of deionized water. Then add 5 mL of 1 M NaOH. Store at room temperature.

2.3 Isolation of Esterified Cholesterol

1. Chloroform.
2. TLC Solvent: Hexane:Ether:Acetic Acid (130:40:1.5). Add 130 mL Hexane, 40 mL Ether, and 1.5 mL Acetic Acid. Store at room temperature.
3. TLC Plate: Silica-coated glass plates.
4. Iodine.
5. Cholesteryl Oleate. Add 1 mg cholesteryl oleate to 1 mL of chloroform. Store at -20°C .

2.4 Cholesterol Quantification

1. 5× Assay Buffer: 0.5 M Potassium Phosphate pH 7.4, 0.25 M NaCl, 25 mM Cholic Acid, 0.5% Triton X-100. Make 500 mL of 0.5 M anhydrous K_2HPO_4 (43.55 g) and 0.5 M anhydrous KH_2PO_4 (34.02 g). To 400 mL of the 0.5 M anhydrous KH_2PO_4 solution, gradually add the 0.5 M anhydrous K_2HPO_4 (43.55 g) until the pH reaches 7.4. Adjust with HCl if necessary. Store solution at 4 °C.
2. 1× Assay Buffer. Add 2.5 mL of 5× Assay Buffer to 10 mL of deionized water.
3. 20 mM Amplex Red Reagent. Add 200 μ L DMSO to 1 mg Amplex Red.
4. 200 U/mL Horseradish peroxidase. Dissolve HRP to 200 U/mL in 1× Assay Buffer. Store at -20 °C.
5. 200 U/mL Cholesterol oxidase. Dissolve cholesterol oxidase to 200 U/mL in 1× Assay Buffer. Store at -20 °C.
6. 200 U/mL Cholesterol Esterase. Dissolve cholesterol esterase to 200 U/mL in 1× Assay Buffer. Store at -20 °C.
7. Working Solution: 0.3 mM Amplex Red, 10 U HRP, 10 U Cholesterol Oxidase, 1 U Cholesterol Esterase, 1× Reaction Buffer. Add 75 μ L Amplex Red Reagent, 50 μ L horse radish peroxidase, 50 μ L Cholesterol Oxidase and 5 μ L Cholesterol Esterase to 4.82 mL 1× Assay Buffer (*see Note 1*).

3 Methods

Carry out all procedures under a ventilated hood unless specified.

3.1 Lipid Extraction

1. Differentiate normal human podocytes (approximately 2×10^5 cells per 10 cm dish) for 14 days at 37 °C (*see Note 2*).
2. Rinse cells with 1× PBS and remove all liquid (*see Note 3*).
3. Add 5 mL of extraction solution to each dish and incubate for 30 min at room temperature.
4. Collect the extraction solution from the plate and transfer to a glass test tube.
5. Repeat **steps 3** and **4**.
6. Allow plates to dry for 5 min at room temperature (*see Note 4*).

3.2 Protein Assay

1. Add lysis buffer to the plate and detach the cells using a cell scraper. Transfer the cell lysate to an Eppendorf tube.
2. Samples were centrifuged at $21,000 \times g$ for 20 min.
3. Transfer supernatants to a new eppendorf tube.
4. Determine protein concentration for each supernatant using standard BCA protein quantification (*see Note 5*).

3.3 Isolation of Esterified Cholesterol

1. Place samples from Subheading 3.1, step 5 in 37 °C water bath and simultaneously dry lipids under a nitrogen (N₂) gas stream (*see Note 6*).
2. Dissolve lipids in 150 μL of chloroform in a glass test tube.
3. Centrifuge samples at 3000 × *g* for 5 min at room temperature.
4. Spot the entire sample and reference sample (cholesterol oleate) onto TLC plates (*see Note 7*).
5. Develop the TLC plate in Hexane:Ether:Acetic Acid (130:40:1.5) in TLC Chamber (*see Fig. 1*) until solvent reaches approximately $\frac{3}{4}$ up plate (*see Note 8*).
6. Remove the TLC plate from the chamber and allow solvents to evaporate at room temperature.
7. Place open Iodine bottle and TLC plate into clean TLC chamber until yellow spots are visible (*see Note 9*).
8. Mark the spots gently using a pencil.
9. Leave plate in a ventilated hood until the yellow color has dissipated.
10. Scrape silica-containing spots off the plates using a razor blade and transfer into glass test tubes.
11. Add 1 mL of chloroform to each test tube and incubate at room temperature for 5 min.
12. Centrifuge samples at 3000 × *g* for 3 min at room temperature.
13. Pipette supernatant to new test tube and repeat steps 11–13 (*see Note 8*).
14. Place samples in 37 °C water bath and simultaneously dry lipids under nitrogen (N₂) gas stream (*see Note 10*).

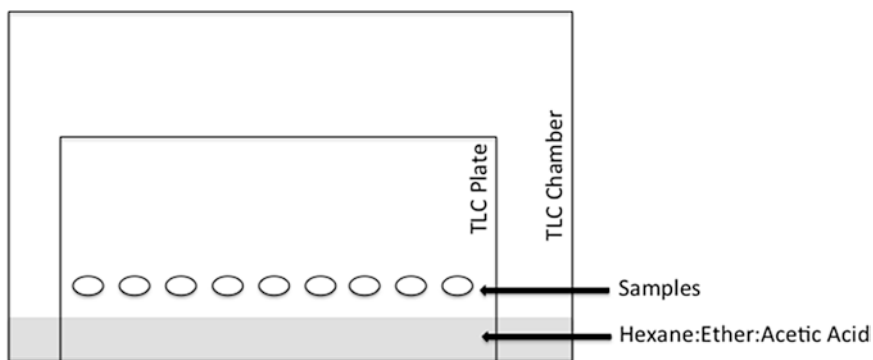


Fig. 1 Cholesterol ester isolation. The TLC chamber is pre-equilibrated chamber with TLC solvent. The TLC plate is placed into the chamber, with the samples above the solvent. Allow the solvent to travel up the plate until approximately $\frac{3}{4}$ to the top at room temperature

3.4 Measurement of Esterified Cholesterol Mass

1. Prepare a standard curve in 1× Assay Buffer with standards ranging from 8 to 0.06 µg/mL.
2. Dilute esterified cholesterol samples in 100 µL of 1× Assay Buffer.
3. Add 50 µL of sample or standard to each well.
4. Add 50 µL of working solution per well.
5. Incubate at 37 °C for 30 min.
6. Measure fluorescence on plate reader, Excitation 530–560 nm and Emission 590 nm.
7. Perform analysis utilizing standard protocol for the determination of analytes by standard curve.

4 Notes

1. The Amplex Red Cholesterol Assay Kit (Invitrogen) can be used as it contains all elements necessary for quantification.
2. At least 10 cm² area dish of differentiated normal human podocytes is necessary for measuring esterified cholesterol content.
3. If long-term storage of samples is required, the cell-containing plates can be stored at –80 °C.
4. If long-term storage of samples is required before proceeding to protein extraction, the cell-containing plates can be stored at –80 °C.
5. Our experience shows no matrix interference using the Pierce BCA protein assay kit.
6. A water bath is not absolutely necessary in this step but will significantly shorten the drying process.
7. Use of an AIS Analytical Instrument Specialties 4A TLC Multi-Spotter will allow for higher sample throughput.
8. The Hexane:Ether:Acetic Acid solvent solution should be added to the TLC chamber prior to the addition of the TLC plate. If necessary, line the inside of the TLC Chamber with filter paper to ensure proper equilibration of solvent solution. Additionally, upon addition of the TLC plate into the TLC chamber, make sure the Hexane:Ether:Acetic Acid fills the bottom of the chamber, but does not directly touch the samples.
9. Pre-equilibration of the TLC chamber with Iodine can reduce the visualization time to less than 5 min.
10. If long-term storage of the samples is necessary before proceeding to the quantification, samples can be stored at –20°C.

Acknowledgments

This work was supported by the NIH and NIDDK (grant numbers DK090316, DK104753) and by Grant Number 1UL1TR000460, University of Miami Clinical and Translational Science Institute, from the National Center for Advancing Translational Sciences and the National Institute on Minority Health and Health Disparities.

References

1. Mendez AJ (1997) Cholesterol efflux mediated by apolipoproteins is an active cellular process distinct from efflux mediated by passive diffusion. *J Lipid Res* 38(9):1807–1821
2. Liebisch G, Binder M, Schifferer R, Langmann T, Schulz B, Schmitz G (2006) High throughput quantification of cholesterol and cholesteryl ester by electrospray ionization tandem mass spectrometry (ESI-MS/MS). *Biochim Biophys Acta* 1761(1):121–128. doi:10.1016/j.bbali.2005.12.007
3. Amundson DM, Zhou M (1999) Fluorometric method for the enzymatic determination of cholesterol. *J Biochem Biophys Methods* 38(1):43–52
4. De Hoff JL, Davidson LM, Kritchevsky D (1978) An enzymatic assay for determining free and total cholesterol in tissue. *Clin Chem* 24(3):433–435
5. Smith RM, Marble A (1937) The colorimetric determination of free and combined cholesterol. *J Biol Chem* 117:673–684
6. DeBarber AE, Lutjohann D, Merckens L, Steiner RD (2008) Liquid chromatography-tandem mass spectrometry determination of plasma 24S-hydroxycholesterol with chromatographic separation of 25-hydroxycholesterol. *Anal Biochem* 381(1):151–153. doi:10.1016/j.ab.2008.05.037
7. Zak B (1977) Cholesterol methodologies: a review. *Clin Chem* 23(7):1201–1214
8. Li L, Han J, Wang Z, Liu J, Wei J, Xiong S, Zhao Z (2014) Mass spectrometry methodology in lipid analysis. *Int J Mol Sci* 15(6):10492–10507. doi:10.3390/ijms150610492

High-Performance Chromatographic Separation of Cerebrosides

Renaud Sicard and Ralf Landgraf

Abstract

High-performance thin-layer chromatography (HPTLC) is a very robust, fast, and inexpensive technique that enables separation of complex mixtures. Here, we describe the analytical separation of glucosylceramide and galactosylceramide by HPTLC. This technique can be used for quantitation purposes but also with small modification for subsequent mass spectrum analyses for structural determination.

Key words High-performance thin-layer chromatography, Cerebrosides, Galactosylceramide, Glucosylceramide, Orcinol reagent

1 Introduction

Thin-layer chromatography (TLC), despite being one of the oldest methods in the analytical chemistry field, remains widely used for routine separation and identification of individual lipids such as cerebrosides [1]. Convenience, low-cost reagents, and equipment in comparison to HPLC, robustness of the method, and the emergence of high-performance TLC (HPTLC) are some of the reasons for its durability. HPTLC plates deliver higher efficiency in the separation of compounds due to the smaller particle size and thinner layers. Although HPTLC does not allow exact structural analysis of cerebrosides (degree of saturation, length of carbon chain, etc.), orcinol reagent reactivity with glycolipids and comparison of chromatographic mobility with standards allows their quantitation. More recently, coupling of HPTLC with mass spectrometry using desorption techniques, such as desorption electrospray ionization (DESI) and matrix-assisted laser desorption/ionization (MALDI), has been implemented allowing combining ease of use and convenience of the HPTLC method and the resolving power of mass spectrometry for structural

Table 1

Overview of the detection limits, applications, and scales of processing of the main techniques for cerebroside analysis

Techniques	Detection range	Level of identification	Scale of processing
High-performance thin-layer chromatography (HPTLC)	Staining and Immunostaining: nanomoles	Hexose identification	Microliters of plasma; several millions of cells.
High-performance liquid chromatography (HPLC) coupled to MS	femtomoles	Structure analysis	Microliters of plasma; several thousands of cells.
Gas chromatography (GC)/GC/MS	femtomoles	Fatty acyl compositions	Microliters of plasma; several hundred of thousands of cells.
Soft ionization mass spectrometry	femtomoles	Structure analysis	Microliters of plasma; thousand of cells.
$^1\text{H}/^{13}\text{C}$ NMR	micromoles	Structure analysis	Microliters of plasma; several millions of cells .

characterization [2, 3]. Depending on the analysis and the rarity of the sample, other techniques may be more appropriate but usually require expansive instrumentation (Table 1).

The objective of this chapter is to provide beginners in the TLC field with an easy-to-follow protocol that generates reproducible and high-quality data for cerebroside separation and analysis (Figs. 1 and 2). Isolation and purification techniques will not be covered in this chapter due to the diversity of sources and protocols. It usually involves lipid extraction using a mixture of chloroform and methanol (2:1 for the Folch method [6] or 1:1 for Bligh and Dyer method [7]) and subsequent chromatographic steps to extract and purify cerebroside. For more general information on lipid purification techniques, the reader is encouraged to consult *Isolation of Glycosphingolipids* by R. Schnaar [8] and *Lipid Analysis-Isolation, Separation, Identification and Lipidomic Analysis* by W. Christie and X. Han [9].

2 Materials

All solvents used should be at least of reagent grade, preferably analytical grade. Milli-Q water is used for aqueous solutions. All solvent mixtures can be prepared at room temperatures and be stored as mentioned. All operations must be done under a chemical hood to avoid exposure to solvent fumes.

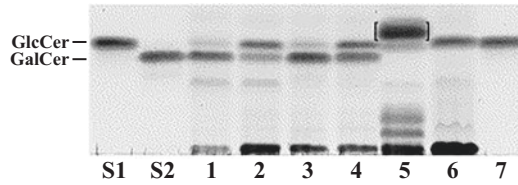


Fig. 1 Comparison of GlcCer and GalCer expression in *A. fumigatus* and *A. nidulans* showing temperature dependence. Lower section of orcinol-stained analytical HPTLC plate compares crude neutral lipids extracted from *A. fumigatus* strains 9197 (lanes 1 and 2) and 237 (lanes 3 and 4), and *A. nidulans* strain A28 (lanes 5 and 6). Mycelia were cultured at 30 °C (lanes 1, 3, and 5) or 37 °C (lanes 2, 4, and 6). Lanes S1 and S2, standards of GlcCer and GalCer from *A. fumigatus* strain 9197 previously characterized by NMR and ⁺ESI-MS. Bracketed band appearing in *A. nidulans* strain A28 only at 30 °C (lane 3) is sterol glucoside. Lane 7, putative GlcCer purified from *A. nidulans*, 37 °C culture (reprinted from [4] with permission from Elsevier)

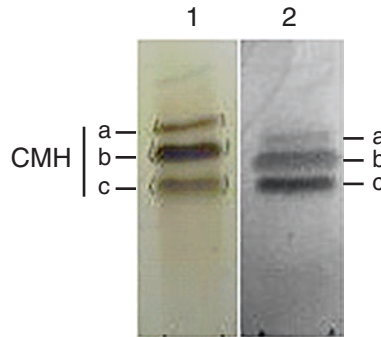


Fig. 2 HPTLC of *S. apiospermum* ceramide monohexosides (CMH) (spots a,b,c), which was developed in CHCl_3 : MeOH: 2 M NH_4OH (40:10:1 v/v). Lane 1: stained with orcinol/ H_2SO_4 ; lane 2: immunostaining with the anti-CMH MAb (reprinted from [5] with permission from PLOS One)

2.1 Special Equipment

1. HPTLC plates: Precoated Silica gel 60 Glass-Backed HPTLC Plates (EMD Millipore, Darmstadt, Germany) are often used for sphingolipid resolution but other brands such as Macherey-Nagel (Düren, Germany) are good alternatives (*see Note 1*).
2. TLC developing tank with lid: any rectangular glass chambers can be used.
3. Fine mist sprayer.
4. Glass capillaries or gel-loading tips.
5. Handheld hair-dryer with cold air option.
6. Heating plate or oven.
7. TLC spray box.

2.2 HPTLC

1. Developing Solvent: chloroform:methanol:2 M ammonium hydroxide solution in a 50:10:1 volume ratio. Prepare 100 mL of a 2 M ammonium hydroxide solution by adding 13.5 mL of a 28–30% ammonium hydroxide solution to 86.5 mL of water in a glass beaker with magnetic stirring. In a glass bottle, mix 100 mL of chloroform, 20 mL of methanol, and 2 mL of the prepared 2 M ammonium hydroxide solution. Mix well to ensure that reagents form one phase and close the bottle until use (*see Note 2*).
2. Orcinol Reagent: dissolve 0.2 g of orcinol in 100 mL of a 2 M solution of sulfuric acid H_2SO_4 which can be prepared by adding carefully and slowly 11.1 mL of concentrated H_2SO_4 to distilled water under magnetic stirring to a final volume of 100 mL (*see Note 3*).
3. Glucosylceramides and galactosylceramides can be purchased, e.g., from Matreya LLC (State College, PA, USA).

3 Methods

All procedures should be carried out at room temperature unless otherwise specified.

3.1 HPTLC Development Tank Setup

1. Add freshly prepared Developing Solvent to the bottom of the tank to a depth of about 1 cm (usually 30–50 mL).
2. Close the tank using the fitted glass lid and allow the solvent system to equilibrate for at least 1 h (*see Note 4*).

3.2 HPTLC Setup

1. Always handle HPTLC plates with gloves to avoid any contamination that could interfere with TLC staining.
2. HPTLC plates should be kept in a dry environment, if it is not the case the plates can be placed in an oven for about 10 min at 60–70 °C.
3. Use a soft pencil to indicate the sample position on the HPTLC. Samples and standards should be located at 1.5–2 cm above the bottom of the plate and at least 2 cm from each side to avoid any edge effects. Samples and standards (0.5–1 cm) should also be separated 1 cm from each other.
4. To improve repeatability between separate plates, a line is drawn at 1–1.5 cm from the top of the HPTLC plates and will be used to remove the plate when the solvent front reaches this line (Fig. 3).

3.3 Sample Loading

1. If using dried samples, resuspend them in chloroform:methanol solution in 2:1 volume ratio.

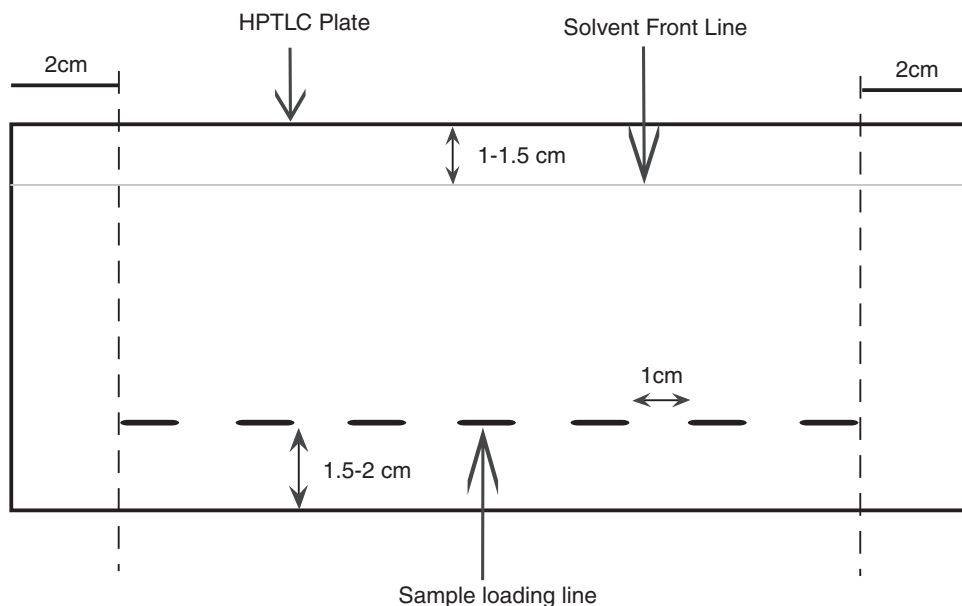


Fig. 3 Representation of HPTLC setup. Samples and standards should be located at 1.5–2 cm above the bottom of the plate and at least 2 cm from each side of the plate. An interval of 1 cm between samples should be respected. The solvent front line allows reproducibility between each experiment

2. Load your standards and samples using microcapillaries or fine gel-loading tips. Between each application evaporate the solvent using hair-dryer (*see Note 5*). Load samples evenly along the marked line drawn to improve reproducibility. Depending on the concentration of the sample a volume between 10 and 50 μL can be deposited.

3.4 Chromatogram Development

1. After removing the lid, carefully place the plate into the developing chamber (*see Note 6*). The solvent (or mobile phase) is drawn through the plate by capillary action and hence should start uniformly to avoid differences in running behavior between samples.
2. Remove the plate once the solvent front reaches the upper line of the HPTLC.
3. Dry the HPTLC plate using the hair dryer using cold air.

3.5 Visualization and Quantitative Determination

1. Place the HPTLC plate upright in a TLC spray box under a chemical hood.
2. Apply Orcinol Reagent (*see Note 7*) using the fine mist sprayer in a zigzag pattern from one edge to another until the whole surface is covered (*see Note 8*).
3. Carefully remove the HPTLC from the spray box and place it on the heat plate or the oven at 150 $^{\circ}\text{C}$ for about 10 min.
4. Scan the HPTLC plate for further quantitation and analysis (*see Note 9*).

4 Notes

1. To assure good reproducibility between experiments, plates should come from the same manufacturer.
2. Different solvent systems can be found in the literature for cerebroside analysis [5, 10–12]. However, a mixture of chloroform, methanol, and ammonium hydroxide is the most widely used solvent mixture.
3. Do not add water to concentrated H_2SO_4 , the reaction is extremely exothermic and may cause explosion. The use of a cold water bath is recommended.
4. The use of solvent-saturated filter paper to cover the inner walls of the TLC tank can facilitate a faster equilibration of the vapor phase.
5. It is very important to load samples slowly and dry the solvent completely between applications using cold air.
6. Use of long tweezers on each upper side of the plate is recommended, especially when using tall TLC tanks.
7. Depending on the intended application, other spray reagents can be used. For example, use of a reversible staining spray made of 0.01% primuline in acetone:water solution (80:20 volume ratio) allows visualization of lipids under UV light. This approach allows scraping and lipid extraction for further analysis such as mass spectrometry [13]. Spray visualization can also be replaced by iodine vapors that will stain all lipids. Immunostaining can be used to confirm the identity of specific cerebroside [14].
8. Staining spray can be dispensed using the air stream available in a chemical hood. The flow should be low enough to obtain a fine mist.
9. For most visualization purposes, a regular image scanner will suffice. However, specific TLC plate readers or TLC visualizer are best suited for precise quantitation purposes.

References

1. Fuchs B, Suss R, Teuber K, Eibisch M, Schiller J (2011) Lipid analysis by thin-layer chromatography--a review of the current state. *J Chromatogr A* 1218(19):2754–2774. doi:10.1016/j.chroma.2010.11.066
2. Meisen I, Mormann M, Muthing J (2011) Thin-layer chromatography, overlay technique and mass spectrometry: a versatile triad advancing glycosphingolipidomics. *Biochim Biophys Acta* 1811(11):875–896
3. Nakamura K, Suzuki Y, Goto-Inoue N, Yoshida-Noro C, Suzuki A (2006) Structural characterization of neutral glycosphingolipids by thin-layer chromatography coupled to matrix-assisted laser desorption/ionization quadrupole ion trap time-of-flight MS/MS. *Anal Chem* 78(16):5736–5743. doi:10.1021/ac0605501
4. Levery SB, Momany M, Lindsey R, Toledo MS, Shayman JA, Fuller M, Brooks K, Doong RL, Straus AH, Takahashi HK (2002)

- Disruption of the glucosylceramide biosynthetic pathway in *Aspergillus nidulans* and *Aspergillus fumigatus* by inhibitors of UDP-Glc:ceramide glucosyltransferase strongly affects spore germination, cell cycle, and hyphal growth. *FEBS Lett* 525(1-3):59–64
5. Rollin-Pinheiro R, Liporagi-Lopes LC, de Meirelles JV, LMd S, Barreto-Bergter E (2014) Characterization of *Scedosporium apiospermum* glucosylceramides and their involvement in fungal development and macrophage functions. *PLoS One* 9(5):e98149
 6. Folch J, Lees M, Sloane Stanley GH (1957) A simple method for the isolation and purification of total lipides from animal tissues. *J Biol Chem* 226(1):497–509
 7. Bligh EG, Dyer WJ (1959) A rapid method of total lipid extraction and purification. *Can J Biochem Physiol* 37(8):911–917
 8. Schnaar RL (1994) Isolation of glycosphingolipids. *Methods Enzymol* 230:348–370
 9. CWH X (2010) Lipid analysis-isolation, separation, identification and lipidomic analysis. Oily Press, Bridgwater, UK
 10. Fewou SN, Bussow H, Schaeren-Wiemers N, Vanier MT, Macklin WB, Gieselmann V, Eckhardt M (2005) Reversal of non-hydroxy:alpha-hydroxy galactosylceramide ratio and unstable myelin in transgenic mice overexpressing UDP-galactose:ceramide galactosyltransferase. *J Neurochem* 94(2):469–481
 11. Pinto MR, Rodrigues ML, Travassos LR, Haido RMT, Wait R, Barreto-Bergter E (2002) Characterization of glucosylceramides in *Pseudallescheria boydii* and their involvement in fungal differentiation. *Glycobiology* 12(4):251–260
 12. Sakaki T, Zahringer U, Warnecke DC, Fahl A, Knogge W, Heinz E (2001) Sterol glycosides and cerebrosides accumulate in *Pichia Pastoris*, *Rhynchosporium secalis* and other fungi under normal conditions or under heat shock and ethanol stress. *Yeast* 18(8):679–695. doi:[10.1002/yea.720](https://doi.org/10.1002/yea.720)
 13. Saito K, Maekawa K, Ishikawa M, Senoo Y, Urata M, Murayama M, Nakatsu N, Yamada H, Saito Y (2014) Glucosylceramide and lysophosphatidylcholines as potential blood biomarkers for drug-induced hepatic phospholipidosis. *Toxicol Sci* 141(2):377–386. doi:[10.1093/toxsci/kfu132](https://doi.org/10.1093/toxsci/kfu132)
 14. Brade L, Vielhaber G, Heinz E, Brade H (2000) In vitro characterization of anti-glucosylceramide rabbit antisera. *Glycobiology* 10(6):629–636

Lipid Identification by Untargeted Tandem Mass Spectrometry Coupled with Ultra-High-Pressure Liquid Chromatography

Gabriel B. Gugiu

Abstract

Lipidomics refers to the large-scale study of lipids in biological systems (Wenk, *Nat Rev Drug Discov* 4(7):594–610, 2005; Rolim et al., *Gene* 554(2):131–139, 2015). From a mass spectrometric point of view, by lipidomics we understand targeted or untargeted mass spectrometric analysis of lipids using either liquid chromatography (LC) (Castro-Perez et al., *J Proteome Res* 9(5):2377–2389, 2010) or shotgun (Han and Gross, *Mass Spectrom Rev* 24(3):367–412, 2005) approaches coupled with tandem mass spectrometry. This chapter describes the former methodology, which is becoming rapidly the preferred method for lipid identification owing to similarities with established *omics* workflows, such as proteomics (Washburn et al., *Nat Biotechnol* 19(3):242–247, 2001) or genomics (Yadav, *J Biomol Tech: JBT* 18(5):277, 2007). The workflow described consists in lipid extraction using a modified Bligh and Dyer method (Bligh and Dyer, *Can J Biochem Physiol* 37(8):911–917, 1959), ultra high pressure liquid chromatography fractionation of lipid samples on a reverse phase C18 column, followed by tandem mass spectrometric analysis and in silico database search for lipid identification based on MSMS spectrum matching (Kind et al., *Nat Methods* 10(8):755–758, 2013; Yamada et al., *J Chromatogr A* 1292:211–218, 2013; Taguchi and Ishikawa, *J Chromatogr A* 1217(25):4229–4239, 2010; Peake et al., *Thermoscientifics* 1–3, 2015) and accurate mass of parent ion (Sud et al., *Nucleic Acids Res* 35(database issue):D527–D532, 2007; Wishart et al., *Nucleic Acids Res* 35(database):D521–D526, 2007).

Key words Lipids, Lipidomics, Lipid extraction, LCMS, UHPLC, Tandem mass spectrometry, Lipid identification, MS/MS, MS²

1 Introduction

Lipidomics [1, 2] is a relatively new field, which developed later than proteomics along with new mass spectrometric techniques and technologies allowing the investigation of structural and biological diversity of lipids [3].

The main relational database of lipids containing the structure and annotation of biologically relevant lipids is Lipid Maps structural database (LMSD) [4] from the lipid maps project. The human

metabolome database (HMDB) also contains many lipid structures and annotations [5]. From the point of view of polarity lipids can be classified into nonpolar lipids (such as triacylglycerol, cholesterol, cholesteryl esters, etc.) and polar lipids (phospholipids, sphingolipids, glycolipids). Based on their chemical structure, lipids are divided in classes with precise nomenclature [6, 7]. Most of these are abundant lipids while others are lipid metabolites (lipids produced by action of enzymes in biological systems, DG, MG, FA, S1P, etc.) [8]. Untargeted lipidomics aims to comprehensively measure lipids in a sample encompassing all the above-mentioned classes of lipids by omic workflows similar to proteomics [9] and genomics [10]. For certain lipids, such as lipid metabolites specific, targeted methods are normally used due to their low abundance [8, 11].

2 Materials

Optima grade LCMS solvents chloroform, methanol, water. Deionized water with a conductivity of 18 M Ω -cm at 25 °C can be used instead of optima grade LCMS. To prevent lipid oxidation during sample processing a metal ion chelator and a radical oxidation inhibitor will be added to the extraction solvent: 2 mM ethylenediaminetetraacetic acid (EDTA) and 100 μ M butylated hydroxytoluene (Sigma-Aldrich). A Kinetex 1.7 μ m 100 Å , 100 \times 2.1 mm UHPLC column (Phenomenex, Torrance, CA, USA), Thermo-Dionex Ultimate 3000 UHPLC, Thermo Orbitrap Fusion Tribrid mass spectrometer (Thermo, West Palm beach, FL, USA), nitrogen gas evaporator (Organomation, Catalog #11250). Phosphate buffer saline or Tris buffer saline can be purchased from Sigma-Aldrich.

3 Methods

3.1 Lipid Extraction

Various methods for lipid extraction were described in the literature from Folch extraction [12] and Bligh and Dyer [13] to MTBE [14]. Here, a modified Bligh and Dyer method is described. In order to prevent unsaturated lipid oxidation during sample handling in the air, a cocktail of inhibitors is usually added prior to lipid extraction. Such inhibitors include chelators like ethylene-diaminetetraacetic acid (EDTA, 2 mM final concentration) and butylated hydroxytoluene (BHT, 100 μ M final concentration) [11]. To prevent unwanted lipase activity tissue samples should be flash frozen in liquid nitrogen and minimally handled before lipid extraction (i.e., weighing). Cell pellets frozen or fresh can be directly extracted to avoid further alteration of lipid composition and the dry lipid samples can be kept at -80 °C under argon until analysis (*see Note 1*).

To a lipid sample, for example, 100 mg flash frozen tissue homogenate or 1×10^7 cells suspended in 500 μ L of 10 mM phosphate

buffer saline (PBS), Tris buffer saline (TBS), or other aqueous buffer containing appropriate oxidation inhibitors (as described above), an equal volume of methanol is added and the mixture is vortexed for a minute and then extracted with chloroform (typically a volume equal to that of buffer plus methanol). The extraction is repeated three times. No plastic containers/vials can be used with chloroform since plasticizers from the material can leach out and contaminate the lipid samples, HPLC column, and mass spectrometer; only glass tubes or vials and preferably a Hamilton syringe or glass pipette should be used. After each extraction (1 min vortexing) a centrifugation at 4 °C for 10 min at 3500 RCF may be required to separate the organic and aqueous phases. The lower chloroform phases are collected, combined, and evaporated to dryness, typically using a nitrogen gas evaporator. When samples are dry the nitrogen can be switched to argon, which is heavier than air. That insures the samples are sealed under a blanket of argon and then can be stored at −80 °C until analysis. Parafilm can be used to seal the vials. This extraction procedure can be applied to cells in suspension, cell pellets, or homogenized tissue.

3.2 Chromatographic Separation of Lipids: HPLC Method

Owing to their great structural diversity lipids have varied chemical properties and polarities and a single system for lipid separation is challenging [1]. An example of a chromatographic separation method involves either HPLC or UHPLC on a reverse phase C18 column using as buffer system; A—10 mM ammonium acetate or formate solution in 40% acetonitrile in water and as buffer B—10 mM ammonium acetate or formate solution in 10% acetonitrile in isopropanol [15]. A typical 27 min separation method, which achieves lipid class separation and some species separation, is provided in Table 1 [15]. Example base peak chromatograms collected in either positive- or negative-ion modes are given in Figs. 1 and 2 and identification information is shown in Figs. 3 and 4 respectively (*see Note 2*).

3.3 Instrument Acquisition Method for Lipid Analysis

A variety of instrumentation can be used for mass spectrometric detection of lipids. However, typically a tandem mass spectrometer

Table 1
Example gradient for chromatographic separation of lipid mixtures on a reverse phase C18 column

Time (min)	Buffer A (%)	Buffer B (%)
0	60	40
1	60	40
16	0	100
20	0	100
22	60	40
27	60	40

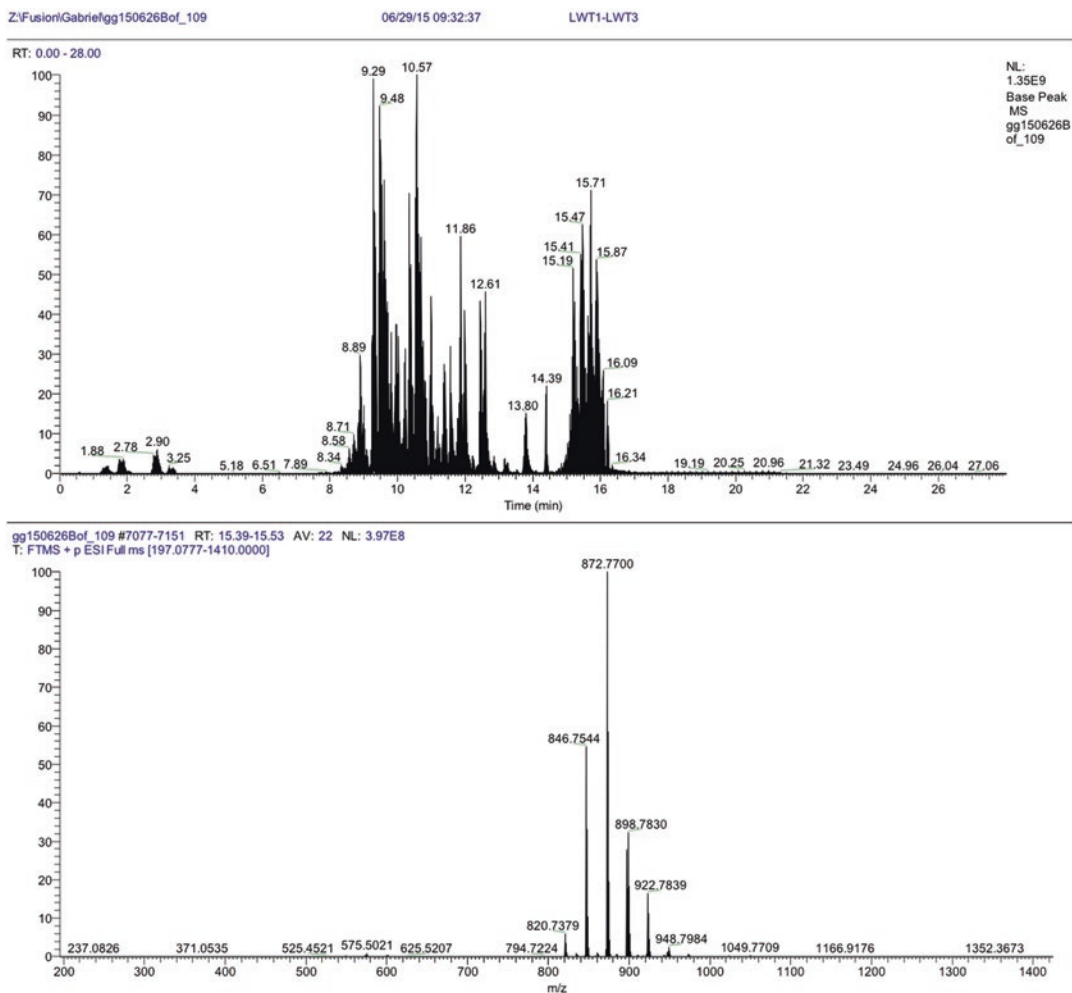


Fig. 1 Example Base peak chromatograms acquired on Thermo Orbitrap Fusion Tribrid of a mouse liver lipid mixture in positive ion mode (upper). Mass spectrum of peak eluted at 15.47 min showing lipid ion with m/z 872.7700 (lower). Lipid Search identification information for this peak is shown in Fig. 3

is used which can acquire full MS, fragment the most intense lipid ions, and acquire fragment ion information on the measured lipids. The most popular instruments for lipid analysis are Orbitraps (Q-Exactive, Orbitrap Fusion) and Q-TOFs (Agilent, Waters, Sciex, Bruker, etc.). A triple quadrupole instrument is usually used for targeted analyses of specific lipids [11, 16].

Herein, the acquisition method on a Thermo Orbitrap Fusion will be described in detail (*see Note 3*).

Examples of base peak chromatograms of a lipid mixture extracted from mouse liver and analyzed on a Thermo Orbitrap Fusion mass spectrometer fitted with a Dionex Ultimate 3000 UHPLC system in positive- and negative-ion mode are shown in Figs. 1 and 2. The acquisition method for a data-dependent analysis (DDA) workflow is shown in Table 2.

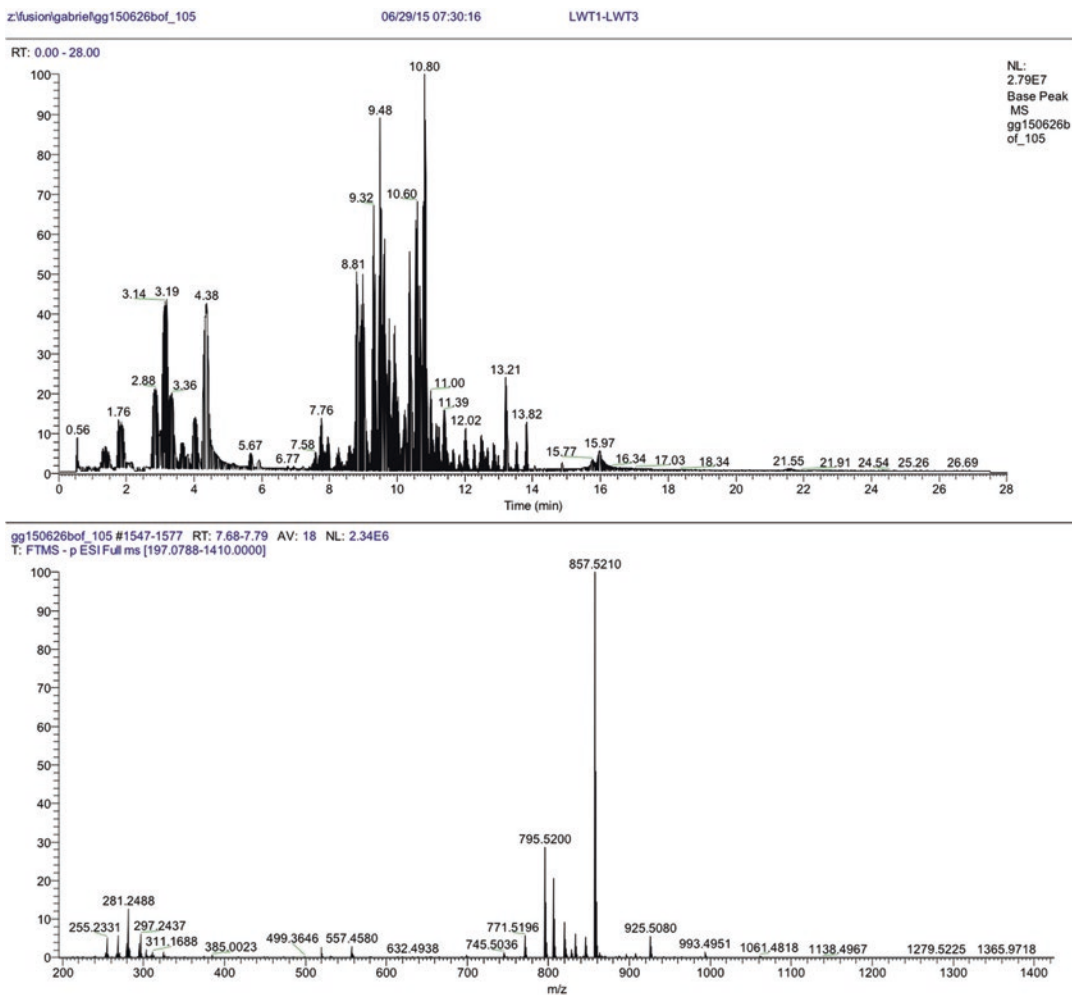


Fig. 2 Example Base peak chromatograms acquired on Thermo Orbitrap Fusion Tribrid mass spectrometer of a mouse liver lipid mixture in negative ion mode (upper). Mass spectrum of peak eluted at 7.76 min showing lipid ion with m/z 857.5210 (lower). Lipid Search identification information for this peak is shown in Fig. 4

3.4 Data Analysis

Several software packages are available for the analysis of mass spectrometric data for lipid identification and quantitation such as Lipid Search (Thermo Fisher) [17–19], Lipidblast [20], Simlipid (Premier Biosoft) [21]. Matching the MS/MS experimental data with spectra from various databases provides the identification. Historically, this used to be done based on accurate mass search due to lack of MS/MS databases. Currently, MS/MS matching against an experimental [4, 5] or in silico [17, 20, 22] database is the preferred identification method used in combination with parent ion accurate mass.

An example of data analysis parameters for Thermo Lipid Search 4.1 is given in Tables 3–9. In Tables 5–8 where multiple options are possible the parameters used are in bold letters (*see* Note 4).

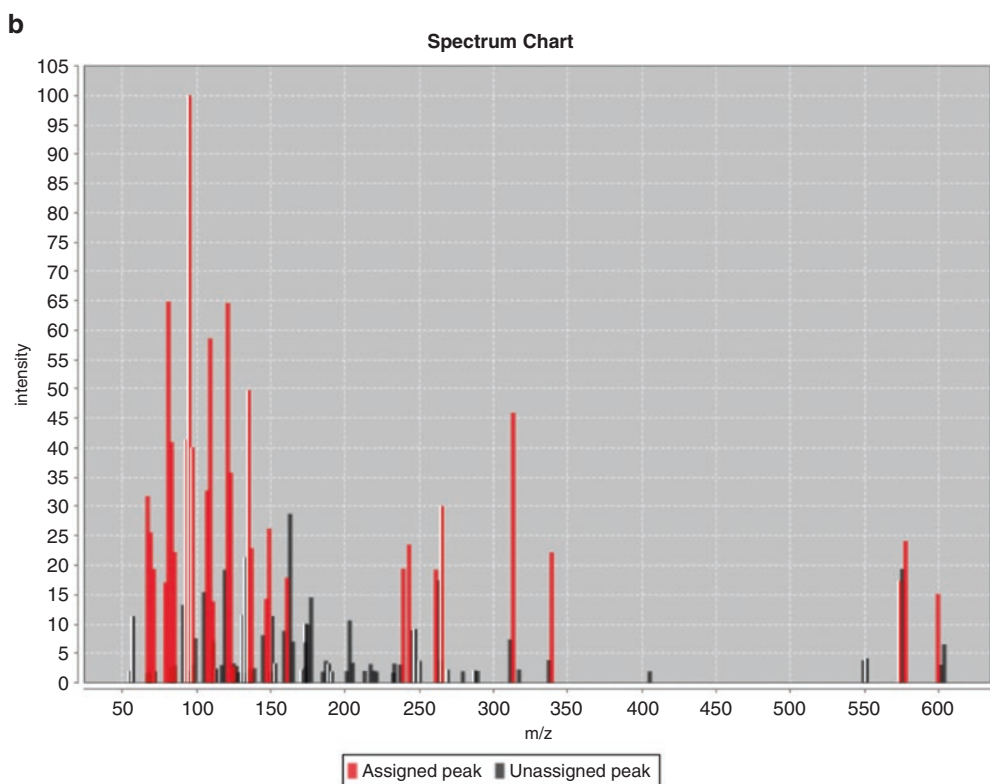
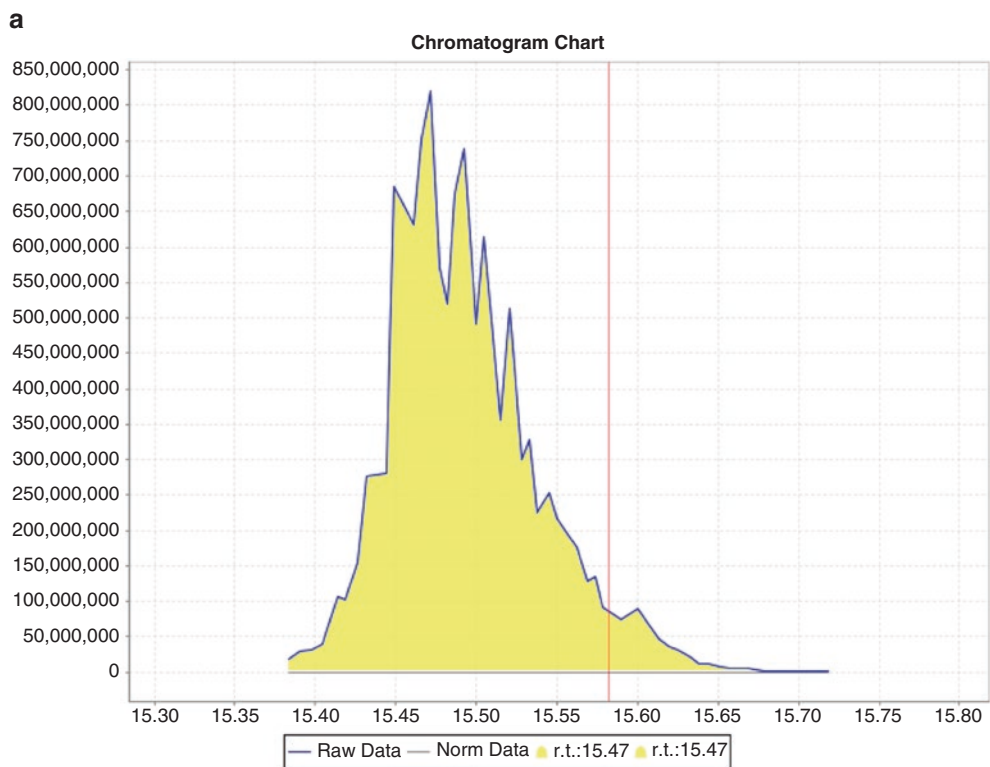


Fig. 3 Thermo Lipid Search identification of lipid ion with m/z 872.7699 (Fig. 1, lower). (a) Extracted ion chromatogram; (b) MS^2 spectrum with matched fragment ions

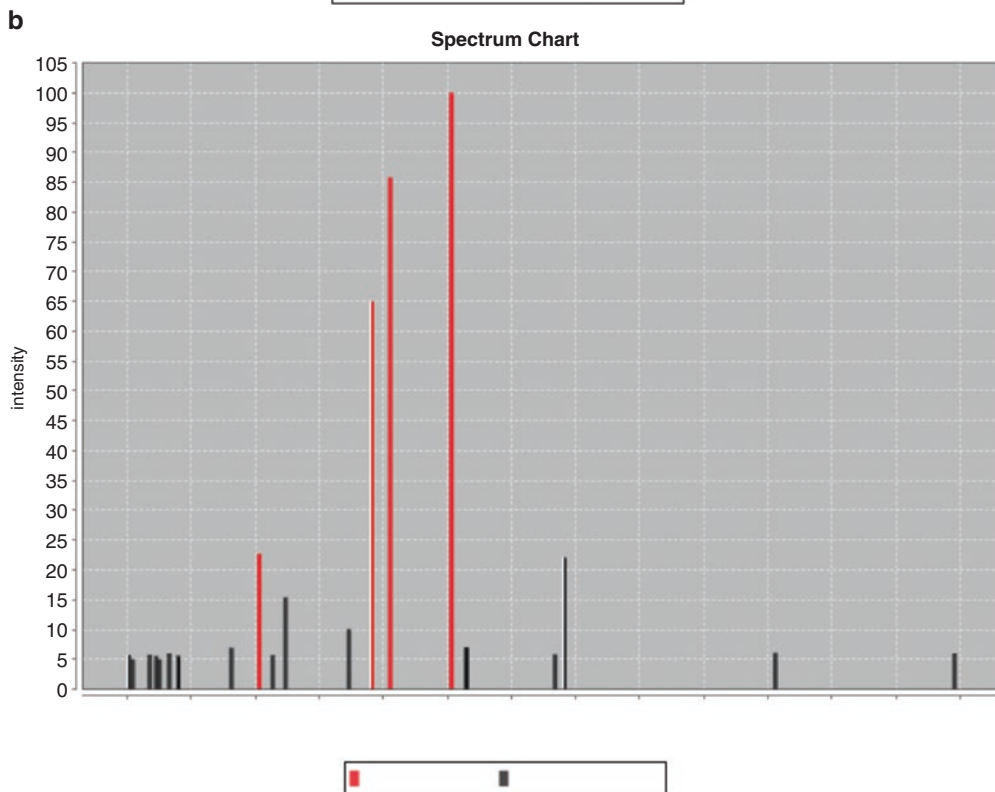
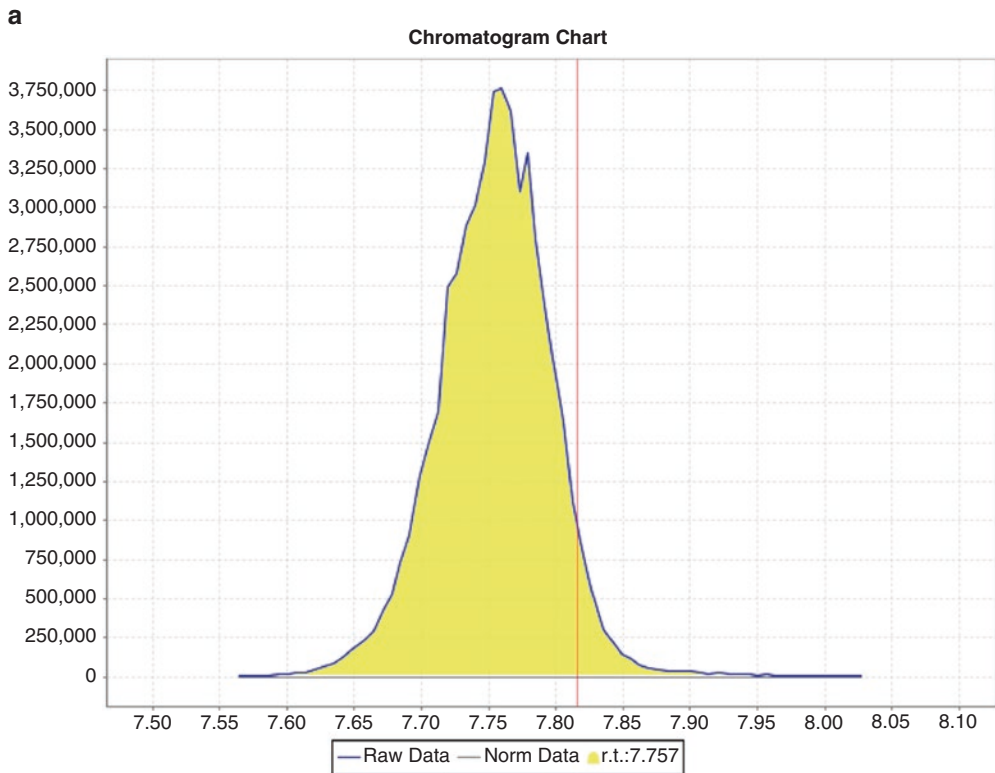


Fig. 4 Thermo Lipid Search identification of lipid ion with m/z 857.5210 (Fig. 2, lower). (a) Extracted ion chromatogram; (b) MS^2 spectrum with matched fragment ions

Table 2
Acquisition method for data-dependent analysis (DDA) on the Thermo Orbitrap Fusion for lipid analysis in positive-ion mode

Method duration	28 min
Ion Source type	HESI
Spray voltage	Static
Positive ion (V)	3500
Negative ion (V)	2500
Sheath gas (Arb)	50
Aux Gas (Arb)	25
Sweep Gas (Arb)	3
Ion Transfer Tube Temp (°C)	325
Vaporizer temp (°C)	320
MS	
Pressure mode	Standard
Default charge state	1
Internal mass calibration	TRUE
Internal mass calibration	EASY-IC
Divert valve	
0 min	1–6
0.5 min	1–2
27.5 min	1–6
Experiment 1	
Start time (min)	0
End time (min)	28
Master scan	
MS OT	
Detector type	Orbitrap
orbitrap resolution	60,000
mass range	normal
use quadrupole isolation	TRUE
scan range (m/z)	210-1410
S-lens RF level (%)	60
AGC Target	2.00E+05
Max injection time (ms)	100

(continued)

Table 2
(continued)

Microscan	1
Data type	Profile
Polarity	Positive
Source fragmentation	Disabled
Use EASY-IC	TRUE
Filter	
MIPS	
Use MIPS	on
Dynamic exclusion	
Exclude after n times	1
Exclusion duration	6
Mass tolerance	ppm
Low	10
High	10
Perform dependent scan on single charge state per precursor	FALSE
Decision	
DDA	Top speed
Precursor priority	Most intense
No. of scan events	1
Scan event type 1	
Condition	Intensity greater than 1000
ddMS2 OT HCD	
MSn Level	2
Isolation mode	Quadrupole
Use isolation m/z offset	FALSE
Activation type	HCD
HCD collision energy (%)	30
Stepped collision energy	FALSE
Detector type	Orbitrap
Scan range mode	Auto m/z normal
Orbitrap resolution	15,000

(continued)

Table 2
(continued)

First mass m/z	75
AGC target	5.00E+04
Inject ions for all available parallelizable times	FALSE
Maximum injection time (ms)	35
Microscans	1
Data type	Profile
Use EASY-IC	TRUE

Table 3
Match detail for TG(16:0/18:1/18:3) from Lipid Search 4.1

ObsMz	Type	It. (%)	Frag.	Delta (Da)
67.0546	MS2	31.833	C ₅ H ₇	0.0003
69.0702	MS2	25.575	C ₅ H ₉	0.0003
71.0857	MS2	19.358	C ₅ H ₁₁	0.0002
79.0545	MS2	17.06	C ₆ H ₇	0.0003
81.0702	MS2	64.851	C ₆ H ₉	0.0003
83.0859	MS2	41.006	C ₆ H ₁₁	0.0004
85.1016	MS2	22.246	C ₆ H ₁₃	0.0005
93.0703	MS2	41.373	C ₇ H ₉	0.0005
95.086	MS2	100	C ₇ H ₁₁	0.0005
97.1017	MS2	40.084	C ₇ H ₁₃	0.0005
107.0859	MS2	32.748	C ₈ H ₁₁	0.0004
109.1017	MS2	58.582	C ₈ H ₁₃	0.0005
111.1172	MS2	13.818	C ₈ H ₁₅	0.0003
121.1016	MS2	64.659	C ₉ H ₁₃	0.0004
123.1173	MS2	35.808	C ₉ H ₁₅	0.0004
125.1331	MS2	2.742	C ₉ H ₁₇	0.0006
135.1174	MS2	49.767	C ₁₀ H ₁₅	0.0006
137.133	MS2	22.931	C ₁₀ H ₁₇	0.0005
147.117	MS2	14.303	C ₁₁ H ₁₅	0.0002
149.1328	MS2	26.261	C ₁₁ H ₁₇	0.0003

(continued)

Table 3
(continued)

ObsMz	Type	It. (%)	Frag.	Delta (Da)
161.1327	MS2	17.878	C ₁₂ H ₁₇	0.0003
239.2374	MS2	19.438	FA(16:0)-OH	0.0004
243.211	MS2	23.515	C ₁₈ H ₂₇	0.0003
261.2226	MS2	19.213	FA(18:3)-OH	0.0013
265.2533	MS2	30.098	FA(18:1)-OH	0.0008
313.275	MS2	45.927	MG(16:0)-OH	0.0013
339.2903	MS2	22.187	MG(18:1)-OH	0.0009
573.4883	MS2	17.33	NL[FA(18:1)- H+NH ₄]	0.0006
577.52	MS2	24.137	NL[FA(18:3)- H+NH ₄]	0.001
599.5074	MS2	15.117	NL[FA(16:0)- H+NH ₄]	0.004

Table 4
Match detail for PI(16:0/20:4) from Lipid Search 4.1

ObsMz	Type	It. (%)	Frag.	Delta (Da)
51.0978	MS2	5.695		
54.1288	MS2	5.042		
67.3232	MS2	5.785		
72.4691	MS2	5.571		
75.0886	MS2	5.024		
82.6744	MS2	5.988		
89.5469	MS2	5.29		
89.6753	MS2	5.638		
131.2233	MS2	6.969		
152.9967	MS2	22.715	GP-H ₃ O	0.0009
163.4947	MS2	5.702		
173.4847	MS2	15.43		
223.0038	MS2	10.089		
241.0125	MS2	64.953	PH(inositol)- H ₂ O-H	0.0006

(continued)

Table 4
(continued)

ObsMz	Type	It. (%)	Frag.	Delta (Da)
255.2344	MS2	85.784	FA(16:0)-H	0.0014
303.234	MS2	100	FA(20:4)-H	0.0011
314.9033	MS2	6.987		
315.0512	MS2	7.034		
383.8999	MS2	5.848		
391.2292	MS2	22.117		
555.9779	MS2	6.088		
695.7428	MS2	6.019		
Lipid Ion	M-Sc. T-Sc. St. Occ.			
PI(16:0/20:4)-H 26.7	0	66.7		

Table 5
Identification parameters in Thermo Lipid Search 4.1

Batch		
Job Name	<i>Test search</i>	
Comment	product ion 1%	
Search options		
Search Type	Product	
Exp Type	LC	
Precursor tolerance	5	ppm
Product tolerance	8	ppm
Merge Range (Min)	0	
Min Peak Width (Min)	0	
Intensity threshold	0.01	Parent ion
Threshold type	Relative absolute	
	1	Product ion
m-Score Threshold	3	
Database		
Target Database	General	Q Exactive
		Orbitrap

(continued)

Table 5
(continued)

	Oxid. GPL
	Labeled GPL, GL, SP, ChE
Peak detection	
Recalc Isotope	On off
R.T. interval(Min)	0
R.T. Range(Min)	—

Table 6
Quantitation parameters in Thermo Lipid Search 4.1. This is useful for determining the ratio between different sample categories such as normal and disease

Quantitation		
Execute Quantitation	On off	
Mz tolerance	-5	5
Tolerance Type	Da ppm	
Rt range (min.)	-1	1

Table 7
Display filter in Thermo Lipid Search 4.1

Display Filter	
Toprank filter	On off
Main node filter	Off Main isomer peak All isomer peaks
m-Score Threshold	3
c-Score Threshold	2
FA Priority	On off
ID Quality filter	A B C D

4 Notes

Potential problems with the method:

1. Very little lipid extract is obtained during the lipid extraction step (Subheading 3.1). Typically, you would need at least 1 million cells or a few mg of tissue samples to be able to successfully extract lipids for this analysis.

Table 8
Ions detected (depends on experimental conditions—polarity, solvent additives, pH)

Polarity	Name
Negative	-H
	+HCOO
	+CH ₃ COO
	+Cl
	-2H
Positive	+H
	+NH ₄
	+Na
	+Li
	+K
	CH ₃ (CH ₂) ₃ NH
	+2H

Table 9
Classes of lipids used for identification in Lipid Search 4.1

Group	classKey	Lipid Name
P-Choline	LPC	lysophosphatidylcholine
PAF	platelet-activating factor	
PC	phosphatidylcholine	
P-Ethanol Amine	LPE	lysophosphatidylethanolamine
LdMePE	lysodimethylphosphatidylethanolamine	
PE	phosphatidylethanolamine	
dMePE	dimethylphosphatidylethanolamine	
P-Serine	LPS	lysophosphatidylserine
PS	phosphatidylserine	
P-Glycerol	LPG	lysophosphatidylglycerol
PG	phosphatidylglycerol	
P-Inositol	LPI	lysophosphatidylinositol
PI	phosphatidylinositol	
PIP, PIP2, PIP3	phosphatidylinositol phosphates	

(continued)

Table 9
(continued)

Group	classKey	Lipid Name
P-Ethanol	LPEt	lysophosphatidylethanol
PEt	phosphatidylethanol	
P-Acid	LPA	lysophosphatidic acid
PA	phosphatidic acid	
cPA	cyclic phosphatidic acid	
P-Methanol	LPMe	lysophosphatidylmethanol
PMe	phosphatidylmethanol	
Sphingolipids	SM	sphingomyelin
LSM	lysosphingomyelin	
phSM	sphingomyelin(phytosphingosine)	
Neutral glycerolipid	MG	monoglyceride
DG	diglyceride	
TG	triglyceride	
Fatty Acid	FA	fatty acid
OAHA	(O-acyl)-1-hydroxy fatty acid	
Cardiolipin	CL	Cardiolipin
Sphingoid base	So	Sphingosine
SoP	Sphingosine phosphate	
Neutral Glycosphingolipids	SoG1	Glucosylsphingosine
Cer(G1, G2, G3, G2GNAc1, G2GNAc2)	Simple Glc series	
Glycosphingolipids	Cer	Ceramides
CerP	Ceramides phosphate	
GM(1, 1a, 1b, 2, 3), GT(1a, 1b, 1c, 2, 3), GQ(1c, 1b)	Gangliosides	
Steroid	ChE	Cholesteryl Ester
ZyE	zymosteryl	
StE	Stigmasteryl ester	
SiE	Sitosteryl ester	
D7ChE	Deuterated Cholesteryl Ester	

(continued)

Table 9
(continued)

Group	classKey	Lipid Name
Coenzyme	Co	Coenzyme
Glycoglycerolipid	MGMG	Monogalactosylmonoacylglycerol
MGDG	Monogalactosyldiacylglycerol	
DGMG	Digalactosylmonoacylglycerol	
DGDG	Digalactosyldiacylglycerol	
SQMG	Sulfoquinovosylmonoacylglycerol	
SQDG	Sulfoquinovosyldiacylglycerol	
Neutral glycerolipid (deuterated)	D5DG	Deuterated diglyceride
D5TG	Deuterated triglyceride	

- If you have chromatographic (Subheading 3.2) problems always make sure your column is well equilibrated, the solvents you are using are fresh and the LC pump/system was purged and equilibrated properly. Typically, the example given would work on most reverse phase C18 columns.
- You think you have adequate amount of lipid but observe very little signal in the mass spectrometer above the noise (Subheading 3.3). It is strongly recommended to purchase some synthetic lipid standards to optimize the mass spectrometer's acquisition parameters as well as LC gradient if required. These lipid standards should preferably be stable isotope labeled and can be used also for within class lipid quantitation when spiked into the lipid mixture to be analyzed, at a known concentration. Check the presence in Lipid Search stable isotope database before ordering labeled lipids. If they are not in the database, they will not be identified or used for ratiometric quantification.
- You identify very few lipids with the typical data analysis (Subheading 3.4) parameters given. Make sure your mass spectrometer can produce data with the mass accuracy in the range described. If not you may want to widen the mass errors for MS and MS/MS and use the General database. Lipid Search manual and Thermo application notes could be very useful to troubleshoot your data analysis issues.

References

1. Wenk MR (2005) The emerging field of lipidomics. *Nat Rev Drug Discov* 4(7):594–610. doi:[10.1038/nrd1776](https://doi.org/10.1038/nrd1776)
2. Rolim AEH, Henrique-Araújo R, Ferraz EG, de Araújo Alves Dutra FK, Fernandez LG (2015) Lipidomics in the study of lipid metabolism: current perspectives in the omic sciences. *Gene* 554(2):131–139. doi:[10.1016/j.gene.2014.10.039](https://doi.org/10.1016/j.gene.2014.10.039)
3. Fahy E, Cotter D, Sud M, Subramaniam S (2011) Lipid classification, structures and tools. *Biochim Biophys Acta* 1811(11):637–647. doi:[10.1016/j.bbali.2011.06.009](https://doi.org/10.1016/j.bbali.2011.06.009)
4. Sud M, Fahy E, Cotter D, Brown A, Dennis EA, Glass CK, Merrill AH, Murphy RC, Raetz CRH, Russell DW, Subramaniam S (2007) LMSD: LIPID MAPS structure database. *Nucleic Acids Res* 35(Database issue):D527–D532. doi:[10.1093/nar/gkl838](https://doi.org/10.1093/nar/gkl838)
5. Wishart DS, Tzur D, Knox C, Eisner R, Guo AC, Young N, Cheng D, Jewell K, Arndt D, Sawhney S, Fung C, Nikolai L, Lewis M, Coutouly MA, Forsythe I, Tang P, Shrivastava S, Jeroncic K, Stothard P, Amegbey G, Block D, Hau DD, Wagner J, Miniaci J, Clements M, Gebremedhin M, Guo N, Zhang Y, Duggan GE, MacInnis GD, Weljie AM, Dowlatabadi R, Bamforth F, Clive D, Greiner R, Li L, Marrie T, Sykes BD, Vogel HJ, Querengesser L (2007) HMDB: the human metabolome database. *Nucleic Acids Res* 35. (Database):D521–D526. doi:[10.1093/nar/gkl923](https://doi.org/10.1093/nar/gkl923)
6. Fahy E, Subramaniam S, Brown H, Glass C, Merrill JA, Murphy R, Raetz C, Russell D, Seyama Y, Shaw W, Shimizu T, Spener F, van Meer G, Vannieuwenhze M, White S, Witztum J, Dennis EA (2005) A comprehensive classification system for lipids. *J Lipid Res* 46:839–861. PubMed ID: 15722563
7. Fahy E, Subramaniam S, Murphy R, Nishijima M, Raetz C, Shimizu T, Spener F, van Meer G, Wakelam M, Dennis EA (2009) Update of the LIPID MAPS comprehensive classification system for lipids. *J Lipid Res* 50:S9–S14. PubMed ID: 19098281
8. Han X, Gross RW (2005) Shotgun lipidomics: electrospray ionization mass spectrometric analysis and quantitation of cellular lipidomes directly from crude extracts of biological samples. *Mass Spectrom Rev* 24(3):367–412. doi:[10.1002/mas.20023](https://doi.org/10.1002/mas.20023)
9. Washburn MP, Wolters D, Yates JR (2001) Large-scale analysis of the yeast proteome by multidimensional protein identification technology. *Nat Biotechnol* 19(3):242–247. doi:[10.1038/85686](https://doi.org/10.1038/85686)
10. Yadav SP (2007) The wholeness in suffix -omics, -omes, and the word om. *J Biomol Tech: JBT* 18(5):277
11. Gugiu BG, Mesaros CA, Sun M, Gu X, Crabb JW, Salomon RG (2006) Identification of oxidatively truncated ethanolamine phospholipids in retina and their generation from polyunsaturated phosphatidylethanolamines. *Chem Res Toxicol* 19(2):262–271. doi:[10.1021/tx050247f](https://doi.org/10.1021/tx050247f)
12. Folch J, Ascoli I, Lees M, Meath JA, leBaron N (1951) Preparation of lipide extracts from brain tissue. *J Biol Chem* 191(2):833–841
13. Bligh EG, Dyer WJ (1959) A rapid method of total lipid extraction and purification. *Can J Biochem Physiol* 37(8):911–917
14. Matyash V, Liebisch G, Kurzchalia TV, Shevchenko A, Schwudde D (2008) Lipid extraction by methyl-tert-butyl ether for high-throughput lipidomics. *J Lipid Res* 49(5):1137–1146. doi:[10.1194/jlr.D700041-JLR200](https://doi.org/10.1194/jlr.D700041-JLR200)
15. Castro-Perez JM, Kamphorst J, DeGroot J, Lafeber F, Goshawk J, Yu K, Shockcor JP, Vreeken RJ, Hankemeier T (2010) Comprehensive LC-MS E lipidomic analysis using a shotgun approach and its application to biomarker detection and identification in osteoarthritis patients. *J Proteome Res* 9(5):2377–2389. doi:[10.1021/pr901094j](https://doi.org/10.1021/pr901094j)
16. Tie C, Hu T, Jia Z-X, Zhang J-L (2015) Automatic identification approach for high-performance liquid chromatography-multiple reaction monitoring fatty acid global profiling. *Anal Chem* 87(16):8181–8185. doi:[10.1021/acs.analchem.5b00799](https://doi.org/10.1021/acs.analchem.5b00799)
17. Yamada T, Uchikata T, Sakamoto S, Yokoi Y, Fukusaki E, Bamba T (2013) Development of a lipid profiling system using reverse-phase liquid chromatography coupled to high-resolution mass spectrometry with rapid polarity switching and an automated lipid identification software. *J Chromatogr A* 1292:211–218. doi:[10.1016/j.chroma.2013.01.078](https://doi.org/10.1016/j.chroma.2013.01.078)
18. Taguchi R, Ishikawa M (2010) Precise and global identification of phospholipid molecular species by an orbitrap mass spectrometer and automated search engine lipid search. *J Chromatogr A* 1217(25):4229–4239. doi:[10.1016/j.chroma.2010.04.034](https://doi.org/10.1016/j.chroma.2010.04.034)
19. Kiyonami R, Peake DA, Liu X, and Huang Y (2015) Large scale lipid profiling of a human

- serum lipidome using a high resolution accurate mass LC/MS/MS approach. Presented at the LIPID MAPS annual meeting, La Jolla, CA, 12–13 May 2015
20. Kind T, Liu K-H, Lee DY, DeFelice B, Meissen JK, Fiehn O (2013) LipidBlast in silico tandem mass spectrometry database for lipid identification. *Nat Methods* 10(8):755–758. doi:[10.1038/nmeth.2551](https://doi.org/10.1038/nmeth.2551)
 21. Kang YP, Lee WJ, Hong JY, Lee SB, Park JH, Kim D, Park S, Park C-S, Park S-W, Kwon SW (2014) Novel approach for analysis of Bronchoalveolar lavage fluid (BALF) using HPLC-QTOF-MS-based lipidomics: lipid levels in asthmatics and corticosteroid-treated asthmatic patients. *J Proteome Res* 13(9): 3919–3929. doi:[10.1021/pr5002059](https://doi.org/10.1021/pr5002059)
 22. Peake DA, Kiyonami R, Yokoi Y, Fukamachi Y (2015) Processing of a complex lipid dataset for the NIST inter-laboratory comparison exercise for lipidomics measurements in human serum and plasma. Presented at the ASMS annual meeting, Saint Louis, MO, 31st May–4th June 2015

Utility of Moderate and High-Resolution Mass Spectrometry for Class-Specific Lipid Identification and Quantification

Maria del Carmen Piqueras

Abstract

The study of lipidomics has been dramatically enhanced by using mass spectrometry techniques.

With the purpose of identification and/or quantification of the lipids object of study, mass spectrometry has been proven to be the best approach, where three main techniques are currently being used: electrospray ionization (ESI), liquid chromatography (LC/MS), and matrix-assisted laser desorption/ionization (MALDI) mass spectrometry (Han et al. *Mass Spectrom Rev* 31:134–178, 2012). In order to avoid the problems generated by gradient concentration using liquid chromatography, here we describe the method used for the lipidomics analysis using moderate and high-resolution mass spectrometry for class-specific lipid identification and quantification for phospholipid species using ESI-MS/MS.

Key words Lipidomics, Mass spectrometry (MS), Lipids, Phospholipids, Electrospray ionization (ESI), Orbitrap

1 Introduction

Lipidomics, a relatively recent field of study part of metabolomics, is focused in the analysis of cellular lipids in biological systems. Lipids play an essential role as structural and functional components of cells, being extremely dynamic in function and composition, and vulnerable to environmental changes [1]. The unique collection of lipid species at any organic level constitutes its lipi-dome. Studying lipidomics establishes a point of reference for the study of diseases based in an altered qualitative or quantitative lipid composition.

Lipids include a great variety of molecules such as sterols, waxes, fats, glycerides, phospholipids, etc., each one with a distinct structure. Although lipids can be categorized in several ways, eight main categories have been established: fatty acyls (FA), glycerolipids (GL), glycerophospholipids (GP), sphingolipids (SP), sterol lipids

(ST), prenol lipids (PR), saccharolipids (LP), and polyketides (PK) [2]. This classification is chemically based, considering the distinct polarity of the constituents of the lipid molecules. According to the structure and nature of each class, different mass spectrometry modes are set to analyze them in tandem mass spectrometry (MS/MS): product-ion analysis mode, precursor-ion scanning mode, neutral-loss scanning mode or selected reaction monitoring mode [2]. Setting different parameters for each lipid class allows specifically targeting the lipid object of interest, due to the specific chemical structure of each one, which renders a particular and definite pattern of fragmentation that will be recognized for identification purposes in the bioinformatics analysis. In order to illustrate it, let us take phospholipids, for example. Phospholipids belong to a lipid class that is glycerol-based, composed by a glycerol backbone linked to a phosphate group, and bonded to several aliphatic chains and a polar head, mainly covalently linked. The polar head can be phosphoethanolamine, phosphocholine, hydrogen, etc. One of the constituents of the lipid molecule is the fatty acyl moiety, while the other is linked through a C-C bond, aliphatic chain containing different number of carbons. Overall, we could consider them generally formed by three distinctive parts [1] that are linked to the glycerol backbone (Fig. 1).

For mass spectrometry analysis purposes, each one of the three parts described before can be represented by distinctive moieties of individual lipid classes. For phospholipids, in this case, two main tandem MS techniques are used: Precursor Ion Scan (PIS) and

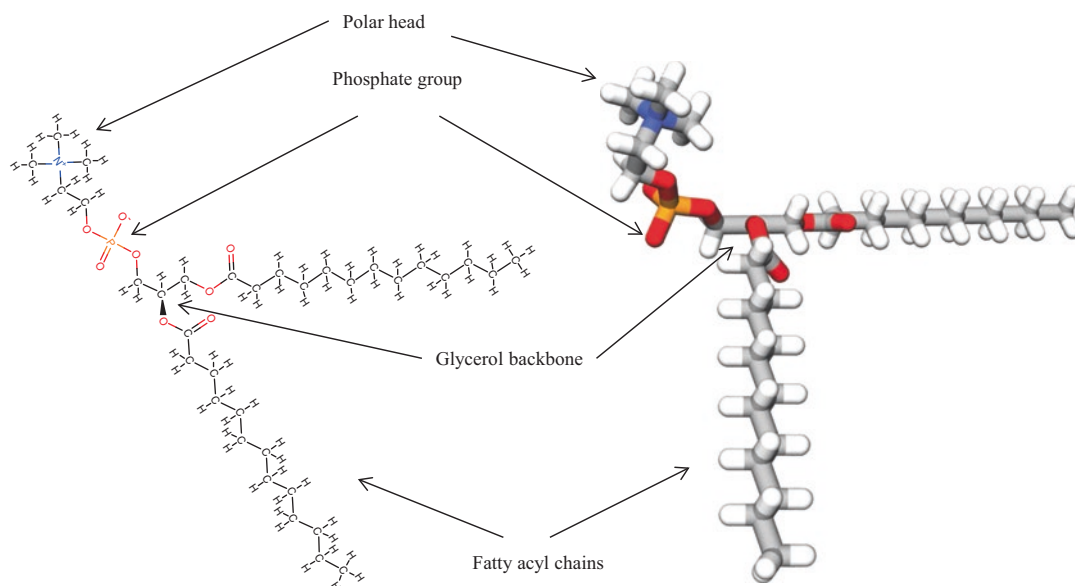
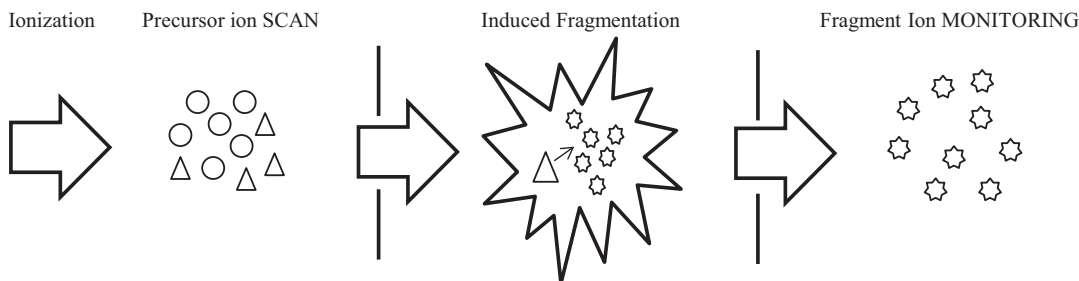


Fig. 1 General structure of glycerophospholipids. Polar heads and fatty acyl chains vary

Precursor Ion Scan (PIS)



Neutral Loss Scan (NLS)

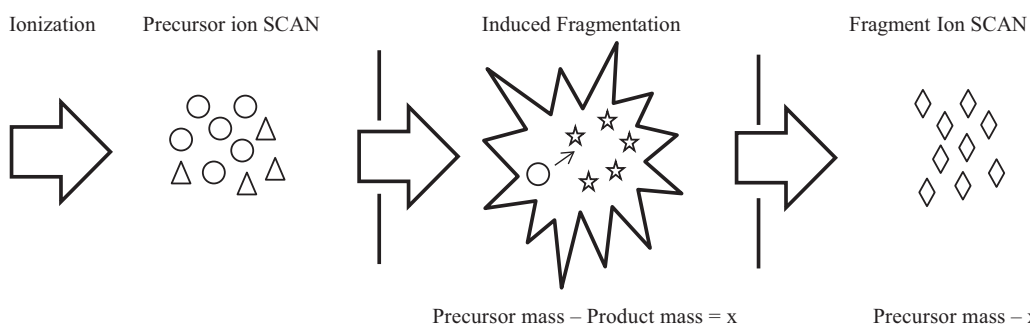


Fig. 2 Schematics of two main tandem MS techniques: Precursor Ion Scan (PIS) and Neutral Loss Scan (NLS). In the first one, after fragmentation, the fragment ions are monitored and the precursor ion is scanned. In the second, both fragment and precursor ions are scanned

Neutral Loss Scan (NLS). The latter mode sets a specific loss of a neutral fragment, while the first is set to scan a specific fragment ion (Fig. 2).

For ESI, we work with direct infusion (Triversa nanomate by Advion Bioscience Ltd., Ithaca NY) which injects the lipids into the ion source directly (Shotgun lipidomics) coupled to a TSQ Quantum Access Max Mass Spectrometer. This approach has the advantage over LC-MS of avoiding the problems originated by the gradient in concentration, among others while rendering high sensitivity. Besides, the procedure is easier and faster [1]. Other authors agree in the fact that maintaining a constant concentration achieved by Shotgun Lipidomics is a critical point for identification and quantification [3]. However, each run is set to detect one specific lipid class, for which the scan parameters are specifically designed. Other approaches in Shotgun Lipidomics, like those including Q-TOF or Orbitrap mass spectrometers, like Q-Exactive from Thermo Fischer, are able to run several PIS simultaneously, with higher mass resolution and accuracy typical to those instruments (0.1 amu).

High resolution and mass accuracy are features especially important in lipidomics. For example, the significant remark made by Schwudke [4] in a paper about high-resolution mass spectrometry, a mass difference between a certain species of PC and a certain species of PS is only 1.9429 Da. This small difference could be isobaric (same nominal mass) in case they have the same number of carbon atoms in their fatty acid moieties and the PS has one double bond more compared to the PC. However, even with the same nominal mass, they state, their exact mass diverges by 0.0726 Da, and it is precisely this fact the reason for which it will be possible to distinguish them in high-resolution mass spectra. Exact masses of lipids from each group do not overlap and their peaks in MS spectra are unique [4].

Our instrument is coupled to an ESI source, a TSQ Quantum Access Max from Thermo Scientific, primarily designed to achieve maximum sensitivity, accuracy, precision, and linear dynamic range. The TSQ Quantum has true hyperbolic electrodes, large field radius, high frequency and voltage, and a long length (25 cm) and hence has the ability to achieve high mass resolution, as by their technical specifications.

2 Materials

2.1 Resuspension of Samples and Standards

1. Acetonitrile: LC/MS Suitable for UHPLC-UV.
2. 2-Propanol: LC/MS Packaged under Nitrogen, 0.2 μm filtered suitable for LC/MS.

2.2 Lipid Standards (Avanti Polar Lipids, Alabaster, AL)

1. 1,2-ditridecanoyl-*sn*-glycero-3-phosphocholine (MW 649.89) (PC).
2. 1,2-dioleoyl-*sn*-glycero-3-phospho-L-serine (MW 810.03) (PS).
3. 1,2-dioleoyl-*sn*-glycero-3-phosphoethanolamine (MW 744.04) (PE).
4. 1,2-dioleoyl-*sn*-glycero-3-phospho-(10-*myo*-inositol) (MW 880.15) (PI).

2.3 Mass Spectrometry Analysis

1. 2.0 TSQ Quantum Access Max triple quadrupole electrospray mass spectrometer (Thermo Fisher Scientific, Pittsburgh, PA).
2. Triversa nanomate (Advion Bioscience Ltd., Ithaca NY) for direct infusion of the samples and the standards.

2.4 Other

1. Argon gas.
2. Nitrogen, compressed, ultra-high purity.

3 Methods

Before running the lipid samples, the lipid standards are run beforehand separately to ensure efficiency and that they render the proper chromatogram and spectra. After this step, run the samples with and without every standard for quantification purposes.

1. Preparation of lipid samples and lipid standards.
 - (a) Dilute each standard to the desired concentration, typically 10 pmol/ μ L, in a mix of acetonitrile and isopropanol (1:1).
 - (b) Resuspend the dried lipid samples from tissues (obtained using the Bligh and Dryer method, stored at $-80\text{ }^{\circ}\text{C}$) in acetonitrile:isopropanol (1:1). Divide the lipid samples into five aliquots each.
2. Run a solvent aliquot in the mass spectrometer to note the most abundant peaks present only in the solvent, in order to obtain a spectra under every set of parameters that will be adjusted for every class of lipids (*see step 3*).
3. Set the different class parameters in Thermo Xcalibur and Tunes Software, which are the following:
 - (a) For Phosphocholine (PC) (Fig. 3a).
 - Set collision energy to 35 V.
 - Set positive mode.
 - Set PIS mode.
 - Set Product ion mass to 184.0 m/z .
 - Set Mass range: 200–1020 m/z .
 - (b) For Phosphoserine (PS) (Fig. 3b).
 - Set collision energy to 24 V.
 - Set negative mode.
 - Set NLS mode.
 - Set Product ion mass to 87.1.
 - Set mass range: 400–1000 m/z .
 - (c) For Phosphoinositol (PI) (Fig. 3c).
 - Set collision energy to 45 V.
 - Set negative mode.
 - Set PIS mode.
 - Set Product ion mass to 241 m/z .
 - Mass range: 500–1000 m/z .
 - (d) For Phosphoethanolamine (PE) (Fig. 3d).
 - Set collision energy to 50 V.

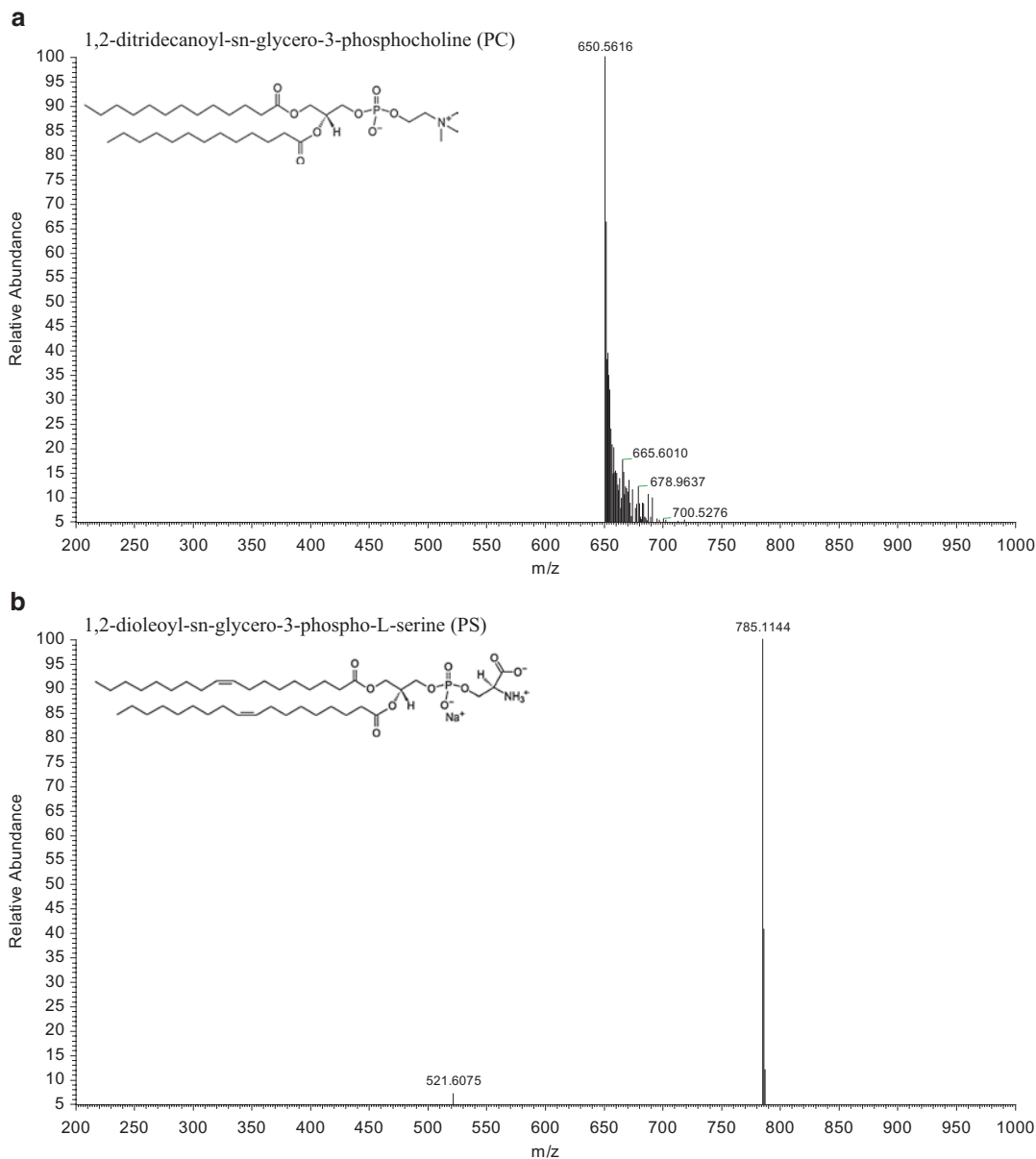


Fig. 3 (a) Mass spectrum obtained in TSQ Quantum Access Max set in parent ion scan (PIS) positive mode for 1,2-ditridecanoyl-*sn*-glycero-3-phosphocholine (PC). (b) Mass spectrum obtained in TSQ Quantum Access Max set in neutral loss scan (NLS) negative mode for 1,2-dioleoyl-*sn*-glycero-3-phospho-L-serine (PS). (c) Mass spectrum obtained in TSQ Quantum Access Max set in parent ion scan (PIS) negative mode for 1,2-dioleoyl-*sn*-glycero-3-phospho-(10-*myo*-inositol) (PI). (d) Mass spectrum obtained in TSQ Quantum Access Max set in parent ion scan (PIS) negative mode for 1,2-dioleoyl-*sn*-glycero-3-phosphoethanolamine (PE)

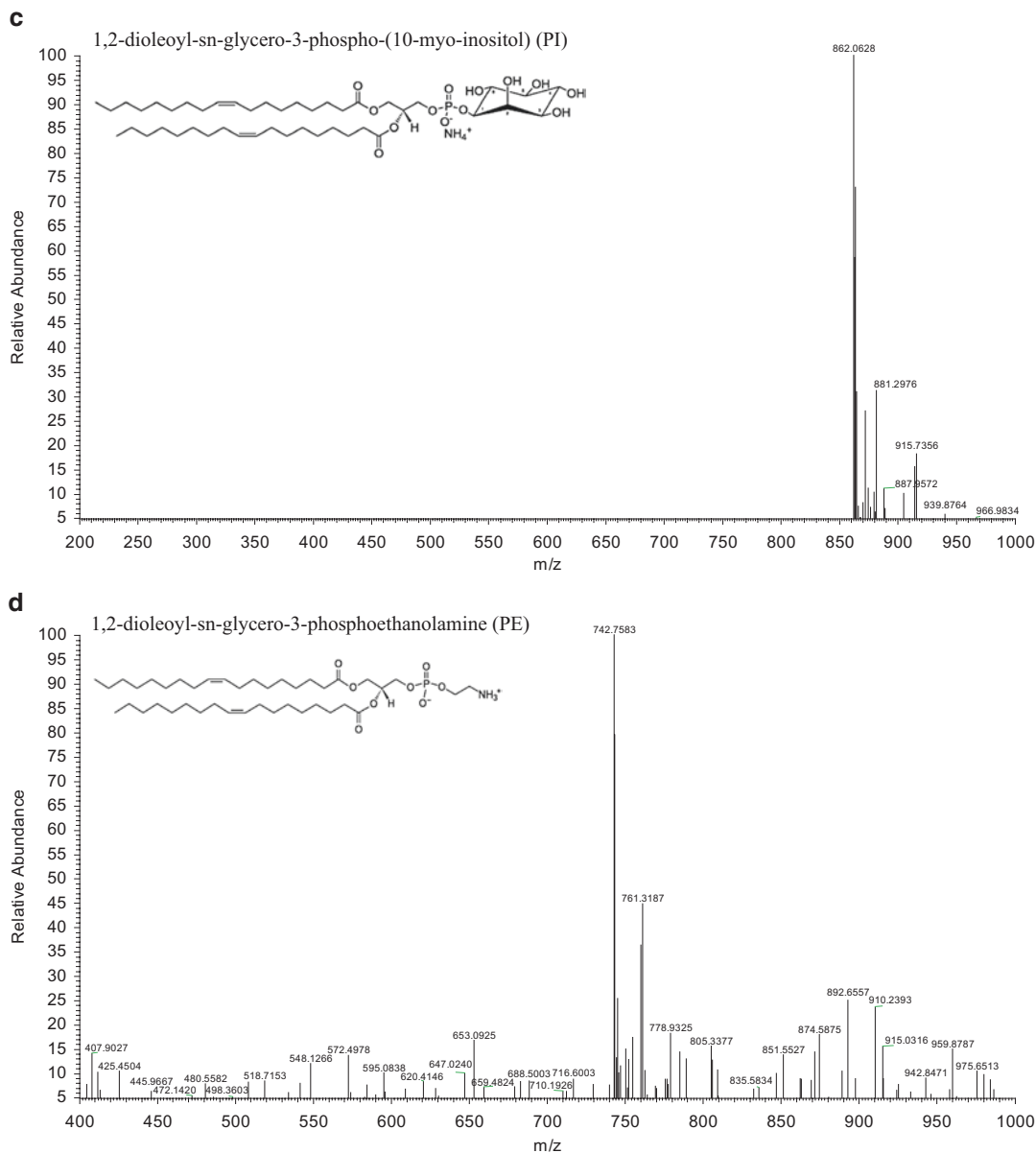


Fig. 3 (continued)

- Set negative mode.
 - Set PIS mode.
 - Set Product ion mass to 196 m/z .
 - Set Mass range: 200–1000 m/z .
4. Set the following parameters for ESI,
- (a) Flow rate infusion to 10 $\mu\text{L}/\text{min}$.
 - (b) Set 2 min for recording spectra.
 - (c) Set 0.5 s scan.

- (d) Set +1.3 kV ionization voltage for positive mode and -1.2 kV for negative.
- (e) Set 0.3 units of gas pressure.
5. Use 5–10 μL of sample or standard per run. That will depend on the available amount of sample object of study. Repeat this process ten times to ensure repeatability.
6. Run every standard separately for identification purposes.
7. Run the samples separately, with and without every standard.
8. For quantification purposes, add 1 μL of each standard to each sample aliquot and run it. Quantification of the different species will be determined by proportionally comparing the peak area of the standard in the spectra with the rest of peaks in the bioinformatics analysis.

4 Notes

Major problems with lipid standards come from their instability and degrading once dissolved. Maintaining them at the proper storage temperature ($-20\text{ }^{\circ}\text{C}$) at all times and using them immediately after preparation are the key to obtain a good result. Following carefully the proper lipid extraction protocol and storage temperature of the lipid object of study are also critical, typically at $-80\text{ }^{\circ}\text{C}$ until used. All samples must be maintained on ice during the preparation to be run in the mass spectrometer. Concentration of standard and samples are critical to obtain good chromatograms and spectra. Running the samples without standard will proportionate information about the presence or absence of each class and the amount of lipids in them. Therefore, the amount of standard used for each sample should be adequate in order to be able to be easily recognized in the spectra, not too elevated or insignificant. In order to achieve a good ratio standard/sample, be sure to dilute your samples accordingly. For relative protein/lipid quantification, it is necessary to measure the amount of protein in the samples obtained in the Bligh and Dryer protocol to calculate the pertinent ratios in the bioinformatics analysis.

References

1. Han X, Yang K, Gross RW (2012) Multi-dimensional mass spectrometry-based shotgun lipidomics and novel strategies for lipidomic analyses. *Mass Spectrom Rev* 31(1):134–178. doi:[10.1002/mas.20342](https://doi.org/10.1002/mas.20342)
2. Almeida R, Pauling JK, Sokol E, Hannibal-Bach HK, Ejsing CS (2015) Comprehensive lipidome analysis by shotgun lipidomics on a hybrid quadrupole-orbitrap-linear ion trap mass spectrometer. *J Am Soc Mass Spectrom* 26(1):133–148. doi:[10.1007/s13361-014-1013-x](https://doi.org/10.1007/s13361-014-1013-x)
3. Wang M, Wang C, Han RH, Han X (2016) Novel advances in shotgun lipidomics for biology and medicine. *Prog Lipid Res* 61:83–108. doi:[10.1016/j.plipres.2015.12.002](https://doi.org/10.1016/j.plipres.2015.12.002)
4. Schwudke D, Schuhmann K, Herzog R, Bornstein SR, Shevchenko A (2011) Shotgun lipidomics on high resolution mass spectrometers. *Cold Spring Harb Perspect Biol* 3(9):a004614. doi:[10.1101/cshperspect.a004614](https://doi.org/10.1101/cshperspect.a004614)

A Robust Lipidomics Workflow for Mammalian Cells, Plasma, and Tissue Using Liquid-Chromatography High-Resolution Tandem Mass Spectrometry

Candice Z. Ulmer, Rainey E. Patterson, Jeremy P. Koelmel, Timothy J. Garrett, and Richard A. Yost

Abstract

Lipids have been analyzed in applications including drug discovery, disease etiology elucidation, and natural products. The chemical and structural diversity of lipids requires a tailored lipidomics workflow for each sample type. Therefore, every protocol in the lipidomics workflow, especially those involving sample preparation, should be optimized to avoid the introduction of bias. The coupling of ultra-high-performance liquid chromatography (UHPLC) with high-resolution mass spectrometry (HRMS) allows for the separation and identification of lipids based on class and fatty acid acyl chain. This work provides a comprehensive untargeted lipidomics workflow that was optimized for various sample types (mammalian cells, plasma, and tissue) to balance extensive lipid coverage and specificity with high sample throughput. For identification purposes, both data-dependent and data-independent tandem mass spectrometric approaches were incorporated, providing more extensive lipid coverage. Popular open-source feature detection, data processing, and identification software are also outlined.

Key words Lipidomics, Ultra-high performance liquid chromatography (UHPLC), High-resolution mass spectrometry, Sample preparation, Biomarker discovery

1 Introduction

Lipids are analyzed in numerous settings including synthetic and natural products industries [1–6] and medical fields [7–10]. The diverse biological functions and ubiquitous occurrence of lipids highlight their potential as clinical biomarkers and as indicators of pathways perturbed by disease or environmental exposure. Lipid diversity in function is enabled by lipid diversity in structure, with over 180,000 possible lipid species at the level of fatty acid constituents [11]. Lipid structural diversity, amphiphilic nature, and concentrations range several million-fold [12], all pose unique analytical challenges in the field of lipidomics.

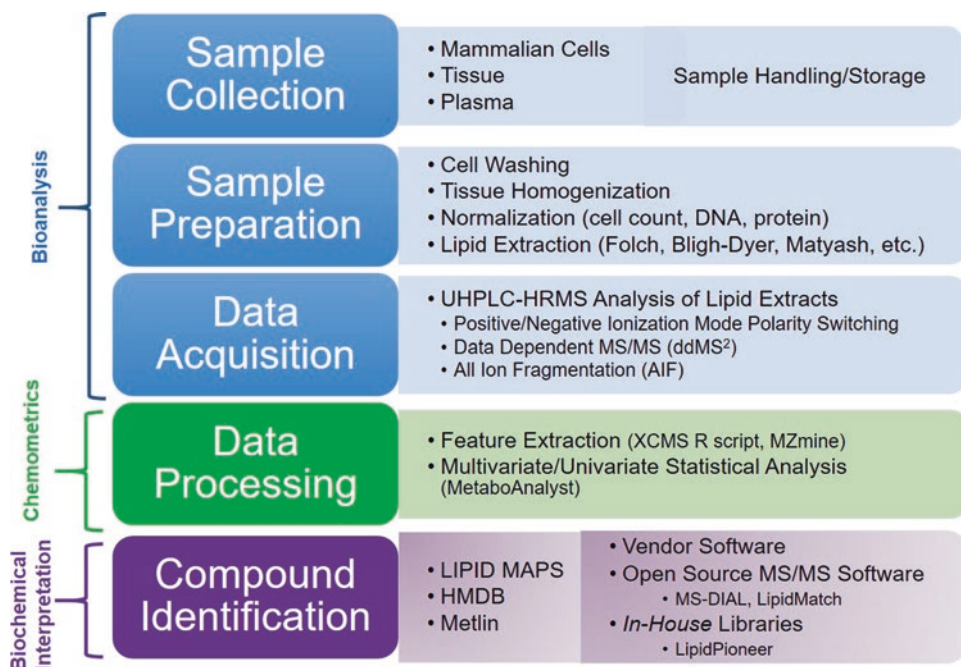


Fig. 1 Lipidomics workflow including the components for bioanalysis, chemometrics with open-source software, and biochemical interpretation of lipid extracts

The most comprehensive lipidomics workflows in terms of the number and accuracy of lipid species analyzed include sample homogenization and extraction, separation by liquid chromatography, ionization and detection by electrospray ionization high-resolution tandem mass spectrometry (ESI-HR MS/MS), feature detection and identification, and statistical analysis (Fig. 1). Because lipids encompass a broad range of chemical and physical properties, lipidomics sample preparation workflows have not been standardized in the literature. In addition, every step of the sample preparation workflow (e.g., storage, sample handling, homogenization, and lipid extraction) may bias the results. Therefore, the lipidomics sample preparation workflow should be tailored to the sample type. The amphiphilic lipids are amenable to reverse phase (RP) chromatography, where research has shown these lipids under RP conditions to separate based on class, fatty acid constituents, and even by *m1* and *m2* positional isomers and double bond positions [13]. Chromatographic separation enhances specificity, reduces ion suppression in ESI-HRMS/MS, and aids in the identification of lipid species. High-resolution tandem mass spectra of precursor ions and fragment ions containing information on lipid class and fatty acid acyl chain information can be used to confidently identify lipid structures.

Here, we describe a workflow that is optimized for various sample types (mammalian cells, plasma, and tissue), which balances extensive lipid coverage and specificity with high sample throughput. In addition, quality control procedures are included to characterize any introduction of non-biological variability. The workflow provides semi-quantitative lipid concentrations using available lipid class-representative standards, allowing comparison of lipid data between different techniques and labs. For identification purposes, both data-dependent and data-independent tandem mass spectrometric approaches are used, providing more extensive lipid coverage. Popular open-source feature detection and identification software are described in the notes with suggested parameters. Data-processing and interpretation strategies are outlined to reduce the chance of false positives and false negatives, providing as much information on up- and down-regulated lipids and lipid signatures as possible. In addition, multivariate statistical techniques and open-source software for predicting and categorizing biological perturbations based on lipid profiles are described.

2 Materials

Prepare all solutions using LC-MS grade solvents. Refrigerate solvents used for sample preparation and store all samples in temperatures at $-80\text{ }^{\circ}\text{C}$ or below. For the purpose of this study, analytical grade solvents (formic acid, chloroform, and methanol) were purchased from Fisher-Scientific (Fairlawn, NJ). Mobile phase solvents were Fisher Optima LC/MS grade (acetonitrile, isopropanol, and water). Triacylglyceride lipid standards (TG 15:0/15:0/15:0 and TG 17:0/17:0/17:0) were purchased from Sigma-Aldrich (St. Louis, MO). Exogenous lysophosphatidylcholine (LPC 17:0 and LPC 19:0), phosphatidylcholine (PC 17:0/17:0 and PC 19:0/19:0), phosphatidylethanolamine (PE 15:0/15:0 and PE 17:0/17:0), phosphatidylserine (PS 14:0/14:0 and PS 17:0/17:0), and phosphatidylglycerol (PG 14:0/14:0 and PG 17:0/17:0) lipid standards were purchased from Avanti Polar Lipids (Alabaster, AL) (*see Note 1*). All lipid standards were diluted prior to analysis in 1:2 (v/v) chloroform:methanol (CHCl_3 :MeOH) and a working standard mix was then prepared by diluting the stock solution with the same solvent mixture. Butylated hydroxytoluene (BHT) was purchased from Sigma Aldrich. All protein and DNA assay measurements were obtained using a Qubit 3.0 Fluorometer purchased from Thermo Fisher Scientific. Lipid extracts were dried down using a MultiVap 118 nitrogen dryer set at $30\text{ }^{\circ}\text{C}$ (Organomation Associates, Inc.).

2.1 Sample Preparation

1. Mammalian cells: minimum of 10^6 cells, cell rinsing solution: deionized water with ammoniated cell washing buffer (*see Note 2*).

2. Tissue: liquid nitrogen-pooled mortar and ceramic pestle, liquid nitrogen, homogenization beads (zirconium oxide or ceramic for soft tissue, and stainless steel for muscle and harder tissues).
3. Plasma collected using EDTA anticoagulant. Stored for long term at -80°C in polypropylene Eppendorf tubes.
4. Centrifuge (*see Note 3*).
5. Polypropylene Eppendorf tubes (1.5 mL and/or 2 mL), polypropylene conical tubes (5 mL and/or 15 mL) (*see Note 4*).

2.2 Sample-Dependent Folch Lipid Extraction

1. Lipid internal standard mix: create a stock solution [1:2 (v/v) chloroform: methanol] of the following lipids: PC 17:0/17:0, PC 19:0/19:0, PE 15:0/15:0, PE 17:0/17:0, PS 14:0/14:0, PS 17:0/17:0, PG 14:0/14:0, PG 17:0/17:0, TG 15:0/15:0/15:0, and TG 17:0/17:0/17:0 (*see Note 1*).
2. Folch lipid extraction solvents: methanol with 1 mM butylated hydroxytoluene (BHT), chloroform, water (*see Note 5*).
3. Re-extraction solvent: 2:1 (v/v) chloroform/methanol (*see Note 6*).
4. Vortex.
5. Nitrogen dryer.

2.3 UHPLC-HRMS Data Acquisition

1. UHPLC C18 column (*see Note 7*).
2. Reconstitution solvent: 100% isopropanol.
3. Solvent A: acetonitrile:water (60:40, v/v) with 10 mM ammonium formate and 0.1% formic acid (*see Note 8*).
4. Solvent B: isopropanol:acetonitrile:water (90:8:2, v/v) with 10 mM ammonium formate and 0.1% formic acid (*see Note 8*).
5. UHPLC system coupled to a high-resolution mass spectrometer capable of employing positive and negative ionization with a heated electrospray probe (*see Note 9*).
6. Glass vials with 200 μL inserts.

3 Methods

All samples and solvents during the Folch lipid extraction should be kept on ice. Avoid exposing samples to room temperature for more than 5 min.

3.1 Sample Preparation

1. Cell preparation: Pellet mammalian cells in a 15 mL conical tube at $311 \times g$ for 5 min at 4°C . Wash cell pellet 2–3 times by adding 1 mL of the cell rinsing solution. During the last washing step, reconstitute the cells in the rinsing solution and obtain a 5 μL aliquot for each assay (protein and/or DNA

measurement). Store the cell pellet at $-80\text{ }^{\circ}\text{C}$ or perform the lipid extraction (*see Note 10*).

2. Plasma preparation: Thaw plasma samples on ice before pipetting $40\text{ }\mu\text{L}$ into a 2.0 mL centrifuge tube prior to the Folch extraction. Maintain samples on ice for the remainder of extraction (*see Note 11*).
3. Tissue Pulverization/Homogenization: Flash freeze tissues in liquid nitrogen quickly after collection and store at $-80\text{ }^{\circ}\text{C}$. Further pulverize individual tissue samples in a liquid nitrogen-cooled mortar with a ceramic pestle. Weigh the fine powder into a homogenization tube using balance tared with homogenization beads (ceramic or zirconium oxide for soft tissues, and stainless steel for muscle or harder tissues). Aim for 50 mg of tissue. Record the weight of the tissue powder as further extraction volumes will be adjusted based on weight of tissue. Add internal standard to the tissue ($125\text{ }\mu\text{L}$ of 160 ppm) and homogenize tissues for lipid extraction in the Folch solvents [chloroform:methanol, (2:1, v:v)] at a volume (μL) at 20 times the weight (mg) (*see Note 12*).
4. Create a pooled sample group quality control (*see Note 13*) and/or use a standard reference material (SRM) (e.g., Red Cross Blood Plasma or National Institute of Standards and Technology (NIST) SRM) as a quality control (*see Note 14*).

3.2 Sample-Dependent Folch Lipid Extraction

1. Spike in an aliquot of the lipid internal standard mix into plasma or mammalian cells and an empty Eppendorf/conical tube as an extraction blank (*see Note 15*).
2. Add ice-cold methanol with 1 mM BHT and chloroform (1:2, v/v) directly to the sample.
3. Incubate on ice for 30 min and vortex occasionally.
4. Add ice-cold water to a final ratio of chloroform/methanol/water (8:4:3, v/v/v) and incubate on ice for an additional 10 min .
5. Centrifuge the sample at $311 \times g$ for 5 min at $4\text{ }^{\circ}\text{C}$ to separate the aqueous and organic layer.
6. Pipette through aqueous layer (upper phase) and transfer the organic layer (lower phase) to a separate Eppendorf/conical tube without contaminating the organic phase with the protein layer.
7. Re-extract on the remaining aqueous layer by adding the re-extraction solvent, vortexing, and centrifuging for 5 min at $4\text{ }^{\circ}\text{C}$.
8. Dry down the organic layer under nitrogen at $30\text{ }^{\circ}\text{C}$ (*see Note 16*).
9. Reconstitute the dried lipid extract with 100% isopropanol (*see Note 17*).
10. Transfer lipid extract to an LC vial with a $200\text{ }\mu\text{L}$ glass insert.

3.3 UHPLC-HRMS Data Acquisition

1. Create an instrument sequence that begins with solvent and extraction blanks to give time for column and instrument equilibration (*see Note 18*).
2. Equilibrate the UHPLC C18 column at 50 °C with starting percentages of Solvent A and B as mobile phases (*see Note 19*).
3. Apply the following LC gradient: 32% B at 0 min, 40% B at 1 min, a hold at 40% B until 1.5 min, 45% B at 4 min, 50% B at 5 min, 60% B at 8 min, 70% B at 11 min, and 80% B at 14 min at a flow rate of 0.5 mL/min (*see Note 20*).
4. Maintain the autosampler at 5 °C.
5. The following heated electrospray ionization (HESI) parameters were used in positive ion mode: spray voltage at 3.3 kV, sheath gas and auxiliary nitrogen pressure at 30 and 5 arbitrary units, respectively, and capillary and heater temperatures at 300 °C and 350 °C, respectively. HESI parameters that differed in negative ion mode were sheath gas and auxiliary gas at 25 and 15 arbitrary units, respectively, and a capillary temperature of 250 °C.
6. The following full-scan MS conditions were used with polarity switching (*see Note 21*) following calibration of the instrument (*see Note 22*): S-lens RF level at 35 V, a resolution of 70,000 with an automatic gain control of 5×10^6 ions, and maximum injection time of 256 ms, scanning from m/z 200–1500 (*see Note 23*). All data were acquired in profile mode. *See Fig. 2* for the TIC of lipid extracts from mammalian cells, tissue, and plasma collected in positive ion mode.
7. For identification (*see Note 24*), pooled samples from each sample group were analyzed in both polarities separately using alternate full scans and all ion fragmentation (AIF) scans with AIF parameters as follows: a resolution of 70,000 with an automatic gain control of 5×10^6 ions and maximum injection time of 256 ms, scanning from m/z 100–1500 with a stepped normalized collision energy (NCE) of 15, 20, and 25 (*see Note 25*).
8. Fragmentation of ions obtained in each polarity separately in pooled samples was acquired using data-dependent top10 (ddMS²-top10) analysis as well. Ions were isolated using a 1 amu window, and isolation was triggered using an intensity threshold of 5×10^4 (setting the underfill ratio to reach this desired target), an apex trigger of 10–20 s, isotope exclusion on, and a dynamic exclusion of 4 s. Ions were fragmented by HCD using NCEs of 15, 20, and 25, and fragments were measured with a resolution of 35,000 with an automatic gain control of 5×10^6 ions and maximum injection time of 175 ms.

3.4 HRMS Lipidomic Data Processing

1. Convert .raw files to an mzXML output using software such as ProteoWizard MSConvert (*see Note 26*).

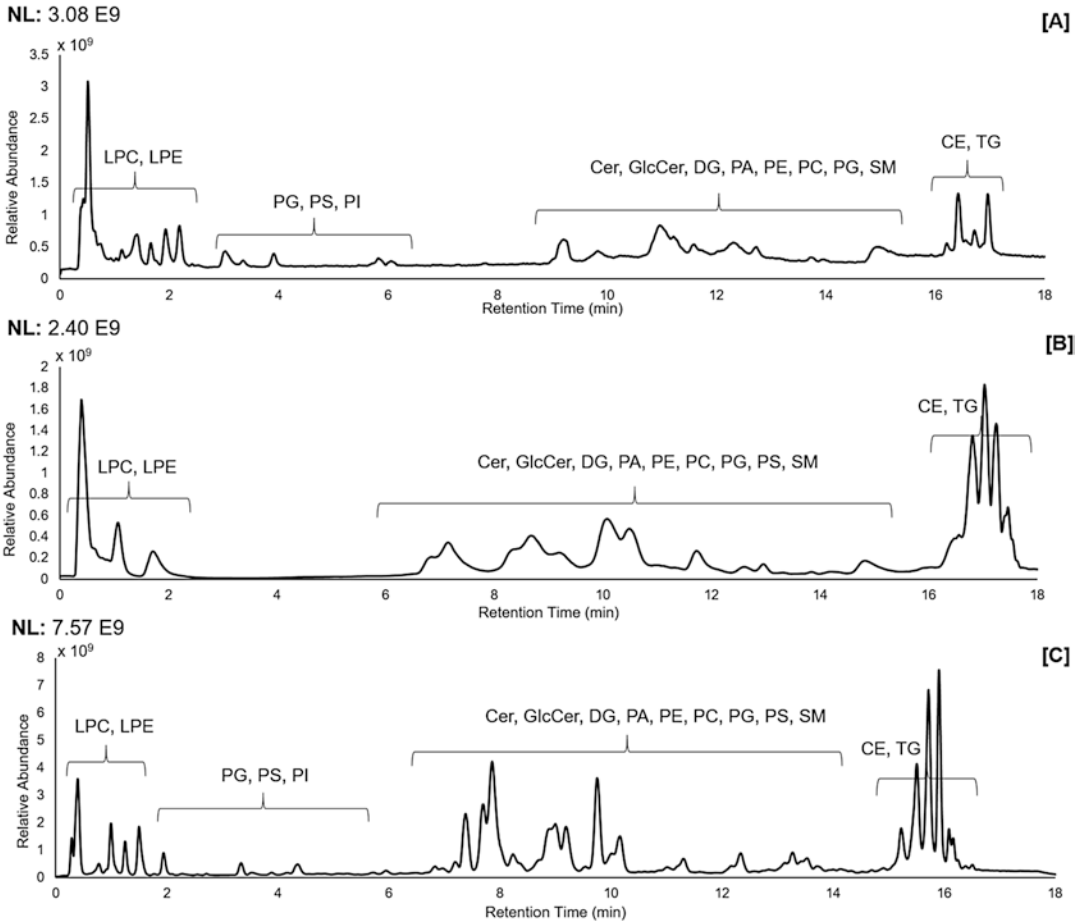


Fig. 2 Total ion chromatogram of the reverse-phase endogenous lipid elution profile for extracted (a) Jurkat T lymphocyte cells, (b) skin tissue, (c) plasma in positive ion mode using a Supelco Analytical Titan C18 column

2. Process the mzXML files using a feature detection and alignment software (*see Note 27*).
3. Export the peak-picked data as a .csv file that can be imported for data analysis and interpretation.

3.5 Data Analysis and Interpretation

1. Apply a univariate and/or multivariate statistical analysis software to the peak-picked data (*see Note 28*).
2. Match features that significantly differ between predefined sample groups from feature detection and alignment software to a database or *in-house* library for annotation. Confidence in annotation increases with information including m/z , adduct, retention time, and fragmentation pattern (*see Notes 24 and 29*).

4 Notes

1. Other lipid internal standards that represent common lipid classes that can be purchased from Avanti Polar lipids include diacylglyceride (DG 14:0/14:0), sphingomyelin SM (d18:1/17:0), and ceramide Cer (d18:1/17:0).
2. A minimum of 10^6 suspension and/or adherent cells are needed for lipidomic studies to ensure a sufficient instrument signal (10^7 – 10^8 peak intensity). Cells should be washed with an ammoniated cell washing buffer as these rinsing solvents are compatible with ESI-LC-MS conditions [14].
3. For mammalian cell lipidomics studies, a centrifuge is needed that can support 5 or 15 mL conical tubes. For plasma and tissue lipidomics studies, a centrifuge is needed that can support 1.5 or 2 mL Eppendorf tubes.
4. Polypropylene tubes should be used when working with chloroform.
5. The methanol contains 1 mM BHT to minimize oxidation of lipid species [15].
6. Because 1 mM BHT was added during the initial steps of the extraction, it is not needed here.
7. Options for a UHPLC C18 columns include: Supelco Analytical Titan C18 (2.1×75 mm, $1.9 \mu\text{m}$) and Waters Acquity™ BEH C18 column (2.1×50 mm, $1.7 \mu\text{m}$). Polar lipid species can be separated on a HILIC column such as the Agilent HILIC Plus RRHD column (2.1×150 mm, $1.8 \mu\text{m}$).
8. Use glass pipettes to aliquot formic acid into mobile phases. A 1 mL ampule of formic acid for each liter of mobile phase can be used to avoid contamination.
9. This work incorporated a Dionex Ultimate 3000 UHPLC system coupled to a Q Exactive Orbitrap mass spectrometer (Thermo Scientific, San Jose, CA).
10. If possible, normalize all samples using the cell count before performing sample preparation. If the cell count information is unavailable, data can be normalized to DNA or protein concentrations post-data acquisition [16].
11. Typically, a consistent volume used for plasma is adequate; however, protein content may be assessed to provide an alternative method of normalization. Another extraction method that works well for lipids from plasma is the Matyash MTBE method [17]. Notes comparing the two methods were published by Patterson, et al. [18].
12. Maintain tissue weight:homogenization solvent ratio at 1 mg:20 μL to avoid tissue weight normalization post-data

acquisition and differences in extraction efficiencies based on lipid concentrations. For example, 50 mg of tissue will require 1000 μL of Folch solvent. Alternatively, tissue can be homogenized in an aqueous buffer (ammonium formate, etc.) and then aliquoted like plasma; however, we have found most efficient homogenization for lipid analysis occurs with organic solvents during homogenization. If the tissue is to be homogenized in the Folch solvents, continue with Subheading 3.2, step 3.

13. Sample pools can be created before or after extraction depending on the sample type. If pooled before extraction, an even aliquot from all samples in the experiment or group should be pooled. For plasma, 10 μL (for example) can be pooled from each sample and combined into one Eppendorf tube. Once mixed well, that pooled sample can be prepared alongside the other samples in the experiment. For tissue, equal weights of pulverized powder can be combined in a separate tube. Once mixed well, this pooled powder can be weighed out and prepared alongside other samples in the experiment. For cells, a reconstituted aliquot of cells (in an ammoniated buffer) can be pooled for each sample group. The advantage of pooling before extraction is that the sample can be maintained as a QC for future experiments using the same samples. If samples are pooled after extraction and reconstitution, an even volume from each sample can be pooled in to a separate LC vial prior to analysis. A dilution series of the pooled sample (e.g., 1:1, 1:2, 1:4, 1:8) analyzed at the end of a sequence can enable discrimination between artifacts and features of biological origin [19]. These samples are made post reconstitution and each contains an aliquot of the pooled QC with increasing amounts of isopropanol.
14. The standard reference material (SRM) can be used in addition to the pooled sample group QCs. The SRM can be prepared alongside samples every day of sample preparation. This SRM provides injections for inter- and intra-day variability comparisons and consistency of instrument and column quality. If pooled QCs are not made, representative samples from each sample group can be used to obtain lipid identification using MS/MS, *see* Subheading 3.3, steps 7 and 8.
15. The amount of internal standard spiked in should be comparable to the intensity level of endogenous lipids in the sample. The concentration of the internal standard required varies with the sample type but should be close to 10–15 ppm. The purpose of the extraction blank is to monitor the sample preparation reproducibility and to identify background interferences due to the sample preparation process. The volume of the Folch extraction solvents is dependent on the sample type. However, the final ratios of the solvents should be chloroform/methanol/water (8:4:3, v/v/v).

16. If the samples cannot be processed on the instrument on the same day, store the dried lipid extract at $-80\text{ }^{\circ}\text{C}$ until analysis.
17. Lipid extracts reconstituted with 100% IPA should undergo data acquisition on the same day to avoid sample degradation and lipid oxidation. Mammalian cell extracts containing 10^6 – 10^7 cells should be reconstituted in 50 μL of IPA. Plasma extracts (from 40 μL of plasma) should be reconstituted in 100 μL IPA. Tissue extracts (from 50 mg of tissue) should be reconstituted in 500 μL IPA. Do not use inserts in vials in this case. For HILIC analysis, the lipid extract should be reconstituted in no less than 80% acetonitrile.
18. Following initial blanks, two solvent blanks followed by QCs should be run and incremented every 10–15 sample injections. Sample injections must be randomized throughout the sequence. The sequence ends with the dilution series of the pooled sample, if available.
19. The column temperature was increased to $50\text{ }^{\circ}\text{C}$ to reduce the column back pressure when the gradient increases to 100% IPA.
20. In order to increase throughput for large-scale lipidomic studies, we recommend shorter chromatographic runs. Be aware that lipids with different fatty acid constituents, but the same total number of carbons and degrees of unsaturation are isomeric and will often coelute. This is especially problematic for triacylglycerides where over ten species identified by MS/MS for a given feature have been determined in our previous work (unpublished). Fig. 3 shows an example for TG(50:6) where increasing the time for chromatographic separation shows multiple peaks (Fig. 3b) which were indistinguishable in shorter chromatographic runs (Fig. 3a). Therefore, changes in

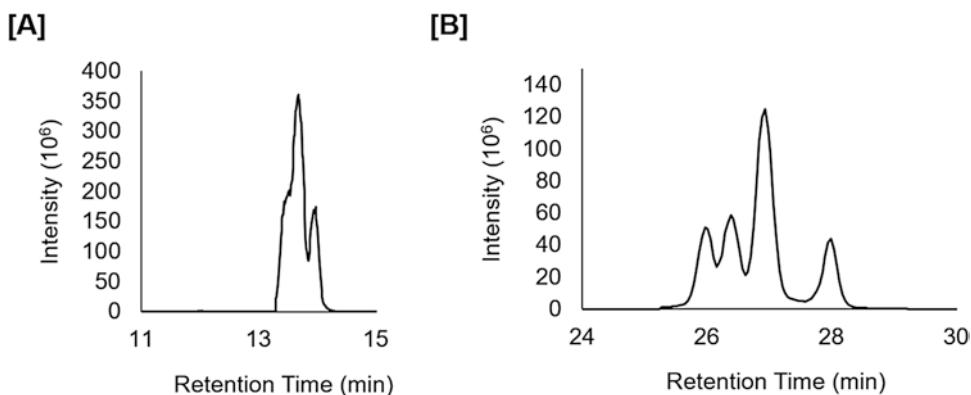


Fig. 3 Reconstructed ion chromatograms of ammoniated TG(50:6) ions using an 18 min chromatographic run (a) and a 45 min chromatographic run (b) on a Waters™ Acquity BEH C18 column. Short chromatographic runs exhibit features that often represent not one, but multiple lipid species

concentrations across sample groups for one feature might represent changes in an average of various lipid species. Even at longer (e.g., 70 min) chromatographic runs, TGs molecular species will often overlap.

21. Polarity switching reduces the number of scans across a peak significantly as it takes 1 s to switch between polarities for which time nearly four full scans can be acquired. In the case that more scans are desired across a peak (e.g., to improve deconvolution of closely eluting peaks), samples can be run in both positive and negative polarity separately, although this nearly doubles data acquisition time. In addition, lipid ions in negative mode are often at least an order of magnitude lower in signal than respective lipid ions in positive mode. In the case where the negative ion mode signal must be increased without increasing positive ion mode signal (due to saturation effects at high concentrations), separate negative mode analysis of more concentrated samples or separate analysis with higher injection volumes for negative mode can be performed. Note that higher injection volumes should not exceed 10 μL , as this could shift retention times.
22. For external calibration, less than a 3 ppm error in mass accuracy should be obtained in positive and negative polarity, with our lab consistently obtaining less than a 1 ppm error in mass accuracy. Lock masses greatly increase the accuracy of mass measurements. Lock masses used for positive ion mode were diisooctyl phthalate (m/z 391.2842) and polysiloxanes (m/z 371.1012 and 445.1200). No known background ions with stable signal across the entire chromatographic region are available to be used as lock masses in negative ion mode.
23. The m/z scan window was increased to m/z 1500 in order to include the $[\text{M}-\text{H}]^-$ adduct of the cardiolipin species.
24. When identifying features, assumptions should be clearly indicated in assigning a specific level of structural resolution. Note that not all lipid identification software annotates lipid structures based on MS/MS data properly, with the danger of over reporting structural resolution. Exact mass alone only gives tentative identification of lipid class and total carbons and double bonds, with class-specific fragments giving more confidence in identifications. If fragments containing fatty acid constituents occur, care should be taken in identifying lipids at this level. Using nominal mass isolation, fatty acid fragments could come from multiple coeluting species, including those without the same exact mass and from different lipid classes. A table of currently accepted notation for lipid assignment with the structural resolution determined by information obtained using mass spectrometry is provided for reference (Table 1).

Table 1
Lipid assignments using tandem mass spectrometry should take into account the structural resolution known. One problem in the field of lipidomics is over reporting structural resolution

Structural resolution	Example
Carbons and double bonds	PC(34:2)
Fatty acid constituents	PC(16:0_18:2)
Positional isomers	PC(16:0/18:2)
Double bond position	PC(16:0/18:2(9,12))
Double bond cis (Z) or trans (E)	PC(16:0/18:2(9Z, 12E))

25. The injection volume will change depending on the sample type. Inject at least 5 μ L for the mammalian cell lipid extracts. Because of the lower ion intensity observed in negative ionization mode, a larger injection volume may be required in which case, polarity switching cannot be used (*see Note 21*).
26. Files should be converted to an mzXML format to centroid the data and reduce the file size. The mzXML files can be directly uploaded to peak picking/detection software.
27. (1) XCMS [20] has an online and R script workflow that can be used for data processing. The built-in workflow was developed for filtering, peak picking/integration, peak matching, RT alignment, and gap filling. (2) The MZmine 2 [21] workflow used in our lab consists of creating a mass peak list, building chromatograms, smoothing chromatograms, peak deconvolution and integration (using a local minimum algorithm), deisotoping peaks, peak list alignment, gap filling, and filtering. A batch-processing file for MZmine containing optimized parameters for column-dependent lipidomic analysis can be created and applied to all samples. (3) MS-DIAL [22] can also be used with the same steps above as in MZmine for feature detection. In our lab MS-DIAL often crashed or outputted erroneous peak picking results when samples sizes greater than eight were used. The advantage of MS-DIAL is that it also incorporates the identification of the lipids using LipidBlast [23] libraries and either data-dependent fragmentation spectra or data-independent fragmentation spectra. While originally designed for SWATH, a text file containing AIF parameters can be used in conjunction with MS-DIAL to identify lipids from AIF data. Both MS-DIAL and MZmine provide user interfaces to view peaks and the resulting peak integration, while XCMS does not. Manual quality control of feature detection is an important step for insuring the correct parameters are used and data quality is sufficient for research goals.

28. MetaboAnalyst is an online processing and bioinformatics tool used to analyze and visualize statistical differences in complex lipidomic datasets [24, 25]. Options for univariate statistical analysis in MetaboAnalyst include fold change, *t*-test, volcano plots, ANOVA, correlations, and significance analysis of microarrays (SAM). Multivariate analysis platforms available include principal component analysis (PCA), partial least squares-discriminant analysis (PLS-DA). Clustering/classification options include, but are not limited to, random forest, *K*-means clustering, and hierarchical clustering. Additional data analysis/identification programs include the web-based MeltDB [26], commercial SIMCA-P software [27], and commercial SAS software.
29. Examples of lipidomic databases used for lipid identification include LIPID MAPS [28], the Human Metabolome Database (HMDB) [29], Metlin [30], vendor software, and *in-house* libraries. Software for annotating lipid structure based on fragmentation for LC-MS/MS data (*see Note 22*) includes LipidSearch [31, 32], MS-DIAL [22], and LipidMatch [33] or an *in-house* fragmentation library/software. The lipid identification software, LipidMatch [33], provides additional unique features in comparison to MS-Dial, including the ability to incorporate MZmine and XCMS outputs, to obtain structurally defined lipid assignments, and to mine simulated MS/MS libraries for oxidized lipids. Table 2 provides a list of 31 of the 56 lipid types with *in silico* fragmentation libraries in LipidMatch for identification of various lipid species. It is common to have less than 50% of features match annotations in databases, depending on thresholds used in peak detection and depth of libraries.

Table 2
Number of simulated fragments for selected lipid classes used by the LipidMatch software [33]

Class	Adducts	Species
Ac(2,3,4)PIM(1,2)	[M-H] ⁻	22,621
AcCa	[M+H] ⁺	53
(L)PC	[M+H] ⁺ , [M+Na] ⁺ , [M+HCO ₂] ⁻	779
LPC(O-34:2)	[M+H] ⁺ , [M+HCO ₂] ⁻	114
LPC(P-36:3)	[M+H] ⁺ , [M+HCO ₂] ⁻	228
(L)PE	[M+H] ⁺ , [M+Na] ⁺ , [M-H] ⁻	779
(L)PE(O-	[M+H] ⁺ , [M-H] ⁻	114
(L)PE(P-	[M+H] ⁺ , [M-H] ⁻	228
(L)PI	[M-H] ⁻ , [M+H] ⁺ , [M+NH ₄] ⁺	779
CE	[M+NH ₄] ⁺	38

(continued)

Table 2
(continued)

Class	Adducts	Species
Cer	[M+H] ⁺	1445
CerG	[M+H] ⁺	30
CerP	[M+H] ⁺ , [M-H] ⁻	169
CL	[M-2H] ⁻	3065
CoQ	[M+NH ₄] ⁺	5
DG	[M+NH ₄] ⁺	741
DGDG	[M+HCO ₂] ⁻	780
Ganglioside	[M-H] ⁻	1353
LipidA_PP	[M-H] ⁻	15,625
MMPE	[M-H] ⁻	742
DMPE	[M-H] ⁻	742
MG	[M+NH ₄] ⁺	50
MGDG	[M+NH ₄] ⁺ , [M+H] ⁺ , [M+NH ₄ -CO] ⁺	2305
Ox(L)PC	[M+H] ⁺ , [M+Na] ⁺ , [M+HCO ₂] ⁻	31,326
Ox(L)PE	[M+H] ⁺ , [M-H] ⁻ , [M+Na] ⁺	31,326
OxTG	[M+NH ₄] ⁺	8557
PA	[M-H] ⁻ , [M+H] ⁺	741
PG	[M-H] ⁻ , [M+NH ₄] ⁺ , [M+Na] ⁺	741
PS	[M-H] ⁻ , [M+H] ⁺ , [M+Na] ⁺	741
PS(O-	[M+H] ⁺ , [M-H] ⁻	114
PS(P-	[M+H] ⁺ , [M-H] ⁻	228
SM	[M+H] ⁺	1445
So	[M+H] ⁺	13
Sulfatide	[M-H] ⁻	169
TG	[M+NH ₄] ⁺	115,520

Acknowledgments

This work was supported by the Southeast Center for Integrated Metabolomics (SECIM)—NIH Grant #U24 DK097209.

References

1. Anonymous (2015) Major fats and oils industry overview. In: Chemical economics handbook. IHS Markit, London
2. Batenburg JJ (1992) Surfactant phospholipids: synthesis and storage. *Am J Phys* 262(4 Pt 1):L367–L385
3. Bhuyan S, Sundararajan S, Yao L, Hammond EG, Wang T (2006) Boundary lubrication properties of lipid-based compounds evaluated using microtribological methods. *Tribol Lett* 22(2):167–172. doi:10.1007/s11249-006-9076-x
4. Brennan L, Owende P (2010) Biofuels from microalgae—a review of technologies for production, processing, and extractions of biofuels and co-products. *Renew Sust Energ Rev* 14(2):557–577. doi:10.1016/j.rser.2009.10.009
5. Piazza GJ, Foglia TA (2001) Rapeseed oil for oleochemical usage. *Eur J Lipid Sci Technol* 103(7):450–454. doi:10.1002/1438-9312(200107)103:7<450::AID-EJLT450>3.0.CO;2-D
6. Uner M, Wissing SA, Yener G, Muller RH (2005) Skin moisturizing effect and skin penetration of ascorbyl palmitate entrapped in solid lipid nanoparticles (SLN) and nanostructured lipid carriers (NLC) incorporated into hydrogel. *Pharmazie* 60(10):751–755
7. Fernandis AZ, Wenk MR (2009) Lipid-based biomarkers for cancer. *J Chromatogr B Anal Technol Biomed Life Sci* 877(26):2830–2835. doi:10.1016/j.jchromb.2009.06.015
8. Kwan BCH, Kronenberg F, Beddhu S, Cheung AK (2007) Lipoprotein metabolism and lipid management in chronic kidney disease. *J Am Soc Nephrol* 18(4):1246–1261. doi:10.1681/asn.2006091006
9. Lukyanov AN, Torchilin VP (2004) Micelles from lipid derivatives of water-soluble polymers as delivery systems for poorly soluble drugs. *Adv Drug Deliv Rev* 56(9):1273–1289. doi:10.1016/j.addr.2003.12.004
10. Sutphen R, Xu Y, Wilbanks GD, Fiorica J, Grendys EC Jr, LaPolla JP, Arango H, Hoffman MS, Martino M, Wakeley K, Griffin D, Blanco RW, Cantor AB, Xiao YJ, Krischer JP (2004) Lysophospholipids are potential biomarkers of ovarian cancer. *Cancer Epidemiol Biomarkers Prev* 13(7):1185–1191
11. Yetukuri L, Ekroos K, Vidal-Puig A, Oresic M (2008) Informatics and computational strategies for the study of lipids. *Mol Biosyst* 4(2):121–127. doi:10.1039/b715468b
12. Lintonen TP, Baker PR, Suoniemi M, Ubhi BK, Koistinen KM, Duchoslav E, Campbell JL, Ekroos K (2014) Differential mobility spectrometry-driven shotgun lipidomics. *Anal Chem* 86(19):9662–9669. doi:10.1021/ac5021744
13. Lin J, Snyder L, McKeon TA (1998) Prediction of relative retention times of triacylglycerols in non-aqueous reversed-phase high-performance liquid chromatography. *J Chromatogr* 808(1):43–49. doi:10.1016/S0021-9673(98)00134-4
14. Ulmer CZ, Yost RA, Chen J, Mathews CE, Garrett TJ (2015) Liquid chromatography-mass spectrometry metabolic and lipidomic sample preparation workflow for suspension-cultured mammalian cells using Jurkat t lymphocyte cells. *J Proteomics Bioinform* 8(6):126–132. doi:10.4172/jpb.1000360
15. Reis A, Rudnitskaya A, Blackburn GJ, Mohd Fauzi N, Pitt AR, Spickett CM (2013) A comparison of five lipid extraction solvent systems for lipidomic studies of human LDL. *J Lipid Res* 54(7):1812–1824. doi:10.1194/jlr.M034330
16. Silva LP, Lorenzi PL, Purwaha P, Yong V, Hawke DH, Weinstein JN (2013) Measurement of DNA concentration as a normalization strategy for metabolomic data from adherent cell lines. *Anal Chem* 85(20):9536–9542. doi:10.1021/ac401559v
17. Matyash V, Liebisch G, Kurzchalia TV, Shevchenko A, Schwudke D (2008) Lipid extraction by methyl-tert-butyl ether for high-throughput lipidomics. *J Lipid Res* 49(5):1137–1146. doi:10.1194/jlr.D700041-JLR200
18. Patterson RE, Ducrocq AJ, McDougall DJ, Garrett TJ, Yost RA (2015) Comparison of blood plasma sample preparation methods for combined LC-MS lipidomics and metabolomics. *J Chromatogr B Anal Technol Biomed Life Sci* 1002:260–266. doi:10.1016/j.jchromb.2015.08.018
19. Vorkas PA, Isaac G, Anwar MA, Davies AH, Want EJ, Nicholson JK, Holmes E (2015) Untargeted UPLC-MS profiling pipeline to expand tissue metabolome coverage: application to cardiovascular disease. *Anal Chem* 87(8):4184–4193. doi:10.1021/ac503775m
20. Smith CA, Want EJ, O’Maille G, Abagyan R, Siuzdak G (2006) XCMS: processing mass spectrometry data for metabolite profiling using nonlinear peak alignment, matching, and identification. *Anal Chem* 78(3):779–787. doi:10.1021/ac051437y
21. Pluskal T, Castillo S, Villar-Briones A, Orešič M (2010) MZmine 2: modular framework for processing, visualizing, and analyzing mass spectrometry-based molecular profile data. *BMC Bioinformatics* 11(1):1–11. doi:10.1186/1471-2105-11-395

22. Tsugawa H, Cajka T, Kind T, Ma Y, Higgins B, Ikeda K, Kanazawa M, VanderGheynst J, Fiehn O, Arita M (2015) MS-DIAL: data-independent MS/MS deconvolution for comprehensive metabolome analysis. *Nat Methods* 12(6):523–526. doi:[10.1038/nmeth.3393](https://doi.org/10.1038/nmeth.3393)
23. Kind T, Liu KH, Lee DY, DeFelice B, Meissen JK, Fiehn O (2013) LipidBlast in silico tandem mass spectrometry database for lipid identification. *Nat Methods* 10(8):755–758. doi:[10.1038/nmeth.2551](https://doi.org/10.1038/nmeth.2551)
24. Xia J, Wishart DS (2011) Web-based inference of biological patterns, functions and pathways from metabolomic data using MetaboAnalyst. *Nat Protoc* 6(6):743–760. doi:[10.1038/nprot.2011.319](https://doi.org/10.1038/nprot.2011.319)
25. Xia J, Mandal R, Sinelnikov IV, Broadhurst D, Wishart DS (2012) MetaboAnalyst 2.0--a comprehensive server for metabolomic data analysis. *Nucleic Acids Res* 40(Web Server issue):W127–W133. doi:[10.1093/nar/gks374](https://doi.org/10.1093/nar/gks374)
26. Kessler N, Neuweger H, Bonte A, Langenkamper G, Niehaus K, Nattkemper TW, Goesmann A (2013) MeltDB 2.0--advances of the metabolomics software system. *Bioinformatics* 29(19):2452–2459. doi:[10.1093/bioinformatics/btt414](https://doi.org/10.1093/bioinformatics/btt414)
27. Wu Z, Li D, Meng J, Wang H (2010) Introduction to SIMCA-P and its application. In: Esposito V, Chin W, Henseler J, Wang H (eds) *Handbook of partial least squares: concepts methods and applications*. Springer, Berlin, Heidelberg, pp 757–774
28. Fahy E, Subramaniam S, Murphy RC, Nishijima M, Raetz CR, Shimizu T, Spener F, van Meer G, Wakelam MJ, Dennis EA (2009) Update of the LIPID MAPS comprehensive classification system for lipids. *J Lipid Res* 50(Suppl):S9–14. doi:[10.1194/jlr.R800095-JLR200](https://doi.org/10.1194/jlr.R800095-JLR200)
29. Wishart DS, Tzur D, Knox C, Eisner R, Guo AC, Young N, Cheng D, Jewell K, Arndt D, Sawhney S, Fung C, Nikolai L, Lewis M, Coutouly MA, Forsythe I, Tang P, Shrivastava S, Jeroncic K, Stothard P, Amegbey G, Block D, Hau DD, Wagner J, Miniaci J, Clements M, Gebremedhin M, Guo N, Zhang Y, Duggan GE, Macinnis GD, Weljie AM, Dowlatbadi R, Bamforth F, Clive D, Greiner R, Li L, Marrie T, Sykes BD, Vogel HJ, Querengesser L (2007) HMDB: the human metabolome database. *Nucleic Acids Res* 35(Database issue):D521–D526. doi:[10.1093/nar/gkl923](https://doi.org/10.1093/nar/gkl923)
30. Smith CA, O'Maille G, Want EJ, Qin C, Trauger SA, Brandon TR, Custodio DE, Abagyan R, Siuzdak G (2005) METLIN: a metabolite mass spectral database. *Ther Drug Monit* 27(6):747–751
31. Taguchi R, Nishijima M, Shimizu T (2007) Basic analytical systems for lipidomics by mass spectrometry in Japan. *Methods Enzymol* 432:185–211. doi:[10.1016/s0076-6879\(07\)32008-9](https://doi.org/10.1016/s0076-6879(07)32008-9)
32. Taguchi R, Ishikawa M (2010) Precise and global identification of phospholipid molecular species by an Orbitrap mass spectrometer and automated search engine lipid search. *J Chromatogr A* 1217(25):4229–4239. doi:[10.1016/j.chroma.2010.04.034](https://doi.org/10.1016/j.chroma.2010.04.034)
33. Koelmel JP, Kroeger NM, Gill EL et al (2017) Expanding lipidome coverage using LC-MS/MS data-dependent acquisition with automated exclusion list generation. *J Am Soc Mass Spectrom* 1–10. doi:[10.1007/s13361-017-1608-0](https://doi.org/10.1007/s13361-017-1608-0)

Chapter 11

Combined Use of MALDI-TOF Mass Spectrometry and ^{31}P NMR Spectroscopy for Analysis of Phospholipids

Jenny Schröter*, Yulia Popkova*, Rosmarie Süß, and Jürgen Schiller*

Abstract

Lipids are important and abundant constituents of all biological tissues and body fluids. In particular, phospholipids (PL) constitute a major part of the cellular membrane, play a role in signal transduction, and some selected PL are increasingly considered as potential disease markers. However, methods of lipid analysis are less established in comparison to techniques of protein analysis. Mass spectrometry (MS) is an increasingly used technique to analyze lipids, especially in combination with electrospray ionization (ESI) MS which is the so far best established ionization method. Matrix-assisted laser desorption/ionization time-of-flight (MALDI-TOF) MS has itself proven to be also useful in the field of lipid analysis. ^{31}P nuclear magnetic resonance (NMR) spectroscopy is another powerful method of PL analysis, represents a direct quantitative method, and does not suffer from suppression effects.

This chapter gives an overview of methodological aspects of MALDI-TOF MS and ^{31}P NMR in lipid research and summarizes the specific advantages and drawbacks of both methods. In particular, suppression effects in MS will be highlighted and possible ways to overcome this problem (use of different matrices, separation of the relevant lipid mixture prior to analysis) will be discussed.

Key words Glycerophospholipids, Lipid analysis, MALDI-TOF MS, Lipid extracts, Matrix, ^{31}P NMR spectroscopy

1 Introduction

1.1 Lipids and Lipid Analysis

Lipids were over decades primarily considered as (1) energy source in nutrition, (2) an effective way to store superfluous energy, and (3) the cellular *packing material* of more important contents, particularly proteins and nucleic acids, within a cell [1, 2]. Nowadays, however, some lipids and particularly PL such as phosphatidic acids or polyphosphoinositides are known to represent important second messenger molecules involved in cellular communication and inflammation [3]. Additionally, lipids such as lysophosphatidylcholines (LPC), which are derived from

*Jenny Schröter, Yulia Popkova, and Jürgen Schiller contributed equally to this work.

phosphatidylcholine (PC) by the removal of one fatty acyl residue, were also recognized as important disease markers, for instance, in atherosclerosis or rheumatoid arthritis [4, 5]. LPC is also increasingly discussed as a measure of the fertilizing ability of human spermatozoa [6]. Accordingly, in addition to terms such as proteomics, genomics, or metabolomics, the term lipidomics [7, 8] was also introduced. In a nutshell, the interest in PL and their analysis has significantly increased in this millennium.

Protocols of lipid analysis are less developed compared to protein analysis. One potential reason is the considerable diversity of lipids which comprises differences in the headgroup (e.g., choline or ethanolamine), the linkage type between the apolar alkyl chains and the glycerol (diacyl, alkyl-acyl- or alkenyl-acyl), and, finally, the large variability of potential fatty acyl or alkyl residues [9]. Therefore, very complex lipid patterns must be expected if crude biological extracts are analyzed.

Although both chromatographic techniques, high-performance liquid chromatography (HPLC) [10] and thin-layer chromatography (TLC) [11], are well established, in the majority of cases a two-dimensional approach (different stationary phases) is necessary: normal phase chromatography is required for the separation of lipids according to their headgroups, whereas reversed phase chromatography is regularly used for the differentiation of lipids according to their fatty acyl or alkyl compositions [11]. Another problem is the detection of lipids within the obtained fractions. If, for instance, an ultraviolet (UV) detector is used, lipids with unsaturated fatty acyl residues are primarily detected, whereas UV detection is not suitable for the detection of lipids with saturated residues because there is no significant UV absorption [1].

Mass spectrometry is increasingly used for the analysis of lipid mixtures [12]. Although ESI MS [13] (either combined with HPLC or as shotgun approach) is the method of choice for lipids, there is increasing evidence that MALDI-TOF MS is also a useful method [2]. The particular advantages of MALDI MS are the convenient handling and the high sensitivity which enables (at least in selected cases) the detection of just a few lipid molecules [14]. The use of MALDI-TOF MS for lipid and PL analysis has been recently reviewed [2, 15] and compared with other MS methods of lipid analysis [16].

Of course, there are also useful spectroscopic methods of lipid analysis, whereby NMR is in our opinion the most powerful method [17]. We will focus here on ^{31}P NMR spectroscopy because this method has some significant advantages in comparison to ^1H and ^{13}C NMR which are summarized in Table 1 and compared with other methods of lipid analysis.

Table 1
Experimental approaches frequently used to determine the PL classes as well as the related fatty acyl compositions

Technique	Applicable to	Advantages	Disadvantages
<i>Mass Spectrometry</i>			
MALDI	All (polar and apolar) lipid classes.	Simple, fast, and sensitive technique. Sample impurities (e.g., salts, detergents) are tolerated. May be easily combined with TLC (desorption technique).	Ion suppression may play a significant role. Limited quantitative data analysis due to irregularities of the crystallization process.
ESI	Principally all lipid classes. Apolar lipids are more difficult than polar compounds.	Can be easily coupled to HPLC. Therefore, suitable for the screening of complex mixtures. Most frequently used in lipid analysis.	Individual lipid classes are detected with different sensitivities. Signal suppression may occur when crude mixtures are analyzed. Sensitive to contaminants (buffers, salts, detergents).
<i>Nuclear Magnetic Resonance (NMR) Spectroscopy</i>			
³¹ P NMR	Phospholipids (at least without derivatization).	Nondestructive. Direct, absolute quantitative analysis of virtually all PL.	Expensive equipment. Relatively low sensitivity. High concentrations of detergent are needed.
¹ H NMR	All lipids.	Nondestructive. More sensitive than ³¹ P NMR.	Crowded spectra when mixtures are analyzed. Expensive equipment. Highly purified solvents required (for diluted samples).
¹³ C NMR	All lipids.	Nondestructive. Enables structure determination (of purified compounds). Provides excellent spectral resolution.	Mixtures of lipids give crowded spectra. Expensive equipment. Very low sensitivity.
<i>Chromatography</i>			
Thin-layer chromatography (TLC)	All lipid classes (solvent system must be adjusted according to the lipid mixture and the stationary phase).	Simple, fast, and inexpensive. Well-established method. Can be easily implemented in all laboratories. Densitometric analysis of spot intensities is possible.	Provides only limited resolution.
High-performance liquid chromatography (HPLC)	All lipid and PL classes (after establishment of a suitable solvent system).	Differentiation of individual lipid classes (normal phase) and fatty acid composition (reversed phase) established. Many well-established methods available.	Relatively large solvent amounts needed. Memory effects may occur.
Gas chromatography (GC)	Works exclusively with volatile compounds. Hydrolysis and derivatization of PL is required prior to fatty acid analysis.	Method of choice to determine the fatty acid composition of mixtures. Excellent resolving power.	Requires volatile compounds and/or derivatization to enhance volatility.

1.2 Strengths of MALDI-TOF MS and ^{31}P NMR in Lipidomics

Since MALDI MS and ^{31}P NMR are very different analytical methods, there were so far not many attempts to compare and to discuss the individual strengths and weaknesses of both techniques [18, 19]. A comprehensive treatise of all related methodological aspects is surely beyond the scope of this short contribution. Therefore, we will focus here on a very few selected aspects: (1) sensitivity—there is no doubt that MS is much more sensitive than NMR! Samples in the μg range (or even lower) are typically used in MS while mg amounts are normally required for successful NMR experiments. This limits the application of NMR to samples which are available in relatively large amounts. (2) Resolving power—MS is surely capable of resolving very small molecular weight differences (at high resolution mass spectrometers less than 1 mDa) but fails to resolve isomeric compounds which have identical masses. If the analysis of isomeric lipids is relevant, previous HPLC separation, tandem MS or combination between MS and ion mobility spectrometry (IMS) [20] is required. We will show here that isomeric PL can be differentiated by ^{31}P NMR already in a simple one-dimensional spectrum. (3) Mixture analysis—This is the most important advantage of NMR! While MS may suffer (depending on the composition of the sample) from strong ion suppression effects [21], NMR is affected only to a minor extent by the sample composition. That is, all relevant PL classes will be detectable in a mixture—at least if the spectral resolution is sufficiently high to enable the differentiation of the individual resonances.

2 Materials

2.1 MALDI-TOF MS

1. Bruker Autoflex MALDI-TOF mass spectrometer (Bremen, Germany) equipped with reflectron, delayed extraction (DE) facility and N_2 laser emitting at 337 nm. The capability to record positive and negative ion spectra must be available (*see Note 1*).
2. MALDI targets made from stainless steel or from aluminum with gold-coated surface (*see Note 2*).
3. Micropipettes (*see Note 3*).
4. Glass (Hamilton) syringes of different sizes.
5. Small, single-use glass vessels for mixing matrix and sample or for diluting stock solutions of lipids (e.g., Knauer, Berlin, Germany).
6. Heat gun or common hair dryer (*see Note 4*).

2.2 ^{31}P NMR Spectroscopy

1. High resolution NMR spectrometer (Bruker BioSpin GmbH, Rheinstetten, Germany). In the optimum case, the device

should be equipped with a narrow bore magnet and the field strength should be at least 7 T (i.e., the ¹H resonance frequency is 300 MHz and that of ³¹P 121.5 MHz) (*see Note 5*).

2. Three channel NMR probe tunable to the resonance frequency of ³¹P (first channel). A *lock* (²H) channel should be available and ¹H decoupling should be possible. Additionally, a thermostat which warrants that all spectra can be recorded at identical temperatures is mandatory.
3. NMR sample tubes with a diameter of 5 mm (*see Note 6*).
4. Micropipettes (*see Note 3*).
5. Sonifier or ultrasound bath.

2.3 Reagents and Biological Mixtures

1. Stock solutions of 1-palmitoyl-2-oleoyl-*sn*-phosphatidylcholine (POPC), -ethanolamine (POPE), and -glycerol (POPG) in chloroform (e.g., Avanti Polar Lipids, Alabaster, AL, USA). These stock solutions should be diluted with chloroform to a concentration of 1 mg/mL.
2. 2,5-Dihydroxybenzoic acid (DHB) and 9-aminoacridine (9-AA) of highest available purity as MALDI matrices (*see Note 7*). DHB is dissolved in methanol (0.5 M) whereas a 10 mg/mL solution of 9-AA is prepared in isopropanol/acetonitrile (60/40 volume ratio). All solvents should be of the highest commercially available quality (*see Note 8*).
3. 50 mM 4-(2-Hydroxyethyl)piperazine-1-ethanesulfonic acid (HEPES) buffer (pH 7.65) containing 200 mM sodium cholate (to suppress the aggregation of PL) and 5 mM ethylenediaminetetraacetic acid (EDTA, disodium salt) (to reduce the line-broadening effects of paramagnetic ions such as iron or copper which may be bound to negatively charged PL). This solution is best prepared in D₂O to provide a sufficient field frequency lock [22].
4. A small amount of hen egg yolk or any other biological fluid or tissue extract. The hen egg yolk can be prepared as follows: Break the eggshell and separate yolk and egg white. Treat the egg yolk with the about twentyfold amount (by weight) of Bligh & Dyer solvent [23] mixture (chloroform:methanol:water in 1:1:0.9 volume ratio) and vortex the resulting turbid mix for a few minutes. Subsequently centrifuge the sample (10 min, 2000 rpm (ca. 400 g), 20 °C) in order to improve the separation of the organic (bottom) and the water/methanol phase (*see Note 9*). Remove the organic (lower) chloroform phase by a Hamilton syringe and transfer it to another unused vial. Do not try to get the complete organic phase in order to avoid the introduction of impurities from the aqueous layer. The lipid concentration (which can be obtained by weighing) is of the order of 15–25 mg/mL.

3 Methods

3.1 Sample Processing

1. MALDI-TOF MS of artificial lipid samples of known composition
 - (a) If sufficient amounts of samples are available, the use of stock solutions in the mg/mL concentration range is recommended—although MS is actually much more sensitive. Therefore, dilute the available lipid samples to about 1 mg/mL with chloroform. Mix one equivalent of the lipid standard solution with either one volume equivalent of DHB or 9-AA matrix solution.
 - (b) Apply the prepared samples to the MALDI target. Do not be surprised if a very large spot is formed and the sample spreads out over the sample plate. This is caused by the smaller surface tension of organic solvents (methanol $\sim 23 \times 10^{-3}$ N/m; acetonitrile $\sim 29 \times 10^{-3}$ N/m; isopropanol $\sim 22 \times 10^{-3}$ N/m) in comparison to water ($\sim 73 \times 10^{-3}$ N/m). Avoid touching the MALDI target with the pipette tip or the needle of the Hamilton syringe because this might negatively affect homogeneous crystallization. The MALDI target should also not be touched with the fingers (but gloves should be worn) to avoid potential contaminations with skin lipids.
 - (c) Evaporate the solvent quickly by drying the sample plate with a hairdryer and load the prepared sample plate directly into the mass spectrometer. Avoid long-term exposition to air: Due to the large surface of the lipid film on the MALDI target, unsaturated lipids may be oxidized (*see Note 10*).
2. MALDI-TOF MS of the lipids in the hen egg yolk extract
 - (a) The obtained crude hen egg yolk lipid extract may be directly used for MALDI-TOF MS by simple dilution of the organic solution with the prepared matrix solution (about 1:10 volume ratio).
 - (b) Use the same method of sample preparation as described in the context of the artificial lipids.

3.2 Preparation of the ^{31}P NMR Samples

1. Take 100 μL of the obtained, original, concentrated egg yolk extract and evaporate the organic solvent under reduced pressure.
2. Resolubilize the lipid residue in about 600 μL of the detergent solution described above (Subheading 2.3). Vortex the sample until all the material has dissolved. If the sample remains opaque, use a sonifier and/or slight heating to convert the obtained suspension into a clear *solution*. This sample can be directly used for NMR but should be allowed to equilibrate for a few hours at room temperature (*see Note 11*).

3.3 Recording MALDI-TOF Mass Spectra

1. Due to the large number of MALDI mass spectrometers that are available from different suppliers, it is impossible to describe the necessary experimental parameters in detail. Therefore, please consult the manual of your device for a suitable data file to start with. You should start with DE conditions and use the reflectron of the device. This results in higher resolution which is particularly beneficial if relatively small compounds are analyzed.
2. It is recommended to start in all cases with the analysis of a known sample of known concentration in order to check if the MS device is properly working and if all parameters are adequately set. This known sample may also be used to check the mass accuracy, i.e., the quality of the applied mass calibration file, as well as the resolution achievable at these instrumental settings. The applied laser fluence normally has the most pronounced effect on the spectral quality [24]. The laser fluence should be set as low as possible.
3. Take always care that the MALDI target is carefully dried before it is inserted into the mass spectrometer in order to avoid a significant decrease of the vacuum—and waiting time until the necessary vacuum is re-established.
4. It is not true that the signal-to-noise (S/N) ratio may be enhanced by increasing the laser fluence. Although absolute signal intensities may be enhanced at elevated laser intensities, the quality of the baseline simultaneously gets poor since more fragment ions are generated. Therefore, the laser intensity should be set as high as needed but as low as possible.
5. Try to move the laser randomly over the sample plate in order to average nonhomogeneous spots resulting from the sample preparation. It is, however, not possible to improve the S/N ratio by averaging a larger number of individual laser shots [25] because the level of unspecific chemical background noise forms the limiting criterion.
6. Try to optimize the required parameters always with a known sample and use these parameters afterwards for the unknown samples, i.e., the organic hen egg yolk extract.

3.4 ³¹P NMR Spectroscopy

1. Load the sample into the magnet of your NMR spectrometer.
2. Set T = 310 K and allow the sample to equilibrate for at least 30 min.
3. Find the lock (²H) signal of the deuterated solvent and lock in.
4. Tune and match the probe to ³¹P (first channel) and ¹H (decoupler channel).
5. Load a suitable dataset for ³¹P.
6. Determine the 90° pulse for ³¹P and the decoupler (¹H) pulse. Follow the instructions given in your NMR spectrometer handbook or in [26].

7. Determine the most suitable receiver gain and record a one-dimensional ^{31}P (^1H decoupled) spectrum. Ensure that the number of points (time domain) is high enough to record the entire free induction decay (FID).
8. Use Fourier transformation to convert your data from intensity versus time to intensity versus frequency, i.e., generate a *spectrum*. Apply a line-broadening factor of not more than 2 Hz. Phase correct your spectrum and set the resonance of PC (normally the most intense one at the right end of the spectrum) to -0.65 ppm.
9. Integrate all observed resonances.

3.5 Results

A coarse overview about the shape of the positive and negative ion MALDI-TOF mass spectra of different PL (as well as their characteristic headgroups) in the presence of two different matrices is shown in Fig. 1. The polarity of the measurements (positive or negative) is indicated directly in the spectra. POPC (Fig. 1a), POPE (Fig. 1b, c), and POPG (Fig. 1c, f) were chosen as typical PL because they are abundant in biological materials but differ in their charge states: POPC and POPE are zwitterionic (but overall neutral) phospholipid, whereas POPG is negatively charged at physiological pH 7.4. In Fig. 1d, g the positive and negative ion spectra, respectively, of 1:1:1 mixtures of these PL are shown to illustrate the problems of mixture analysis by MALDI-TOF MS. However, the situation would be very similar if ESI MS instead of MALDI would be used.

It is evident that the spectra differ significantly: POPC gives—in the presence of the DHB matrix—two signals at m/z 760.6 and 782.6 in the positive ion mode corresponding to the generation of the H^+ and the Na^+ adduct (Fig. 1a). Due to the permanent positive charge of the quaternary ammonia group [27], PC is not (or only with very low intensity) detectable as negative ion under the applied conditions (data not shown) [28].

It is important to note that the PC does not give any fragmentation products under these conditions. In contrast, the PE (Fig. 1b) and the PG (Fig. 1c) give significant yields of a fragment ion that corresponds to the loss of the polar headgroup [2]. As the fatty acyl composition is identical, both compounds give the same fragment at m/z 577.5. Additionally, it is evident that the POPE with a monoisotopic neutral mass of 717.5 g/mol gives only rather small yields of the H^+ adduct (m/z 718.5) but significant amounts of the Na^+ adduct (m/z 740.5) as well as the Na^+ adduct subsequent to the exchange of one H^+ by one Na^+ (m/z 762.5) [28]. The latter adduct is caused by the exchangeable protons of the $-\text{NH}_3^+$ group but not seen in the case of PC. The reason why POPE and POPG give more pronounced fragmentation products (m/z 577.5) than POPC is not yet known. However, it is possible that

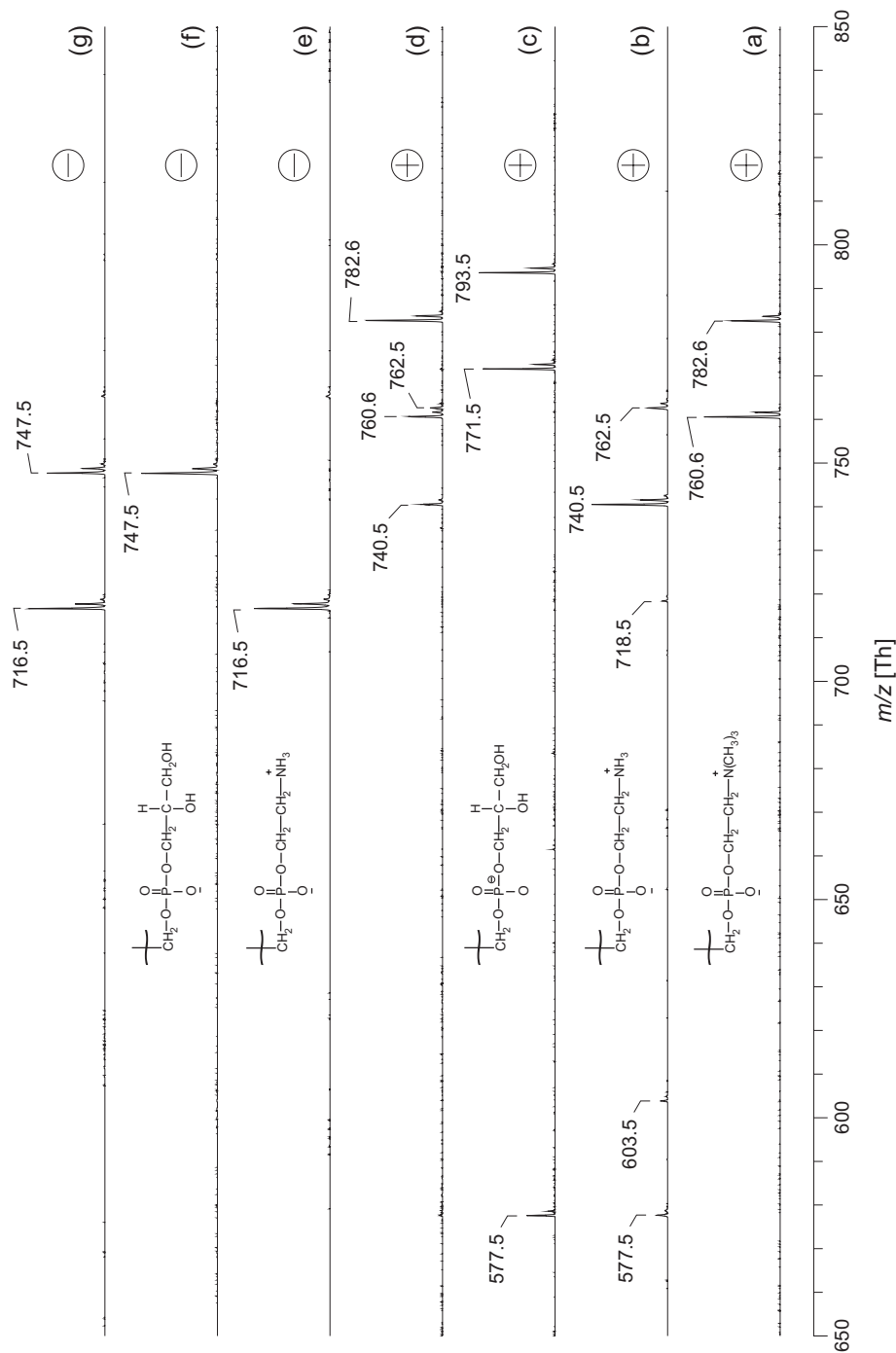


Fig. 1 Positive and negative ion MALDI-TOF mass spectra of 1-palmitoyl-2-oleoyl-*sn*-phosphatidylcholine (POPC; **a**), 1-palmitoyl-2-oleoyl-*sn*-phosphatidylethanolamine (POPE; **b, e**), 1-palmitoyl-2-oleoyl-*sn*-phosphatidylglycerol (POPG; **c, f**) and a 1:1 mixture of these three compounds (**d, g**). The polarities of the measurements are indicated directly at the individual spectra. Positive ion spectra were recorded with a 0.5 M solution of DHB in methanol, whereas a 10 mg/mL solution of 9-AA in isopropanol:acetonitrile (60:40 volume ratio) was used as matrix for the negative ion spectra. PL sample solutions (1 mg/mL in CHCl_3) were diluted in 1:1 volume ratio with the corresponding matrix and afterwards spotted onto the MALDI target. All peaks are marked according to their m/z ratios and the structures of the headgroups of the relevant PL classes are also given

the stability of the H^+ adduct of POPE is not high enough to allow these ions to reach the mass analyzer. A similar observation was already made in the case of triacylglycerols [29], where no H^+ adducts were detectable at all, even if the spectra were recorded from acidified solutions.

Using 9-AA as an alkaline matrix [28], POPE is also detectable as negative ion at m/z 716.5 (Fig. 1e). Note that the detectability of POPE as negative ion (data not shown) in the presence of DHB would be very low due to the acidic properties of this matrix. POPG can be detected as negative ion in the presence of DHB (data not shown) as well as 9-AA (Fig. 1f; m/z 747.5) as negative ion because of its enhanced acidity in comparison to POPE.

Significant differences are obtained between the positive and the negative ion spectra regarding mixture analysis: in the positive ion mode (Fig. 1d), the spectrum of the POPC/POPE/POPG mixture is clearly dominated by the POPC (m/z 760.6 and 782.6). The POPE is only detectable with low intensity (m/z 740.5 and 762.5) although it is present in the same amount as the POPC. POPG is (due to its negative charge) not detectable at all under these conditions. Therefore, the presence of PC prevents the detection of other PL species in mixtures [21, 30].

In contrast, the POPC is completely absent in the negative ion spectrum (Fig. 1g) and only POPE and POPG are detectable in the mixture. Although this is indeed a very simple example, it is evident that mixture analysis by MALDI-TOF MS must be regarded with great caution—at least if only one polarity mode is considered.

The problem of signal suppression is even more evident if the organic hen egg yolk extract is investigated (Fig. 2). The hen egg yolk extract was chosen as an educational example because it can be easily prepared with good reproducibility and is available in huge amount.

The polarities of the measurements and the used matrices are directly indicated in the spectra (Fig. 2) and the most intense peaks are directly assigned to the corresponding PL. The positive ion spectra recorded in the presence of either DHB or 9-AA are similar: the by far most intense peaks correspond to the H^+ adducts of PC 16:0/18:2 (m/z 758.6) and PC 16:0/18:1 (m/z 760.6). Unfortunately, the assignments of some smaller peaks are not straightforward. For instance, m/z 810.6 might be stemming from the H^+ adduct of PC 18:0/20:4 or the Na^+ adduct of PC 18:0/18:1. This assignment problem can be overcome, without the need to use tandem MS (MS/MS) or more sophisticated MS methods, when the 9-AA spectrum is considered because 9-AA is known to generate nearly exclusively the H^+ adducts [31]. Therefore, m/z 788.6 (Fig. 2b) can be unequivocally assigned to the H^+ adduct of PC 18:0/18:1. This simple approach makes assignments possible even if only a mass spectrometer with a limited resolution is available.

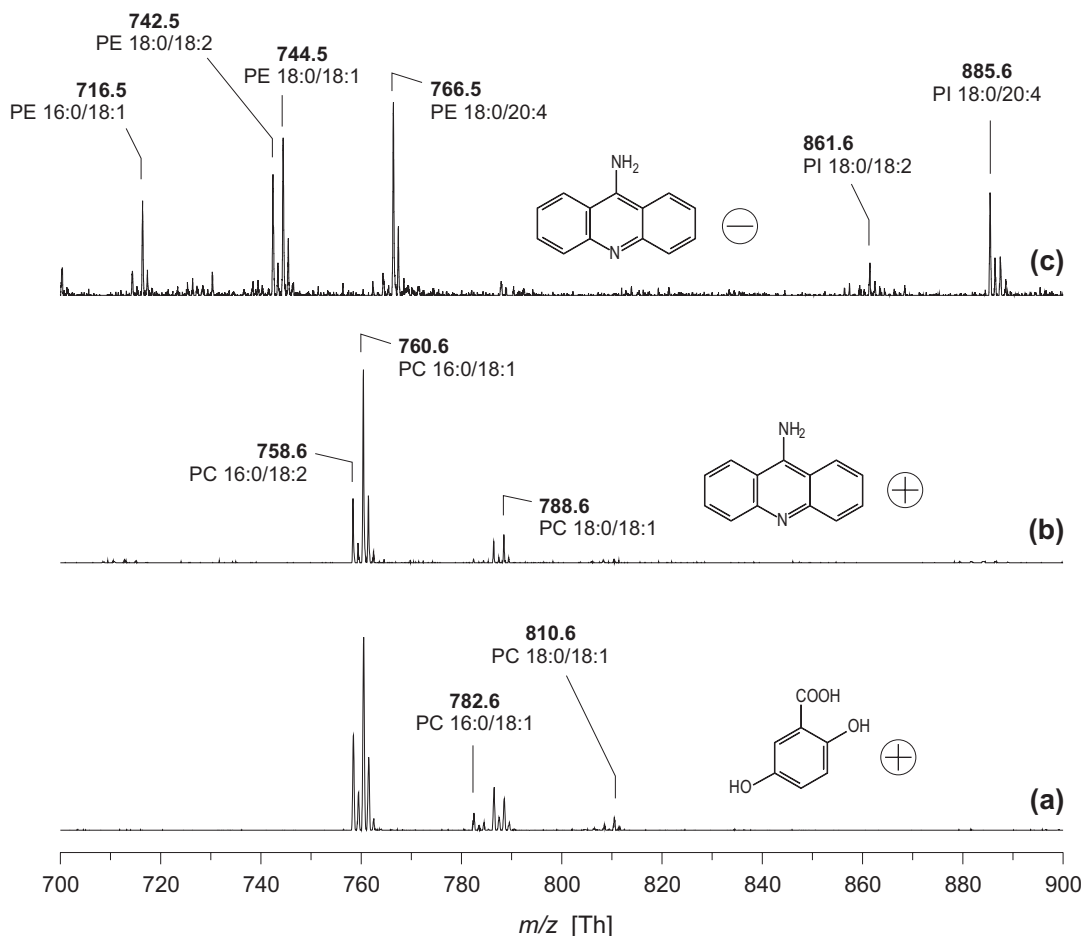


Fig. 2 Positive and negative ion MALDI-TOF mass spectra of an organic hen egg yolk extract (**a** positive ion, DHB; **b** positive ion, 9-AA; **c** negative ion, 9-AA). Polarities of the measurements, the used matrices, and assignments of the most prominent peaks are given at the relevant spectra. Note the complete suppression of PE and PI in the presence of PC in the positive ion mode spectra

Anyway, the positive ion spectra seem to suggest the exclusive presence of PC species and neither PE nor phosphatidylinositol (PI) can be detected, because these species are completely suppressed by the PC [21]. However, this problem can be overcome by using the negative ion spectrum which is shown at the top of Fig. 2 (trace 2c). The presence of different PE and PI species is obvious and assignments are straightforward because each PL species results in just a single peak and interferences with PC species can be completely excluded. Using these data, the relative compositions of PL mixtures can be easily determined by using the intensity of a dedicated peak and dividing this intensity by the sum of the intensities of all peaks of a dedicated PL class. However, what can be done if absolute concentrations and not only relative amounts are required?

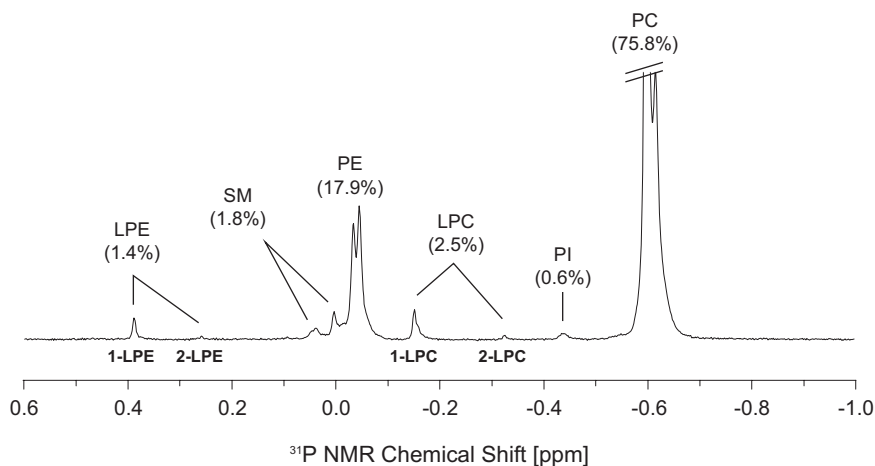


Fig. 3 High resolution ^{31}P NMR spectrum of a total hen egg yolk extract. The spectrum was recorded in aqueous sodium cholate (pH 7.65) in order to suppress PL aggregation and, thus, to maximize resolution. All peaks are assigned to the corresponding PL class, and the relative contributions of the individual resonances with reference to the total phosphorus content are also provided. Please note that some PL classes give rise to more than one resonance. Additionally, migration of the fatty acyl residue in lysophospholipids occurs in protic solvents and detergents. Thus, LPE and LPC show two resonances each. Sphingomyelin (SM) results in two resonances due to differences in the chain lengths of the different species

If absolute data are required, the addition of internal standards (in the optimum case the addition of one deuterated lipid per each lipid class) is mandatory. Unfortunately, this is quite expensive and requires a first rough knowledge about the amounts of lipid to avoid the addition of an excess of the standard.

If NMR is available, absolute quantitative information can be also obtained in the presence of just a single PL standard. This is illustrated by the ^{31}P NMR spectrum of hen egg yolk in Fig. 3. As it can be easily seen each PL is characterized by a dedicated chemical shift which makes spectral separation of the PL quite simple. The relative contributions of the different PL classes can be easily calculated into absolute amounts as soon as there is one internal standard which is present in a known concentration. It is also obvious that some PL resonances do not appear as singlets but are split into two resonances. This is caused by differences in the fatty acyl compositions which can be, however, only partially resolved [32].

4 Notes

1. Of course, all commercially available MALDI-TOF MS devices can be used independent of the company. If product or company names are provided here, this only means that these dedicated products were used for performing the illustrated

experiments. This is sometimes important as different nomenclatures are used. For instance, DE and energy lag focusing are synonyms and mean the same—improvement of resolution. However, MALDI-TOF mass spectrometers which are exclusively capable of recording linear mode spectra are less suitable for lipid analysis because resolution as well as mass accuracy is reduced in comparison to reflector mode spectra.

2. Under the conditions described here, the co-crystals between matrix and analyte give a relatively thick layer (about 100 μm) on the target. Only the upper layers are ablated by the laser because UV irradiation does not penetrate deeply into the sample. Therefore, the MALDI target material is not very important. We are using by default gold-coated targets as they are expected to have a lower content of catalytically active transition metals (such as Fe²⁺) than stainless steel which may reduce unwanted lipid oxidation processes.
3. Normally, the use of plastic pipettes (as well as other plastic material) is strongly discouraged because chloroform is a rather aggressive solvent that leaches impurities such as plasticizers or antioxidants from the plastic material that may interfere with the lipid signals. However, according to our experience grey original Eppendorf pipette tips (up to a volume of 20 μL) may be used without problems. It is, however, recommended to check the potential contribution of impurities by using a sample of known composition.
4. Different solvents are normally required to dissolve matrix and lipid. In the majority of cases, the lipid stock solutions will be prepared in chloroform or chloroform/methanol mixtures. Unfortunately, the most common MALDI matrix—DHB—is nearly insoluble in chloroform, but well soluble in methanol. Due to the different volatilities of both solvents (the boiling point of chloroform is 61.2 °C and that of methanol 64.5 °C, respectively) the lipid will crystallize prior to the DHB resulting in inhomogeneous co-crystals. This problem can be minimized by drying the native matrix/sample mixtures rapidly under a warm stream of air. The extent of lipid oxidation induced by air-drying of the sample is (according to our experience) negligible.
5. The use of low-field NMR spectrometers has two important disadvantages: on the one hand, the achievable spectral resolution is reduced. On the other hand, the sensitivity of the NMR spectrometer correlates directly with the field strength of the magnet. Thus, more instrument time (a larger number of scans) is needed at a low-field NMR spectrometer to obtain the same S/N ratio.

6. 10 mm NMR sample tubes were formerly widely used at older NMR spectrometers because an enhanced sample size increases the achievable sensitivity. However, this normally compromises the achievable resolution. Modern probes are nowadays nearly exclusively designed for 5 mm tubes. This sample size should be sufficient because ^{31}P is a very sensitive nucleus.
7. Special attention should be paid to the salt content of the matrix as well as the solvents. Changes of the salt content may lead to changes of the peak patterns and affect the ratio between H^+ and Na^+ adducts. Additionally, the peaks stemming from the DHB matrix (or cluster ions derived thereof) are also influenced by changes of the salt content and their intensities are favored by high salt concentrations: note that a spectrum of DHB crystallized from pure methanol differs from that in the presence of salts.
8. All used solvents should be of highest quality! Due to the high sensitivity of MS, even very minor impurities within the solvents can be detected: The detection of small amounts of the analytes of interest is normally a minor problem than *NOT* detecting impurities stemming from the solvents or the used reagents.
9. It is not implied that under the used experimental conditions all lipids are completely extracted: some lipids may stick to the proteins that precipitate at the interphase between the aqueous and the organic layer and are, thus, lost. If protein-rich samples are investigated, higher ionic strengths, i.e., a high salt concentration (0.14 M or higher) are recommended in order to reduce the loss of lipids due to the binding to the protein. Complete extraction of lipids from biological tissues is a science of its own!
10. Unwanted lipid oxidation first leads to the generation of peroxides which decay (under scission at the position of the original double double) into aldehydes or carboxylic acids. This leads to characteristic mass differences which are summarized in [33]. For instance, oxidation of POPC (m/z 760.6 and 782.6) is reflected by the characteristic aldehyde peaks at m/z 650.5 and 672.5 [33].
11. It is very important to have a significant excess (about 100:1) of the detergent over the PL. Sodium cholate forms very small micelles which consist of just about 4 cholate molecules [34]. In the best case, one single PL molecule is entrapped in each of these small micelles—and this requires a considerable excess of the detergent.

Acknowledgements

This study was supported by the German Research Council (DFG Schi 476/16-1 and SFB 1052/Z3). We would also like to thank all our colleagues who helped us in performing the related experiments. We are particularly indebted to the Merck & Co. Inc. for the continuous support.

References

1. Christie WW (2003) Lipid analysis. Oily Press, Bridgewater
2. Fuchs B, Süß R, Schiller J (2010) An update of MALDI-TOF mass spectrometry in lipid research. *Prog Lipid Res* 49(4):450–475. doi:10.1016/j.plipres.2010.07.001
3. Hawkins PT, Stephens LR (2015) PI3K signalling in inflammation. *Biochim Biophys Acta* 1851(6):882–897. doi:10.1016/j.bbaliip.2014.12.006
4. Fuchs B, Schiller J, Wagner U, Häntzschel H, Arnold K (2005) The phosphatidylcholine/lysophosphatidylcholine ratio in human plasma is an indicator of the severity of rheumatoid arthritis: investigations by ³¹P NMR and MALDI-TOF MS. *Clin Biochem* 38(10):925–933. doi:10.1016/j.clinbiochem.2005.06.006
5. Matsumoto T, Kobayashi T, Kamata K (2007) Role of lysophosphatidylcholine (LPC) in atherosclerosis. *Curr Med Chem* 14(30):3209–3220
6. Nimptsch A, Pyttel S, Paasch U, Mohr C, Heinrich JM, Schiller J (2014) A MALDI MS investigation of the lysophosphatidylcholine/phosphatidylcholine ratio in human spermatozoa and erythrocytes as a useful fertility marker. *Lipids* 49(3):287–293. doi:10.1007/s11745-013-3870-7
7. Hyotylainen T, Oresic M (2016) Bioanalytical techniques in nontargeted clinical lipidomics. *Bioanalysis* 8(4):351–364. doi:10.4155/bio.15.244
8. Wang M, Wang C, Han RH, Han X (2016) Novel advances in shotgun lipidomics for biology and medicine. *Prog Lipid Res* 61:83–108. doi:10.1016/j.plipres.2015.12.002
9. Fahy E, Subramaniam S, Murphy RC, Nishijima M, Raetz CR, Shimizu T, Spener F, van Meer G, Wakelam MJ, Dennis EA (2009) Update of the LIPID MAPS comprehensive classification system for lipids. *J Lipid Res* 50(Suppl):S9–14. doi:10.1194/jlr.R800095-JLR200
10. Peterson BL, Cummings BS (2006) A review of chromatographic methods for the assessment of phospholipids in biological samples. *Biomed Chromatogr* 20(3):227–243. doi:10.1002/bmc.563
11. Fuchs B, Süß R, Teuber K, Eibisch M, Schiller J (2011) Lipid analysis by thin-layer chromatography—a review of the current state. *J Chromatogr A* 1218(19):2754–2774. doi:10.1016/j.chroma.2010.11.066
12. Murphy SA, Nicolaou A (2013) Lipidomics applications in health, disease and nutrition research. *Mol Nutr Food Res* 57(8):1336–1346. doi:10.1002/mnfr.201200863
13. Fuchs B (2014) Mass spectrometry and inflammation—MS methods to study oxidation and enzyme-induced changes of phospholipids. *Anal Bioanal Chem* 406(5):1291–1306. doi:10.1007/s00216-013-7534-5
14. Northen TR, Yanes O, Northen MT, Marrinucci D, Uritboonthai W, Apon J, Golledge SL, Nordstrom A, Siuzdak G (2007) Clathrate nanostructures for mass spectrometry. *Nature* 449(7165):1033–1036. doi:10.1038/nature06195
15. Cho YT, Su H, Huang TL, Chen HC, Wu WJ, Wu PC, Wu DC, Shiea J (2013) Matrix-assisted laser desorption ionization/time-of-flight mass spectrometry for clinical diagnosis. *Clin Chim Acta* 415:266–275. doi:10.1016/j.cca.2012.10.032
16. Roberts LD, McCombie G, Titman CM, Griffin JL (2008) A matter of fat: an introduction to lipidomic profiling methods. *J Chromatogr B Anal Technol Biomed Life Sci* 871(2):174–181. doi:10.1016/j.jchromb.2008.04.002
17. Mierisova S, Ala-Korpela M (2001) MR spectroscopy quantitation: a review of frequency domain methods. *NMR Biomed* 14(4):247–259
18. Schiller J, Süß R, Fuchs B, Müller M, Zschörnig O, Arnold K (2006) Recent applications of MALDI-TOF mass spectrometry and ³¹P NMR spectroscopy in phospholipid research. *Futur Lipidol* 1(1):115–125. doi:10.2217/17460875.1.1.115

19. Popkova Y, Meusel A, Breittfeld J, Schleinitz D, Hirrlinger J, Dannenberger D, Kovacs P, Schiller J (2015) Nutrition-dependent changes of mouse adipose tissue compositions monitored by NMR, MS, and chromatographic methods. *Anal Bioanal Chem* 407(17):5113–5123. doi:[10.1007/s00216-015-8551-3](https://doi.org/10.1007/s00216-015-8551-3)
20. Fenn LS, McLean JA (2008) Biomolecular structural separations by ion mobility-mass spectrometry. *Anal Bioanal Chem* 391(3):905–909. doi:[10.1007/s00216-008-1951-x](https://doi.org/10.1007/s00216-008-1951-x)
21. Eibisch M, Fuchs B, Schiller J, Süß R, Teuber K (2011) Analysis of phospholipid mixtures from biological tissues by matrix-assisted laser desorption and ionization time-of-flight mass spectrometry (MALDI-TOF MS): a laboratory experiment. *J Chem Educ* 88(4):503–507. doi:[10.1021/ed1004905](https://doi.org/10.1021/ed1004905)
22. Pearce JM, Komoroski RA (2000) Analysis of phospholipid molecular species in brain by $(31)P$ NMR spectroscopy. *Magn Reson Med* 44(2):215–223
23. Bligh EG, Dyer WJ (1959) A rapid method of total lipid extraction and purification. *Can J Biochem Physiol* 37(8):911–917. doi:[10.1139/o59-099](https://doi.org/10.1139/o59-099)
24. Bresler K, Pyttel S, Paasch U, Schiller J (2011) Parameters affecting the accuracy of the MALDI-TOF MS determination of the phosphatidylcholine/lysophosphatidylcholine (PC/LPC) ratio as potential marker of spermatozoa quality. *Chem Phys Lipids* 164(7):696–702. doi:[10.1016/j.chemphyslip.2011.07.006](https://doi.org/10.1016/j.chemphyslip.2011.07.006)
25. Hillenkamp F, Peter-Katalinic J (2014) MALDI-MS. Weinheim, Wiley-Blackwell
26. Berger S, Braun S (2004) 200 and more NMR experiments: a practical course. Wiley-VCH, Weinheim
27. Petkovic M, Schiller J, Müller M, Benard S, Reichl S, Arnold K, Arnhold J (2001) Detection of individual phospholipids in lipid mixtures by matrix-assisted laser desorption/ionization time-of-flight mass spectrometry: phosphatidylcholine prevents the detection of further species. *Anal Biochem* 289(2):202–216. doi:[10.1006/abio.2000.4926](https://doi.org/10.1006/abio.2000.4926)
28. Fuchs B, Bischoff A, Süß R, Teuber K, Schürenberg M, Suckau D, Schiller J (2009) Phosphatidylcholines and -ethanolamines can be easily mistaken in phospholipid mixtures: a negative ion MALDI-TOF MS study with 9-aminoacridine as matrix and egg yolk as selected example. *Anal Bioanal Chem* 395(8):2479–2487. doi:[10.1007/s00216-009-3032-1](https://doi.org/10.1007/s00216-009-3032-1)
29. Gidden J, Liyanage R, Durham B, Lay JO Jr (2007) Reducing fragmentation observed in the matrix-assisted laser desorption/ionization time-of-flight mass spectrometric analysis of triacylglycerols in vegetable oils. *Rapid Commun Mass Spectrom* 21(13):1951–1957. doi:[10.1002/rcm.3041](https://doi.org/10.1002/rcm.3041)
30. Fuchs B, Schiller J, Süß R, Schürenberg M, Suckau D (2007) A direct and simple method of coupling matrix-assisted laser desorption and ionization time-of-flight mass spectrometry (MALDI-TOF MS) to thin-layer chromatography (TLC) for the analysis of phospholipids from egg yolk. *Anal Bioanal Chem* 389(3):827–834. doi:[10.1007/s00216-007-1488-4](https://doi.org/10.1007/s00216-007-1488-4)
31. Sun G, Yang K, Zhao Z, Guan S, Han X, Gross RW (2008) Matrix-assisted laser desorption/ionization time-of-flight mass spectrometric analysis of cellular glycerophospholipids enabled by multiplexed solvent dependent analyte-matrix interactions. *Anal Chem* 80(19):7576–7585. doi:[10.1021/ac801200w](https://doi.org/10.1021/ac801200w)
32. Schiller J, Müller M, Fuchs B, Arnold K, Huster D (2007) ^{31}P NMR spectroscopy of phospholipids: from micelles to membranes. *Curr Anal Chem* 3:283–301
33. Fuchs B, Schiller J, Süß R, Nimptsch A, Schürenberg M, Suckau D (2009) Capabilities and disadvantages of combined matrix-assisted laser desorption/ionization time-of-flight mass spectrometry (MALDI-TOF MS) and high-performance thin-layer chromatography (HPTLC): analysis of egg yolk lipids. *J Planar Chromatogr* 22:35–42
34. le Maire M, Champeil P, Moller JV (2000) Interaction of membrane proteins and lipids with solubilizing detergents. *Biochim Biophys Acta* 1508(1–2):86–111

Global Monitoring of the Mammalian Lipidome by Quantitative Shotgun Lipidomics

Inger Ødum Nielsen, Kenji Maeda, and Mesut Bilgin

Abstract

The emerging field of lipidomics presents the systems biology approach to identify and quantify the full lipid repertoire of cells, tissues, and organisms. The importance of the lipidome is demonstrated by a number of biological studies on dysregulation of lipid metabolism in human diseases such as cancer, diabetes, and neurodegenerative diseases. Exploring changes and regulations in the huge networks of lipids and their metabolic pathways requires a lipidomics methodology: Advanced mass spectrometry that resolves the complexity of the lipidome. Here, we report a comprehensive protocol of quantitative shotgun lipidomics that enables identification and quantification of hundreds of molecular lipid species, covering a wide range of lipid classes, extracted from cultured mammalian cells.

Key words Global monitoring, Lipidomics, Shotgun lipidomics, Quantification, Mammalian cells, Mass spectrometry, Lipid extraction, Systems biology

1 Introduction

Every living organism from bacteria to mammals is equipped with metabolic pathways that produce structurally and functionally diverse lipids. Lipids are essential components of cells, assembling lipid bilayers and determining the architecture of cellular membranes. Lipids orchestrate numerous biological processes taking place at cellular membranes by participating in complex networks of physical interactions with each other and with other macromolecules. Besides forming membranes, lipids play other roles such as serving as storage compounds, sources of energy, and signaling molecules [1]. The regulation of lipid metabolism is poorly illuminated, yet of pivotal importance since imbalances in the lipid metabolism have been linked to the pathophysiology of cancer and other diseases [2].

Lipids have been divided into eight categories based on their core structures: fatty acyls, glycerolipids, glycerophospholipids, sphingolipids, sterol lipids, prenol lipids, saccharolipids, and

polyketides [3]. The great diversity of lipids arises from the myriad of different combinations of building blocks: Lipids differ in terms of headgroups, the presence, length and number of fatty acyl chains, the numbers and positions of double bonds, the presence of additional modifications such as hydroxylation or glycosylation, to name a few. From the combinations of these, many thousands of structurally diverse lipid species may be generated [4]. The entire lipid repertoire of cells, tissues, or organisms is referred to as the lipidome and the systems biology approach to identify and quantify the lipidome is termed lipidomics. The emerging field of lipidomics has experienced rapid progress in the past decade, mainly through advances in mass spectrometry technologies and applications delivering sensitive and accurate quantitative lipid analysis [1, 5, 6]. Lipid studies increasingly contribute to the integrated picture presented in life science, showing how genes, proteins, and metabolites work together to perform cellular functions.

This protocol presents a methodology of mass spectrometry-based quantitative shotgun lipidomics on cultured mammalian cells. A mass spectrometer separates charged molecular ions (e.g., lipids) based on the mass-to-charge ratio (m/z , expressed in amu or Da) and measures the intensity of each ion. The signals obtained in the mass analyzer are translated into m/z values and intensities [7]. The m/z value and intensity peak of each lipid ion are used for identification and quantification of specific lipid species.

Shotgun lipidomics is a mass spectrometry-based direct analysis of crude lipid extracts from various biological materials [1, 8–12] without prior chromatographic lipid separation. Lipidomics setups in which mass spectrometry is coupled to upstream chromatographic lipid separation procedures such as gas chromatography and liquid chromatography may have drawbacks and limitations in lipidome-wide analysis (reviewed in [13]). Shotgun lipidomics is advantageous in that it requires small sample amounts and in being a simple and fast procedure that is easily automated for high-throughput analysis. It detects and quantifies hundreds of lipid species covering 15–20 lipid classes in a single shotgun lipidomics experiment [11, 14–16]. With the high resolution and high sensitivity of modern mass spectrometers, shotgun lipidomics enables global monitoring of the cellular lipidome [13].

The protocol presented here combines a two-step lipid extraction with direct lipid infusion into a hybrid quadrupole-Orbitrap mass spectrometer for analysis (*see* Fig. 1). Lipids are analyzed by an optimized high resolution (HR) MS^{All}, a tandem mass spectrometry approach starting with a MS scan that detects all lipid ions within a broad m/z range, e.g., 335–1215. Subsequently, lipid ions are subjected to an MS/MS scan, where they are fragmented and the resulting fragment ions are detected in the Orbitrap mass analyzer. The combination of precursor ion m/z values obtained in the MS scan and the m/z values of their corresponding fragment

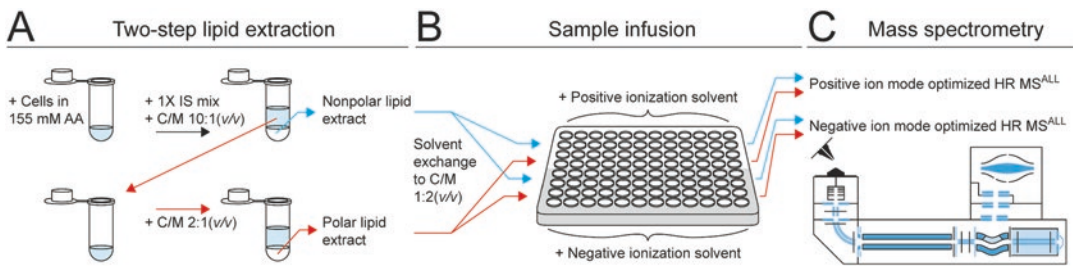


Fig. 1 The protocol workflow. **(a)** Lipids are extracted by a two-step lipid extraction, separating the nonpolar lipids in the first chloroform/methanol extraction (fraction 10:1) from the polar lipids in the second chloroform/methanol extraction (fraction 2:1). **(b)** Lipids from fraction 10:1 and fraction 2:1 are separately mixed with either positive or negative ionization solvent in a 96-well PCR plate, from which the samples are ionized and infused with positive or negative automated robotic nanoelectrospray ionization. **(c)** Lipids are detected by the hybrid quadrupole-Orbitrap mass spectrometer. *AA* ammonium acetate, *C* chloroform, *HR* high resolution, *IS mix* internal standard mix, *M* methanol

Table 1
Separation of lipid classes by lipid fraction and ionization mode

Ionization mode	Lipid fraction	Lipid class
Positive mode	10:1	CE, Cer, Chol, DAG, HexCer, LCB, LSM, SM, TAG
	2:1	diHexCer, triHexCer
Negative mode	10:1	PG, PG O ⁻ , LPG, LPG O ⁻
	2:1	LCBP, CerP, SHexCer, PA, PA O ⁻ , LPA, LPA O ⁻ , PI, PI O ⁻ , LPI, LPI O ⁻ , PS, PS O ⁻ , LPS, LPS O ⁻
Both positive and negative mode	10:1	PC, PC O ⁻ , LPC, LPC O ⁻ , PE, PE O ⁻ , LPE, LPE O ⁻
	2:1	–

This is a list of lipids, separated by the fraction in which they are extracted and the ion mode in which they are detected. *O⁻* indicates a glycerophospholipid with one fatty alcohol chain attached to the glycerol backbone. The lipids that are detected in both positive and negative ionization modes can be analyzed in either modes for quantification (*see Note 21*)

ions obtained in the MS/MS scan is used for lipid identification. In the following section, details of the protocol are described.

The two-step lipid extraction separates lipids based on their physicochemical properties, extracting nonpolar and polar lipids in the first and second step, respectively (*see Table 1*). This increases the analytical sensitivity of the method compared to one-step lipid extraction [11]. Ionization of the lipids is a crucial step to the procedure. Lipids form different adduct ions depending on their ionization polarity and solvent system [11, 17, 18]. To maximize the

Table 2
***m/z* ranges used for optimized HR MS^{ALL} settings**

Ionization mode	Lipid fraction	Scan type	Low range, <i>m/z</i>	High range, <i>m/z</i>	Inclusion list, <i>m/z</i>
POS	10:1	MS	400–730	575–1,050	–
		SIM	402–410	–	–
		tPRM	–	–	404.3887, 408.4138
		MS/MS	–	–	400.3000–1050.8200
	2:1	MS	–	790–1,215	–
		MS/MS	–	–	806.6248–1,185.9280
NEG	10:1	MS	400–675	500–1,025	–
		MS/MS	–	–	400.2000–1,000.6800
	2:1	MS	335–675	500–1,000	–
		MS/MS	–	–	335.1480–1,000.6800

Here the specific *m/z* ranges used for the optimized HR MS^{ALL} are presented. The ranges are chosen to encompass the lipids isolated in each fraction. Analyzing the 2:1 fraction in positive ionization mode only includes a high range *m/z* MS scan. In tPRM only 2 *m/z* values are chosen for analysis, specific for cholesterol and the cholesterol internal standard

number of detected lipid ions, samples are divided and mixed with either positive or negative ionization solvent (we use ammonium acetate and triethylamine, respectively), enhancing the formation of positive and negative lipid ions, respectively. Lipids are ionized through automated robotic nanoelectrospray ionization and delivered to a hybrid quadrupole-Orbitrap mass spectrometer. The samples dissolved in positive ionization solvent are analyzed by the mass spectrometer in positive ion mode, detecting positive ions, while samples dissolved in negative ionization solvent are analyzed in negative ion mode, detecting negative ions. The initial MS scans an interval of *m/z* values expected to cover most lipid ions (e.g., 335–1215) (*see* Table 2). Following the MS scan, ions in a selected *m/z* range (*see* Table 2) are sequentially subjected to fragmentation. The *m/z* window changes stepwise and allows for MS/MS scans to be acquired separately for all ions. Fragmentation is achieved by higher-energy collisional dissociation (HCD), a type of collision-induced dissociation specific to the Orbitrap mass spectrometers.

Due to difficult ionization, the shotgun approach may leave some lipid species undetected. Cholesterol ionizes suboptimally without derivatization [19, 20]; therefore the optimized HR MS^{ALL} is adjusted by including selected ion monitoring (SIM): a MS scan on a small *m/z* range centered around the *m/z* value of cholesterol is performed. This enhances the detection sensitivity by increasing the relative amount of cholesterol ions within the MS scan. Following the SIM, we perform a targeted parallel reaction

monitoring (tPRM), where MS/MS is done on specific ions with the m/z value of cholesterol.

The lipids detected in the positive ion mode mainly form $[M+H]^+$ and $[M+NH_4]^+$ adducts, while the lipids detected in the negative ion mode mainly form $[M-H]^-$ and $[M-CH_3OCOO]^-$ adducts (*see* Tables 3 and 4). Identification is done by matching theoretical m/z values with the observed. A lipid is identified if the m/z value in MS matches the theoretical m/z value of a lipid ion, and if the corresponding fragment ion(s) m/z value(s) observed in MS/MS match the theoretical fragment ion(s). For quantification of individual lipid species, known and appropriate amounts of specific lipid species (internal standards) are added to the biological sample prior to lipid extraction. The peak intensities of lipid ions in the MS scans are then compared to those of the corresponding internal standards. The internal standard mixture is a collection of lipids representing the common lipid classes present in mammalian cells without the specific species being present.

This protocol presents a methodology of quantitative global profiling of the mammalian cell lipidome by combining a two-step lipid extraction with shotgun lipidomics, performed using an optimized HR MS^{ALL}. The methodology is not limited to mammalian cells, but can be adapted for quantitative global lipid profiling of other organisms such as bacteria, yeast etc. The protocol presented here is a generic approach that can readily be applied using other platforms and serve as an additional routine in the repertoire of mass spectrometry applications for lipidome-wide quantification [11, 12, 21].

2 Materials

Throughout this procedure it is paramount to keep all solvents, pipette tips, tubes, and plates cool and clean to prevent contamination and degradation of lipids. Clean all glassware with chloroform/methanol 1:1 (v/v) before use. Avoid using plasticware as the organic solvents may dissolve plastic polymers, which will affect the quality of the mass spectrometry data.

2.1 Sample Preparation

1. Chloroform/methanol 1:1 (v/v): Mix 10 mL chloroform with 10 mL methanol in a 20 mL graduated cylinder.
2. Chloroform/methanol 10:1 (v/v): Mix 90 mL chloroform with 9 mL methanol in a 100 mL graduated cylinder.
3. Chloroform/methanol 2:1 (v/v): Mix 60 mL chloroform with 30 mL methanol in a 100 mL graduated cylinder.
4. Chloroform/methanol 1:2 (v/v): Mix 30 mL chloroform with 60 mL methanol in a 100 mL graduated cylinder.

Table 3
Detection of lipid classes in positive ion mode

Lipid class	MS, Precursor ion	MS/MS, Fragment ion	MS/MS, Neutral loss	MS/MS, m/z
PE/PE O ⁻ /LPE/LPE O ⁻	[M+H] ⁺	–	Phosphoethanolamine	141.0191
PC/PC O ⁻ /LPC/LPC O ⁻ –/SM/LSM	[M+H] ⁺	[Phosphorylcholine+H] ⁺	–	184.0733
Chol/CE	[M+NH ₄] ⁺	[Chol–NH ₃ –H ₂ O] ⁺	–	369.3516
Cer/HexCer/diHexCer/ trihexCer/LCB	[M+H] ⁺	[LCB+H–H ₂ O] ⁺	–	Depend on species
Cer/HexCer/diHexCer/ trihexCer/LCB	[M+H] ⁺	[LCB+H–2H ₂ O] ⁺	–	Depend on species
Cer/HexCer/diHexCer/ trihexCer/LCB	[M+H] ⁺	[LCB+H–CH ₄ O ₂] ⁺	–	Depend on species
DAG/TAG	[M+NH ₄] ⁺	–	Fatty acid –H+NH ₄	Depend on species

A list of lipid classes and their precursor ions, fragment ions, and neutral loss of species used for detection in the positive ionization mode. O⁻ indicates a glycerophospholipid with one fatty alcohol chain attached to the glycerol backbone

Table 4
Detection of lipid classes in negative ion mode

Lipid class	MS, Precursor ion	MS/MS, Fragment ion	MS/MS, Neutral loss	MS/MS, m/z
CerP/LCBP	[M-H] ⁻	[Phosphoric acid -H-H ₂ O] ⁻	-	78.959
PS/PS O ⁻ /LPS/LPS O ⁻	[M-H] ⁻	-	[C ₃ H ₅ NO ₂]	87.032
SHexCer	[M-H] ⁻	[Sulfuric acid -H] ⁻	-	96.9601
PA/PA O ⁻ /LPA/LPA O ⁻ /PC/ PC O ⁻ /LPC/LPC O ⁻ /PG/ PG O ⁻ /LPG/LPG O ⁻ /PI/ PI O ⁻ /LPI/LPI O ⁻ /PS/PS O ⁻ /LPS/LPS O ⁻	[M-H] ⁻	[Glycerophosphate -H-H ₂ O] ⁻	-	152.9958
PC/PC O ⁻ /LPC/LPC O ⁻	[M+CH ₃ OCOO] ⁻	[Cholinephosphate -H-CH ₃] ⁻	-	168.0431
PE/PE O ⁻ /LPE/LPE O ⁻	[M-H] ⁻	[Ethanolaminephosphate -H-H ₂ O] ⁻	-	196.038
PI/PI O ⁻	[M-H] ⁻	[Inositolphosphate -H-2H ₂ O] ⁻	-	223.0013
PI/PI O ⁻	[M-H] ⁻	[Inositolphosphate -H-H ₂ O] ⁻	-	241.0119
PI/PI O ⁻	[M-H] ⁻	[Inositolphosphate -H] ⁻	-	259.0224
Glycerophospholipid species	[M-H] ⁻	[Fatty acid -H] ⁻	-	depend on species
Glycerophospholipid species O ⁻	[M-H] ⁻	[Fatty acid -H] ⁻	-	depend on species
Glycerophospholipid species O ⁻	[M-H] ⁻	[M-Fatty acid -H+OH] ⁻	-	depend on species
Polyunsaturated glycerophospholipid species	[M-H] ⁻	[Fatty acid -H-CO ₂] ⁻	-	depend on species

A list of lipid classes and their precursor ions, fragment ions, and neutral loss of species used for detection in the negative ionization mode. O⁻ indicates a glycerophospholipid with one fatty alcohol chain attached to the glycerol backbone

5. 155 mM ammonium acetate in H₂O: Add 25 mL water to a 100 mL graduated cylinder. Weigh 0.597 g ammonium acetate and add to the graduated cylinder. Add 25 mL water, and mix gently until ammonium acetate is fully dissolved.
6. Positive ionization solvent, 13.3 mM ammonium acetate in isopropanol: Pour 25 mL isopropanol into a 100 mL blue cap bottle. Weigh 0.102 g ammonium acetate and add it to the bottle, followed by 75 mL of isopropanol. Close the cap and heat the bottle to 50 °C till the ammonium acetate is completely dissolved.
7. Negative ionization solvent, 0.2% triethylamine in chloroform/methanol 1:5 (v/v): Mix 15 mL chloroform, 75 mL methanol, and 180 µL triethylamine in a 100 mL graduated cylinder.
8. 10× Internal Standard Mix (10× IS mix), 30 µM cholesteryl ester (CE 15:0-D7), 20 µM ceramide (Cer 18:1;2/12:0;0), 20 µM ceramide phosphate (CerP 18:1;2/12:0;0), 200 µM cholesterol (Chol-D4), 10 µM diacylglycerol (DAG 12:0/12:0), 20 µM dihexose ceramide (diHexCer 18:1;2/12:0;0), 25 µM hexose ceramide (HexCer 18:1;2/12:0;0), 20 µM long-chain base (LCB 17:0;2), 20 µM long-chain base phosphate (LCBP 17:0;2), 25 µM lysophosphatidic acid (LPA 17:0), 20 µM lysophosphatidylcholine (LPC 17:1), 25 µM lysophosphatidylethanolamine (LPE 13:0), 15 µM lysophosphatidylglycerol (LPG 17:1), 20 µM lysophosphatidylinositol (LPI 13:0), 20 µM lysophosphatidylserine (LPS 17:1), 20 µM lysosphingomyelin (LSM 17:1;2), 25 µM phosphatidic acid (PA 12:0/12:0), 20 µM phosphatidylcholine (PC-OO 18:1/18:1), 25 µM phosphatidylethanolamine (PE 12:0/12:0), 15 µM phosphatidylglycerol (PG 12:0/12:0), 15 µM phosphatidylinositol (PI 8:0/8:0), 20 µM phosphatidylserine (PS 12:0/12:0), 20 µM sulfatide (SHexCer 18:1;2/12:0;0), 20 µM sphingomyelin (SM 18:1;2/12:0;0), 10 µM triacylglycerol (TAG 17:0/17:0/17:0), and 20 µM trihexose ceramide (triHexCer 18:1;2/17:0;0) dissolved in chloroform/methanol 1:1 (v/v) (*see* **Notes 1–2**). Store 10× IS mix at –80 °C in small aliquots in glass ampules.
9. IS mix (1×): Dilute 100 µL 10× IS mix with 900 µL chloroform/methanol 1:1 (v/v). Ampules of IS mix are saved (siphoned with N₂ before closing) at –80 °C until use.
10. 1.5 mL and 2 mL tubes.
11. 96-well PCR plate (*see* **Note 3**).
12. Aluminum sealing tape (*see* **Note 4**).
13. Table centrifuge.
14. Thermomixer.
15. Vacuum centrifuge (*see* **Note 5**).

2.2 Mass Spectrometry

1. TriVersa NanoMate, an automated robotic nanospray ionization source (Advion, Ithaca, NY, USA).
2. Ionization nozzles (D-Chip).
3. Q-Exactive, a hybrid quadrupole-Orbitrap mass spectrometer (Thermo Fischer Scientific, Waltham, MA, USA).

3 Methods

3.1 Sample Preparation

Keep everything at 4 °C or on ice during this procedure, unless otherwise specified. For a list of lipids extracted during the two-step extraction (*see* Table 1).

1. Cells are prepared according to standard procedures (adherent cells are, e.g., trypsinized and resuspended in media) and counted.
2. Prepare 3e5 cells as a minimum for lipidomics analysis (*see* Note 6).
3. Centrifuge cell suspension in a tube for 5 min at 500 RCF. Discard media.
4. Wash cells with 155 mM ammonium acetate in H₂O.
5. Centrifuge cells for 5 min at 500 RCF and discard the supernatant.
6. Repeat Subheading 3.1, steps 4 and 5 twice (to a total of three washes).
7. Add 155 mM ammonium acetate in H₂O to a final concentration of 3,000 cells/μL.
8. If the samples are not to be subjected to lipid extraction immediately, freeze as fast as possible and store at -80 °C.

3.2 Two-Step Lipid Extraction

(*See* Fig. 1 for overview)

1. First Step: Extracting the nonpolar lipids from the sample (*see* Table 1 for a list of lipids extracted in this step and *see* Note 7).
 - (a) Mix 990 μL freshly prepared chloroform/methanol 10:1 (v/v) with 10 μL IS mix, 33 μL sample (corresponding to 1e5 cells), and 167 μL 155 mM ammonium acetate in H₂O, in 2.0 mL tubes.
 - (b) Shake the samples in the Thermomixer for 60 min at 2,000 rpm and 4 °C.
 - (c) Centrifuge samples at 2,000 RCF for 2 min at 4 °C.
 - (d) Transfer the lower organic phase to new 1.5 mL tubes. Store these at -20 °C until the second extraction step is done.

2. Second Step: Extracting the polar lipids from the sample (*see* Table 1 for a list of lipids extracted in this step).
 - (a) Mix 990 μL of freshly prepared chloroform/methanol 2:1 (v/v) with the upper phase from Subheading 3.2, steps 1d.
 - (b) Shake the samples on Thermomixer for 60 min at 2,000 rpm and 4 °C.
 - (c) Centrifuge for 2 min at 2,000 RCF and 4 °C.
 - (d) Transfer the lower organic phase to new 1.5 mL tubes.
3. Both the organic phases from the first and second extraction steps: Open the tubes and carefully place them in a vacuum centrifuge for evaporation of solvent for approximately 60 min, until all solvent is evaporated and the lipids are dry (*see* Note 8).
4. Dissolve the dried lipids in 100 μL chloroform/methanol 1:2 (v/v).
5. Place the samples in Thermomixer, and shake them for 120 s at 2,000 rpm and 4 °C.
6. Centrifuge the samples for 3 min at 13,000 RCF and 4 °C to pellet insoluble materials.

3.3 Ionization and Mass Spectrometry

In this protocol, the extracted lipids are analyzed by direct infusion mass spectrometry. The lipid extract is analyzed in conditions optimal for either positive or negative lipid ionization. This involves mixing lipid extract with either positive or negative ionization solvent, specific settings for either ionization types during nanoelectrospray ionization, and performing mass spectrometry analysis in positive and negative ion mode (*see* Figs. 1 and 2 for overview and Notes 9 and 10).

1. Set up a 96-well PCR plate and keep it cool in a cool rack or freeze system.
 - (a) To all wells analyzed in positive mode: Load 15 μL positive ionization solvent in a well, followed by loading of 11.7 μL extract (dissolved in chloroform/methanol 1:2 (v/v)) to the same well. The final solvent composition is 7.5 mM ammonium acetate in chloroform/methanol/isopropanol 1:2:4 (v/v), which is optimal for positive mode shotgun lipidomics (for lipid species detected in this mode *see* Table 2).
 - (b) To all wells analyzed in negative mode: Load 14 μL negative ionization solvent in a well, followed by loading of 14 μL extract (dissolved in chloroform/methanol 1:2 (v/v)) to the same well. The final solvent composition is 0.1% triethylamine in chloroform/methanol 1:3.5 (v/v), which

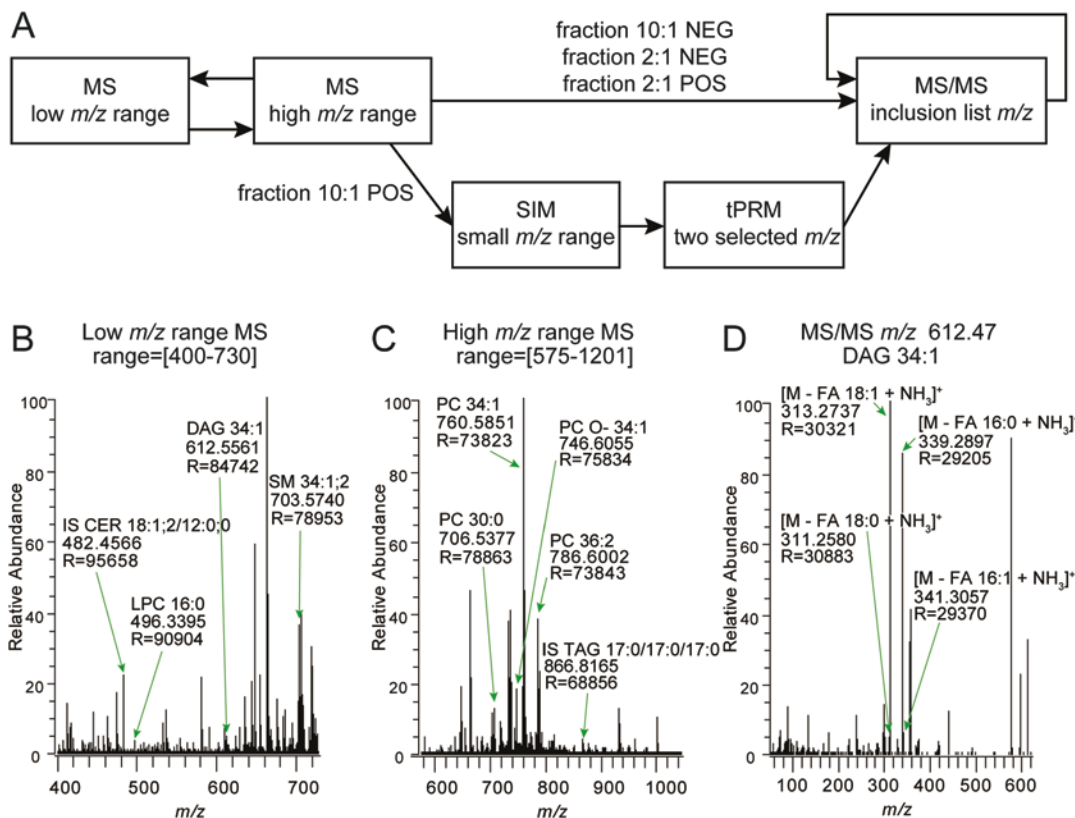


Fig. 2 The MS workflow and examples of the acquired spectra of HR MS and HR MS/MS. **(a)** The optimized HR MS^{ALL} comprises the elements presented here. For HR MS analysis of fraction 2:1 in positive ion mode (fraction 2:1 POS) and 10:1 and 2:1 in negative ion mode (fraction 2:1 and 10:1 NEG), lipid ions are subjected to alternating HR MS analysis in the low and high m/z range. This is followed by sequential HR MS/MS that uses quadrupole isolation of precursor ions followed by higher-energy collision dissociation (*see* Table 2 for the specific m/z ranges and inclusion lists). HR MS analysis of fraction 10:1 in positive ion mode includes an additional step of selected ion monitoring (SIM) on a small m/z range of 10 Da, followed by targeted parallel reaction monitoring (tPRM) of two specific precursor ion masses. **(b-d)** Examples of acquired spectra from extract 10:1 in positive ionization mode. R indicates the resolution of the peak at a given m/z value. **(b)** Low m/z range positive ion mode HR MS spectrum. **(c)** High m/z range positive ion mode HR MS spectrum. **(d)** HR MS/MS spectrum of the precursor ion of m/z 612.47 (DAG 34:1). Based on the fragments indicated in the figure, this lipid is annotated and identified as DAG 16:0/18:1 and DAG 16:1/18:0. The arrows annotate the high intensity peaks of fragment ions $[M-FA16:0+NH_3]^+$ (m/z 339.2897) and $[M-FA18:1+NH_3]^+$ (m/z 313.2737) with lower peak intensities of fragment ions $[M-FA16:1+NH_3]^+$ (m/z 341.3057) and $[M-FA18:0+NH_3]^+$ (m/z 311.2580). This indicates that although both species are present in the sample, DAG 16:0/18:1 is more abundant than DAG 16:1/18:0

is optimal for negative mode shotgun lipidomics (for lipid species detected in this mode *see* Table 2).

2. Seal the plate with aluminum sealing tape to decrease evaporation and risk of contamination.
3. Insert the 96-well PCR plate into the TriVersa NanoMate, the automated robotic nanospray ion source used for sample infusion.

- (a) TriVersa NanoMate settings (*see Note 11*): Allow the TriVersa NanoMate to cool to a temperature of 5 °C (*see Note 12* for optional settings) before use. Use 10 µL as sample volume. Unused sample should not be returned to the well following injection.
 - (b) For positive mode sample delivery, gas pressure should be 1.25 psi, and applied voltage 0.96 kV.
 - (c) For negative mode sample delivery, gas pressure should be 0.7 psi and applied voltage -1.06 kV.
4. Perform optimized HR MS^{ALL} consisting of MS and MS/MS (*see Fig. 2* for overview). For positive mode MS^{ALL}, we include a SIM with tPRM to enhance the detection sensitivity of cholesterol. Therefore the positive mode MS^{ALL} method lasts 11 min, while the negative mode MS^{ALL} method takes 10 min (*see Note 13*).
 - (a) Mass spectrometer source settings: Set the capillary temperature to 200 °C and the S-lens RF level to 80.
5. Start with MS scans using alternating HR MS in low and high m/z range (*see Table 2*).
 - (a) MS settings in both positive and negative ion modes: Average 3 µscans per scan. *Lock masses* are used if there are known masses that can be utilized for internal calibration (*see Note 14*). Use 1e6 as automatic gain control (AGC) target. Set resolution to 140,000 and use a maximal injection time of 150 ms.
6. SIM and tPRM (*see Table 2* and *Fig. 2*): To obtain good signals on cholesterol, we optimize the settings for this particular species by doing a specific MS scan of precursor ions in a small range of m/z values, followed by tPRM of the exact m/z values of cholesterol and its internal standard. These additional steps are only added to the positive ion mode MS^{ALL}, as cholesterol is detected in positive ion mode.
7. Perform a 30 s MS scan on a small 10 Da window centered around the m/z value of cholesterol (*see Table 2* and *Note 15*).
 - (a) SIM settings: Average 3 µscans per scan. Use 1e6 as AGC target. Resolution is set to 140,000.
8. Perform tPRM for 30 s (*see Table 2* for the m/z inclusion list).
 - (a) tPRM settings: Use an isolation window width of 1.2 Da and normalized stepped collision energies of 12, 18, and 23 (*see Note 16*). Set resolution to 35,000 and the AGC target to 1e5 and 1 µscans per scan.
9. Following the SIM/tPRM scan, perform HR MS/MS analysis on all ions within the selected m/z range (*see Table 2* for the inclusion list ranges in positive or negative mode). Use an iso-

lation window width of 1.2 Da for each scan, sequentially stepping by 1.008 Da.

- (a) MS/MS settings in positive mode: ACG target is 5e4 and the resolution 35,000, with only 1 μ scan being performed. Normalized collision steps should be 15, 20, and 25.
 - (b) MS/MS settings in negative mode: ACG target is 5e4 and the resolution 35,000, with only 1 μ scan being performed. Normalized collision steps should be 18, 28, and 38.
10. Precursor ions, fragment ions, and neutral loss used for the identification of sample lipids are listed in Tables 3 and 4.
 11. Spectra assessment: Look carefully through the spectra of each sample as soon as possible following the MS scan. Use the total ion intensities in both high and low m/z range MS scans and in the MS/MS scan of a few internal standard species to assess the quality (*see Note 17* for our assessment thresholds).

3.4 Data Extraction and Quantification

1. For data extraction, we use LipidXplorer [22], a python based program that extracts and processes spectra data, and identifies specific molecular species of ionizable lipid classes by comparing the obtained MS and MS/MS spectra with known or assumed lipid fragmentation patterns (*see Note 18*).
2. Quantification is done by comparing peak intensities of the endogenous lipid with that of its corresponding internal standard with known quantity, e.g., internal standard PS 12:0/12:0 represents all endogenous PS and PS O– species (*see Notes 2, 19–21*).

$$\frac{\text{endogenous lipid}}{\text{IS lipid}} \times \text{spiked [pmol]} \times \frac{\rho \text{ endogenous lipid}}{\rho \text{ IS lipid}} = \text{endogenous lipid [pmol]}$$

3. This calculation includes the isotope correction factor ρ endogenous lipid/ ρ IS lipid, where ρ is the intensity of the mono-isotopic peak relative to the total intensity of peaks in the isotopic cluster. In most lipid analysis software this correction factor however is not necessary, as the ion intensity output is often including isotope correction.

4 Notes

1. The internal standards should be chosen based on prior analysis of the cells/tissue used to ensure that the chosen standards are not found as endogenous species.
2. In case an internal standard is isobaric with endogenous lipid(s) from different classes, the lipid ion species can often be distin-

guished by either using the fragment ion(s) or a different ionization mode (where they are not isobaric).

3. Use of Eppendorf twin.tec PCR Plate 96, skirted, is recommended to avoid plastic material contamination.
4. Use of aluminum foil from Corning Incorporated, Costar, and Thermowell is recommended to minimize plastic contamination.
5. Use of a vacuum centrifuge, Christ, RVC, 2–25 CD plus is recommended. Make sure the inner material is resistant to organic solvents.
6. The minimum amount of cells used for lipid extraction should ensure enough samples for technical triplicates. For the actual extraction sample (each replicate) we consider 50,000–150,000 cells to be sufficient.
7. It is possible to do a single step extraction only using chloroform/methanol 2:1 (v/v); however this has limitations as the fractionation of the lipids enhances the sensitivity.
8. All liquid should have evaporated before continuing from this step. However, try to minimize the time of vacuum centrifugation to avoid plastic contamination.
9. The solvent system should be chosen to increase the ionization efficiency of the samples upon sample infusion in either positive or negative ion mode. Other solvent systems include methyl amine and ammonium formate.
10. Some low abundant lipid species, e.g., LCB, are not easily detected in either positive or negative ion modes. For better quantification of these species, chemical derivatization can be performed with, e.g., methane iodide before MS scan [23, 24].
11. Direct infusion of lipid samples can also be done using a capillary, nano needles, syringe, flow injection, etc.
12. We program the TriVersa NanoMate to move to a new nozzle, if the spray current drops below 5 nA or rises above 7,000 nA for more than 30 s. This helps to minimize loss of sample analysis.
13. The lipids detected in the 2:1 fraction analyzed in positive ion mode are primarily di- and triHexCer. The m/z range of this scan is therefore changed to a smaller m/z interval, 790–1215, increasing the sensitivity of the detection of these specific lipids and shortening the acquisition time (to 6 min).
14. We use the following lock masses: 529.4626 and 1175.7766 for negative ion mode and 388.2541, 680.48022, and 1194.8179 for positive ion mode. For other locked masses, please *see* [14].

15. The 10 Da window used for SIM of cholesterol covers both the m/z values of cholesterol and its internal standard.
16. To achieve the optimal fragmentation of ions in MS/MS we use stepped collision energy, which applies three different energies, normalized to the m/z value of the precursor ion.
17. The assessment of the spectra quality depends on the sample and lipid species in question. We consider the total ion intensity threshold to be $1e6$ in both low and high m/z range MS. If values are lower, the sample should be run again or prepared anew. For the quality of the MS/MS scans, the fragment ions of a few internal standard species are assessed and a total ion intensity of minimum $1e3$ is considered the threshold.
18. For an overview of software available, please *see*: omictools.com/lipid-identification-category.
19. The obtained lipid quantities in pmol can be converted to mol % to account for changes caused by different cell amounts.
20. Before quantification, it is important that potential isobaric overlaps are considered: As an example, PC O⁻ and PS detected in negative ion mode can have some isobaric overlap with the ion species [PC O-32:4-H-CH₃OCOO]⁻ and [PS 36:2-H]⁻, both with m/z 786.5290. To solve this problem, the MS/MS fragmentation spectra can be used for individual quantification. On the other hand, as PC O-32:4 is not a lipid species commonly occurring in biological systems, this problem could also be ignored. Another example is the isobaric overlap of primary and secondary adducts of PC, e.g., [PC 36:5+H]⁺ and [PC 34:2+Na]⁺ with m/z 780.5538 and 780.5513 respectively. With a difference of 25 mDa, *in silico* simulation shows that their separation requires a resolving power of 1,000,000 (not common in mass spectrometers). To solve the problem, quantification of the species can be done in negative ion mode or using MS/MS fragmentation spectra. Since sodiated PC molecules do not produce the same headgroup-specific fragment ion of m/z 184.0733 as protonated PC does [25].
21. In the special circumstances, where MS ion spectra are not sufficient for lipid detection and quantification, we use the MS/MS spectra of the fragment ions for identification and quantification, *see* [10, 24].

Acknowledgements

This work was supported by the Scientific Committee of the Danish Cancer Society (KBVU) (K.M) (R124-A7929-15-S2).

References

1. Shevchenko A, Simons K (2010) Lipidomics: coming to grips with lipid diversity. *Nat Rev Mol Cell Biol* 11(8):593–598. doi:10.1038/nrm2934
2. Menendez JA, Lupu R (2007) Fatty acid synthase and the lipogenic phenotype in cancer pathogenesis. *Nat Rev Cancer* 7(10):763–777. doi:10.1038/nrc2222
3. Fahy E, Subramaniam S, Murphy RC, Nishijima M, Raetz CR, Shimizu T, Spener F, van Meer G, Wakelam MJ, Dennis EA (2009) Update of the LIPID MAPS comprehensive classification system for lipids. *J Lipid Res* 50(Suppl):S9–14. doi:10.1194/jlr.R800095-JLR200
4. van Meer G, Voelker DR, Feigenson GW (2008) Membrane lipids: where they are and how they behave. *Nat Rev Mol Cell Biol* 9(2):112–124. doi:10.1038/nrm2330
5. Wenk MR (2005) The emerging field of lipidomics. *Nat Rev Drug Discov* 4(7):594–610. doi:10.1038/nrd1776
6. Brugger B (2014) Lipidomics: analysis of the lipid composition of cells and subcellular organelles by electrospray ionization mass spectrometry. *Annu Rev Biochem* 83:79–98. doi:10.1146/annurev-biochem-060713-035324
7. Hu Q, Noll RJ, Li H, Makarov A, Hardman M, Graham Cooks R (2005) The orbitrap: a new mass spectrometer. *J Mass Spectrom* 40(4):430–443. doi:10.1002/jms.856
8. Horn PJ, Chapman KD (2012) Lipidomics in tissues, cells and subcellular compartments. *Plant J* 70(1):69–80. doi:10.1111/j.1365-313X.2011.04868.x
9. Blanksby SJ, Mitchell TW (2010) Advances in mass spectrometry for lipidomics. *Annu Rev Anal Chem (Palo Alto, Calif)* 3:433–465. doi:10.1146/annurev.anchem.111808.073705
10. Han X, Gross RW (2003) Global analyses of cellular lipidomes directly from crude extracts of biological samples by ESI mass spectrometry: a bridge to lipidomics. *J Lipid Res* 44(6):1071–1079. doi:10.1194/jlr.R300004-JLR200
11. Ejsing CS, Sampaio JL, Surendranath V, Duchoslav E, Ekroos K, Klemm RW, Simons K, Shevchenko A (2009) Global analysis of the yeast lipidome by quantitative shotgun mass spectrometry. *Proc Natl Acad Sci U S A* 106(7):2136–2141. doi:10.1073/pnas.0811700106
12. Sampaio JL, Gerl MJ, Klose C, Ejsing CS, Beug H, Simons K, Shevchenko A (2011) Membrane lipidome of an epithelial cell line. *Proc Natl Acad Sci U S A* 108(5):1903–1907. doi:10.1073/pnas.1019267108
13. Bou Khalil M, Hou W, Zhou H, Elisma F, Swayne LA, Blanchard AP, Yao Z, Bennett SA, Figeys D (2010) Lipidomics era: accomplishments and challenges. *Mass Spectrom Rev* 29(6):877–929. doi:10.1002/mas.20294
14. Schuhmann K, Almeida R, Baumert M, Herzog R, Bornstein SR, Shevchenko A (2012) Shotgun lipidomics on a LTQ orbitrap mass spectrometer by successive switching between acquisition polarity modes. *J Mass Spectrom* 47(1):96–104. doi:10.1002/jms.2031
15. Almeida R, Pauling JK, Sokol E, Hannibal-Bach HK, Ejsing CS (2015) Comprehensive lipidome analysis by shotgun lipidomics on a hybrid quadrupole-orbitrap-linear ion trap mass spectrometer. *J Am Soc Mass Spectrom* 26(1):133–148. doi:10.1007/s13361-014-1013-x
16. Almeida R, Berzina Z, Arnspang EC, Baumgart J, Vogt J, Nitsch R, Ejsing CS (2015) Quantitative spatial analysis of the mouse brain lipidome by pressurized liquid extraction surface analysis. *Anal Chem* 87(3):1749–1756. doi:10.1021/ac503627z
17. Han X, Yang K, Cheng H, Fikes KN, Gross RW (2005) Shotgun lipidomics of phosphoethanolamine-containing lipids in biological samples after one-step in situ derivatization. *J Lipid Res* 46(7):1548–1560
18. Han X, Gross RW (2005) Shotgun lipidomics: electrospray ionization mass spectrometric analysis and quantitation of cellular lipidomes directly from crude extracts of biological samples. *Mass Spectrom Rev* 24(3):367–412. doi:10.1002/mas.20023
19. Liebisch G, Binder M, Schifferer R, Langmann T, Schulz B, Schmitz G (2006) High throughput quantification of cholesterol and cholesteryl ester by electrospray ionization tandem mass spectrometry (ESI-MS/MS). *Biochim Biophys Acta* 1761(1):121–128. doi:10.1016/j.bbailip.2005.12.007
20. Casanovas A, Hannibal-Bach HK, Jensen ON, Ejsing CS (2014) Shotgun lipidomic analysis of chemically sulfated sterols compromises analytical sensitivity: recommendation for large-scale global lipidome analysis. *Eur J Lipid Sci Technol* 116(12):1618–1620. doi:10.1002/ejlt.201400451
21. Kalvodova L, Sampaio JL, Cordo S, Ejsing CS, Shevchenko A, Simons K (2009) The lipidomes of vesicular stomatitis virus, semliki for-

- est virus, and the host plasma membrane analyzed by quantitative shotgun mass spectrometry. *J Virol* 83(16):7996–8003. doi:[10.1128/JVI.00635-09](https://doi.org/10.1128/JVI.00635-09)
22. Herzog R, Schuhmann K, Schwudke D, Sampaio JL, Bornstein SR, Schroeder M, Shevchenko A (2012) LipidXplorer: a software for consensual cross-platform lipidomics. *PLoS One* 7(1):e29851. doi:[10.1371/journal.pone.0029851](https://doi.org/10.1371/journal.pone.0029851)
23. Bilgin M, Markgraf DF, Duchoslav E, Knudsen J, Jensen ON, de Kroon AI, Ejsing CS (2011) Quantitative profiling of PE, MMPE, DMPE, and PC lipid species by multiple precursor ion scanning: a tool for monitoring PE metabolism. *Biochim Biophys Acta* 1811(12):1081–1089. doi:[10.1016/j.bbali.2011.09.018](https://doi.org/10.1016/j.bbali.2011.09.018)
24. Ejsing CS, Duchoslav E, Sampaio J, Simons K, Bonner R, Thiele C, Ekroos K, Shevchenko A (2006) Automated identification and quantification of glycerophospholipid molecular species by multiple precursor ion scanning. *Anal Chem* 78(17):6202–6214
25. Al-Saad KA, Siems WF, Hill HH, Zabrouskov V, Knowles NR (2003) Structural analysis of phosphatidylcholines by post-source decay matrix-assisted laser desorption/ionization time-of-flight mass spectrometry. *J Am Soc Mass Spectrom* 14(4):373–382. doi:[10.1016/s1044-0305\(03\)00068-0](https://doi.org/10.1016/s1044-0305(03)00068-0)

Bioinformatics Pertinent to Lipid Analysis in Biological Samples

Justin Ma, Ulises Arbelo, Yenifer Guerra, Katyayini Aribindi, Sanjoy K. Bhattacharya, and Daniel Pelaez

Abstract

Electrospray ionization mass spectrometry has revolutionized the way lipids are studied. In this work, we present a tutorial for analyzing class-specific lipid spectra obtained from a triple quadrupole mass spectrometer. The open-source software MZmine 2.21 is used, coupled with LIPID MAPS databases. Here, we describe the steps for lipid identification, ratiometric quantification, and briefly address the differences to the analyses when using direct infusion versus tandem liquid chromatography–mass spectrometry (LC–MS). We also provide a tutorial and equations for quantification of lipid amounts using synthetic lipid standards and normalization to a protein amount.

Key words Bioinformatic analysis, Lipidomic analysis, Lipid profile, Standards, Ratiometric quantification, MZmine 2.21

1 Introduction

Lipids are biomolecules that play essential roles in cell structure and homeostasis. As structural components, they influence cellular transport, signaling, and membrane elasticity. The cellular lipi-dome is composed of thousands of different lipid molecules that are classified according to their backbone structure, head groups, or aliphatic chain linkages [1]. Based on their functional backbone structure, lipids are divided into eight classes: fatty acyls, polyketides, glycerolipids, sphingolipids, glycerophospholipids, sterol lipids, prenol lipids, and saccharolipids [2]. Lipidomics is a subfield of metabolomics that specializes in the characterization of lipid species within cells, tissues, and other fluids. Changes in the lipid profile occur during cell growth, adherence, apoptosis, and migration; and have been linked with disturbances that lead to disease and have potential applications as biomarkers and in clinical usage [3]. Bioinformatics for lipids aims to identify and quantify these changes efficiently and reliably. Although extensive research has been done

in lipidomics, accurately identifying and quantifying individual species remains a challenge.

Lipid extraction is the first step in lipidomics, in which lipids are recovered from the nonpolar fraction of a liquid-liquid extraction procedure. One extraction method commonly used is a modified Bligh and Dyer method [4] where lipids and proteins are separated into two distinct phases. The recent availability of sensitive analytical platforms has allowed for the detection and quantification of many intact lipid species. Mass spectrometry (MS), fluorescence spectroscopy, and magnetic resonance (NMR), among other techniques, are currently used to determine lipid profiles. Electrospray ionization mass spectrometry (ESI-MS) has revolutionized the way lipids are studied [5] and consists of two main approaches, shotgun and liquid chromatography (LC). The shotgun approach offers a constant lipid concentration while the concentration with LC varies over time.

Data analysis and interpretation follows MS experiments. The LIPIDMAPS website is a free resource founded by the National Institute of General Medical Sciences (NIGMS) that facilitates lipid research [6, 7]. The website offers structural databases, a classification system, pathways, and a mass-to-charge (m/z) calculator. In this work, we present a tutorial guide for analyzing class-specific lipids obtained by LC-MS. The open-source software MZmine 2.21, coupled with LIPID MAPS databases, is used to identify lipid species [8, 9]. Further analysis can be conducted for quantification with the ion intensity (peak area) for each identified lipid species and the calibration curve of the internal standard.

2 Materials

This open-source software, designed specifically for mass spectrometry data, allows for processing of a variety of vendor-specific formats. The software's primary capabilities include processing spectra and building chromatograms for identification and export.

1. MZmine 2.21.
2. Sample Spectra Data.
3. Custom Database (Optional).

3 Methods

3.1 *Raw Data Import*

1. Raw Data Methods > Raw Data Import. The software supports such vendor-specific formats as mzXML, NetCDF, Waters Raw, Agilent CSV, and Thermo CSV.

2. Select and open the desired spectra. The spectra selected should appear in the left half of the interface (Raw Data Files) once successfully imported.

3.2 Mass Detection

The purpose of this step is to create a list of masses for each raw file. The settings depend on how the data was acquired and the scan quality. For centroided data, the Centroid Mass Detector is applied and assumes that every signal above the specified noise level is a peak.

1. Raw Data Methods > Peak Detection > Mass Detection.
2. Adjust the parameters according to data resolution and precision:
 - (a) MS level: depends on type of scan. 2 for NLS and 1 for PIS or full MS1 scans.
 - (b) Polarity: depends on type of ionization.
 - (c) Mass Detector: Centroid.
 - (d) Noise level = 0.
 - (e) Mass list name: masses.
3. Other mass detectors may be used as the exact mass detector: local maxima, recursive threshold, or wavelength transform mass detectors.

3.3 Chromatogram Builder (See Note 1)

After running the mass detection, the chromatogram builder makes a constant chromatogram across the scans for each mass. While ideal setting for each chromatogram may change depending on the data set, common baseline settings for several classes are given.

The min time span parameter specifies the minimum duration of time over which a peak must be detected to be included in the chromatogram. Min height is determined by the least possible intensity of the highest data point. Any chromatogram found below the set level is rejected as noise. The m/z tolerance is the greatest allowed m/z difference between data points to be grouped into the same chromatogram.

1. Raw Data Methods > Peak Detection > Chromatogram Builder.
2. Parameters:
 - (a) Mass list: masses.
 - (b) Set filters (MS level and polarity should be the same as the parameters for mass detection):

PC

- Min time span: 0.
- Min height: 5.00E3.
- m/z tolerance 0.3.

PS, PE, PI

- Min time span: 0.
 - Min height: 1.00E2.
 - m/z tolerance 0.3.
3. The completed chromatograms should now appear under the Peak List column on the right side of the interface. Clicking on a completed chromatogram should display a window with the ID, average m/z, retention time, peak shape, height, and area in table form.
 4. Troubleshooting.
 - (a) If the chromatograms do not appear, an error was made in file selection or in applying the settings.
 - (b) If the chromatogram table appears blank, the parameters may have been set too high, causing all data to be discounted as noise.

3.4 Isotopic Peak Correction

The isotopic peaks grouper leaves one representative peak for a group of isotopes.

1. Peal List Methods > Isotopes > Isotopic Peak Grouper.
 - (a) m/z tolerance: 0.05.
 - (b) RT tolerance: entire duration of analysis.
 - (c) Monotopoic shape: checked.
 - (d) Maximum charge: 1.
 - (e) Representative isotope: Lowest m/z.

3.5 Identification

Identification of the generated peaks is done using either custom databases or those provided by the software. Below are the instructions for identifying lipids from a custom database. If no custom database is available, the software provides an adduct ion search, a peak complex search, and an online database search. Note that a custom database may be created by the user (*see* Subheading 3.7).

1. Peak list methods > Identification > Custom Database Search > Select the correct database to which you are analyzing.
2. Parameters:
 - (a) Field separator: , (comma).
 - (b) Field order: ID, m/z, Retention time, Identity, Formula.
 - (c) Ignore First List: Checked.
 - (d) m/z tolerance: 0.3 (*see* **Note 2**).
 - (e) RT tolerance: the entire duration of the direct infusion analysis.

3.6 Export of CSV File

1. Select file (individually) > Peak list methods > Export/Import > Export to CSV.
2. Parameters:
 - (a) Filename.
 - (b) Field separator: , (comma).
 - (c) Export common elements: *Export row m/z* only.
 - (d) Export identity elements: *Name* only.
 - (e) Export data file elements: *Export peak area* only.
3. After the files are exported, they can be combined and further analyzed and quantified outside of MZmine if needed (*see* Subheading 3.8). However, MZmine offers several analysis and visual representation methods. Other export formats can be selected, such as MzTAB, XML and SQL that may open alternatives for later analysis.

3.7 Creating a Class-Specific Database (See Note 3)

Each lipid class will require a corresponding database that contains the attributes to each species. These databases can be obtained from a variety of Internet sources, such as ThermoFisher's Lipidizer or the NIH's LIPIDMAPS. Guidelines for using LIPIDMAPS are given.

1. Visit LIPIDMAPS website > Resources > Classification.
2. Open the desired main class from the eight categories.
3. At the bottom of the list find the *Download results* tab, choose the CSV format and all pages.
4. Open the file in excel and place the columns in the order of ID, m/z, Retention Time, Identity (Common name), Formula.
5. Save as .csv.
6. The new custom database can now be selected in the custom data base search interface for identification.

3.8 Post-MZmine Analysis

For experimental purposes it is often useful to organize and analyze the data as presented in the MZmine-exported file. Further manipulation is often required to analyze data from large experiments or for selecting species for a detailed study.

1. **Ratiometric Quantification:** If a standard of known amount was used during mass spectrometry, its peak area can be assigned as the standard area. The ratio becomes a known amount of standard with a known peak area of the standard, compared to an unknown amount of lipid species with a known peak area of the lipid species. The ratiometric quantification can be outlined in the following mathematical equations:

$$\frac{\text{Known amount of standard}}{\text{Known peak area of standard}} = \frac{\text{unknown amount of lipid species}}{\text{known peak area of lipid species}}$$

where

$$\begin{aligned} & \text{Known amount of standard (pmol of lipid)} \\ & = \text{concentration of standard} \times \text{volume of sample injected} \end{aligned}$$

The amount of lipid species obtained from the ratiometric quantification analyses above should be divided by the total amount of protein in the sample for normalization with regard to differences in tissue size. The Bradford method is used as a method of protein concentration as described elsewhere [10]. The final amount of lipid is expressed in pmol of lipid/ μg protein amount.

2. Multi-sample analysis: The nature of experimentation often requires manipulations of parameters across different sheets to obtain a single data point. For lipidomics this may include selecting the lowest m/z and manually averaging the associated peak areas for a single species in many data sheets in tandem, quickly becoming a very time-consuming task. Third-party software exists but may be difficult to locate and secure. As such, it can be necessary to design simple programs (e.g., in Excel's VBA language). Some useful program schematics follow:
 3. Programs that will average the m/z and peak area values for each occurrence of a certain named species, assigning results to a new sheet.
 4. Programs that can indicate the frequency of occurrence of identified peaks across multiple sheets from different replicates.
 5. Programs that conduct a search comparison between data sheets, indicating the species that are unique to a set or present in both sets.
 6. Programs that can carry out other statistical analyses.

4 Notes

1. The chromatogram builder assumes a liquid chromatographic separation has preceded the mass spectrometric analysis and thus will analyze the data as a chromatogram (peak as a function of retention time). However, mass spectrometric analyses using direct infusion will still allow for analyses and undergo a *pseudochromatogram* builder, with the understanding that the retention time (RT) is the total analysis time and the peak intensity at any time point has no bearing on identification or quantification of the spectra.

2. The mass spectrometer used for these analyses has a moderate resolution instrument, meaning the accuracy of the m/z is within ± 0.3 Da.
3. For accurate identification of peaks the custom database may need to be altered to reflect mass changes in the species such as adducts.

References

1. Han X, Yang K, Gross RW (2012) Multi-dimensional mass spectrometry-based shotgun lipidomics and novel strategies for lipidomic analyses. *Mass Spectrom Rev* 31(1):134–178. doi:[10.1002/mas.20342](https://doi.org/10.1002/mas.20342)
2. Shevchenko A, Simons K (2010) Lipidomics: coming to grips with lipid diversity. *Nat Rev Mol Cell Biol* 11(8):593–598. doi:[10.1038/nrm2934](https://doi.org/10.1038/nrm2934)
3. Hannun YA, Obeid LM (2008) Principles of bioactive lipid signalling: lessons from sphingolipids. *Nat Rev Mol Cell Biol* 9(2):139–150. doi:[10.1038/nrm2329](https://doi.org/10.1038/nrm2329)
4. Bligh EG, Dyer WJ (1959) A rapid method of total lipid extraction and purification. *Can J Biochem Physiol* 37(8):911–917. doi:[10.1139/o59-099](https://doi.org/10.1139/o59-099)
5. Bhattacharya SK (2013) Recent advances in shotgun lipidomics and their implication for vision research and ophthalmology. *Curr Eye Res* 38(4):417–427. doi:[10.3109/02713683.2012.760742](https://doi.org/10.3109/02713683.2012.760742)
6. Fahy E, Sud M, Cotter D, Subramaniam S (2007) LIPID MAPS online tools for lipid research. *Nucleic Acids Res* 35(Web Server issue):W606–W612. doi:[10.1093/nar/gkm324](https://doi.org/10.1093/nar/gkm324)
7. Sud M, Fahy E, Cotter D, Brown A, Dennis EA, Glass CK, Merrill AH Jr, Murphy RC, Raetz CR, Russell DW, Subramaniam S (2007) LMSD: LIPID MAPS structure database. *Nucleic Acids Res* 35(Database issue):D527–D532. doi:[10.1093/nar/gkl838](https://doi.org/10.1093/nar/gkl838)
8. Katajamaa M, Miettinen J, Oresic M (2006) MZmine: toolbox for processing and visualization of mass spectrometry based molecular profile data. *Bioinformatics* 22(5):634–636. doi:[10.1093/bioinformatics/btk039](https://doi.org/10.1093/bioinformatics/btk039)
9. Pluskal T, Castillo S, Villar-Briones A, Oresic M (2010) MZmine 2: modular framework for processing, visualizing, and analyzing mass spectrometry-based molecular profile data. *BMC Bioinformatics* 11:395. doi:[10.1186/1471-2105-11-395](https://doi.org/10.1186/1471-2105-11-395)
10. Bradford MM (1976) A rapid and sensitive method for the quantitation of microgram quantities of protein utilizing the principle of protein-dye binding. *Anal Biochem* 72:248–254

Chapter 14

LC–MS–Based Lipidomics and Automated Identification of Lipids Using the LipidBlast *In-Silico* MS/MS Library

Tomas Cajka and Oliver Fiehn

Abstract

This protocol describes the analysis, specifically the identification, of blood plasma lipids. Plasma lipids are extracted using methyl *tert*-butyl ether (MTBE), methanol, and water followed by separation and data acquisition of isolated lipids using reversed-phase liquid chromatography coupled to quadrupole/time-of-flight mass spectrometry (RPLC–QTOFMS) operated in MS/MS mode. For lipid identification, acquired MS/MS spectra are converted to the mascot generic format (MGF) followed by library search using the *in-silico* MS/MS library LipidBlast. Using this approach, lipid classes, carbon-chain lengths, and degree of unsaturation of fatty-acid components are annotated.

Key words Liquid chromatography–mass spectrometry, Tandem mass spectrometry, Lipidomics, Lipids, Identification, LipidBlast

1 Introduction

Advances in mass spectrometry have had a big impact on overall lipidomics workflows over the last decade. Analytical protocols were streamlined and fast data acquisition mass spectrometers were introduced, enabling collecting multiple types of mass spectrometric data within a single run [1–3]. One of the key advantages of mass spectrometry is its ability to be used for quantification as well as molecule identification. By utilizing tandem mass spectrometry (MS/MS), the lipid class head group, the lengths of carbon-chains, and the degree of unsaturation of fatty-acid components of these acyl groups are annotated [4]. Licensed MS/MS repositories such as Metlin and NIST14, as well as public libraries such as MassBank, do not cover lipids well because these libraries are based on the acquisition of MS/MS spectra of pure chemical standards. For many lipids there are no commercially available lipid standards. Fortunately, many lipids break in an MS/MS experiment in a predictable manner. Fragmentation rules were compiled from the literature and from authentic standards for 29 lipid classes, and

these rules were then applied to lipid structures that were generated using *in-silico* methods to yield a really comprehensive lipidomics library for compound annotations [5].

Generating an *in-silico* MS/MS library consists of the following steps: (1) selecting lipid classes of interest and defining structural boundaries to exclude biologically improbable compounds; (2) generating all possible structures *in-silico* within these structural boundaries; (3) interpreting experimental MS/MS spectra from literature, other libraries, and authentic standards; (4) generating rules based on characteristic fragmentations; (5) modeling MS/MS spectra including ion abundances for each *in-silico* molecular species; (6) validating the *in-silico* MS/MS spectra with additional compounds that were not included in the rule generation; (7) demonstrating the applicability of such library in proof-of-principle studies (Fig. 1) [5]. Besides the protocol presented here, different software solutions for lipid identification are available either from vendors (e.g., LipidView, Lipid Search, SimLipid) or as independent platforms (e.g., LipidBlast [5], LipidXplorer [6], LipidQA [7]) for untargeted LC-MS/MS-based lipidomics. However, no thorough comparison of advantages and disadvantages of these programs has been published.

Here, we present a protocol for using the *in-silico* MS/MS library LipidBlast for the identification of blood plasma lipids separated using reversed-phase liquid chromatography coupled to high-resolution mass spectrometry with a quadrupole/time-of-flight mass analyzer (RPLC-QTOFMS) (Fig. 2). With slight modifications, the protocol can be used also with high-resolution mass analyzer such as a quadrupole/orbital ion trap, or unit resolution mass spectrometers such as an ion trap or a single quadrupole.

2 Materials

2.1 Equipment

1. Calibrated pipettes 1–10 μL , 10–200 μL , and 100–1000 μL .
2. Vortexer.
3. Orbital mixing chilling/heating plate.
4. Centrifuge.
5. Centrifugal vacuum concentrator.
6. Agilent 1290 Infinity LC system (Agilent Technologies, Santa Clara, CA, USA) with a pump (G4220A), a column oven (G1316C), and an autosampler (G4226A).
7. Agilent 6550 iFunnel QTOFMS system (Agilent) with an electrospray ion source operated in positive and negative ion polarity.

2.2 Reagents

1. LC-MS-grade solvents: water, acetonitrile, isopropanol.
2. Mobile-phase modifiers: formic acid, ammonium formate, ammonium acetate.

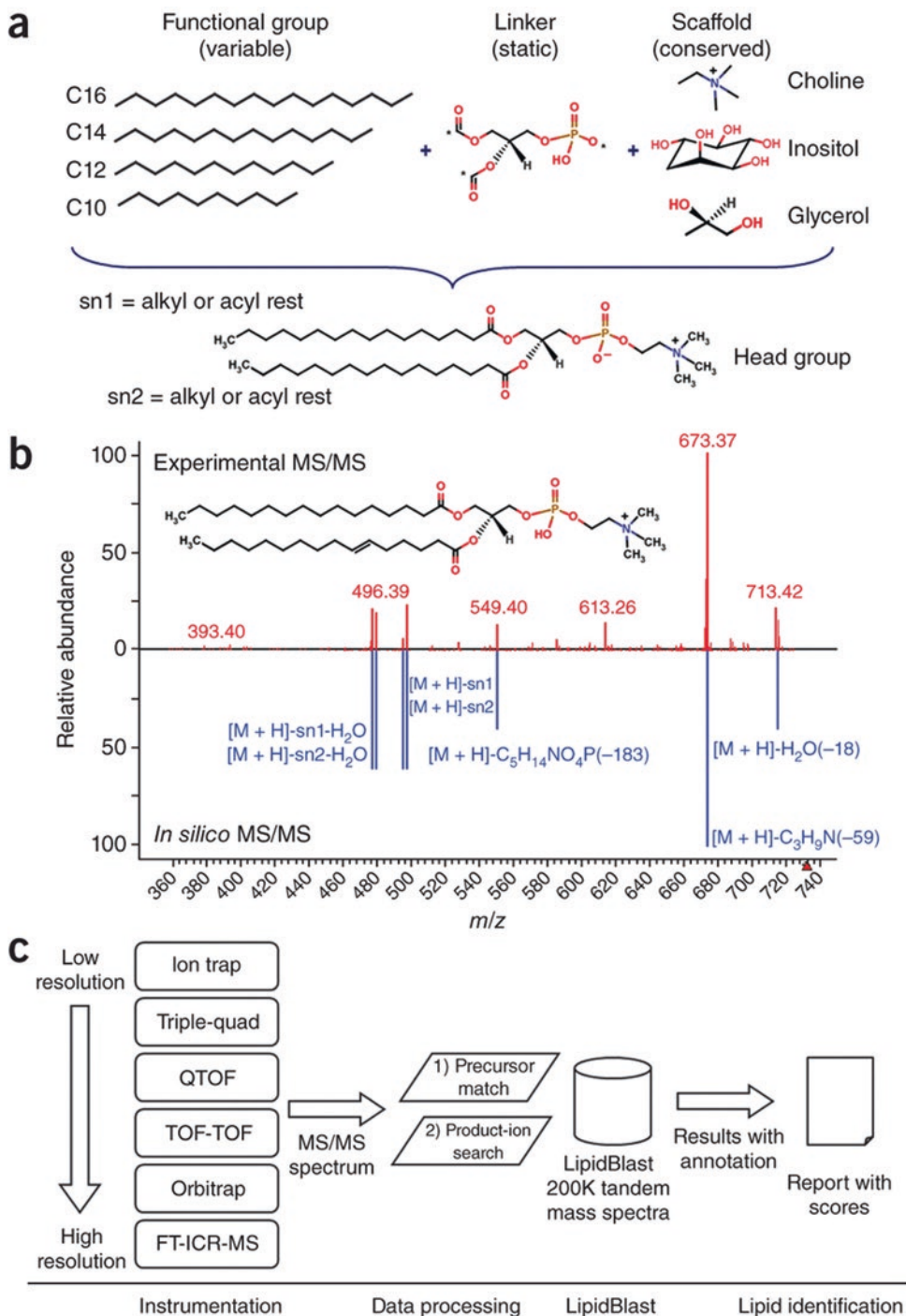


Fig. 1 Creating, validating, and applying *in-silico* generated MS/MS spectra in LipidBlast. **(a)** Lipid compound structures are generated using *in-silico* methods. Lipid core structure scaffolds are connected via a linker to fatty acyls with different chain lengths and different degrees of unsaturation. Asterisks denote connection points. **(b)** Reference tandem spectra (top) are used to simulate mass spectral fragmentations and ion abundances of the *in-silico* spectra (bottom). The compound shown is a phosphatidylcholine (PC), PC (16:0/16:1) at precursor m/z 732.55 $[M+H]^+$. **(c)** For lipid identification, MS/MS spectra obtained from LC-MS/MS experiments are submitted to LipidBlast. An m/z precursor-ion filter filters the data based on m/z precursors. If accurate mass data are used, usually 10 ppm precursor windows are used. Subsequently, experimental fragment ions are matched against the library spectra, generating a hit score that reflects the level of confidence for compound annotation. (Reproduced from [5] with permission from Nature Publishing Group)

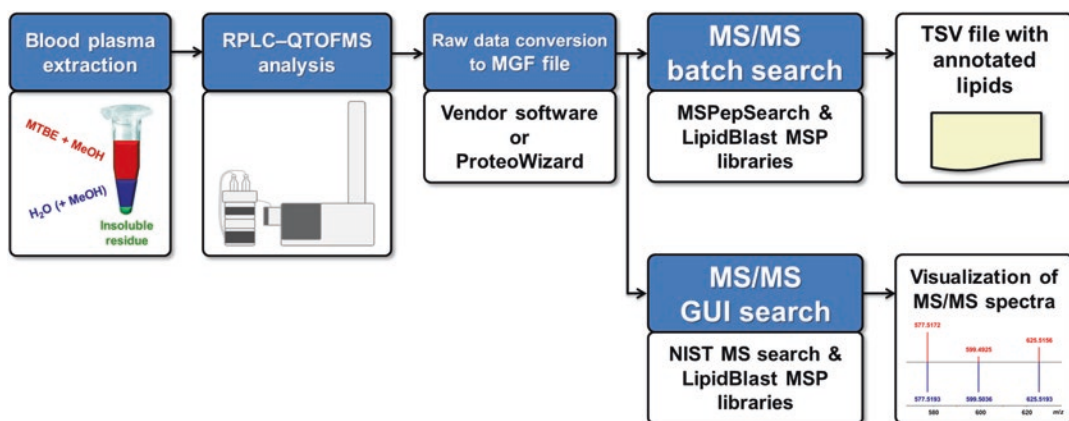


Fig. 2 Workflow of LC–MS-based lipidomics and automated identification of lipids using the LipidBlast *in-silico* MS/MS library. (Legend: RPLC–QTOFMS reversed-phase liquid chromatography coupled to quadrupole/time-of-flight mass spectrometry, MGF mascot generic format, MSP text files containing spectra in the NIST MS Search format, TSV tab-separated values, GUI graphical user interface)

- Solvents for sample preparation: methanol, methyl *tert*-butyl ether, toluene, water.

2.3 Human Plasma

- Disodium EDTA plasma, HMPLEDTA (Bioreclamation IVT, Westbury, NY, USA) stored at -80°C prior to analysis.

2.4 Supplies

- 1.5 mL Eppendorf tubes, uncolored.
- Tips for organic solvents such as acetonitrile, methanol, and methyl *tert*-butyl ether.
- Glass amber vials (2 mL volume).
- Glass inserts for 2 mL standard opening vial (50 μL volume).
- Screw caps for vials.
- Acquity UPLC CSH C18 column (100 \times 2.1 mm; 1.7 μm) (Waters, Milford, MA, USA).
- Acquity UPLC CSH C18 VanGuard pre-column (5 \times 2.1 mm; 1.7 μm) (Waters).

3 Methods

Blood plasma lipids are extracted using a biphasic solvent system of methanol, methyl *tert*-butyl ether (MTBE), and water with some modification [8]. This extraction protocol extracts all main lipid classes in plasma with high recoveries, specifically phosphatidylcholines (PC), sphingomyelins (SM), phosphatidylethanolamines (PE), lysophosphatidylcholines (LPC), ceramides (Cer), cholesterol esters (CholE), and triacylglycerols (TG). The plasma lipids are then separated using a short microbore column (100 \times 2.1 mm

I.D.) with 1.7 μm particle size with C18 sorbent, which represents the currently preferred method in LC-MS-based lipidomics [1]. Using positive and negative electrospray ionization with different mobile-phase modifiers for each polarity increases the coverage of detected lipids [9]. Fig. 3 shows typical positive and negative electrospray ionization chromatograms of plasma lipids.

High-resolution mass spectrometry employing a quadrupole/time-of-flight mass analyzer is used for tandem MS/MS spectra collection. For the system used, different fixed collision energies (+20 eV and -40 eV for ESI(+) and ESI(-), respectively) are used to obtain information-rich MS/MS spectra. After data

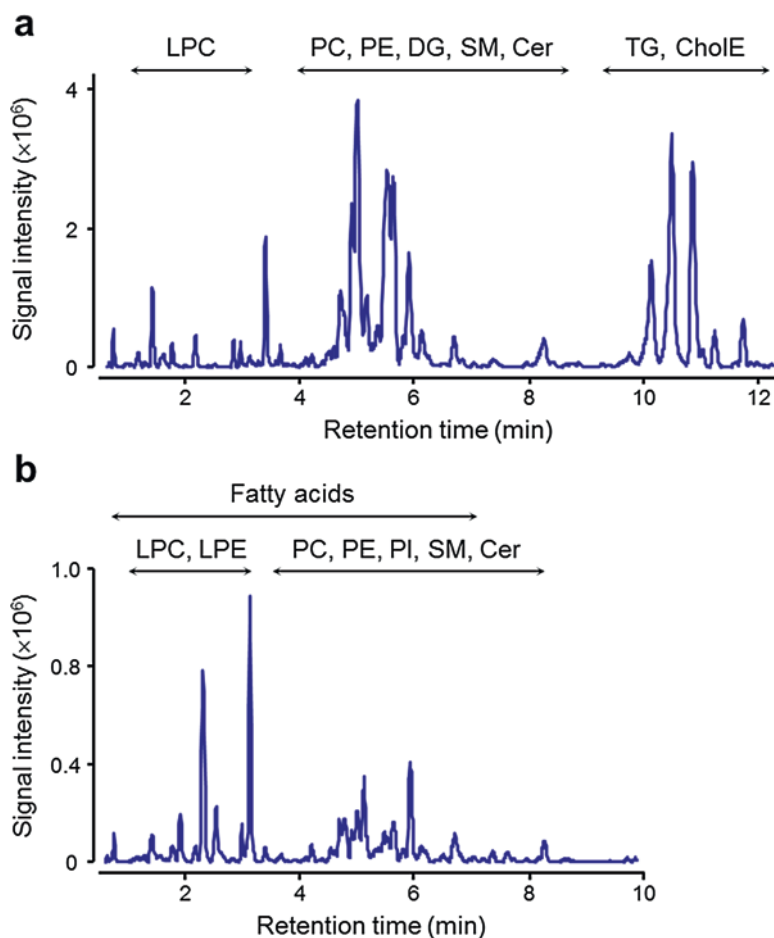


Fig. 3 Total ion chromatograms of plasma lipids, highlighting retention time ranges of particular lipid classes. (a) LC-ESI(+)-MS analysis; (b) LC-ESI(-)-MS analysis. (Legend: Cer ceramides, CholE cholesteryl esters, DG diacylglycerols, LPC lysophosphatidylcholines, LPE lysophosphatidylethanolamines, PC phosphatidylcholines, PE phosphatidylethanolamines, PI phosphatidylinositols, SM sphingomyelins, TG triacylglycerols)

acquisition, MS/MS spectra are converted to an MGF file. This MGF file is queried for lipid annotation using the *in-silico* MS/MS library LipidBlast [5].

3.1 Sample Preparation

1. Add 225 μL of cold methanol (*see* **Notes 1** and **2**) to a 10 μL blood plasma aliquot (*see* **Note 3**) in a 1.5 mL tube (*see* **Note 4**).
2. Vortex at maximum for 10 s.
3. Add 750 μL of cold MTBE (*see* **Note 1**).
4. Vortex for 10 s.
5. Shake for 6 min at 4 °C in the orbital mixer.
6. Add 188 μL of MS-grade water (*see* **Note 5**).
7. Vortex for 20 s.
8. Centrifuge the sample for 2 min at 14,000 $\times g$.
9. Collect two 200 μL aliquots (*see* **Note 4**).
10. Evaporate the aliquots.
11. For LC-ESI(+)-QTOFMS analysis:
 - (a) Resuspend dry extract using 150 μL of a methanol/toluene (9:1, v/v) mixture (*see* **Note 4**).
 - (b) Vortex for 10 s.
 - (c) Centrifuge the extract for 2 min at 14,000 $\times g$.
 - (d) Transfer 100 μL to a glass amber vial with a micro-insert.
 - (e) Cap the vial.
 - (f) Perform LC-ESI(+)-QTOFMS analysis.
12. For LC-ESI(-)-QTOFMS analysis:
 - (a) Resuspend dry extract using 50 μL of a methanol/toluene (9:1, v/v) mixture (*see* **Note 4**).
 - (b) Vortex for 10 s.
 - (c) Centrifuge the extracts for 2 min at 14,000 $\times g$.
 - (d) Transfer 45 μL to a glass amber vial with a micro-insert.
 - (e) Cap the vial.
 - (f) Perform LC-ESI(-)-QTOFMS analysis.

3.2 LC-MS Analysis

3.2.1 Pre-Run Procedures

1. Prepare the tuning solution: 10 mL Agilent Low Concentration ESI Tuning mix (Agilent), 88.5 mL acetonitrile, 4.5 mL water, 3 μL 0.1 mM HP-0321. Make sure to add the components in the order listed to avoid precipitation of any components of the tuning mix.
2. Tune the instrument in both polarities using tuning solution.
3. Prepare the reference ion mass solution: 95 mL acetonitrile, 5 mL water, 100 μL 5 mM 921 Reference Ion, and 100 μL

10 mM Purine Reference Ion. This solution is used for mass correction during the analyses (lock mass).

- (a) In ESI(+), check the intensity of ions m/z 121.0509 and m/z 922.0098, which should be between 5000 and 50,000 with 0.6 mL/min column flow rate. Adjust recipe to attain this intensity.
 - (b) In ESI(-), check the intensity of ions m/z 119.0363 and m/z 980.0164, which should be between 5000 and 50,000 with 0.6 mL/min column flow rate. Adjust recipe to attain this intensity.
4. Check the backpressure of the LC column. Backpressure should be within the range 500–580 bar at the beginning of each run [elution at 15% of the mobile phase (B)] and should not exceed the range 850–1000 bar [elution at 99% of the mobile phase (B)].
 5. Use a new column after approximately 1000 sample injections. The LC column must be coupled to a VanGuard pre-column. The VanGuard pre-column is replaced after approximately 330 sample injections.

3.2.2 Analysis in ESI(+)

1. Prepare mobile phases: (A) 60:40 (v/v) acetonitrile:water with 10 mM ammonium formate and 0.1% formic acid; (B) 90:10 (v/v) isopropanol:acetonitrile with 10 mM ammonium formate and 0.1% formic acid (*see Note 6*).
2. LC gradient: 0 min 15% (B); 0–2 min 30% (B); 2–2.5 min 48% (B); 2.5–11 min 82% (B); 11–11.5 min 99% (B); 11.5–12 min 99% (B); 12–12.1 min 15% (B); 12.1–15 min 15% (B).
3. Column flow and temperature: 0.6 mL/min; 65 °C.
4. Injection volume: 3 μ L (*see Note 4*).
5. Sample temperature: 4 °C.
6. MS conditions: MS¹ mass range, m/z 100–1700; MS/MS mass range, m/z 100–1700; collision energy, +20 eV; capillary voltage, +3.5 kV; nozzle voltage, +1 kV; gas temperature, 200 °C; drying gas (nitrogen), 14 L/min; nebulizer gas (nitrogen), 35 psi; sheath gas temperature, 350 °C; sheath gas flow (nitrogen), 11 L/min.
7. MS data acquisition: MS¹, 10 spectra/s (100 ms); MS/MS, 13 spectra/s (77 ms); total cycle time, 0.508 s; number of precursor ion per cycle, 4; mass range for selection of precursor ions, m/z 300–1200; isolation width, narrow (1.3 m/z); precursor threshold, 2000 counts; active exclusion, excluded after 3 spectra, released after 0.07 min.
8. Reference masses: m/z 121.0509, m/z 922.0098.

3.2.3 Analysis in ESI(-)

1. Prepare mobile phases: (A) 60:40 (v/v) acetonitrile:water with 10 mM ammonium acetate; (B) 90:10 (v/v) isopropanol:acetonitrile with 10 mM ammonium acetate (*see Note 6*).
2. LC gradient: 0 min 15% (B); 0–2 min 30% (B); 2–2.5 min 48% (B); 2.5–9.5 min 76% (B); 9.5–9.6 min 99% (B); 9.6–10.5 min 99% (B); 10.5–10.6 min 15% (B); 10.6–13.5 min 15% (B).
3. Column flow and temperature: 0.6 mL/min; 65 °C.
4. Injection volume: 5 µL (*see Note 4*).
5. Sample temperature: 4 °C.
6. MS conditions: MS¹ mass range, m/z 100–1700; MS/MS mass range, m/z 100–1700; collision energy, –40 eV; capillary voltage, –3.5 kV; nozzle voltage, –1 kV; gas temperature, 200 °C; drying gas (nitrogen), 14 L/min; nebulizer gas (nitrogen), 35 psi; sheath gas temperature, 350 °C; sheath gas flow (nitrogen), 11 L/min.
7. MS data acquisition: MS¹, 10 spectra/s (100 ms); MS/MS, 13 spectra/s (77 ms); total cycle time, 0.508 s; number of precursor ion per cycle, 4; mass range for selection of precursor ions, m/z 250–1100; isolation width, narrow (1.3 m/z); precursor threshold, 500 counts; active exclusion, excluded after 3 spectra, released after 0.07 min.
8. Reference masses: m/z 119.0360, m/z 980.0164 (acetate adducts).

3.2.4 Reducing Carryover between Sample Injections

Carryover between sample injections represents a critical point during LC–MS-based lipidomics analysis (*see Note 7*). For the LC system used we set up *Injector Cleaning* option in MassHunter Data Acquisition software.

1. Gradient for LC–ESI(+)-MS: Time 1: 0.1 min (bypass), Time 2: 11.6 min (mainpass/bypass), Time 3: 13.0 min (mainpass/bypass).
2. Gradient for LC–ESI(-)-MS: Time 1: 0.1 min (bypass), Time 2: 10.1 min (mainpass/bypass), Time 3: 11.5 min (mainpass/bypass).

3.3 Conversion of MS/MS Spectra to an MGF File

Mascot generic format (MGF) files are a common standard for MS/MS searches for small molecules. Each MS/MS scan is defined with the precursor ion (PEPMASS=), charge (CHARGE=) and m/z -abundance pairs (Fig. 4). Multiple product ion scans are usually combined into a single MGF file.

MGF files can be created either using vendor software or open software such as ProteoWizard.

1. Agilent .D format: Use MassHunter Qualitative Analysis software.


```

BEGIN IONS
PEPMASS=874.7866
CHARGE=1+
TITLE=CSH_pos_plasma_MSMS.d, MS/MS of 874.7866 1+ at 10.41 mins
RTINSECONDS=624.627
549.4851 416
575.5002 1693
576.1730 149
577.5222 347
578.5131 171
601.5133 440
603.5312 828
604.5497 104
857.7447 129
874.7862 750
875.7847 531

END IONS

```

Fig. 4 Example of a product ion scan in mascot generic format (MGF)

2. Thermo .raw format: Use `extractMSn` and `MSFileReader` plus dependency libraries.
3. SCIEX .wiff format: Use `PeakView` software and installation of `MS Data Converter` (downloadable at <http://sciex.com/software-downloads-x2110>).
4. Alternatively, `ProteoWizard` software can be used to create MGF files (Fig. 5).
 - (a) Download and install the latest version of the `ProteoWizard` from the following website: <http://proteowizard.sourceforge.net>.
 - (b) Run `MSConvert.exe` from `ProteoWizard` folder.
 - (c) Browse and add files using `MSConvert` application.
 - (d) Select output directory.
 - (e) Select output format: `mgf`; binary encoding precision: 32-bit.
 - (f) Select appropriate filters such as *MS Level* to work with MS/MS data only, *Peak Picking* to centroid data, and *Threshold Peak Filter* (count; most intense; 50).
 - (g) Start conversion using *Start*, check the progress and create the MGF file.

3.4 LipidBlast in-Silico MS/MS Library

3.4.1 Installation

1. Download the latest version of the `LipidBlast` from the following website: <http://fiehnlab.ucdavis.edu/projects/LipidBlast> (section *Download LipidBlast*)
2. Unzip the file. The `LipidBlast` folder contains several sub-folders:

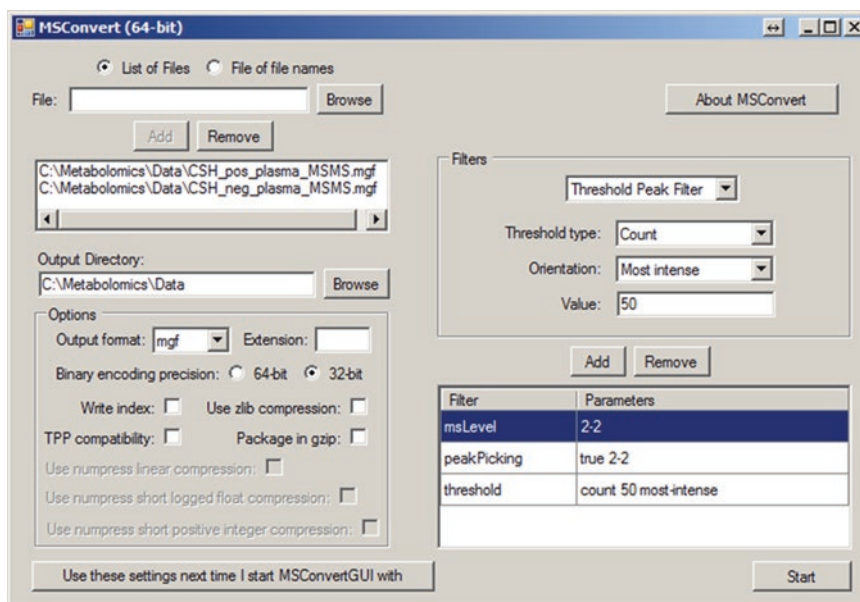


Fig. 5 MSConvert (ProteoWizard) settings for converting raw MS/MS data files to MGF files

- (a) LipidBlast-ASCII-spectra.
- (b) LipidBlast-Development.
- (c) LipidBlast-Examples.
- (d) LipidBlast-HandBook.
- (e) LipidBlast-MSSearch.
- (f) LipidBlast-mz-lookup.
- (g) LipidBlast-Paper.
- (h) LipidBlast-Validation.

3. Download MS PepSearch software from this website: <http://chemdata.nist.gov/dokuwiki/doku.php?id=peptidew:mspepsearch>.
4. Unzip 2013_11_14_MSPepSearch_x32.zip file to \\LipidBlast-Full-Release-3\2013_06_04_MSPepSearch_x32 folder.

3.4.2 MS/MS Batch Search

1. Run MSPepSearchGUI_x64.exe or MSPepSearchGUI_x32.exe from \\LipidBlast-Full-Release-3\2013_06_04_MSPepSearch_x32 and follow settings in Figs. 6 and 7 based on polarity used.
2. Upload MGF file: Input → ☉ File → Open → Select MGF file.
3. Set up Output directory path.
4. Upload MS/MS libraries to search → Select → Select MS/MS library in MSP format from folder \\LipidBlast-Full-Release-3\LipidBlast-MSSearch. Name of MSP libraries, ionization mode, lipid class, and molecular species covered are listed in

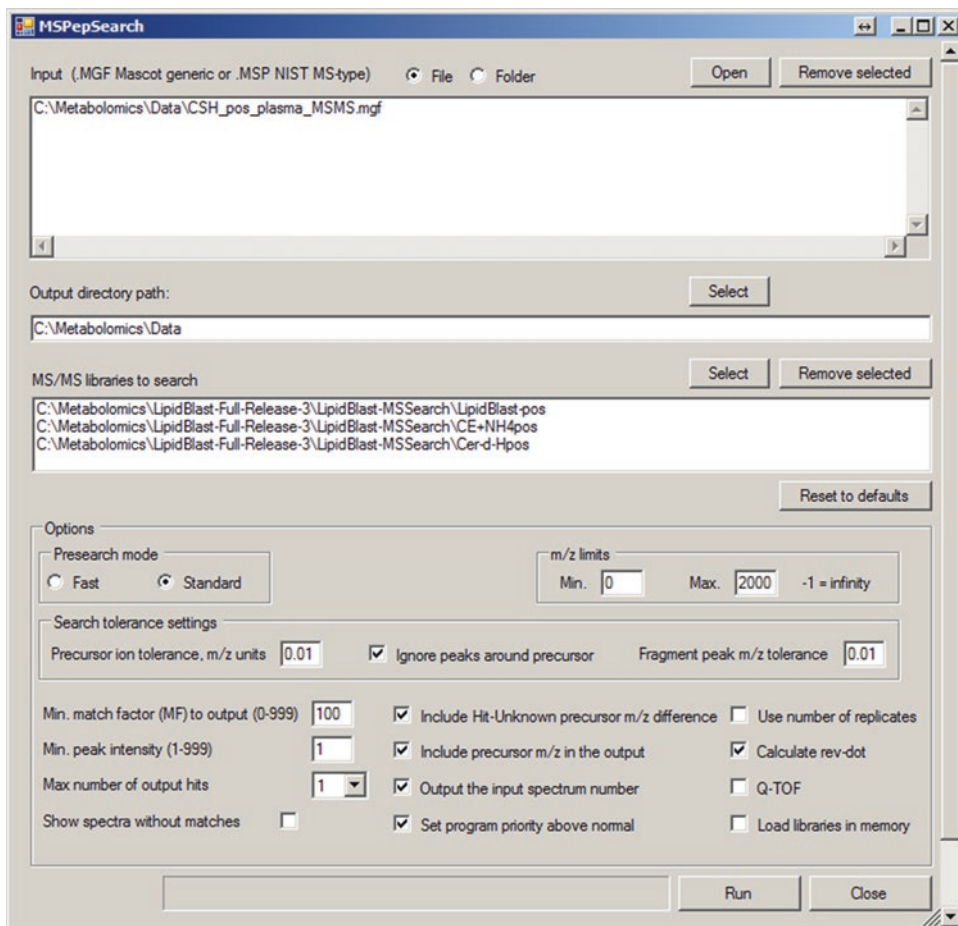


Fig. 6 General settings for MSPepSearch for ESI(+)

Table 1. A maximum of four MSP libraries can be uploaded for one search (*see Note 8*).

5. Change Options for Presearch mode from Fast to Standard.
6. Adjust Search tolerance settings:
 - (a) Precursor ion tolerance, m/z units: 0.01 (*see Note 9*).
 - (b) Fragment peak m/z tolerance: 0.01 (*see Note 9*).
 - (c) Ignore peaks around precursor: keep checked.
7. Adjust other Options parameters:
 - (a) Match factor (MF) to output (0–999): 100.
 - (b) Min. peak intensity: 1.
 - (c) Max. number of output hits: 1.
 - (d) Load libraries in memory: unchecked.
8. Click Run bottom to start MS/MS library search.

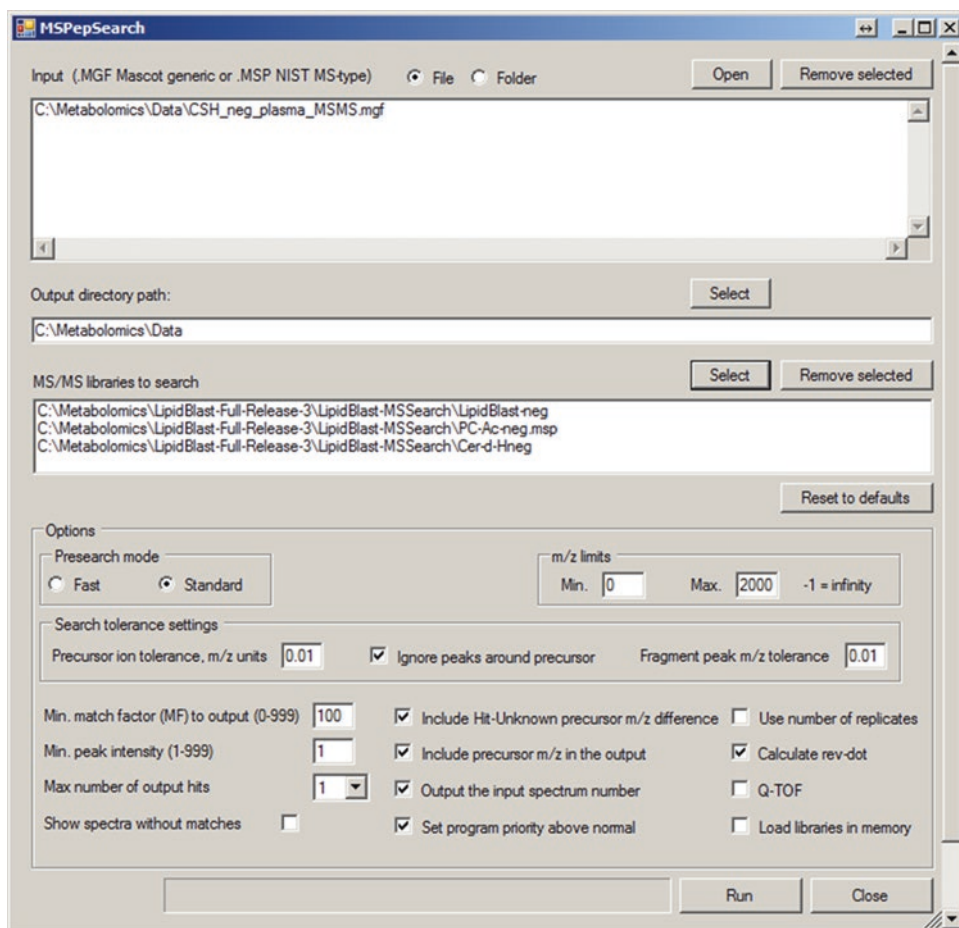


Fig. 7 General settings for MSPepSearch for ESI(–) (see **Note 8** for selecting MSP libraries)

9. For selected MGF file the MSPepSearch program will create TSV (tab-separated values) file containing results of MS/MS search.
10. Open TSV file in Excel for manual inspection (Fig. 8). Use *Dot Product* and *Rev.-Dot* scores for further filtering of data set.
 - (a) Spectral dot product (*Dot Product*) calculation uses the cosine of the angle between the unknown and library spectral vectors.
 - (b) Reverse dot product (*Rev-Dot*) scores are calculated in a similar manner but ignore all ions that are present in the sample spectrum but absent from the library spectrum.

As a general guide for reverse dot product scores, a match >900 is an excellent match; scores between 800 and 900 are good matches; scores between 700 and 800 are fair matches. Scores less than 600 are regarded as very poor matches. MS/MS spectra with many peaks will tend to yield lower spectral dot products

Table 1
Lipid classes covered by the LipidBlast *in-silico* MS/MS library

MSP library	Ionization mode	Lipid class	Abbreviation in LipidBlast	Molecular species covered
LipidBlast-pos	(+)	Ceramide-1-phosphates	CerP	[M+H] ⁺
		Diacylglycerols	DG	[M+NH ₄] ⁺ , [M+Li] ⁺
		Digalactosyl/diacylglycerols	DGDG	[M+Na] ⁺
		Lysophosphatidylcholines	lysoPC	[M+H] ⁺ , [M+Na] ⁺
		Lysophosphatidylethanolamines	lysoPE	[M+H] ⁺ , [M+Na] ⁺
		Monoacylglycerols	MG	[M+NH ₄] ⁺ , [M+Li] ⁺
		Monogalactosyl/diacylglycerols	MGDG	[M+NH ₄] ⁺ , [M+Na] ⁺ , [M+NH ₄ -CO] ⁺
		Phosphatidic acids	PA	[M+Na ₂ -H] ⁺ , [M+Na] ⁺
		Phosphatidylcholines	PC	[M+H] ⁺ , [M+Na] ⁺
		Phosphatidylethanolamines	PE	[M+H] ⁺ , [M+Na] ⁺
		Plasmenylphosphatidylcholines	plasmenyl-PC	[M+H] ⁺ , [M+Na] ⁺
		Plasmenylphosphatidylethanolamines	plasmenyl-PE	[M+H] ⁺ , [M+Na] ⁺
		Phosphatidylserines	PS	[M+H] ⁺ , [M+Na] ⁺
		Sphingomyelins	SM	[M] ⁺ , [M+Na] ⁺
		Triacylglycerols	TG	[M+NH ₄] ⁺ , [M+Na] ⁺ , [M+Li] ⁺
CE + NH ₄ pos	(+)	Cholesteryl esters	CE	[M+NH ₄] ⁺
Cer-d-Hpos	(+)	N-Acylsphingosines (ceramides)	Cer-d	[M+H] ⁺
custom-lysoPC + Hpos	(+)	Lysophosphatidylcholines	lysoPC	[M+H] ⁺
CustomPC + Hpos.msp	(+)	Phosphatidylcholines	PC	[M+H] ⁺
CustomPC + Napos.msp	(+)	Phosphatidylcholines	PC	[M+Na] ⁺

(continued)

Table 1
(continued)

MSP library	Ionization mode	Lipid class	Abbreviation in LipidBlast	Molecular species covered
custom-SM + Hpos	(+)	Sphingomyelins	SM	[M] ⁺
lysoPA + Hpos.msp	(+)	Lysophosphatidic acids	LPA	[M+H] ⁺
LipidBlast-neg	(-)	Diacylated phosphatidylinositol monomannoside	Ac2PIM1	[M-H] ⁻
		Diacylated phosphatidylinositol dimannoside	Ac2PIM2	[M-H] ⁻
		Triacylated phosphatidylinositol dimannoside	Ac3PIM2	[M-H] ⁻
		Tetraacylated phosphatidylinositol dimannoside	Ac4PIM2	[M-H] ⁻
		Ceramide-1-phosphates	CerP	[M-H] ⁻
		Cardiolipins	CL	[M-H] ⁻ , [M-2H] ²⁻
		Digalactosyldiacylglycerols	DGDG	[M-H] ⁻
		Gangliosides	[glycan]-Cer	[M-H] ⁻
		Diphosphorylated hexaacyl Lipid A	LipidA-PP	[M-H] ⁻
		Lysophosphatidylethanolamines	lysoPE	[M-H] ⁻
		Monogalactosyldiacylglycerols	MGDG	[M-H] ⁻
		Phosphatidic acids	PA	[M-H] ⁻
		Phosphatidylethanolamines	PE	[M-H] ⁻
		Phosphatidylglycerols	PG	[M-H] ⁻
		Phosphatidylinositols	PI	[M-H] ⁻
		Phosphatidylserines	PS	[M-H] ⁻
		Sulfoquinovosyldiacylglycerols	SQDG	[M-H] ⁻
		Sulfatides	ST	[M-H] ⁻

Cer-d-Hneg	(-)	<i>N</i> -Acylsphingosines (ceramides)	Cer-d	[M-H] ⁻
PC-Ac-neg.msp	(-)	Phosphatidylcholines	PC	[M+CH ₃ COO] ⁻
PC-Form-neg.msp	(-)	Phosphatidylcholines	PC	[M+HCOO] ⁻
PC-Me-neg.msp	(-)	Phosphatidylcholines	PC	[M-CH ₃] ⁻

(1)	(2)	(3)	(4)	(5)	(6)	(7)	(8)	(9)	(10)	(11)			
Num	Unknown	Precursor m/z	Rank	Library	id	Mass	Delta(m/z)	Lib Precursor m/z	Score	Dot Product	Prob(%)	Rev-Dot	Peptide
1	> MS/MS Search ver. 0.91 build Jun 3 2013 19:11:46. Command line:												
2	> "C:\Metabolomics\2013_06_04_MSPSearch_x64\MSPSearch.exe" /INP "C:\Metabolomics\Data\CSH_pos_plasma_MSMS.mgf" /OUTTAB "C:\Metabolomics\Data\CSH_pos_plasma_MSMS.mgf.tsv" /LIB "C:\Metabolomics\LipidBlast-Full-Release-3\LipidBlast-MSSearch\Lipid												
3													
4													
5	134 CSH_pos_plasma_MSMS.d	MS/MS of 544.3387909	1+	at 1.1364 mins	RT:1.13640	9231	544	0.0015	544.3403	128	516	33.3	937 IsoPC 20:4; [MHH] ⁺ ; PC(20:4)SE.1E.1E(1E)/000
6	135 CSH_pos_plasma_MSMS.d	MS/MS of 544.3387909	1+	at 1.14191666666667 mins	RT:1.14192	9231	544	0.0015	544.3403	356	616	33.3	883 IsoPC 20:4; [MHH] ⁺ ; PC(20:4)SE.1E.1E(1E)/000
7	154 CSH_pos_plasma_MSMS.d	MS/MS of 520.3391647	1+	at 1.21858333333333 mins	RT:1.21858	9209	520	0.0012	520.3403	117	592	16.7	835 IsoPC 18:2; [MHH] ⁺ ; PC(18:2)E.1E(1E)/000
8	182 CSH_pos_plasma_MSMS.d	MS/MS of 466.3294047	1+	at 1.33558333333333 mins	RT:1.33558	9355	466	-0.0008	466.3934	113	458	100	671 IsoPC 17:1; [MHH] ⁺ ; PE(17:1)E(1E)/000
9	187 CSH_pos_plasma_MSMS.d	MS/MS of 546.3328086	1+	at 1.3549 mins	RT:1.35490	9229	546	0.0022	546.356	397	971	50	971 IsoPC 20:3; [MHH] ⁺ ; PC(20:3)SE.2E.1E(1E)/000
10	192 CSH_pos_plasma_MSMS.d	MS/MS of 518.3228048	1+	at 1.40456666666667 mins	RT:1.40457	9269	518	-0.0005	518.3223	110	840	100	995 IsoPC 16:0; [MHNA] ⁺ ; PC(16:0)/000
11	193 CSH_pos_plasma_MSMS.d	MS/MS of 518.3228048	1+	at 1.41048333333333 mins	RT:1.41048	9269	518	-0.0005	518.3223	265	635	100	995 IsoPC 16:0; [MHNA] ⁺ ; PC(16:0)/000
12	194 CSH_pos_plasma_MSMS.d	MS/MS of 496.3396423	1+	at 1.41601666666667 mins	RT:1.41602	9189	496	0.0007	496.3403	188	630	100	874 IsoPC 16:0; [MHH] ⁺ ; PC(16:0)/000
13	198 CSH_pos_plasma_MSMS.d	MS/MS of 496.3396423	1+	at 1.42563333333333 mins	RT:1.42563	9189	496	0.0007	496.3403	201	639	100	886 IsoPC 16:0; [MHH] ⁺ ; PC(16:0)/000
14	210 CSH_pos_plasma_MSMS.d	MS/MS of 518.3228048	1+	at 1.47418333333333 mins	RT:1.47418	9269	518	-0.0005	518.3223	266	633	100	995 IsoPC 16:0; [MHNA] ⁺ ; PC(16:0)/000
15	212 CSH_pos_plasma_MSMS.d	MS/MS of 496.3396423	1+	at 1.4869 mins	RT:1.48690	9189	496	0.0007	496.3403	200	622	100	873 IsoPC 16:0; [MHH] ⁺ ; PC(16:0)/000
16	290 CSH_pos_plasma_MSMS.d	MS/MS of 898.7847222	0	at 10.10693333333333 mins	RT:10.10693	8987847	898	0.0012	898.7859	478	735	97.7	953 TG 54:5; [M+NH4] ⁺ ; TG(18:1/18:2/18:2)
17	298 CSH_pos_plasma_MSMS.d	MS/MS of 872.7698181	0	at 10.12616666666667 mins	RT:10.1262	8727698	872	0.0004	872.7702	412	679	96.4	949 TG 52:4; [M+NH4] ⁺ ; TG(16:0/18:2/18:2)
18	2902 CSH_pos_plasma_MSMS.d	MS/MS of 872.7698181	1+	at 10.13578333333333 mins	RT:10.13578	8727698	872	0.0004	872.7702	414	678	96.5	949 TG 52:4; [M+NH4] ⁺ ; TG(16:0/18:2/18:2)
19	2910 CSH_pos_plasma_MSMS.d	MS/MS of 846.7548218	1+	at 10.15501666666667 mins	RT:10.15502	8467548	846	-0.0002	846.7546	353	758	98.9	938 TG 50:3; [M+NH4] ⁺ ; TG(16:0/16:1/18:2)
20	2914 CSH_pos_plasma_MSMS.d	MS/MS of 846.7548218	1+	at 10.16443333333333 mins	RT:10.16443	8467548	846	-0.0002	846.7546	359	575	61.1	938 TG 50:3; [M+NH4] ⁺ ; TG(16:0/16:1/18:2)
21	2915 CSH_pos_plasma_MSMS.d	MS/MS of 690.6188354	1+	at 10.166 mins	RT:10.1660	6906188	25	690.619	690.6189	314	706	100	849 CE(20:4); [M+NH4] ⁺ ; 20:4 Cholesteryl ester
22	2916 CSH_pos_plasma_MSMS.d	MS/MS of 820.7402242	1+	at 10.16735 mins	RT:10.16735	75731	820	-0.0013	820.739	284	611	99	953 TG 48:2; [M+NH4] ⁺ ; TG(16:0/16:1/16:1)
23	2918 CSH_pos_plasma_MSMS.d	MS/MS of 898.7847222	1+	at 10.17423333333333 mins	RT:10.17423	8987847	898	0.0012	898.7859	457	696	96.1	953 TG 54:5; [M+NH4] ⁺ ; TG(18:1/18:2/18:2)
24	3588 CSH_pos_plasma_MSMS.d	MS/MS of 964.3240112	1+	at 12.05845 mins	RT:12.05845	79572	964	0.0026	964.3267	171	355	100	674 TG 58:0; [M+NH4] ⁺ ; TG(16:0/21:0/21:0)
25	3612 CSH_pos_plasma_MSMS.d	MS/MS of 992.3559611	0	at 12.12886666666667 mins	RT:12.12887	77640	992	0.002	992.3579	119	381	77.3	674 TG 60:0; [M+NH4] ⁺ ; TG(19:0/19:0/22:0)
26	3617 CSH_pos_plasma_MSMS.d	MS/MS of 992.3559611	1+	at 12.1415 mins	RT:12.1415	7752	992	0.002	992.3579	179	555	86.4	913 TG 60:0; [M+NH4] ⁺ ; TG(20:0/20:0/20:0)
27	>												
28	> Completed. 3790 spectra in 1.209 sec, process time = 1.211 sec (read 0.062s; print 0.0125 init pio 0.002s aux 0.008s; sp 0.002s; search only: 0.639s+0.487s=1.126s; 3365.80 spec/s) 3134.44 spec/s Compared 17430 spec. No spectra compared 3023, peaks/spec 3.63												

Fig. 8 Example of TSV file containing an overview of identified lipids based on MS/MS and LipidBlast search. Legend: (1) scan number in MGF file; (2) name of data file processed with particular precursor ion and retention time; (3) precursor m/z; (4) rank; (5) MSP library name; (6) identification number in particular MSP library; (7) difference between theoretical (Lib Precursor m/z) and experimental (Precursor m/z) masses; (8) theoretical mass of precursor ion; (9) spectral dot product; (10) reverse dot product; (11) annotated lipid

(*Dot Product*) than similar spectra with fewer peaks. This can be the case when using higher collision energy leading to extensive fragmentation of precursor ion (Fig. 9).

11. If lipid annotations occur multiple times, there can be two reasons: (1) a true separation of isomers, as in Fig. 10, where two triacylglycerols have the same precursor mass and the same number of acyl carbons and double bonds, however, differ in acyl chain lengths. (2) If MS/MS spectra are annotated with identical isomeric structures, peaks should be at least one peak width apart from each other to exclude erroneous MS/MS selection of the same peak.
12. Some lipids may have lower dot product score because their MS/MS spectra represent a mixture of two or even more lipid isomers having the same number of carbon and double bonds but differ in acyl chain lengths (Fig. 11). Such coelutions unavoidably occur during LC-MS-based lipidomic profiling of complex samples. In this case, the particular lipid is annotated using both species (e.g., TG 52:3; TG 16:1_18:1_18:1 and TG 16:0_18:1_18:2). To get these annotations in TSV file change the *Max number of output hits* parameter from 1 to 2 or 3 in the MSPepSearch (Figs. 6 and 7).

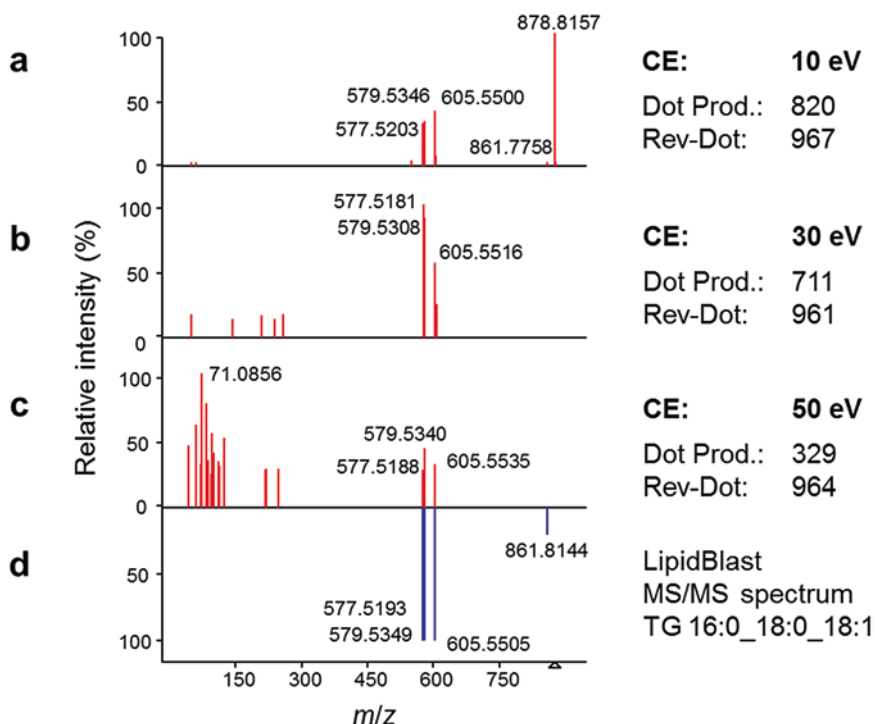


Fig. 9 Experimental MS/MS spectra of TG 16:0_18:0_18:1 (a, b, c) with a precursor ion m/z 878.8172 $[M+NH_4]^+$ and LipidBlast MS/MS spectrum (d). Using different collision energies (CE) yields more fragment ions and thus impacts calculating spectral dot products (Dot Prod.) and reversed dot products (Rev-Dot)

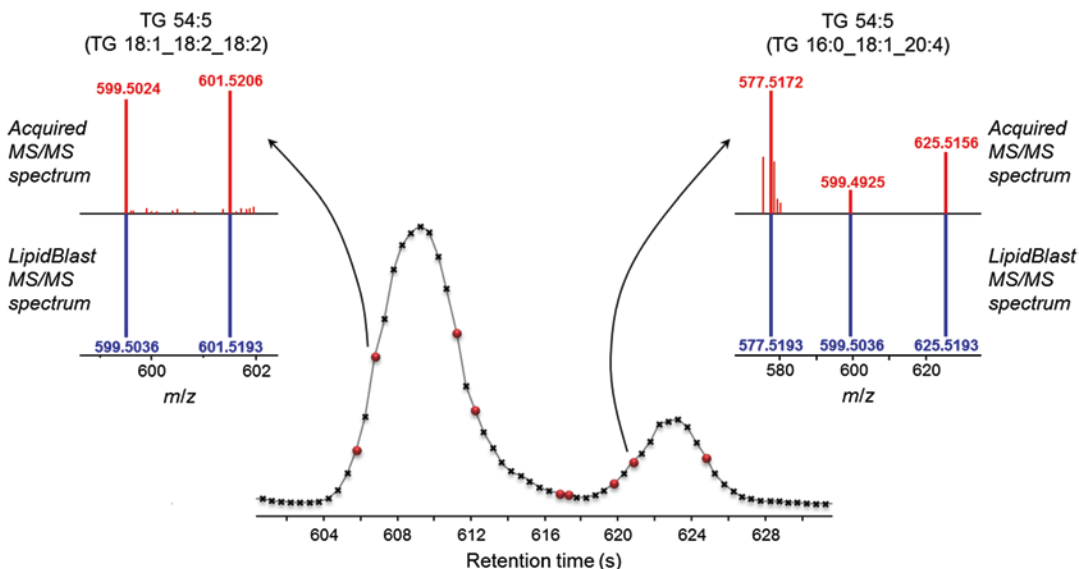


Fig. 10 Extracted ion chromatograms of TG 54:5, m/z 898.7859 $[M+NH_4]^+$ with marked data points per peak: ● MS/MS spectrum acquired, ✕ no MS/MS data acquired

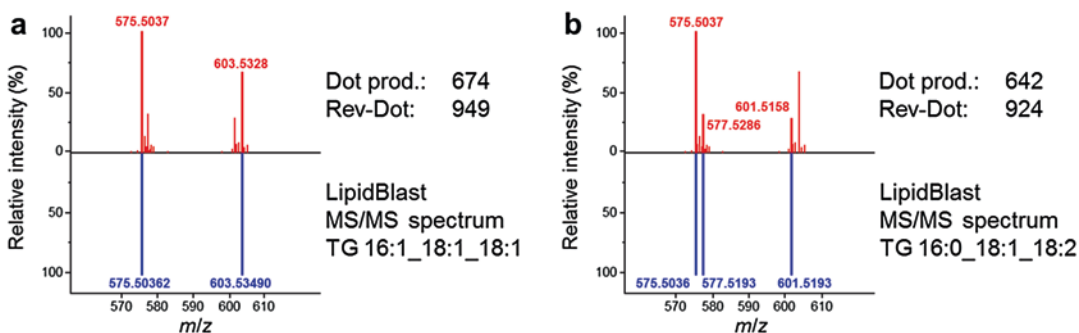


Fig. 11 MS/MS spectrum of TG 52:3 (precursor ion m/z 874.7859 $[M+NH_4]^+$) with two different MS/MS annotations from the LipidBlast library

13. Each identified lipid can be manually inspected based on scan number using *MS/MS Graphical User Interface (GUI)-based search*.

3.4.3 MS/MS Graphical User Interface (GUI)-Based Search

1. Run `nistms.exe` from `\\LipidBlast-Full-Release-3\LipidBlast-MSSearch` folder.
2. Upload MGF file: File → Open → Choose file for spectra/structures import with files of type MGF.

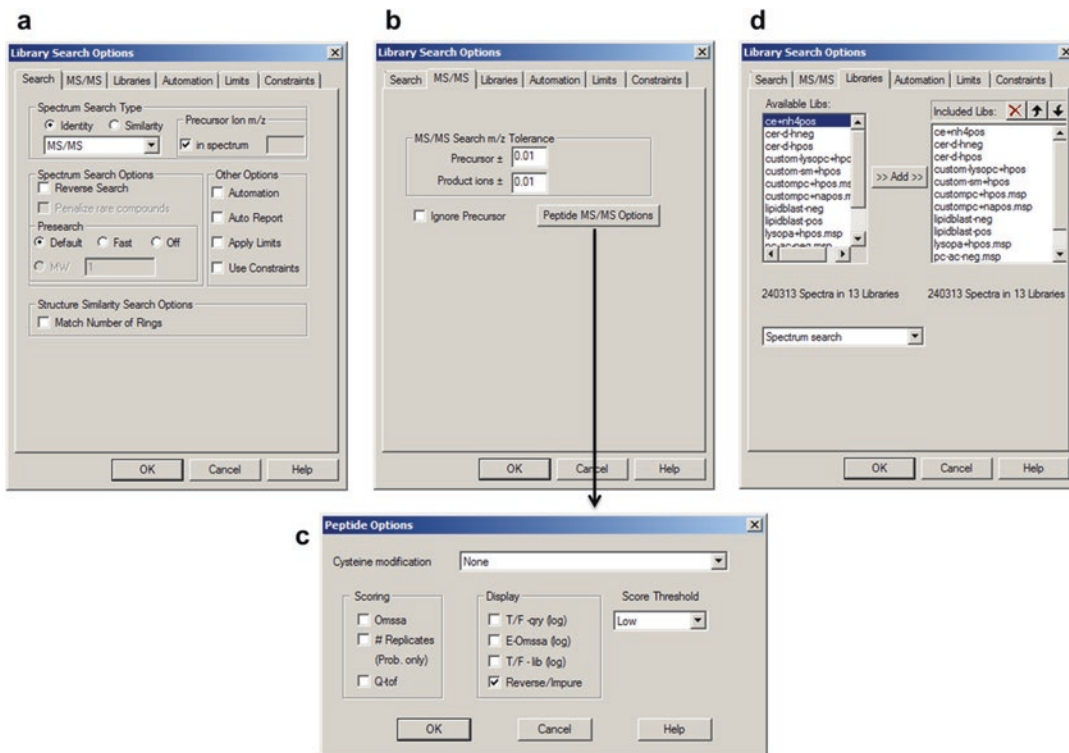


Fig. 12 Settings for MS/MS searches in the NIST MS graphic user interface

3. Check or change LipidBlast libraries including the settings and precursor and product ion window (Fig. 12):
 - (a) Options → Library Search Options → Search → Identity (MS/MS).
 - (b) Options → Library Search Options → MS/MS → MS/MS Search m/z Tolerance → Precursor ± 0.01 ; Product ions ± 0.01 .
 - (c) Options → Library Search Options → MS/MS → Peptide MS/MS Options → Cysteine modification: None; Display: Reverse/Impure; Score Threshold: Low.
 - (d) Options → Library Search Options → MS/MS → Libraries → Add all libraries from Available Libs to Included Libs.
4. Double click on m/z value at a particular retention time to check if there is an MS/MS match with the LipidBlast MS/MS library (Fig. 13).

4 Notes

1. Store solvents (methanol, MTBE) in the $-20\text{ }^{\circ}\text{C}$ freezer to prechill.
2. To prevent contamination disposable material is used. To prevent inhalation of organic solvent vapor, use fume hood during lipid extraction.
3. Thaw each plasma sample on ice. During the extraction keep the Eppendorf tubes either on ice or use prechilled ($-20\text{ }^{\circ}\text{C}$) block.
4. This extraction procedure has been optimized for the Agilent 6550 iFunnel QTOFMS system. For other LC-MS systems differing in their sensitivity the protocol can be modified including (1) volume of blood plasma for analysis (10–30 μL), (2) aliquot taken during the extraction (up to $\sim 700\text{ }\mu\text{L}$ MTBE/methanol layer), (3) volume of resuspension solvent, and (4) volume injected. To avoid band broadening during LC-MS analysis, we recommend a maximum volume of 5 μL during injection.
5. Store water in the $+4\text{ }^{\circ}\text{C}$ fridge to prechill.
6. To enhance solubilization of ammonium formate and ammonium acetate after their addition in the mobile phase, dissolve these salts in a small volume of water before their addition in the mobile phases (0.631 g ammonium formate or 0.771 g ammonium acetate/1 mL water/1 L mobile phase). Mix each mobile phase with modifiers, sonicate them for 15 min to achieve complete dissolving of modifiers (salts), mix them again, and then sonicate for another 15 min.
7. Run plasma extract followed by injection of solvent mixture (methanol:toluene, 9:1, v/v) for checking the carryover. The carryover effect is observed mainly for triacylglycerols. Check the most intensive species such as TG 52:2 (m/z 876.802 $[\text{M}+\text{NH}_4]^+$) and TG 52:3 (m/z 874.786 $[\text{M}+\text{NH}_4]^+$) to evaluate the carryover. Carryover $<0.2\%$ for these most abundant lipid species is acceptable. If possible use different wash solvents during the sample injections, for instance, weak wash solvent: acetonitrile/water (50:50, v/v) followed by a strong wash solvent: isopropanol. If only one solvent for washing is available, use isopropanol and also check a software option to clean the injector using valve switching (e.g., Agilent) at the different composition of mobile phase to release adsorbed lipids.
8. $[\text{M}+\text{Li}]^+$ ions are observed if a base such as LiOH is used as a mobile-phase modifier or coinjected during ionization. For phosphatidylcholines, the formation of $[\text{M}+\text{HCOO}]^-$ and $[\text{M}+\text{CH}_3\text{COO}]^-$ adducts depends on mobile-phase modifier used. Use *PC-Ac-neg.msp* library if using ammonium acetate

(i.e., acetate adducts) and *PC-Form-neg.msp* library if using ammonium formate (i.e., formate adducts) mobile phase modifier.

9. Precursor and fragment ion tolerance depend on the mass accuracy of the particular instrument. Keep in mind that fixed mass tolerance in mDa has different values in ppm. For instance, using 0.01 Da mass tolerance this corresponds to 33, 20, 12, and 10 ppm mass tolerance for precursor ions m/z 300, 500, 800, and 1000, respectively. A wider ion tolerance (0.02–0.05 Da) can be used if precursor ions are very abundant, because mass accuracy is biased if the mass detector is saturated. However, default values should use narrower precursor window tolerances in order to limit false-positive peak detections.

Acknowledgments

This study was supported by the U.S. National Institutes of Health (NIH) Grants P20 HL113452 and U24 DK097154.

References

1. Cajka T, Fiehn O (2014) Comprehensive analysis of lipids in biological systems by liquid chromatography-mass spectrometry. *Trac-Trend Anal Chem* 61:192–206. doi:[10.1016/j.trac.2014.04.017](https://doi.org/10.1016/j.trac.2014.04.017)
2. Hyotylainen T, Oresic M (2015) Optimizing the lipidomics workflow for clinical studies--practical considerations. *Anal Bioanal Chem* 407(17):4973–4993. doi:[10.1007/s00216-015-8633-2](https://doi.org/10.1007/s00216-015-8633-2)
3. Cajka T, Fiehn O (2016) Toward merging untargeted and targeted methods in mass spectrometry-based metabolomics and lipidomics. *Anal Chem* 88(1):524–545. doi:[10.1021/acs.analchem.5b04491](https://doi.org/10.1021/acs.analchem.5b04491)
4. Blanksby SJ, Mitchell TW (2010) Advances in mass spectrometry for lipidomics. *Annu Rev Anal Chem* 3:433–465. doi:[10.1146/annurev.anchem.111808.073705](https://doi.org/10.1146/annurev.anchem.111808.073705)
5. Kind T, Liu KH, Lee do Y, DeFelice B, Meissen JK, Fiehn O (2013) LipidBlast in silico tandem mass spectrometry database for lipid identification. *Nat Methods* 10 (8):755–758. doi:[10.1038/nmeth.2551](https://doi.org/10.1038/nmeth.2551)
6. Herzog R, Schuhmann K, Schwudke D, Sampaio JL, Bornstein SR, Schroeder M, Shevchenko A (2012) LipidXplorer: A software for consensual cross-platform lipidomics. *Plos One* 7(1.) ARTN:e29851. doi:[10.1371/journal.pone.0029851](https://doi.org/10.1371/journal.pone.0029851)
7. Song H, Hsu FF, Ladenson J, Turk J (2007) Algorithm for processing raw mass spectrometric data to identify and quantitate complex lipid molecular species in mixtures by data-dependent scanning and fragment ion database searching. *J Am Soc Mass Spectr* 18(10):1848–1858. doi:[10.1016/j.jasms.2007.07.023](https://doi.org/10.1016/j.jasms.2007.07.023)
8. Matyash V, Liebisch G, Kurzchalia TV, Shevchenko A, Schwudke D (2008) Lipid extraction by methyl-tert-butyl ether for high-throughput lipidomics. *J Lipid Res* 49(5):1137–1146. doi:[10.1194/jlr.D700041-JLR200](https://doi.org/10.1194/jlr.D700041-JLR200)
9. Cajka T, Fiehn O (2016) Increasing lipidomic coverage by selecting optimal mobile-phase modifiers in LC-MS of blood plasma. *Metabolomics* 12(2):article 34. doi:[10.1007/s11306-015-0929-x](https://doi.org/10.1007/s11306-015-0929-x)

Single-Step Capture and Targeted Metabolomics of Alkyl-Quinolones in Outer Membrane Vesicles of *Pseudomonas aeruginosa*

Pallavi Lahiri and Dipankar Ghosh

Abstract

Outer membrane vesicles (OMVs) are secreted by all Gram-ve pathogens. These nano-scale delivery vehicles contain discrete arrays of prokaryotic pathogenic determinants, including a family of low molecular weight (MW) lipidic quorum signaling alkyl-quinolones (AQs). These are synthesized from β -keto-fatty acids and function like primordial lipidic hormones, which regulate numerous pathogenic factors both inter-species and intra-species. Significantly, AQs can also directly exacerbate pathogenesis by cross-kingdom signaling with the host immune, metabolic, and other systems. In *Pseudomonas aeruginosa* more than 50 AQs are reported; many with pathogenic mechanisms that are largely unknown. Some of these AQs are exclusively associated with OMVs. Accurate characterization of these OMV-AQs may reveal novel mechanism of diseases and *Pseudomonas aeruginosa* presents an ideal model. Matrix-free laser desorption/ionization mass spectrometry (LDI-MS) technologies enjoy unique advantages in mass spectrometry (MS)-based imaging and low MW analysis. We report single-step isolation of *Pseudomonas aeruginosa* OMV on inert ceramic filters and high-resolution mass spectrometry (HRMS) analysis of AQs vesicle in situ.

Key words *Pseudomonas sp.*, Gram negative, Outer membrane vesicle (OMV), Alkyl-quinolones, Laser desorption/ionization mass spectrometry (LDI-MS)

1 Introduction

Extracellular secretory vesicles are produced by all living organisms from prokaryotes and eukaryotes [1–3]. This evolutionary conservation underlines critical fitness advantage through controlled release of clusters of membrane bound molecular determinants that allows cells to sense and respond to external environment. In bacteria, particularly the Gram-ve, secretory vesicles originate by external spherical bulges in the outer membrane (OM) and ultimately severalize into environment as OMVs, 20–250 nm in diameter (Fig. 1) [4]. These vesicles share features of the bacterial OM, with an outer layer of lipopolysaccharide

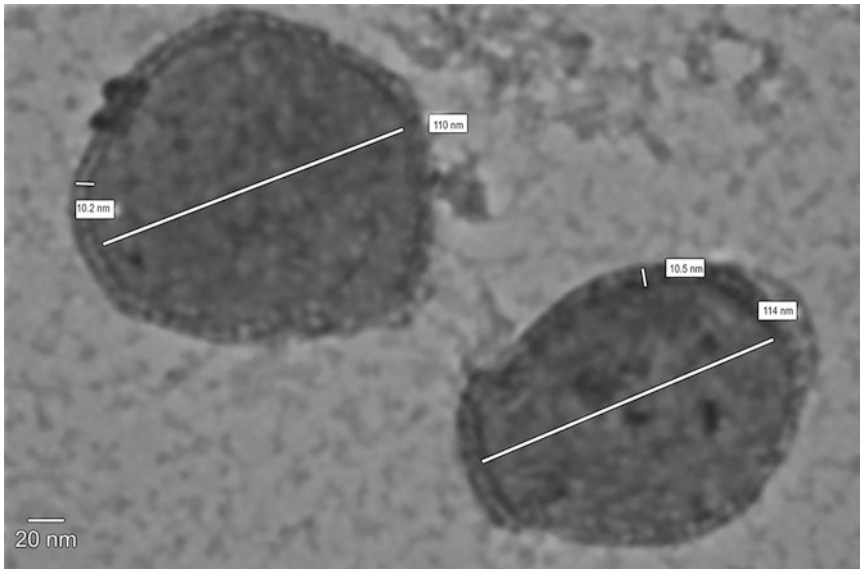


Fig. 1 Transmission electron microscopy (TEM) images of *Pseudomonas aeruginosa* OMVs. Purified OMVs *P. aeruginosa* biofilm culture supernatant exhibit discrete two-layer membrane bound organelles ~100 nm diameter (8000 \times)

(LPS) and an inner phospholipid layer [5, 6]. However, significant differences do exist between the OM and the OMV in the context of its composition and cargo. The OMV membrane contains discrete LPS, phospholipids, and fatty acids and a diverse cargo including nucleic acids, membrane proteins, lipids, and metabolites, which are often species specific [7]. It is clear that this cargo and traffic mechanisms are not consequences of random apoptotic blebbing, but evolutionarily conserved processes that play diverse roles in bioremediation, nutrient acquisition, signaling, drug resistance, pathogenesis, among other functions [3, 7–10]. The concept of *nano-size* bacterial vesicles, strategically packaged with multiple pathogenic determinants, argues for a paradigm shift in the understanding of many infectious diseases. Owing to their small size and unique constituents, OMVs can easily bypass host physiological barriers that otherwise restrict the larger pathogen [11–13]. Subsequently, the vesicles fuse directly with the lipid rafts in the host plasma membrane, delivering a complex cargo that activate signaling cascades and multi-factorial pathologies, which are largely uncharacterized [1, 6, 13].

The Gram-ve bacteria *Pseudomonas aeruginosa* is paradigm of these novel mechanisms of OMV pathogenesis [1, 3, 14]. This pathogen has emerged as a global public health threat with increasingly multiple drug resistant (MDR) infections in diverse sites, including respiratory, skin, genitourinary, gastrointestinal, and others. Many evidences support that *P. aeruginosa* OMVs are discrete and potent tool for pathogenesis [2, 13, 15, 16]. For one, the

P. aeruginosa OMV membrane exclusively contains B-band LPS (O-antigen) which contributes to drug resistance and virulence [1, 17]. However, a major interest in *Pseudomonas aeruginosa* OMVs is the exclusive presence of a discrete class of alkyl-quinolones (AQs) signaling molecules [18, 19]. These lipidic signaling molecules are synthesized by discrete biochemical pathway through the condensation of anthranilate with β -keto-fatty acids, which are the direct precursors of AQs. In *Pseudomonas aeruginosa* more than 50 AQs are reported and grouped into seven discrete classes [20]; the most significant being 4-hydroxy-2-heptylquinoline (HHQ) and corresponding dihydroxylated derivatives, such as 2-heptyl-3,4-dihydroxyquinoline (PQS; also known as the *Pseudomonas quinolone signal*). Broadly, these AQs function in quorum signaling which modulate biofilms, large set of pathogenic factors [2, 3, 20], and other bacteria [21]. However, accumulating reports support that many AQs may be expressed in strain/disease-specific manner and exhibit discrete cross-kingdom signaling [22]. HHQ and PQS modulate human immunity [23, 24] and physiology [25] using discrete pathways. Due to their lipid origin, all AQs are hydrophobic molecules; PQS is an order of magnitude more hydrophobic than the N-acylhomoserine lactone quorum signaling family and exclusively packaged in the OMV membrane [3, 26]. PQS is present in sputum and broncho-alveolar lavage (BAL) of chronic *P. aeruginosa* infections in cystic fibrosis [27, 28], ventilator-associated pneumonia (unpublished data), urinary tract infections [29], and others. The knowledge of HHQ and PQS implies that other OMV AQs may enjoy discrete, hitherto unknown functions and potential as biomarkers of specific diseases [30].

Analysis of OMV lipids and AQs have depended on biosensors [31], thin-layer chromatography (TLC)-based reporter assays, and liquid chromatography-mass spectrometry (LC-MS) [20, 32–34]. These assays require offline sample processing and are not adaptable for high-throughput clinical analysis. Many vesicular metabolites and membrane components are highly unstable when extracted. Metabolomics databases such as the METLIN do not cover all bacterial AQs since chemically pure standards are not available. However, native AQs are easily ionized and produce tandem mass signatures [20, 35]. Although matrix-assisted laser desorption/ionization (MALDI) is ideally suited for high-throughput analysis, the latter generates inherent interference signals <1000 m/z range resulting in loss of sensitivity and resolution in the analysis of small MW metabolites. These limitations may be largely resolved by matrix-free laser desorption and ionization methods and large volume of reports support the competitive advantage of this principle in MS imaging and metabolomics [36–40]. In this report, LDI-MS of AQs is described by direct adsorption and ionization of OMVs on inert silica-based ceramic ultrafiltration membranes. This technique enjoys several advantages. It is fast and offers targeted analysis

of AQs on captured OMVs, concurrently filtering out soluble contaminants and ion-suppressing agents from cultures and biofluids. It is highly sensitive, capable of analyzing picomolar quantities of AQs. Since it uses soft-ionization techniques, it produces negligible in source decay or fragmentation of native AQs. Since LDI-MS spectra predominantly contain singly charged AQs in either protonated, sodiated or potassiated forms, it is easy to interpret this data.

2 Materials

2.1 Reagents and Instrumentation

1. Pure calibration standards: 3-oxo-C12-acyl-homoserine lactone, 2-heptyl-3-hydroxy-4-quinolone, 2-heptyl-4-quinolone (Sigma-Aldrich, Saint Louis, MO, USA).
2. Inert ceramic ultrafiltration membrane filters with 300 kDa MW cutoff (Sterlitech Corp., Kent, WA, USA).
3. UV-based ozone generator and cleaner.
4. 96-well dot-blot unit attached to a laboratory vacuum pump, capable of generating 100 psi or higher.
5. Ultrapure Super Dihydroxybenzoic acid MALDI Matrix (Protea Biosciences Inc., Morgantown, WV, USA); 10 mg/mL in 50:50 methanol:water, 0.1% trifluoroacetic acid (TFA), applied as spray using a 0.3/0.5 mm dual action airbrush.
6. Modified CDC bioreactor bottle(s) containing medical grade polyurethane foam submerged in M9 minimal medium supplemented with 100 μM FeCl_2 .
7. Milli-Q Water. HEPES (4-(2-hydroxyethyl)-1-piperazineethanesulfonic acid) buffer 10 mM, pH 7.4.
8. MALDI plate and conductive carbon tape (with adhesive that does not outgas), to attach the target membrane. TOF/TOF 5800 System (Ab Sciex, Framingham, MA, USA).
9. The mass spectrometry data, analyzed by TOF/TOF series Explorer (Ab Sciex, Framingham, MA, USA), mMass [41] and METLIN.
10. The putative exact mass of AQs is derived using ChemDraw Ultra version 9.0 (CambridgeSoft Corp., Cambridge, MA, USA). The logP (log octanol-water partition coefficient) values of AQs are derived by ACD/ChemSketch (ACD/Labs, Toronto, ON, Canada).

2.2 Bacterial Cultures and Samples

Culture biofilms of *Pseudomonas aeruginosa* PAO1 in modified CDC bioreactor bottle(s) on polyurethane foam, in M9 minimal medium supplemented with 100 μM FeCl_2 . After 72 h (or OD_{600} 1.5), harvest the culture supernatants by centrifuge. Use the supernatants for isolating OMVs or any other biological or clinical fluid containing OMVs for these studies.

3 Methods

3.1 Isolation of OMVs from *P. aeruginosa* Cultures and Biofluids

1. Centrifuge the biofilm culture supernatant or suitable biological fluid at $15,000 \times g$, 4°C for 30 min to remove bacterial cells and debris. Carefully aspirate the supernatant, leaving the pellet undisturbed and store at 4°C .
2. Clarify the supernatant through $0.22 \mu\text{M}$ syringe filter to further ensure the filtrate is cell-free. Check the cell-free supernatant by plating on nutrient agar.
3. Centrifuge the sample at $100,000 \times g$, 4°C for 60 min. Wash the pellet with HEPES buffer and store at 4°C . Reconstitute the pellet with same buffer before use.
4. In case of biological samples with high protein content, (serum, blood or other), dilute the sample with HEPES buffer in a 1:1 volume ratio and centrifuge at $100,000 \times g$, 4°C for 60 min. Wash the pellet with HEPES buffer.
5. Analyze the OMV quality in the pellet by transmission electron microscopy [42].

3.2 Single-Step Analysis of OMV Quinolone Metabolites by LDI-MS

1. Clean the ceramic filter with UV/ozone system for 15 min, wash in Milli-Q water for ~ 20 min, and dry the filter under nitrogen (Fig. 2).
2. Assemble the dot blot apparatus with the ceramic filter on the top of a sheet of Whatman Grade 520 filter paper and attach the vacuum pump. Wet the papers with Milli-Q water and run the pump till excess water is removed.
3. Apply the OMV-containing filtrate or biofluid to individual wells ($100 \mu\text{L}/\text{well}$) of the dot blot apparatus.
4. For higher volume samples, repeat the process. Wash the wells with chilled HEPES buffer when the flow rate is decreased.
5. Load pure standards of PQS and HHQ in discrete wells or directly on the MALDI plate.
6. Dismantle the dot-blot apparatus and remove the membrane. Mark the individual wells with spot of a graphite pencil.
7. Carefully place the membrane on a Sciex MALDI plate and fix the sides with tape.
8. Uniformly spray thin layer of DHB using a $0.3/0.5 \text{ mm}$ Dual Action Airbrush Spray.
9. Dry the membrane under dust-free conditions.
10. Load the MALDI plate into the Sciex 5800. Use the AB Sciex spot-set editor to mark the circular spots defining the diameter of the dot (blots) with center-to-center spacing.

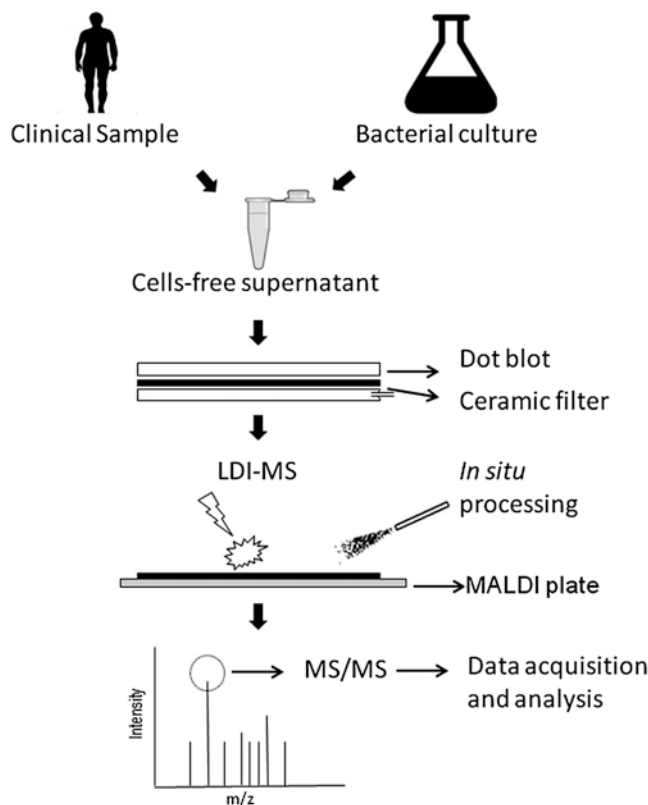




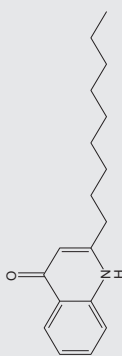
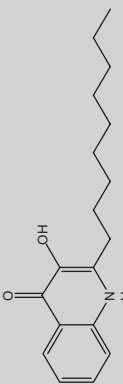
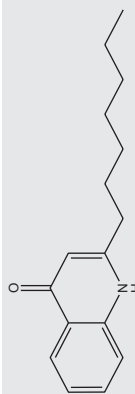
Fig. 2 Flow-chart of OMV capture and analysis on ceramic ultrafiltration membrane and LDI-MS

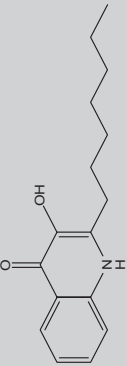
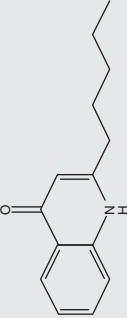
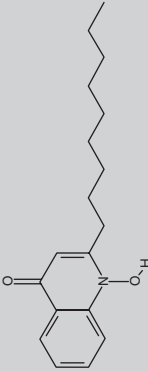
11. Ionize the individual spot using a pulsed Nd/YAG laser at 355 nm with intensity set to 4300 a.u and a repetition rate of 200 Hz.
12. Record total 100 sub-spectra for each spot on a spiral pattern of ablation. Apply delayed extraction of 500 ns. for all acquisitions in positive ion mode.
13. Calibrate the mass spectrometer externally by using the synthetic AQ (PQS and HHQ) standards (*see* **Notes 4** and **5**) or internally using appropriate deuterated standards.
14. Perform TOF MS analysis using mass range 100–1000 Da. with precursor selection from strongest to weakest in reflectron mode using low-mass detector cutoff set at 600 Da. Accumulate Spectra in case of weak AQ signals (*see* **Note 1**).
15. Perform MS/MS acquisitions of targeted precursor ions by high-energy collision-induced dissociation (CID) using Argon (collision gas) at 1×10^{-6} Torr and a laser repetition rate of 1000 Hz (*see* **Note 2–6**).

4 Notes

1. All AQs are easily ionized on ceramic filters and exhibit discrete mono-protonated, sodiated, and potassiumated precursor ions at picomolar sensitivity (Table 1). Application of trace DHB improves signal intensity, but this is not mandatory. All AQs are soluble in methanol and matrix-free LDI-MS preceded by spraying methanol alone generates excellent signals.
2. Untargeted LDI-MS of AQs in OMVs reveal group of eight major AQs expressed in the OMV. These are the 2-alkyl-quinolones (2-heptyl-quinolone; HHQ), 3,4-dihydroxy-2-alkylquinolines (3,4-dihydroxy-2-heptylquinoline, PQS), and 2-alkyl-4-hydroxyquinolines N-oxide (2-Nonyl-4-hydroxyquinoline N-oxide, NQNO) classes respectively (Fig. 3 and Table 1).
3. The association with AQ within the OMV membrane is directly related to their relative expression and hydrophobicity. AQs with $\log P$ (log octanol-water partition coefficient) >5.5 are present in OMV (Table 1). AQ like DHQ ($\log P$ 2.33 ± 0.27), 2-Heptyl-4-hydroxyquinoline N-oxide ($\log P$ 4.90 ± 0.90) and the 3-alkyl-2,3-dihydroxy-4-quinolones ($\log P$ <5) are present in the culture supernatant but not in the OMV.
4. The CID of HHQ exhibit a signature product ion at m/z 159 (the quinolone ring) which is common in all AQs of this class including UHQ, NHQ, PHQ, and DHQ (Fig. 4). This product ion is generated by cleavage between the α and β carbon of water; m/z 216, produced by neutral loss of CO and m/z 200, produced by neutral loss of CO₂. Besides, another product ion at m/z 145 is formed due to loss of methyl group from the quinolone ring.
5. The CID of C7PQS produces a major signature product ion at m/z 175 and m/z 188, which corresponds to quinolone ring with an OH group at R1 and produced by a similar cleavage between the α and β carbon and β and γ carbon of the side chain as in HHQ (Fig. 5). Neutral loss of this OH generates m/z 159, but this species is not consistent in PQS. Other ions are m/z 242, produced from the neutral loss of water; m/z 232, produced from neutral loss of CO; and m/z 216, resulting from the neutral loss of CO₂.
6. The 2-alkyl-4-hydroxyquinoline N-oxide class is present in the form of NQNO (and trace amounts of UQNO, 2-Undecyl-4-hydroxyquinoline N-oxide). The precursor ion of NQNO is m/z 288 (M+H⁺) which produces signature product ions at m/z 159, m/z 172, and m/z 188. 10, by the loss of a tandem MS (MS/MS). Further product ions are m/z 244.18 by neutral loss of CO and m/z 270.29 by neutral loss of water (Fig. 6). This AQ is particularly

Table. 1
List of OMV-associated AQs analyzed by LDI-MS

OMV Quorum signaling molecules	Structure	logP	Precursor mass (observed) (M+H ⁺) (M+Na ⁺) (M+K ⁺)	Product mass (observed)
UHQ (C ₂₀ H ₂₉ NO)		8.40+/- 0.77	300.23 (322.21) (338.18)	159.06, 282.22, 272.23, 256.24
Cl1PQS (C ₂₀ H ₂₉ NO ₂)		8.17+/- 0.77	316.22 (338.20) (354.18)	175.06, 188.09, 298.21, 288.23, 272.23
NHQ (C ₁₈ H ₂₅ NO)		7.34+/- 0.77	272.20 (294.18) (310.15)	159.06, 254.19, 244.20, 228.21
C9PQS (C ₁₈ H ₂₅ NO ₂)		7.10+/- 0.77	288.19 (310.17) (326.15)	175.06, 188.09, 270.18, 260.20, 244.20
HHQ (C ₁₆ H ₂₁ NO)		6.28+/- 0.7	244.17 (266.15) (282.12)	159.06, 226.15, 216.17, 200.18 145.09

C7 PQS ($C_{16}H_{21}NO_2$)		6.04+/- 0.77	260.16 (282.14) (298.12)	175.06, 188.13, 242.15, 232.17, 216.17
PHQ ($C_{14}H_{17}NO$)		5.21+/- 0.77	216.13 (238.12) (254.09)	159.06, 198.12, 188.14, 172.14
NQNO ($C_{18}H_{25}NO_2$)		5.96+/- 0.90	288.19 (310.17) (326.15)	159.09, 172.10, 186.10, 244.18, 270.29

Three distinct classes of AQs are present in *P. aeruginosa* OMV, distinguished by the presence of either a hydroxyl group at the position 3 or a N-oxide group in position 1 of the quinolone ring. Each class exhibits at least one signature product ion and other products rationalized with their structure. This helps discriminate isomers (NQNO and C9PQS) with discrete product ions that are easily characterized by CID tandem mass spectra

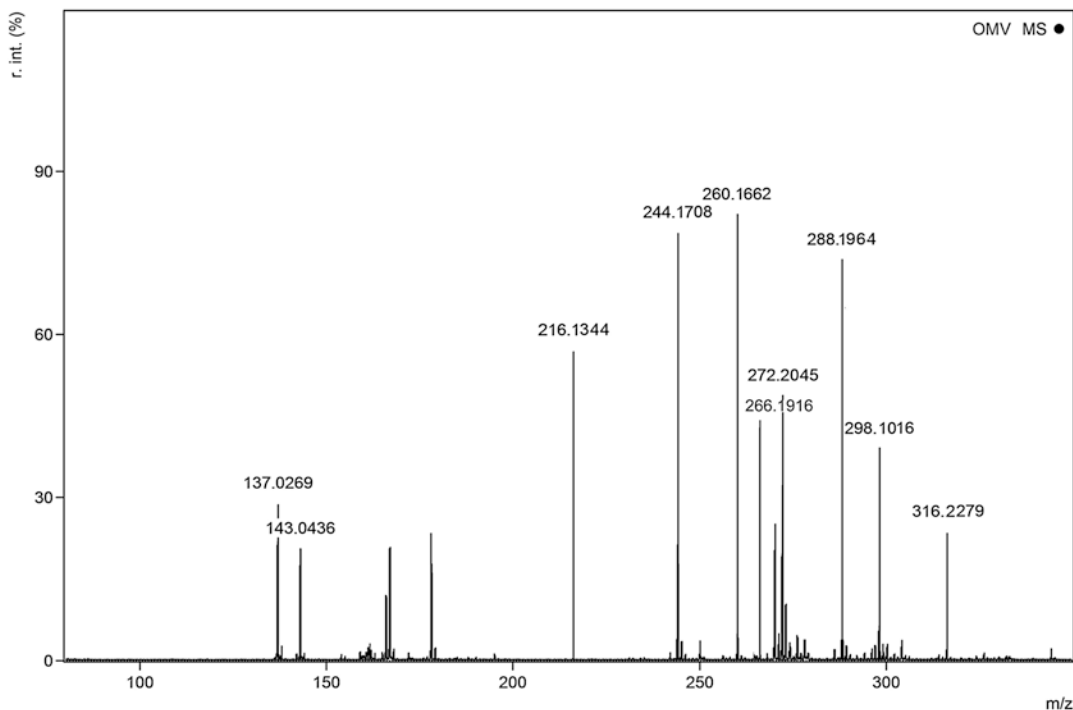


Fig. 3 LDI-MS spectrum of *P. aeruginosa* OMVs captured on ceramic ultrafiltration membrane. Clarified biofilm culture supernatants of *P. aeruginosa* were subjected to ultrafiltration on ceramic membranes and analyzed by LDI-MS in situ. All AQs were confirmed by MS/MS

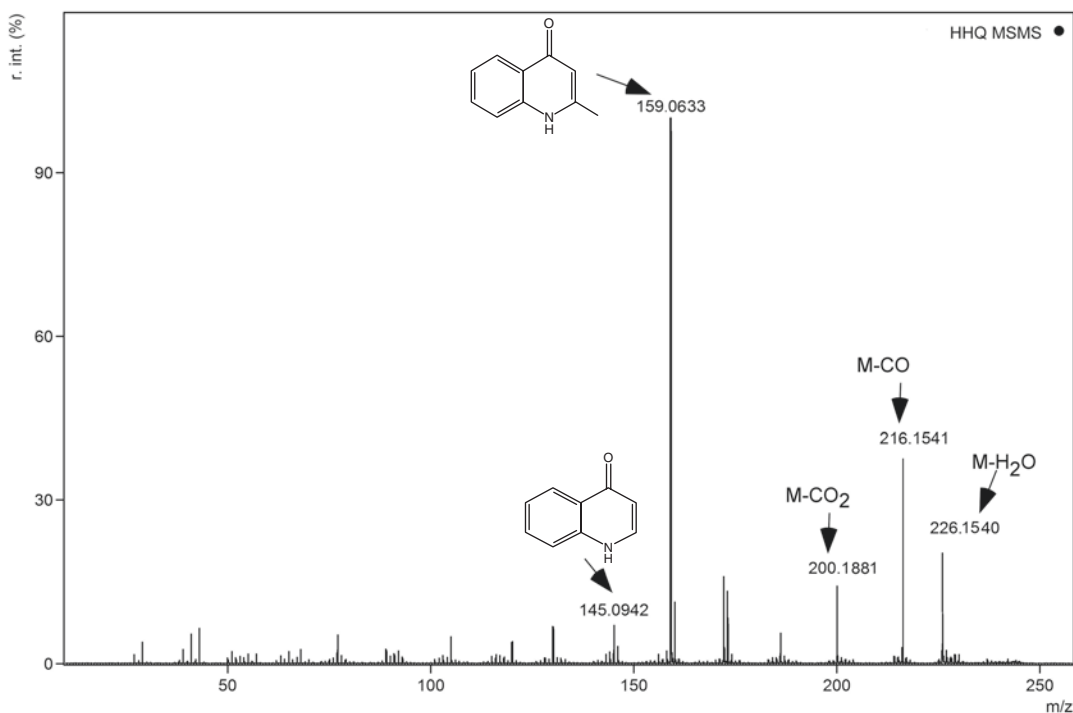


Fig. 4 Laser desorption/ionization-tandem mass spectrometry (LDI-MS/MS) spectrum of the **C7 PQS**. Precursor ion m/z 260 ($M+H^+$) produces signature product ion at m/z 175, and m/z 188 which corresponds to quinolone ring with an OH group at R1 generated by cleavage between the α and β carbon and β and γ carbon of the side chain. Neutral loss of this OH generates m/z 159. Other ions are m/z 242, produced from the neutral loss of water; m/z 232, produced from neutral loss of CO; and m/z 216, resulting from the neutral loss of CO₂

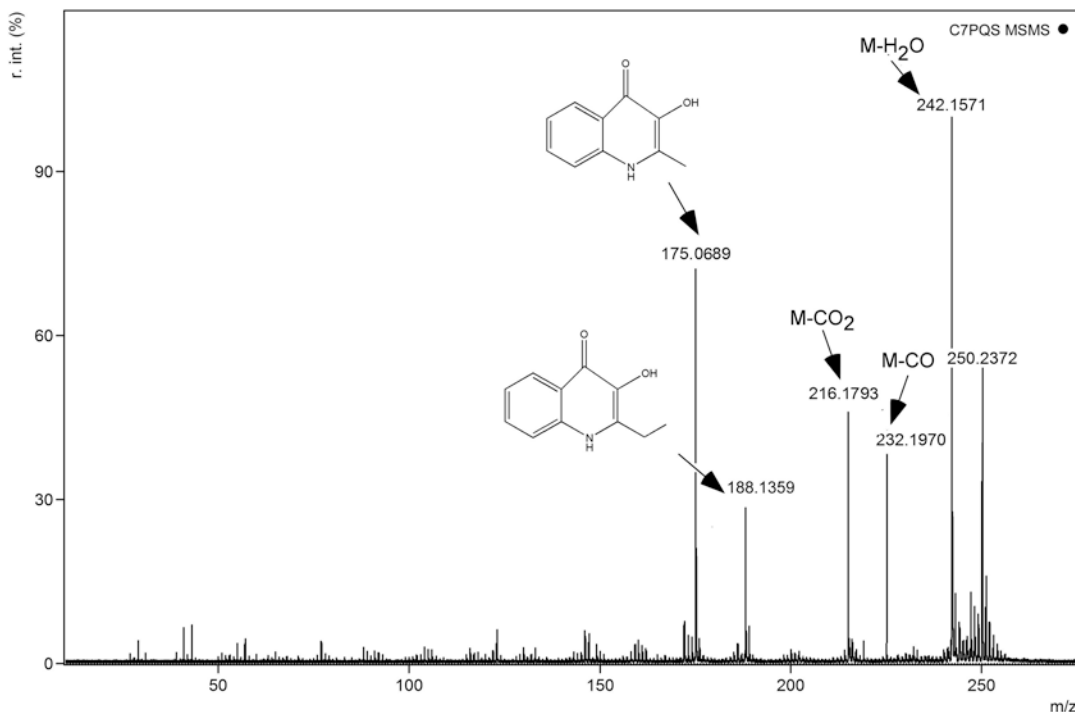


Fig. 5 LDI-MS/MS spectrum of the HHQ. Precursor ion m/z 244 ($M+H^+$) produces signature product ion at m/z 159 (the quinolone ring) and m/z 172 resulting from the cleavage of HHQ side chain. Further product ions are m/z 226, produced by neutral loss of water; m/z 216 produced by neutral loss of CO; and m/z 200, produced by neutral loss of CO₂. Besides, another product ion at m/z 145 is formed due to loss of methyl group from the quinolone ring

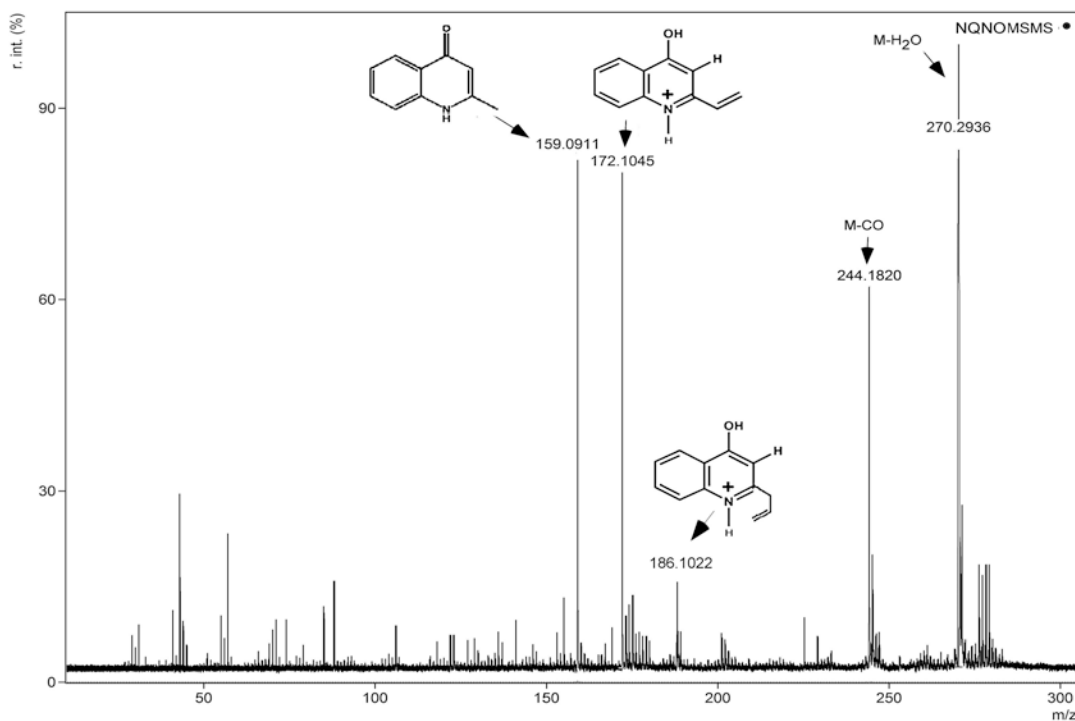


Fig. 6 LDI-MS/MS spectrum of NQNO. Precursor ion m/z 288 ($M+H^+$) from the OMV, ($M+H^+$) produces signature product ion at m/z 159 (the quinolone ring) and m/z 172. Further product ions are m/z 244.18 produced by neutral loss of CO and m/z 270.29 by neutral loss of water

subject to sodiation and strong sodiated precursor ion peak for NQNO is often observed.

Whereas this method allows single-step capture and targeted metabolomics to confirm presence of AQs in clinical samples or cultures, the quality of the OMV is not equal to samples purified over standard ultracentrifugation protocols. The filters efficiently capture bacterial flagella, cell debris, and mammalian exosomes. Since AQs are expressed only in bacterial OMV, targeted AQ metabolomics usually circumvents these problems. However when contaminant-induced signal suppression is suspected the samples must be subjected to a second cycle of ultracentrifugation or density gradient centrifugation

References

1. Kulp A, Kuehn MJ (2010) Biological functions and biogenesis of secreted bacterial outer membrane vesicles. *Ann Rev Microbiol* 64:163–184. doi:10.1146/annurev.micro.091208.073413
2. Schwachheimer C, Kuehn MJ (2015a) Outer-membrane vesicles from gram-negative bacteria: biogenesis and functions. *Nat Rev Microbiol* 13(10):605–619. doi:10.1038/nrmicro3525
3. Mashburn LM, Whiteley M (2005) Membrane vesicles traffic signals and facilitate group activities in a prokaryote. *Nature* 437(7057):422–425. doi:10.1038/nature03925
4. Schwachheimer C, Kuehn MJ (2015b) Outer-membrane vesicles from gram-negative bacteria: biogenesis and functions. *Nat Rev Microbiol* 13(10):605–619. doi:10.1038/nrmicro3525
5. Wessel AK, Liew J, Kwon T, Marcotte EM, Whiteley M (2013) Role of *Pseudomonas aeruginosa* peptidoglycan-associated outer membrane proteins in vesicle formation. *J Bacteriol* 195(2):213–219. doi:10.1128/JB.01253-12
6. Vella BD, Schertzer JW (2015) Understanding and exploiting bacterial outer membrane vesicles. In: Ramos J-L, Goldberg JB, Filloux A (eds) *Pseudomonas*, New aspects of *pseudomonas* biology, vol 7. Springer, Dordrecht, pp 217–250. doi:10.1007/978-94-017-9555-5_9
7. Roier S, Zingl FG, Cakar F, Durakovic S, Kohl P, Eichmann TO, Klug L, Gadermaier B, Weinzerl K, Prassl R, Lass A, Daum G, Reidl J, Feldman MF, Schild S (2016) A novel mechanism for the biogenesis of outer membrane vesicles in gram-negative bacteria. *Nat Comm* 7:10515. doi:10.1038/ncomms10515
8. Chatterjee SN, Chaudhuri K (2012) Gram-negative bacteria: the cell membranes. In: *Outer membrane vesicles of bacteria*. Springer, Berlin, Heidelberg, pp 15–34. doi:10.1007/978-3-642-30526-9_2
9. Choi CW, Park EC, Yun SH, Lee SY, Lee YG, Hong Y, Park KR, Kim SH, Kim GH, Kim SI (2014) Proteomic characterization of the outer membrane vesicle of *pseudomonas putida* KT2440. *J Proteome Res* 13(10):4298–4309. doi:10.1021/pr500411d
10. Tashiro Y, Sakai R, Toyofuku M, Sawada I, Nakajima-Kambe T, Uchiyama H, Nomura N (2009) Outer membrane machinery and alginate synthesis regulators control membrane vesicle production in *Pseudomonas aeruginosa*. *J Bacteriol* 191(24):7509–7519. doi:10.1128/JB.00722-09
11. Bomberger JM, Maceachran DP, Coutermarsh BA, Ye S, O'Toole GA, Stanton BA (2009a) Long-distance delivery of bacterial virulence factors by *Pseudomonas aeruginosa* outer membrane vesicles. *PLoS Pathog* 5(4):e1000382. doi:10.1371/journal.ppat.1000382
12. Wispelwey B, Hansen EJ, Scheld WM (1989) Haemophilus influenzae outer membrane vesicle-induced blood-brain barrier permeability during experimental meningitis. *Infect Immun* 57(8):2559–2562
13. Bomberger JM, MacEachran DP, Coutermarsh BA, Ye SY, O'Toole GA, Stanton BA (2009b) Long-distance delivery of bacterial virulence factors by *Pseudomonas aeruginosa* outer membrane vesicles. *PLoS Pathog* 5(4):e1000382. doi:10.1371/journal.ppat.1000382
14. Kulkarni HM, Jagannadham MV (2014) Biogenesis and multifaceted roles of outer membrane vesicles from gram-negative bacteria. *Microbiology* 160(Pt 10):2109–2121. doi:10.1099/mic.0.079400-0
15. Kuehn MJ, Kesty NC (2005) Bacterial outer membrane vesicles and the host-pathogen

- interaction. *Genes Dev* 19(22):2645–2655. doi:10.1101/gad.1299905
16. Schertzer JW, Whiteley M (2013) Bacterial outer membrane vesicles in trafficking, communication and the host-pathogen interaction. *J Mol Microbiol Biotechnol* 23(1–2):118–130. doi:10.1159/000346770
 17. Dean CR, Franklund CV, Retief JD, Coyne MJ Jr, Hatano K, Evans DJ, Pier GB, Goldberg JB (1999) Characterization of the serogroup O11 O-antigen locus of *Pseudomonas aeruginosa* PA103. *J Bacteriol* 181(14):4275–4284
 18. Dubern JF, Diggle SP (2008) Quorum sensing by 2-alkyl-4-quinolones in *Pseudomonas aeruginosa* and other bacterial species. *Mol Biosyst* 4(9):882–888. doi:10.1039/b803796p
 19. Camara M, Williams P, Barrett D, Halliday N, Knox A, Smyth A, Fogarty A, Barr H, Forrester D (2016) Alkyl quinolones as biomarkers of *pseudomonas aeruginosa* infection and uses thereof. US Patent 20,160,131,648
 20. Lepine F, Milot S, Deziel E, He J, Rahme LG (2004) Electrospray/mass spectrometric identification and analysis of 4-hydroxy-2-alkylquinolines (HAQs) produced by *Pseudomonas aeruginosa*. *J Am Soc Mass Spectrom* 15(6):862–869. doi:10.1016/j.jasms.2004.02.012
 21. Inaba T, Oura H, Morinaga K, Toyofuku M, Nomura N (2015) The pseudomonas quinolone signal inhibits biofilm development of *Streptococcus mutans*. *Microbes Environ* 30(2):189–191. doi:10.1264/jsmc2.ME14140
 22. Liu YC, Chan KG, Chang CY (2015) Modulation of host biology by *Pseudomonas aeruginosa* quorum sensing signal molecules: messengers or traitors. *Front Microbiol* 6:1226. doi:10.3389/fmicb.2015.01226
 23. Kim K, Kim YU, Koh BH, Hwang SS, Kim SH, Lepine F, Cho YH, Lee GR (2010) HHQ and PQS, two *Pseudomonas aeruginosa* quorum-sensing molecules, down-regulate the innate immune responses through the nuclear factor-kappaB pathway. *Immunology* 129(4):578–588. doi:10.1111/j.1365-2567.2009.03160.x
 24. Kaparakis-Liaskos M, Ferrero RL (2015) Immune modulation by bacterial outer membrane vesicles. *Nat Rev Immunol* 15(6):375–387. doi:10.1038/nri3837
 25. Legendre C, Reen FJ, Mooij MJ, McGlacken GP, Adams C, O’Gara F (2012) *Pseudomonas aeruginosa* alkyl quinolones repress hypoxia-inducible factor 1 (HIF-1) signaling through HIF-1alpha degradation. *Infect Immun* 80(11):3985–3992. doi:10.1128/IAI.00554-12
 26. Huse H, Whiteley M (2011) 4-Quinolones: smart phones of the microbial world. *Chem Rev* 111(1):152–159. doi:10.1021/cr100063u
 27. Collier DN, Anderson L, McKnight SL, Noah TL, Knowles M, Boucher R, Schwab U, Gilligan P, Pesci EC (2002) A bacterial cell to cell signal in the lungs of cystic fibrosis patients. *FEMS Microbiol Lett* 215(1):41–46
 28. Gruber JD, Chen W, Parnham S, Beauchesne K, Moeller P, Flume PA, Zhang YM (2016) The role of 2,4-dihydroxyquinoline (DHQ) in *Pseudomonas aeruginosa* pathogenicity. *PeerJ* 4:e1495. doi:10.7717/peerj.1495
 29. Bala A, Chhibber S, Harjai K (2014) *Pseudomonas* quinolone signalling system: a component of quorum sensing cascade is a crucial player in the acute urinary tract infection caused by *Pseudomonas aeruginosa*. *Int J Med Microbiol* 304(8):1199–1208. doi:10.1016/j.ijmm.2014.08.013
 30. Palmer GC, Schertzer JW, Mashburn-Warren L, Whiteley M (2011) Quantifying *Pseudomonas aeruginosa* quinolones and examining their interactions with lipids. *Methods Mol Biol* 692:207–217. doi:10.1007/978-1-60761-971-0_15
 31. Diggle SP, Fletcher MP, Camara M, Williams P (2011) Detection of 2-alkyl-4-quinolones using biosensors. *Methods Mol Biol* 692:21–30. doi:10.1007/978-1-60761-971-0_2
 32. Choi DS, Kim DK, Choi SJ, Lee J, Choi JP, Rho S, Park SH, Kim YK, Hwang D, Gho YS (2011) Proteomic analysis of outer membrane vesicles derived from *Pseudomonas aeruginosa*. *Proteomics* 11(16):3424–3429
 33. Bala A, Gupta RK, Chhibber S, Harjai K (2013) Detection and quantification of quinolone signalling molecule: a third quorum sensing molecule of *Pseudomonas aeruginosa* by high performance-thin layer chromatography. *J Chromatogr B Anal Technol Biomed Life Sci* 930:30–35. doi:10.1016/j.jchromb.2013.04.027
 34. Chutkan H, Macdonald I, Manning A, Kuehn MJ (2013) Quantitative and qualitative preparations of bacterial outer membrane vesicles. *Methods Mol Biol* 966:259–272. doi:10.1007/978-1-62703-245-2_16
 35. Baig NF, Dunham SJ, Morales-Soto N, Shrout JD, Sweedler JV, Bohn PW (2015) Multimodal chemical imaging of molecular messengers in emerging *Pseudomonas aeruginosa* bacterial communities. *Analyst* 140(19):6544–6552. doi:10.1039/c5an01149c
 36. Peterson DS (2007) Matrix-free methods for laser desorption/ionization mass spectrometry. *Mass Spectrom Rev* 26(1):19–34. doi:10.1002/mas.20104

37. Coffinier Y, Boukherroub R (2014) Porous Silicon-Based Mass Spectrometry. In: Canham L (ed) Handbook of Porous Silicon. Springer International Publishing, Cham, pp 869–885. doi:10.1007/978-3-319-05744-6_88
38. Kusano M, Kawabata S, Tamura Y, Mizoguchi D, Murouchi M, Kawasaki H, Arakawa R, Tanaka K (2014) Laser Desorption/Ionization Mass Spectrometry (LDI-MS) of lipids with iron oxide nanoparticle-coated targets. Mass Spectrom (Tokyo) 3(1):A0026. doi:10.5702/massspectrometry.A0026
39. Ghosh D, Panchagnula V, Dhaware D (2016) Selective detection and analysis of small molecules. EU Patent EP 2676287 A2.
40. Pluháček T, Lemr K, Ghosh D, Milde D, Novák J, Havlíček V (2016) Characterization of microbial siderophores by mass spectrometry. Mass Spectrom Rev 35(1):35–47
41. Strohalm M, Kavan D, Novak P, Volny M, Havlicek V (2010) mMass 3: a cross-platform software environment for precise analysis of mass spectrometric data. Anal Chem 82(11):4648–4651
42. Kadurugamuwa JL, Beveridge TJ (1995) Virulence factors are released from *Pseudomonas aeruginosa* in association with membrane vesicles during normal growth and exposure to gentamicin: a novel mechanism of enzyme secretion. J Bacteriol 177(14):3998–4008

Analysis of Fatty Acid and Cholesterol Content from Detergent-Resistant and Detergent-Free Membrane Microdomains

Mark E. McClellan and Michael H. Elliott

Abstract

The compartmentalization of cellular membranes into discrete membrane microdomains (known as *lipid rafts*) challenged the original definition of membranes as containing randomly distributed lipid and protein components. The lipid microdomain hypothesis has generated significant controversy and rigorous inquiry based on the attractive idea that such domains concentrate machinery to mediate cellular events such as signaling and endocytosis. As such, numerous studies have used biochemical, cell biological, and biophysical methodologies to define the composition of such domains in a variety of experimental contexts. In this chapter, we describe methodologies to isolate membranes from cell or tissue sources with biophysical/biochemical properties of membrane microdomains that are amenable to subsequent classical or mass spectrometry-based lipid analytical approaches.

Key words Membrane microdomains, Density gradient centrifugation, Lipid extraction, Cholesterol, Fatty acids

1 Introduction

The description of cell membranes as a sea of lipids with randomly distributed proteins defined by Singer and Nicolson's fluid mosaic model advanced our understanding of plasma membrane organization [1]. Our definition of cell membrane organization was later expanded to incorporate observations of thermodynamically stable clusters of lipids [2, 3], later defined as *lipid rafts* [4]. The ability of lipids to exhibit lateral heterogeneity in model membranes is clear but the challenge of biochemically defining such domains in cellular contexts has been complicated [5, 6]. Subclasses of membrane microdomains such as caveolae can be visualized ultrastructurally and lateral segregation of *raft* lipid and protein probes has suggested that both stable and dynamic phase separations of lipids occur in cell membranes [7]. In 2006, a consensus definition of rafts as *small (10–200 nm), heterogeneous, highly*

dynamic, sterol- and sphingolipid-enriched domains that compartmentalize cellular processes [8] emerged based on a variety of biophysical, biochemical, and cell biological analyses [5]. Biochemical techniques to isolate membranes with the biochemical properties of rafts (e.g., cholesterol, sphingolipid, and raft protein enrichment) commonly use detergent-based or detergent-free isolation coupled with density gradient centrifugation [9–15]. Although care in interpretation of compositional analyses of such biochemically isolated membrane domains is warranted, the basic methodologies described herein provide a rational framework for the analysis of membranes with raft-like characteristics.

Our work has focused mainly on the isolation of membrane domains from well-characterized parent membranes from ocular cells (e.g., photoreceptor outer segment membranes). By comparing the compositions of the resulting membrane microdomains to parent membrane fractions, whether they be from plasma or organellar membranes, the investigator can reduce the analytical complexities that arise from the potential mixing of raft membranes that result from the chosen membrane disruption and fractionation strategies employed. Although our prior work did not employ mass spectrometric-based lipidomics, these approaches have been used by other investigators to define raft membrane lipid composition [16]. Recently, other investigators have applied such comprehensive lipidomic analysis of detergent-resistant membrane composition derived from plasma membranes isolated by colloidal silica perturbation, a technique that results in a pure parent plasma membrane fraction [17]. Thus, the basic methodologies for raft isolation and downstream lipid extraction described herein are amenable to comprehensive lipidomic-based strategies in a variety of experimental systems.

2 Materials

2.1 Solutions for Detergent-Free Preparation of Membrane Microdomains/Caveolae by Carbonate Extraction (Modified from Song et al. [11])

1. 500 mM 2-(N-morpholine)-ethane sulphonic acid (MES), pH 6.5 adjusted with NaOH.
2. 500 mM sodium carbonate (Na_2CO_3), pH 11. The pH will be ~11 without any further adjustment.
3. 2 M NaCl.
4. MES-buffered saline. 25 mM MES, 150 mM NaCl, with protease inhibitors (Roche, Mannheim, Germany).
5. 90% (w/v) sucrose (in 25 mM MES, 150 mM NaCl): For 100 mL, add 5 mL of 500 mM stock MES buffer and 7.5 mL of 2 M NaCl to a beaker with a stir bar and slowly dissolve 90 g of sucrose with heating to assist dissolving sucrose. Bring up to 100 mL with ddH₂O. Store at room temperature (*see Note 1*).

6. 35% (w/v) sucrose (in 25 mM MES, 150 mM NaCl, 250 mM Na₂CO₃): For 100 mL, add 5 mL of 500 mM MES buffer, pH 6.5, 7.5 mL of 2 M NaCl, and 50 mL of 500 mM sodium carbonate (Na₂CO₃), pH 11 to a beaker with a stir bar. Slowly dissolve 35 g of sucrose and bring up to 100 mL with ddH₂O. Store at 4 °C for short term and at -20 °C for longer term.
7. 5% (w/v) sucrose (in 25 mM MES, 150 mM NaCl, 250 mM Na₂CO₃): For 100 mL: add 5 mL of 500 mM MES buffer, pH 6.5, 7.5 mL of 2 M NaCl, and 50 mL of 500 mM sodium carbonate (Na₂CO₃), pH 11 to a beaker with a stir bar. Dissolve 5 g of sucrose and bring up to 100 mL with ddH₂O. Store at 4 °C for short term and at -20 °C for longer term.

2.2 Solutions for Detergent-Free Preparation of Membrane Microdomains by Simplified Optiprep Method (Macdonald and Pike Method [10])

1. Base buffer A: 20 mM Tris-HCl, pH 7.8, 250 mM sucrose with 1 mM CaCl₂ and 1 mM MgCl₂, and protease inhibitors.
2. OptiPrep density gradient medium (Sigma-Aldrich, St Louis, MO). 50% and 20% prepared in base buffer A.

2.3 Solutions for Preparation of Detergent-Resistant Membranes (Elliott et al. [13] Modified from Seno et al. [18])

1. Base buffer B: 10 mM Tris-HCl, pH 7.4, 70 mM NaCl, 2 mM MgCl₂, 0.5 mM EDTA and protease inhibitors.
2. 1% Triton X-100 in base buffer B.
3. 2.4 M (82% w/v) sucrose in base buffer B.
4. Additional sucrose solutions for discontinuous gradient steps: (0.9 M/30.8% (w/v), 0.8 M/27.4% (w/v), 0.7 M/24% (w/v), 0.6 M/20.5% (w/v), and 0.5 M/17.1%(w/v)) all prepared in base buffer B (*see* Note 2).

2.4 Materials for Two-Part Extraction of Saponifiable and Nonsaponifiable Lipids

1. 19-hydroxycholesterol internal standard (Steraloids, Inc., Newport, RI).
2. Pentadecanoic acid (15:0), heptadecanoic acid (17:0), and heneicosanoic acid (21:0) internal fatty acid standards (Nu-Chek Prep, Elysian, MN).
3. 2% (w/v) KOH in ethanol.
4. Concentrated HCl.
5. Hexane.
6. Toluene.
7. 2% sulfuric acid (H₂SO₄) in methanol.
8. Nonane.

3 Methods

The methodologies to prepare membrane microdomains can be used on purified membrane fractions or whole cell/tissue homogenates. As mixing of membranes from different cellular compartments during preparation may complicate interpretation of results, the use of specific membrane fractions (e.g., plasma membranes) isolated by subcellular fractionation is recommended. Methods of choice to prepare starting membranes should be determined by the investigator. The downstream microdomains preparations described are amenable to whole cell or postnuclear lysates, crude microsomes, or highly purified organellar or plasma membrane fractions [10, 13–15, 17, 19].

3.1 Isolation of Detergent-Free Membrane Microdomains/Caveolae by Carbonate Extraction (Modified from Song et al. [11])

1. Resuspend cell or membrane pellet in 2.1 mL ice-cold 500 mM sodium carbonate (*see Note 3*).
2. Homogenize with Dounce or Teflon/glass homogenizer by ten passes on ice.
3. Sonicate three times for 15 s using ultrasonic processor (Cole-Parmer Instrument Co., Vernon Hills, IL). Allow sample to rest on ice for 30 s between bursts (*see Note 4*).
4. Remove and save ~0.1 mL of lysate for subsequent comparison of starting membranes to isolated membrane microdomains. Add equal volume (2 mL in this case) of 90% sucrose solution to the cell lysate and mix well. (Thus, final sucrose = 45%; Final volume = 3.6 mL).
5. Divide into four SW60 tubes (1 mL/tube) (*see Note 5*).
6. Overlay each gradient with 1.3 mL of 35% sucrose in MBS and 1.3 mL of 5% sucrose in MBS.
7. Centrifuge at $175,000 \times g$ for 16–20 h at 4 °C in Beckman SW 60 swinging bucket rotor.
8. After centrifugation, a faint band of material is usually visible at the 35%/5% interface. These are the membrane microdomain/caveolae fractions. Membrane microdomains can either be collected by directly pipetting the material at the 35%/5% interface or by collecting equivalent volume fractions from the gradient.

3.2 Isolation of Detergent-Free Preparation of Membrane Microdomains by Simplified Optiprep Method (Macdonald and Pike Method [10])

1. Cells or membrane pellets are resuspended in 1.5 mL of base buffer A (Tris-sucrose buffer containing divalent cations and protease inhibitors).
2. Cells/membranes are disrupted by 20 passes through a 22-G needle.
3. Lysates are centrifuged at $1000 \times g$ for 10 min and the post-nuclear supernatant is collected.

4. The pelleted material is resuspended in 1.5 mL of fresh base buffer A and again passed 20 times through a 22-G needle.
5. Lysates are again centrifuged at $1000 \times g$ for 10 min and the first and second postnuclear supernatants are combined. At this point, an aliquot ~10% should be collected if comparison of subsequently isolated membrane microdomains to the parent membrane/lysate is to be made.
6. Add an equal volume (~3 mL) of 50% OptiPrep (in base buffer A) to the combined starting lysate (final concentration 25% Optiprep in final volume of 6 mL). Mix well and place at the bottom of a 16 mL Ultra-Clear centrifuge tube.
7. Pour a 10 mL gradient of 0%–20% OptiPrep in base buffer A on the top of the lysate.
8. Centrifuge at $52,000 \times g$ for 90 min at 4 °C in a Beckman SW 32 swinging bucket rotor.
9. Gradients are fractionated in 1 mL fractions for subsequent downstream analyses (e.g., protein content, cholesterol content, western blotting [10]) (*see Note 6*).

**3.3 Isolation
Detergent-Resistant
Membranes (Elliott
et al. [13] Modified
from Seno et al. [18])**

1. Bulk cell membranes are solubilized on ice in 1% Triton X-100 in base buffer B (*see Note 7*). After the addition of detergent-containing buffer, membranes are disrupted by 3–4 passes through a 20-G needle (*see Note 8*). Lysates are then allowed to stand on ice for 10 min.
2. The detergent lysate is then adjusted to 0.9 M sucrose by the addition of 2.4 M sucrose in base buffer B.
3. Detergent lysates in 0.9 M sucrose are transferred to the bottom of appropriate volume ultracentrifuge tubes and are carefully overlaid sequentially with 0.8 M, 0.7 M, 0.6 M, and 0.5 M sucrose solutions in base buffer B to form a 5-step discontinuous sucrose gradient.
4. Gradients are centrifuged at $250,000 \times g$ for 16–20 h in a swinging bucket rotor (Beckman-Coulter, Fullerton, CA).
5. After centrifugation, tubes are carefully removed and material at the 0.6 M/0.5 M interface (low buoyant density, detergent resistant membranes) can be collected or the gradient can be fractionated as described.

**3.4 Evaluation
of Membrane Domains**

Recovered membranes (or membrane fractions) can be evaluated by immunoblot analysis for microdomain/caveolae inclusion and exclusion markers (*see Note 9*). Comparisons can be made across equivalent proportional fractions (if the gradient is fractionated) or to the starting membrane fractions. In addition to protein markers, lipid markers such as cholesterol content can be evaluated.

3.5 Analytical Approaches to Examine Lipid Composition of Membrane Microdomains

The membrane domains isolated by the described procedures are amenable to a variety of lipid analytical approaches. While the theme of this volume is lipidomic methodologies, our prior compositional work on membrane microdomains used only classical quantitative lipid analytical procedures including analysis of total fatty acids [14, 15], cholesterol [13, 14], and fatty acid composition of specific lipid classes separated by two-dimensional thin-layer chromatography [15]. Other investigators have used similarly isolated domains for shotgun mass spectrometric lipidomic analyses [16, 17, 20] and the interested reader is invited to examine these papers. In the following section, we describe a two-part extraction procedure to analyze nonsaponifiable and saponifiable lipid extracts for the measurement of cholesterol and fatty acids from the same lipid extract.

3.5.1 Two-Part Extraction Procedure for Saponifiable and Nonsaponifiable Lipids

1. Membrane samples (50–100 μg of protein) are placed in 16×100 mm screw cap tubes.
2. Samples are spiked with internal standards (19-hydroxycholesterol and 15:0, 17:0, 21:0 fatty acid standards) (*see Note 10*).
3. Two milliliters of 2% KOH in ethanol is added and samples are vortexed and tubes are capped under nitrogen with Teflon-lined caps.
4. Heat tubes at 100°C for 1 h and then cool on ice.
5. Add 3 mL of H_2O and then extract $3\times$ into 2 mL of hexane. The recovered organic phases containing nonsaponifiable lipids (e.g., cholesterol) are pooled.
6. To the aqueous phase, add 0.2 mL of concentrated HCl and cap under nitrogen.
7. Vortex for 10 s, sonicate for 10 min in bath sonicator, vortex again for 10 s.
8. Extract $3\times$ into 2 mL of hexane. This organic phase is the saponifiable fatty acid extract.
9. Dry both saponifiable and nonsaponifiable extracts under nitrogen, rinsing the sides of the tubes $2\times$ with hexane.

3.5.2 Analysis of Cholesterol by High-Performance Liquid Chromatography (HPLC)

1. To the dried nonsaponifiable lipid extract, add 50 μL of methanol and sonicate for 10 min in a bath sonicator.
2. Inject 35 μL into the HPLC system.
3. Cholesterol is separated on a C18 column (Supelcosil LC-18, $25\text{ cm} \times 4.6\text{ mm}$, 5 μm particle size) with an isocratic mobile phase of 1 mL/min of methanol.
4. Cholesterol is quantified based on absorbance at 208 nm detected by an Agilent 1100 series photodiode array detector in comparison to an authentic cholesterol standard within linear response range. Cholesterol content is corrected for the recovery of the 19-hydroxycholesterol internal standard.

3.5.3 *Preparation of Fatty Acid Methyl Esters and Analysis by Gas Chromatography and Flame Ionization Detection*

1. To the dried saponifiable fatty acid extract, add 0.2 mL of toluene and 1 mL of 2% H₂SO₄ in methanol.
2. Cap tubes with Teflon-lined caps under nitrogen and vortex for 10 s.
3. Heat tubes at 100 °C for 1 h and then cool on ice.
4. Add 1.2 mL of H₂O and then extract 3× with 2.4 mL of hexane.
5. Dry the pooled hexane extracts under nitrogen rinsing the sides of the tubes 2× with hexane.
6. Resuspend dried fatty acid methyl esters in 20 µL of nonane and sonicate for 10 min and transfer to a gas chromatography vial.
7. The fatty acid composition is determined by injecting 3 µL of nonane extract at 250 °C with the split ratio set to 20:1 using a DB-225 capillary column (30 m × 0.53 mm inner diameter; J&W Scientific, Folsom, CA) in a gas-liquid chromatography system with autosampler (Agilent Technologies, Wilmington, DE). The column temperature is held at 160 °C for 1 min, then increased to 200 °C at 1 °C/min, and then held at 220 °C for 10 min. Helium carrier gas flows at 4.2 mL/min. The hydrogen flame ionization detector temperature is set at 270 °C. Chromatographic peaks are integrated and processed using ChemStation software (Agilent Technologies). Fatty acid methyl esters are identified by comparison of their relative retention times with authentic standards and the relative mole percentages are calculated.

4 Notes

1. The concentrated sucrose stock solution requires heating to dissolve sucrose. Once prepared, the solution should be stored at room temperature to avoid precipitation of sucrose.
2. A simplified gradient using 45%, 35%, and 5% sucrose (as described for the detergent-free carbonate preparation) is also frequently used for DRM isolation [17]. The gradient steps used in the provided protocol were developed for DRM isolation from photoreceptor membranes [13–15, 18] but can be used for other membrane sources.
3. The volumes can vary depending on how much starting material is used and the volumes of the tubes used for gradient centrifugation. We have used as small as 4 mL gradients (4 mL Ultra-Clear tubes for SW60 rotor, Beckman-Coulter) and up to 16 mL (17 mL Ultra-Clear tubes SW32) depending on starting material. The volumes in the described protocol can

be adjusted proportionately to account for different amounts of starting material and tube volumes.

4. The shear provided by sonication is the critical step to free membrane microdomains such as caveolae from the bulk membranes in this detergent-free procedure. The power setting needs to be empirically determined based on the ultrasonic disrupter available and the cells/membranes used as the shear force applied will affect the yield. If too much power is applied, membrane domains can be disrupted and if too little power is applied then domains may not be released from bulk membranes. In either case, this would result in a higher proportion of membrane domain components, (e.g., caveolins) to be found in higher density fractions after density gradient centrifugation.
5. Depending on the available equipment, it is also possible to place the entire 4 mL volume in a single tube (e.g., SW41 Ultra-Clear tube) and overlay equal volumes (4 mL) of each sucrose solution. However, be sure that the swinging bucket rotor to be used can reach $175,000 \times g$.
6. The detergent-free OptiPrep method yields more diffuse banding and thus fractionation is recommended. Fractions should be evaluated by immunoblotting for marker proteins of interest. Once the fractionation pattern is determined (e.g., identification of caveolin- and/or flotillin-enriched fractions), then selected fractions could be evaluated for lipid composition by classical or mass spectrometric methodologies.
7. The use of detergents to isolate *lipid rafts* is controversial and care should be taken in defining such detergent-resistant membranes as bona fide rafts [21, 22]. However, these methodologies can suggest the potential of molecular components to associate with raft domains. Although the most common detergent used for detergent-resistant membrane isolation is Triton X-100, a variety of different detergents have been used including Brij detergents, LUBROL detergents, and ocytlglucoside among others [20, 23].
8. The detergent-lipid phosphorous molar ratio should be approximately 3:1. Thus, it is recommended that determination of lipid phosphorous on parent membrane fractions be empirically determined such that this ratio can be established for efficient solubilization bulk membrane lipids and for release of insoluble, detergent-resistant membranes.
9. Inclusion markers, including known membrane domain resident proteins, e.g., caveolins and flotillins, can be evaluated by immunoblotting. These protein markers should be enriched in membrane domain fractions relative to either high-density fractions (if fractions are collected) or relative to the starting

parent membrane/post-nuclear supernatant fraction by any of the isolation procedures described. Exclusion markers (non-raft proteins) such as transferrin receptor, β -COP, and nucleoporin should also be evaluated. If material collected at the low buoyant density interface is used, we typically concentrate these membranes by diluting the density gradient medium with appropriate base buffer at least fivefold. This diluted fraction is mixed well and then centrifuged at $100,000 \times g$ for 1 h at 4 °C in a swinging bucket rotor. The resulting pellet can then be resuspended and a protein concentration can be determined by bicinchoninic acid (BCA) assay using bovine serum albumin as a standard. Then, equivalent amounts of membrane domain protein and starting material can be resolved by SDS-PAGE, electrotransferred to nitrocellulose or PDF membranes, and immunoblotted with appropriate antibodies.

10. Fatty acid internal standard stocks are typically 1 mM and the 19-hydroxycholesterol is 0.15 mg/mL and we typically add 20 μ L of each standard solution to the sample prior to extraction. The amount of standard to add to sample should be empirically determined based on the samples analyzed to be sure that internal standard and sample peaks are in the same range.

Acknowledgments

This work was supported by NIH Grant R01EY019494, NIH Core Grant P30EY021725, and by an unrestricted grant from Research to Prevent Blindness, Inc. to the Department of Ophthalmology, University of Oklahoma Health Science Center.

References

1. Singer SJ, Nicolson GL (1972) The fluid mosaic model of the structure of cell membranes. *Science* 175(4023):720–731
2. Lee AG, Birdsall NJ, Metcalfe JC, Toon PA, Warren GB (1974) Clusters in lipid bilayers and the interpretation of thermal effects in biological membranes. *Biochemistry* 13(18):3699–3705
3. Karnovsky MJ, Kleinfeld AM, Hoover RL, Klausner RD (1982) The concept of lipid domains in membranes. *J Cell Biol* 94(1):1–6
4. Simons K, Ikonen E (1997) Functional rafts in cell membranes. *Nature* 387(6633):569–572. doi:10.1038/42408
5. Pike LJ (2009) The challenge of lipid rafts. *J Lipid Res* 50(Suppl):S323–S328. doi:10.1194/jlr.R800040-JLR200
6. Munro S (2003) Lipid rafts: elusive or illusive? *Cell* 115(4):377–388
7. Sonnino S, Prinetti A (2013) Membrane domains and the "lipid raft" concept. *Curr Med Chem* 20(1):4–21
8. Pike LJ (2006) Rafts defined: a report on the keystone symposium on lipid rafts and cell function. *J Lipid Res* 47(7):1597–1598. doi:10.1194/jlr.E600002-JLR200
9. Brown DA, Rose JK (1992) Sorting of GPI-anchored proteins to glycolipid-enriched membrane subdomains during transport to the apical cell surface. *Cell* 68(3):533–544
10. Macdonald JL, Pike LJ (2005) A simplified method for the preparation of detergent-free lipid rafts. *J Lipid Res* 46(5):1061–1067. doi:10.1194/jlr.D400041-JLR200

11. Song KS, Li S, Okamoto T, Quilliam LA, Sargiacomo M, Lisanti MP (1996) Co-purification and direct interaction of Ras with caveolin, an integral membrane protein of caveolae microdomains. Detergent-free purification of caveolae microdomains. *J Biol Chem* 271(16):9690–9697
12. Smart EJ, Ying YS, Mineo C, Anderson RG (1995) A detergent-free method for purifying caveolae membrane from tissue culture cells. *Proc Natl Acad Sci U S A* 92(22):10104–10108
13. Elliott MH, Fliesler SJ, Ghalayini AJ (2003) Cholesterol-dependent association of caveolin-1 with the transducin alpha subunit in bovine photoreceptor rod outer segments: disruption by cyclodextrin and guanosine 5'-O-(3-thiotriphosphate). *Biochemistry* 42(26):7892–7903. doi:[10.1021/bi027162n](https://doi.org/10.1021/bi027162n)
14. Elliott MH, Nash ZA, Takemori N, Fliesler SJ, McClellan ME, Naash MI (2008) Differential distribution of proteins and lipids in detergent-resistant and detergent-soluble domains in rod outer segment plasma membranes and disks. *J Neurochem* 104(2):336–352. doi:[10.1111/j.1471-4159.2007.04971.x](https://doi.org/10.1111/j.1471-4159.2007.04971.x)
15. Martin RE, Elliott MH, Brush RS, Anderson RE (2005) Detailed characterization of the lipid composition of detergent-resistant membranes from photoreceptor rod outer segment membranes. *Invest Ophthalmol Vis Sci* 46(4):1147–1154. doi:[10.1167/iovs.04-1207](https://doi.org/10.1167/iovs.04-1207)
16. Opreanu M, Tikhonenko M, Bozack S, Lydic TA, Reid GE, McSorley KM, Sochacki A, Perez GI, Esselman WJ, Kern T, Kolesnick R, Grant MB, Busik JV (2011) The unconventional role of acid sphingomyelinase in regulation of retinal microangiopathy in diabetic human and animal models. *Diabetes* 60(9):2370–2378. doi:[10.2337/db10-0550](https://doi.org/10.2337/db10-0550)
17. Ogiso H, Taniguchi M, Okazaki T (2015) Analysis of lipid-composition changes in plasma membrane microdomains. *J Lipid Res* 56(8):1594–1605. doi:[10.1194/jlr.M059972](https://doi.org/10.1194/jlr.M059972)
18. Seno K, Kishimoto M, Abe M, Higuchi Y, Mieda M, Owada Y, Yoshiyama W, Liu H, Hayashi F (2001) Light- and guanosine 5'-3-O-(thio)triphosphate-sensitive localization of a G protein and its effector on detergent-resistant membrane rafts in rod photoreceptor outer segments. *J Biol Chem* 276(24):20813–20816. doi:[10.1074/jbc.C100032200](https://doi.org/10.1074/jbc.C100032200)
19. Ostrom RS, Liu X (2007) Detergent and detergent-free methods to define lipid rafts and caveolae. *Methods Mol Biol* 400:459–468. doi:[10.1007/978-1-59745-519-0_30](https://doi.org/10.1007/978-1-59745-519-0_30)
20. Pike LJ, Han X, Gross RW (2005) Epidermal growth factor receptors are localized to lipid rafts that contain a balance of inner and outer leaflet lipids: a shotgun lipidomics study. *J Biol Chem* 280(29):26796–26804. doi:[10.1074/jbc.M503805200](https://doi.org/10.1074/jbc.M503805200)
21. Lichtenberg D, Goni FM, Heerklotz H (2005) Detergent-resistant membranes should not be identified with membrane rafts. *Trends Biochem Sci* 30(8):430–436. doi:[10.1016/j.tibs.2005.06.004](https://doi.org/10.1016/j.tibs.2005.06.004)
22. Lingwood D, Simons K (2007) Detergent resistance as a tool in membrane research. *Nat Protoc* 2(9):2159–2165. doi:[10.1038/nprot.2007.294](https://doi.org/10.1038/nprot.2007.294)
23. Roper K, Corbeil D, Huttner WB (2000) Retention of prominin in microvilli reveals distinct cholesterol-based lipid micro-domains in the apical plasma membrane. *Nat Cell Biol* 2(9):582–592. doi:[10.1038/35023524](https://doi.org/10.1038/35023524)

Chapter 17

Computational Functional Analysis of Lipid Metabolic Enzymes

Carolina Bagnato, Arjen Ten Have, María B. Prados, and María V. Beligni

Abstract

The computational analysis of enzymes that participate in lipid metabolism has both common and unique challenges when compared to the whole protein universe. Some of the hurdles that interfere with the functional annotation of lipid metabolic enzymes that are common to other pathways include the definition of proper starting datasets, the construction of reliable multiple sequence alignments, the definition of appropriate evolutionary models, and the reconstruction of phylogenetic trees with high statistical support, particularly for large datasets. Most enzymes that take part in lipid metabolism belong to complex superfamilies with many members that are not involved in lipid metabolism. In addition, some enzymes that do not have sequence similarity catalyze similar or even identical reactions. Some of the challenges that, albeit not unique, are more specific to lipid metabolism refer to the high compartmentalization of the routes, the catalysis in hydrophobic environments and, related to this, the function near or in biological membranes.

In this work, we provide guidelines intended to assist in the proper functional annotation of lipid metabolic enzymes, based on previous experiences related to the phospholipase D superfamily and the annotation of the triglyceride synthesis pathway in algae. We describe a pipeline that starts with the definition of an initial set of sequences to be used in similarity-based searches and ends in the reconstruction of phylogenies. We also mention the main issues that have to be taken into consideration when using tools to analyze subcellular localization, hydrophobicity patterns, or presence of transmembrane domains in lipid metabolic enzymes.

Key words Data-mining, Functional annotation, Hydrophobicity, Multiple sequence alignment, Phylogenetic tree, Superfamily

1 Introduction

The large numbers of sequences that have become available in recent years provide both opportunities and challenges for bio-computational function prediction. Complete proteomes often show that many protein families have several paralogs and are, hence, part of intricate protein superfamilies. The evolution of protein superfamilies is complex [1] and obfuscates function assignment. On a positive end, the same great amount of sequence information can be used to study the exact challenge just

mentioned: how did a particular superfamily evolve and what predictions regarding the functional characterization of its members can, as such, be made? This endeavor has many technical requirements, such as high fidelity multiple sequence alignments (MSAs), statistically supported phylogenies and, if available, structural information. Some of the issues and requirements are common to the whole protein universe, while others will be more specific to lipid metabolic enzymes.

Lipids are a heterogeneous group of macromolecules characterized by being soluble in organic solvents and poorly soluble in water. Contrary to other major macromolecules, which are polymers of similar monomers (e.g., monosaccharides, amino acids, or nucleotides), lipids are chemically very diverse. Nevertheless, most lipids are fatty acid derivatives formed by their esterification to alcohol hydroxyl groups, for instance those present in glycerol, cholesterol or sphingol, or by a nucleophilic substitution and amide formation starting from amines and fatty acids. Another common feature in lipid chemistry is the formation of phosphodiester bonds, present in various species of glycerophospholipids. These prevalent characteristics have had an effect on the evolution of the lipid metabolic enzymes that pose great challenges for bio-computational analysis. For instance, analysis of a number of examples shows that, in some cases, proteins that act on the same or similar functional groups on different molecules have evolved from common ancestors, having undergone structural and functional diversification to form very complex superfamilies, such as the phospholipase D (PLD) superfamily [2]. On the opposite end, other groups of enzymes (e.g., phosphoinositide kinases) seem to have originated from many different ancestral proteins, but have somehow converged to catalyze similar or even identical reactions, triggered by the similarity of the substrates and catalytic mechanisms [3]. Sometimes, proteins that catalyze related reactions have no significant sequence similarity, but share a few amino acids that constitute the actual core of the catalytic activity. An example of this is the histidine (H) that seems to be mandatory for catalysis in most acyltransferases [4, 5]. Although none of these issues is unique to lipid enzymes, any bio-computational analysis will profit from a profound knowledge of not only the enzymes of interest but also its homologous proteins.

A key particularity of lipid enzymes comes from the fact that catalysis has to deal with hydrophobic or amphipathic substrates that, in many cases, are inserted in a membrane. This implies that lipid enzymes must have, at least, some hydrophobic regions or lipid-binding domains to properly interact with the substrates and/or the membrane environment, while most frequently the enzymes themselves are more or less inserted in a membrane. In this scenario, the presence of transmembrane domains and hydrophobicity analyses are essential parts of lipid enzyme computational

studies. This information might not only contribute to sequence characterization, but also to sequence identification and annotation, since these features are usually shared between the members of the same family. The second peculiarity of lipid metabolism relates to the fact that the anabolic and catabolic reactions are usually carried out in different cell organelles or compartments, such as membrane, cytosol, chloroplast, or mitochondria, or they can even act extracellularly. In this context, the prediction of the presence of signal peptides for protein transit or targeting is of major relevance.

In this work, we will outline a general procedure intended to guide in the process of obtaining robust MSAs, phylogenies, and functional characterization of enzymes, with a particular emphasis on those that participate in the metabolism of lipids.

2 Materials

Figure 1 shows a flowchart of a stepwise procedure that can be used for protein bio-computational analysis. The procedure can be divided into a number of processes, each one with its particular details and resources. The flowchart intends to provide general guidelines using the major tools we have used in our previous computational analyses. However, this protocol can admit modifications, supplementations, or even simplifications depending on the case. Table 1 shows a non-exhaustive list of the main tools we have used in each process of the pipeline.

3 Methods

3.1 Dataset Definition

The most important step of the procedure is the definition of the objective. Two common interests we can outline are: (a) The identification and annotation of a particular pathway, including all the involved activities, and (b) The more profound analysis of a particular activity, in an effort to understand the origin and evolution of the corresponding sequences and their functional characteristics. The common challenge is to identify sequences, assign them plausible functions, and obtain relevant information that could guide experimental design and data interpretation. The objective will have a clear impact on both the initial set of sequences that will be used as seed or query for similarity-based searches and the sequence collection that will be used to search for hits using the previous seed. The seed or query dataset should consist, if available, of protein sequences with high quality annotation, as encountered in databases such as Swissprot (or UniProtKB) [14] (*see Note 1*) or Protein Databank (PDB) [13]. The selection of the target dataset depends on the taxonomic interests, which should

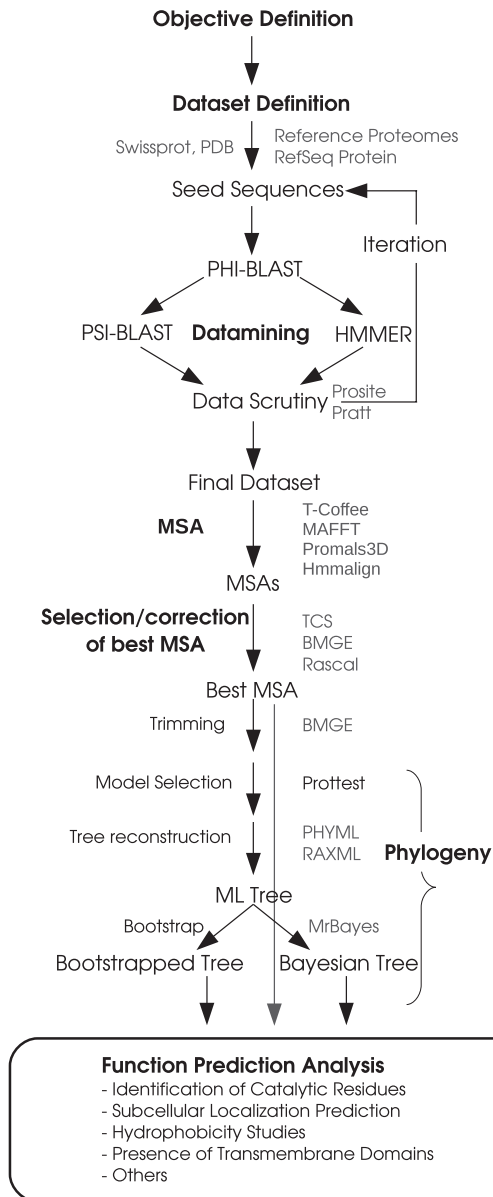


Fig. 1 Sequence mining flowchart depicting a basic pipeline for the analysis of protein superfamilies. Major processes as described in the text are in *bold*, resources in *gray*. Upon the definition of the objective and the corresponding dataset, sensitive sequence identification can be achieved by either iterative HMMER or PSI-BLAST, both can be seeded with a specific data seed obtained by PHI-BLAST. Upon scrutiny, the final data-set should be aligned with a variety of methods and the best MSA should be selected and corrected. When the objective involves only proper annotation, this MSA can be used directly for functional characterization. When the objective involves evolutionary questions, the MSA is used for phylogenetic tree reconstruction. Prior to running a phylogeny, the MSA should be trimmed and the correct evolutionary model should be determined. A maximum likelihood tree should be reconstructed and accompanied by bootstrap analysis; optionally it can serve as a starting tree for Bayesian analysis. In this case, MSA and phylogeny can also be used for a great number of functional prediction analyses

Table 1**List of common tools used for the bio-computational functional analysis of lipid metabolic enzymes**

Tool (Acronym)	Sources/Websites	Reference
<i>Dataset definition: hallmarks/proteins</i>		
Superfamily	http://supfam.org/SUPERFAMILY/	[6]
The comprehensive enzyme information system (Brenda)	http://www.brenda-enzymes.org/	[7]
Kyoto Encyclopedia of Genes and Genomes (KEGG)	http://www.genome.jp/kegg/	[8]
The European Bioinformatics Institute (EMBL-EBI, Pfam)	http://pfam.xfam.org/	[9]
Bioinformatics Resource Portal (ExPASy, Prosite)	http://prosite.expasy.org/	[10]
The European Bioinformatics Institute (EMBL-EBI, Interpro)	https://www.ebi.ac.uk/interpro/	[11]
John Craig Venter Institute (JCVI, TIGRFAM)	http://www.jcvi.org/cgi-bin/tigrfams/index.cgi	[12]
Protein Data Bank (PDB)	http://www.rcsb.org/pdb/home/home.do	[13]
<i>Dataset definition: general databases</i>		
The European Bioinformatics Institute (EMBL-EBI, Uniprot)	http://www.uniprot.org/	[14]
National Center for Biotechnology Information (NCBI)	http://www.ncbi.nlm.nih.gov/	[15]
DNA Data Bank of Japan (DDBJ)	http://www.ddbj.nig.ac.jp/	[16]
<i>Dataset definition: specific genomes</i>		
The Joint Genome Institute (JGI)	http://genome.jgi.doe.gov/	[17]
Broad Institute	https://www.broadinstitute.org/	[18]
National Center for Biotechnology Information (NCBI Genome)	http://www.ncbi.nlm.nih.gov/genome/browse/	[15]
Eukaryotic Pathogen Database Resources (EuPathDB)	http://eupathdb.org/eupathdb/	[19]

(continued)

Table 1
(continued)

Tool (Acronym)	Sources/Websites	Reference
Wellcome Trust Sanger Institute	http://www.sanger.ac.uk/	[20]
John Craig Venter Institute (JCVI, Genomics)	http://www.jcvi.org/cms/home/	[21]
<i>Data-mining</i>		
Biosequence analysis using profile hidden Markov models (HMMER)	http://hmmer.org/	[22]
Protein-protein Blast (BLAST)	NCBI and Other platforms	[23]
Position-Specific Iterated Blast (PSI-BLAST)	NCBI and Other platforms	[24]
Pattern Hit Initiated Blast (PHI-BLAST)	NCBI and Other platforms	[25]
<i>Sequence clustering and comparison</i>		
CD-HIT	http://weizhongli-lab.org/cd-hit/	[26]
<i>Multiple sequence alignment</i>		
T-coffee Multiple sequence alignment server	http://www.ebi.ac.uk/Tools/msa/tcoffee/	[27]
Multiple Alignment using Fast Fourier Transform (MAFFT)	http://mafft.cbrc.jp/alignment/server/index.html	[28]
Multiple Sequence Comparison by Log-Expectation (MUSCLE)	http://www.ebi.ac.uk/Tools/msa/muscle/	[29]
PROfile Multiple Alignment with Local Structure (PROMALS3D)	http://prodata.swmed.edu/promals3d/promals3d.php	[30]
Hidden Markov Model alignment (hmmalign)	http://hmmer.org/	[31]
<i>Alignment visualization/editing</i>		
GeneDoc	http://iubio.bio.indiana.edu/soft/molbio/ibmpc/genedoc-readme.html	[32]
AliView	http://www.ormbunkar.se/aliview/	[33]
SeaView	http://doua.prabi.fr/software/seaview	[34]
<i>MSA selection and correction</i>		
Block Mapping and Gathering using Entropy (BMGE)	http://mobyle.pasteur.fr/cgi-bin/portal.py#forms::BMGE	[35]

(continued)

Table 1
(continued)

Tool (Acronym)	Sources/Websites	Reference
Rapid Scanning and Correction of multiple Sequence Alignments (RASCAL)	ftp://ftp-igbmc.u-strasbg.fr/pub/RASCAL	[36]
Automated quality improvement for MSAs (AQUA)	http://www.bork.embl.de/Docu/AQUA/	[37]
Transitive Consistency Score (TCS)	http://tcoffee.crg.cat/apps/tcoffee/do:core	[27]
<i>Phylogeny: evolutionary model selection</i>		
ProtTest	http://darwin.uvigo.es/software/protest2_server.html	[38]
<i>Tree reconstruction—ML</i>		
Randomized Axelerated Maximum Likelihood (RAxML)	http://sco.h-its.org/exelixis/web/software/raxml/index.html	[39]
Phyml	http://www.atgc-montpellier.fr/phyml/	[40]
IQ-Tree	http://iqtree.cibiv.univie.ac.at/	[41]
<i>Tree reconstruction—Bayesian</i>		
Bayesian Inference of Phylogeny (Mr. Bayes)	http://mrbayes.sourceforge.net/	[42]
Bayesian Evolutionary Analysis Sampling Trees (Beast)	http://beast.bio.ed.ac.uk/	[43]
<i>3D modeling</i>		
Protein Homology/AnalogY Recognition Engine (PHYRE)	http://www.sbg.bio.ic.ac.uk/phyre2/html/page.cgi?id=index	[44]
Iterative Threading ASSEmbley Refinement (I-Tasser)	http://zhanglab.ccmb.med.umich.edu/I-TASSER/	[45]
<i>Subcellular localization: general</i>		
TargetP	http://www.cbs.dtu.dk/services/TargetP/	[46]
SignalP	http://www.cbs.dtu.dk/services/SignalP/	[46]
WoLF PSORT	http://www.genscript.com/wolf-psort.html	[47]
Predotar	https://urgi.versailles.inra.fr/predotar/predotar.html	

(continued)

Table 1
(continued)

Tool (Acronym)	Sources/Websites	Reference
<i>Subcellular localization: location-specific</i>		
ChloroP	http://www.cbs.dtu.dk/services/ChloroP/	[48]
MitoProt	https://ihg.gsf.de/ihg/mitoprot.html	[49]
SecretomeP	http://www.cbs.dtu.dk/services/SecretomeP/	[50]
<i>Subcellular localization: group-specific</i>		
PredAlgo	https://giavap-genomes.ibpc.fr/predalgo/	[51]
Hectar	http://webtools.sb-roscoff.fr/	[52]
Prediction of Apicomplast Targeted Sequences (PATS)	http://gecco.org.chemie.uni-frankfurt.de/pats/pats-index.php	[53]
<i>Hydrophobicity</i>		
ProtScale	http://web.expasy.org/protscale/	[54]
<i>Transmembrane vs. soluble</i>		
Transmembrane Hidden Markov Model (TMHMM)	http://www.cbs.dtu.dk/services/TMHMM	[55]
Hidden Markov Model Topology Prediction (HMMTOP)	http://www.enzim.hu/hmmtop/	[56]
Constrained Consensus Topology Prediction (CCTOP)	http://cctop.enzim.ttk.mta.hu/	[57]

guide and limit the analysis. Certain questions will require an unbiased dataset, consisting of phylogenetically representative or randomly chosen taxa, such as those provided by EBI's Reference Proteome dataset. Other studies will focus on only a portion of the tree of life, which might result in a desired over-representation of taxa within certain taxonomical clades (*see Note 2*).

There are a number of protein sequence resources. The three major generic online sequence resources are provided by NCBI [15], EMBL-EBI [58], and DDBJ [16] (*see Note 3*). The complete proteomes can be selected using RefSeq Protein, although not all RefSeq Protein datasets correspond to a complete proteome.

3.2 Data-Mining

Sequence identification, referred to as data-mining, is hampered by precision problems. An optimal sequence dataset is the one that contains all the sequences that correspond to the superfamily of interest and has no false positives. However, the protein space is so

complex that this is difficult to achieve. In order to improve sensitivity, we recommend an iterative procedure with two safeguards to maintain specificity: biochemical and sequence quality restrictions.

1. Biochemical restrictions: enzymes have motifs that are highly conserved, and this information should be used to restrict data-mining. PHI-BLAST [25] is useful for this purpose, since it restricts the sequence database with an inclusion pattern that corresponds to the biochemical restrictions of a protein family (*see Note 4*). Patterns for many protein families can be identified at Prosite [10] that also provides a method (PRATT) to construct custom patterns. A PHI-BLAST search using a single or a number of initial seed sequences yields a specific dataset that can be subsequently used for a sensitive sequence mining, with either HMMER [22] or PSI-BLAST [24] (*see Note 5* for a basic description of both methods).
2. Sequence quality restrictions: once a single sequence mining cycle is performed, the obtained sequences should be scrutinized. Many sequences will be partial, lacking either N- or C-termini, or even internal portions of the peptide. The absence of key amino acids or subsequences involved in secondary structure is indicative for faulty sequences and those should be eliminated (*see Note 6*). The scrutinized dataset can then be used to perform batch BLAST and/or HMMER searches (we recommend HMMER) until convergence or contamination occurs.

3.3 Multiple Sequence Alignment

Once the final sequence set has been obtained, proteins should be aligned to obtain information regarding functional characteristics. Given the already mentioned complexity of evolution, obtaining solid MSAs has turned out to be one of the major obstacles in protein bio-computation. More than 100 algorithms for MSA have been published since the initial ClustalW [59] became available [60]. A number of different heuristic approaches are being employed, often in combination. Furthermore, several auxiliary methods have also been developed with the goal of reducing errors introduced during alignment. Given the complexity of superfamily evolution and the different approaches used by the MSA software, *ab initio* it cannot be predicted which method will result in the best MSA. Benchmarking analysis of MSA software has clearly shown that many recent programs (*see Table 1*, which includes a list of good alignment programs) outperform ClustalW but also that different datasets appear to require different programs to generate the best MSA. Therefore, our recommendation is to use at least three different methods for building MSAs and then to evaluate their reliability. MSAs can be tested according to a structural criterion, an evolutionary criterion, and a similarity criterion. Each of these criteria has a bias and, as such, an empirical method is preferred.

An intuitive and quick method to evaluate MSA quality is the use of MSA trimming software, such as BMGE [35], which removes columns with high gap content and/or high entropy and maintains the most reliable parts of the MSA. Hence, the largest trimmed alignment should be considered the most reliable or the best MSA. Another method is the Transitive Consistency Score (TCS) [27], part of the T-coffee package. The output of TCS is very useful, since it provides consistency scores not only for the MSA but also for each sequence and even each residue. This allows for the identification of problematic sequences and possibly incorrectly aligned residues (*see Note 7*). The latest developments try to combine several methods. AQUA (Automated quality improvement for MSAs) [37] consists of a pipeline that uses two alignment programs (MUSCLE [20] and MAFFT [28]), one refinement program (RASCAL) [36], and one assessment program (NORMD) [61] to optimize the process of alignment.

If the objective of the analysis requires the reconstruction of phylogenies, BMGE or other MSA trimming methods should be used for the removal of phylogenetically unreliable or ambiguous columns prior to tree reconstruction (*see Note 8*).

3.4 Phylogenetic Tree Reconstruction

Phylogenies are not a mandatory step in functional analysis, but they provide very useful information for proper protein annotation. After trimming of the MSA, the best evolutionary model should be determined. ProtTest [38] is a software that can be used for the selection of the best-fit model of evolution of an MSA. Finally, a number of methods for the reconstruction of phylogenetic trees is available. Distance methods are only used for exceedingly large datasets. Maximum parsimony methods can be used for datasets with very similar sequences. Superfamilies will have highly variable MSAs that do not correspond considerably to the parsimony criterion. Hence, the current standard for protein superfamily phylogeny is the computational costly Maximum Likelihood (ML) method. Popular packages such as RAxML [39] and PhyML [40] provide reliable trees and other faster, but less reliable, methods are available for larger datasets.

The hierarchical clustering of trees requires statistical branch support, which determines the high computational cost of phylogenetic tree reconstruction. The best known analysis is bootstrap analysis in which random columns are copied to replace other random columns (*see Note 9* for details). As a general consensus, 1000 bootstrap replicates are required to gain considerable confidence, but lower numbers are usually computed in real-world studies. A second and much faster method consists of the approximate likelihood ratio test (aLRT) [62]. This does not require additional phylogeny, since it simply compares the local likelihoods of the best tree with the second best tree. If both trees are similar, high global support is obtained (*see Note 10*).

The latest developed tree reconstruction methods, such as MrBayes [42], use Bayesian statistics to sample trees from the tree space and calculate, for each bifurcation, a posterior probability using the probability distribution of these trees. For proper sampling, the methodology uses a Markov Chain Monte Carlo (MCMC) approach and recommends doing at least two independent runs. The convergence of runs is indicative of having reached a global peak and, hence, the best tree (*see Note 11*). Convergence is supposedly reached when the standard deviation between runs is <0.01. However, we recommend analyzing convergence using AWTY, a system for the graphical exploration of MCMC convergence in Bayesian phylogenetic inference [63].

3.5 Functional Analysis

The final stage of functional sequence analysis is the most variable one and depends markedly on the original objective of the analysis. Although this is by all means the most interesting part of structure-function studies, here we will not go into detail into the numerous analyses that can be done on a protein or group of proteins. We will only describe three types that are particularly important for enzymes that participate in the lipid pathways: subcellular localization, hydrophobicity, and presence of transmembrane domains.

3.5.1 Subcellular Localization Prediction

The vast majority of the prediction tools are available online and have friendly and easy interfaces, some of them are listed in Table 1. The aim of this section is to only mention the most important considerations of using subcellular localization prediction tools. The most conserved targeting signal is the secretory signal peptide (SP), which targets a protein for translocation across the plasma membrane in prokaryotes and across the endoplasmic reticulum (ER) membrane in eukaryotes (*see Note 12*). Targeting to mitochondria or to chloroplasts is mediated by different transit peptides, mTP and cTP respectively (*see Note 13*). Prediction tools employ the amino acid sequence of the protein of interest as input data and give *prediction scores*, which are not necessarily probabilities, that a protein goes to a particular localization. Two categories of methods have been developed: those that predict the presence of sorting signals, such as TargetP [46], ChloroP [48], and Predotar [64], and those that also rely on some features shared by proteins found in a specific organelle (reflected in their amino acid composition), such as WoLF PSORT [47] and SecretomeP [50]. For the first group of methods, the presence of the N-terminus of the sequence is mandatory, since they only search for the specific signals included in the N-terminal region that determine primary cell sorting. The second group of methods uses the complete sequence and can still make a prediction when no leader sequence is detected.

Most of the current computational prediction tools are machine learning methods, which have been trained with a specific

set of sequences. Therefore, when choosing a method, it is important to consider how extensive the training set was. Otherwise, the localization of those proteins that are not taxonomically close to the set of sequences used in the training might not be predicted accurately. For example, algal sequences were not included in the training set used to construct TargetP. Therefore, in spite of the fact that the *plant* version of TargetP could be used to analyze algal sequences, the results could be unreliable. Currently, softwares for analyzing specific groups are becoming available, for example, Hectar [52] for heterokonts or PredAlgo [51] for green algae. When a taxon-specific tool is not available, it is recommended to choose the most suitable general tool and apply the *winner-takes-all* criterion for determining the potential subcellular localization.

A particular issue should be taken into consideration with organisms containing complex plastids, originated by secondary endosymbiosis. In these organisms, nuclear-encoded proteins are targeted to the complex plastid via the secretory pathway. These proteins have a *bipartite signal*, which can be easily confused with the SP of secreted proteins. The N-terminus of the bipartite signal functions as a classical SP, mediating entry to the ER. Upon cleavage of this signal, a transit peptide required for targeting to the plastid is exposed. Therefore, it is recommended for these proteins to determine the presence of a SP first and, if present, manually remove it and test the remaining sequence for the presence of plastid targeting peptides [65].

3.5.2 Protein Hydrophobicity Analysis

There are a series of tools to predict protein hydrophobicity and the majority are based on the analysis of the relative polarity of single amino acid residues. Hydrophobic indexes are calculated as an average of the individual hydrophobicity of a short sequence of amino acids, and the results are interpreted and represented in 2D plots. ProtScale [54] is a commonly used tool to construct hydrophobicity plots of proteins, available at ExPASy, that provides many scales and allows for large window size ranges. The window size can be selected based on the user's criteria, corresponding to, for instance, the minimal size of a membrane-spanning helix (*see Note 14*). When used in conjunction with MSAs and 3D structures, conservation of hydrophobic subsequences can yield important clues on functional characteristics.

3.5.3 Membrane Protein Topology

Closely related to the hydrophobicity is the topology of membrane-bound proteins, which involves the identification of transmembrane segments (TMSs) or helices, loops, and their orientation across the membrane. Many membrane integral proteins present segments that cross the lipid bilayer one or several times. A good example is diacylglycerol acyltransferase 1 (DGAT1), which spans the ER membrane between 9 and 12 times depending on the

organism. Besides determining the amount and localization of TMSs, it is important to know which compartment the loops are facing, since this has implications on substrate availability, product delivery, and might aid in the characterization of the catalytic mechanism. There are several programs dedicated to the identification of TMSs (Table 1). As a general consensus, a protein with a segment of more than 20 hydrophobic amino acids is likely to present a transmembrane segment. Although the initial approaches to determine TMSs were based on the analysis of protein sequence hydrophobicity [66–68], recently global approaches based on Hidden Markov Models such as TM-HMM [55] or HMMTOP [56] became prevalent because of their high prediction efficiency. These methods are based on the fact that particular signatures of transmembrane proteins are not randomly distributed throughout a protein. In our analyses, we use TM-HMM, since it was shown to have the best performance among several methods of topology prediction [69]. The output indicates the number and location of predicted transmembrane segments or helices. In addition, a 2D plot shows posterior probabilities of the inner, outer, and transmembrane segments. A careful analysis of the length and position of predicted features should be done (*see Note 15*).

3.6 Examples

In the following section, we will provide two examples that portrait common challenges of the computational analysis of lipid metabolic enzymes, based on our experience, as well as the general procedure followed in both cases.

3.6.1 Phospholipase D HKD Superfamily

PLDs are enzymes that catalyze the hydrolysis of structural phospholipids at their terminal phosphoester bond. PLDs are part of a larger superfamily of proteins that share a similar reaction mechanism, but act on a range of substrates other than phospholipids, including neutral lipids and even polynucleotide backbones. PLDs are characterized by a HxKxxxxD motif that is more or less strict depending on the subfamily. Many PLDs are well-conserved proteins that are quite easily identified using straightforward similarity-based search tools such as BLASTP. However, many of the homologs have diverged considerably, and the difficulty with these proteins is to predict with some level of confidence whether they have retained the PLD activity or if they are actually non-PLD members of the superfamily.

Based on the importance of PLDs in higher plants we set out to investigate PLDs in algae, taking into consideration that algae are taxonomically very diverse and that they occur in various ecological niches. Rather than using a PHI-BLAST with a pattern based on an overly strict HxKxxxxD motif, our initial approach consisted in generating a very broad collection of well-characterized PLD homologs, which were scrutinized, aligned, and used to generate an initial profile hmm. This profile was then used to search a compiled FASTA file

containing the complete proteomes of a group of selected eukaryotic species. Sequences scoring above the default inclusion threshold (E-value = 0.01) were retrieved. A set of nonredundant sequences obtained by CD-HIT [26] was aligned using MAFFT. The resulting MSA was manually corrected and used for the generation of a new HMMER profile. This process was iterated until convergence. In order to analyze eukaryotic PLD homologs in a true phylogenetic context, both the seed and the final profile hmms were used to search for prokaryotic homologs. This was done by searching the SwissProt and EBI Reference Proteome databases at the HMMER website, restricted to Bacteria and Archaea. In this case, hmalign proved to yield the best final MSA. BMGE was used both to test MSA reliability and to eliminate unreliable regions of the MSA prior to tree reconstruction. Phylogenetic analysis was done using PhyML and Mr. Bayes. Even though our main interest was on algae, inclusion of other eukaryotic and prokaryotic representative taxa improved tree reconstruction and statistical support. In order to ensure that we obtained the most complete dataset of eukaryotic PLDs possible, the sequences from each phylogenetic group were retrieved and used in group-specific data-mining following the same procedure as the one described above. Phylogenetic and clustering analysis allowed us to identify novel subclades, to provide insights into the required conservation levels of the HxKxxxxD motif for each subfamily, and to construct sequence logos with a better representation of the tree of life [2].

3.6.2 *Acyltransferases in the Glycerolipid Synthesis Pathway*

Acyltransferases catalyze the transfer of a fatty acid to a hydroxyl group in a condensation reaction that ends up in the formation of an ester. Activated fatty acids, mostly in the form of an acyl-CoA, are the most common donors, whereas the acyl acceptor varies considerably, from carbohydrates to amino acid residues and a wide variety of lipids. For lipids, we can distinguish between acyltransferases in the glycerophospholipid pathway that act on different acyl-CoA acceptors (such as glycerol-3-phosphate, acylglycerol-3-phosphate and diacylglycerol), and acyltransferases that utilize esterified fatty acids for TAG synthesis and phospholipid remodeling. Our main interest in the TAG pathway involved the characterization and functional annotation of proteins from algae, a group of organisms for which proper annotation is just emerging. Bio-computational analysis of acyltransferases in the TAG pathway is troubled by the fact that these activities are related to other activities in very intricate manners. Some of this complexity is exemplified by their Pfam relationships [9], as shown in Table 2. The five acyltransferase enzymes that participate in the TAG pathway mostly derive from three clans and at least four families. Many of the activities belong to clans with other enzymes that act on non-lipidic compounds. Particularly complex is the clan of abhydrolases

Table 2
Acyltransferases in the TAG synthesis pathway

Clan ^a	Family ^b	Family name ^b	Family description	Enzyme activity (TAG pathway) ^c	Enzyme acronym	Other members of the clan ^d
CL0517	PF03062	MBOAT	Membrane Bound O-Acyltransferase	Diacylglycerol acyltransferase 1 EC 2.3.1.20	DGAT1, DAGAT1	Sterol O-acyltransferase (SOAT) EC 2.3.1.26
CL0228	PF01553	Acyltransferase	Acyltransferase	Glycerol-3-phosphate acyltransferase EC 2.3.1.15 Acylglycerol-3-phosphate acyltransferase EC 2.3.1.51	GPAT AGPAT, LPAAT	1. Lysocardiolipin acyltransferase (LYCAT) EC 2.3.1.51 2. Glyceronophosphate O-acyltransferase (GNPAT) EC 2.3.1.42. 3. Lipid A biosynthesis
	PF03982	DAGAT	Diacylglycerol acyltransferase	Diacylglycerol acyltransferase 2 EC 2.3.1.20	DGAT2, DAGAT2	Palmitoleoyltransferase EC 2.3.1.242
CL0028	PF02450	LCAT	Lecithin:cholesterol acyltransferase	Phospholipid diacylglycerolacyl transferase EC 2.3.1.158	PDAT	1. Lecithin:cholesterol acyltransferase (LCAT) EC 2.3.1.43 2. Phospholipase A1 (PLA1) EC 3.1.1.32

^aPfam clan IDs. Please, see the Pfam glossary for a full description of the terms clan and family

^bPfam family PF IDs and names

^cCatalytic activities of each family that participate in the TAG synthesis pathway, including the Enzyme Commission (EC) numbers. Note that DGAT1 and DGAT2 catalyze the same activity and have, hence, the same EC number, but belong to different protein clans

^dExamples of members of each clan that participate in other lipid pathways other than TAG synthesis

(CL0028), which contains the enzyme phospholipid diacylglycerol acyltransferase (PDAT), as well as other 65 families [9]. Furthermore, PDAT is part of a family also composed of lecithin:cholesterol acyltransferases (LCAT), a group of acyltransferases that do not act on the TAG pathway, but on sterols.

Other activities, such as the three types of diacylglycerol acyltransferases (DGATs), catalyze the same reaction but belong to different protein superfamilies, having little or no sequence similarity. From a bio-computational point of view, this implies that three different patterns or profiles hmms have to be built to identify and annotate all DGATs.

Similar to the PLDs, the challenge for these enzymes was to build a sensitive profile hmm that could identify distant homologs, while maintaining sufficient specificity to exclude false positives or incorrect annotation. However, contrary to the PLD analysis, which was aimed at describing the PLD superfamily, the aim of this work was to do an accurate annotation of the activities of the pathway, without so much emphasis on phylogenetic aspects. To define the seed datasets, we used reviewed and well-characterized sequences, taken from SwissProt, for each activity, which were: human GPAT3 (Q53EU6), human LPAAT4 (Q643R3), human DGAT1 (O75907), human DGAT2 (Q96PD7), and *Arabidopsis thaliana* PDAT (Q9FNA9). Using these sequences, we performed a BLAST search on the SwissProt database to identify properly annotated proteins. The retrieved sequences were used to build initial hmm profiles that were used to search SwissProt again. The output was scrutinized based on the presence of key amino acids and domains described in the literature. The sequences resulting from this search were used to build other profile hmms, which were used to search FASTA files containing the genomes of all the algae of interest, some of them not contained in Uniprot or NCBI. Since curation for some of these genomes is preliminary, the algae sequences were carefully scrutinized for the presence of key amino acids. In addition, and due to the scarce information available for this pathway in algae, the hydrophobicity pattern, in particular in the vicinity of the putative catalytic site, the presence of transmembrane domains, and the predicted subcellular localization were included to make decisions on sequence identity. As expected, it was difficult to clearly distinguish between GPAT and AGPAT sequences, mainly because there is a certain grade of substrate ambiguity and activity overlapping for these enzymes [70, 71]. However, our models were more effective at discriminating between both activities than the Pfam database, in which they are represented with a single hmm.

4 Notes

1. Swissprot or UniProtKB have five different quality levels of annotation. Levels 1 (with protein evidence) and 2 (with transcript evidence) form the most reliable part.
2. Even questions that are focused on specific taxonomic groups are frequently best approached when using a more general set of proteomes. It should be noted that a certain bias will always exist, even by simply considering that many taxa are still unknown.
3. Proteome sets from recently sequenced organisms might only be available on the websites of the particular sequencing consortia (e.g., JGI, Broad, JCVI). In these cases, particular attention should be paid to the quality of the protein sequences, since recently sequenced genomes tend to suffer from unfinished manual curation.
4. Patterns are deterministic descriptions of proteins in the sense that a sequence either does or does not correspond to a pattern. Patterns should not be confused with profiles, which are probabilistic descriptions of proteins. Patterns should be carefully determined, since any bias in their construction can result in the exclusion of homologs. In addition, when conserved sites tolerate some level of variation, patterns should be avoided and replaced with probabilistic profiles, such as those constructed with HMMER.
5. In HMMER profiling, sequences are compared with query MSAs, which are used to make probabilistic models called *profile hidden Markov models* (profile hmms). Pfam [9] and Superfamily [6] make use of HMMER by comparing query sequences with a database of well-annotated profile hmms. In practical data-mining, HMMER is more sensitive than BLAST, since it uses more information. PSI-BLAST is an iterative procedure in which, following a BLAST, a Position-Specific Substitution Matrix (PSSM) is built based on pseudo-MSAs of the hits, and used for subsequent iterations.
6. Sequence scrutiny is delicate and can easily result in the removal of positives, since substitution at presumed strictly conserved sites by similar residues can occur.
7. To strengthen the reliability, ideally the best MSA should be determined by means of two partially independent methods, such as TCS and BMGE. Manual MSA corrections might also be required but, since these are subject to human error, they should be verified using the aforementioned methods.
8. A point of reference is required to determine which levels of entropy should be tolerated. Given the thermodynamic

requisite of secondary structure in general and beta sheets in particular, trimming should ideally not remove subsequences corresponding to these elements. The inclusion of structural information can therefore be important.

9. Bootstrapping actually determines if the rate of evolution is comparable over all columns of the MSA dataset. Since this rate will arguably never be identical for all columns, bootstrapping is not a method that estimates if a tree or the underlying MSA is correct. Nevertheless, low bootstrap values can indicate possible errors and clades with good support are less likely to be incorrectly placed than clades with poor support. Since bootstrap analysis is known to underestimate support, low bootstrap support does not necessarily mean poor support [72]. A bootstrap support of 50/100 means that 50 of the 100 bootstrapped trees coincide with the bifurcation. However, it does not yield information regarding the other 50 trees. These might be all identical or different.
10. Since other trees with worse global likelihood can have higher local likelihoods, it becomes evident that, although the aLRT method is very practical, it overestimates support. Therefore, the current standard for ML phylogeny mostly requires bootstrap analysis.
11. Bayesian phylogeny has been suggested to be better and faster than bootstrapping. In our experience with complex datasets, convergence is not easily reached, even when applying multiple adjustments and the recent incorporation of heated chains using Metropolis Coupled MCMC. Future improvements regarding how to search complex tree spaces (e.g., using genetic algorithms) will be required to successfully apply Bayesian statistics to all complex phylogenies without depending on large high-performance computation clusters.
12. Not all secretory proteins have SPs, nonclassically secreted proteins were found in both prokaryotes and eukaryotes. SecretomeP, for example, is a useful tool to identify secretory proteins targeted via the nonclassical secretory pathway.
13. Sometimes, computational tools cannot discriminate between mitochondrial or chloroplast targeting peptides in a precise manner. It should be noted that, although targeting of nuclear-encoded proteins to the mitochondria and chloroplast is specific, numerous examples of proteins imported to both organelles were described in plants. This indicates that several TPs can carry out dual targeting, which complicates prediction.
14. ProtScale provides data of hydrophobicity signal but it does not provide a reliability score. Data interpretation needs to be done by including positive and negative controls. Identification of truly strong signal areas can be done by slightly changing

the window size or by replacing the scale and checking if the segments with strong signal remain present.

15. Short loops are predicted to be of five amino acids minimum and membrane spanning segments are expected to be of about 20–22 amino acids, so loops or helices shorter than that deserve special attention. For example, the size of the amino acids in the very short loop should be scrutinized, ideally it should be composed of small amino acids like glycine. The hydrophobic segments present in signal peptides (SP) are often misidentified as transmembrane domains by computational prediction methods. SignalP latest versions (4.0 or later) have an improved power to discriminate between SPs and transmembrane regions. If the SP and the transmembrane domain are difficult to discern, the use of Phobius [73] is recommended [65].

References

1. Eirin-Lopez JM, Rebordinos L, Rooney AP, Rozas J (2012) The birth-and-death evolution of multigene families revisited. *Genome Dyn* 7:170–196. doi:[10.1159/000337119](https://doi.org/10.1159/000337119)
2. Beligni MV, Bagnato C, Prados MB, Bondino H, Laxalt AM, Munnik T, Ten Have A (2015) The diversity of algal phospholipase D homologs revealed by biocomputational analysis. *J Phycol* 51(5):943–962. doi:[10.1111/jpy.12334](https://doi.org/10.1111/jpy.12334)
3. Brown JR, Auger KR (2011) Phylogenomics of phosphoinositide lipid kinases: perspectives on the evolution of second messenger signaling and drug discovery. *BMC Evol Biol* 11:4. doi:[10.1186/1471-2148-11-4](https://doi.org/10.1186/1471-2148-11-4)
4. Cao H (2011) Structure-function analysis of diacylglycerol acyltransferase sequences from 70 organisms. *BMC Res Notes* 4:249. doi:[10.1186/1756-0500-4-249](https://doi.org/10.1186/1756-0500-4-249)
5. Das A, Davis MA, Rudel LL (2008) Identification of putative active site residues of ACAT enzymes. *J Lipid Res* 49(8):1770–1781. doi:[10.1194/jlr.M800131-JLR200](https://doi.org/10.1194/jlr.M800131-JLR200)
6. Wilson D, Pethica R, Zhou Y, Talbot C, Vogel C, Madera M, Chothia C, Gough J (2009) SUPERFAMILY—sophisticated comparative genomics, data mining, visualization and phylogeny. *Nucleic Acids Res* 37(Database issue):D380–D386. doi:[10.1093/nar/gkn762](https://doi.org/10.1093/nar/gkn762)
7. Schomburg I, Chang A, Placzek S, Sohngen C, Rother M, Lang M, Munnareto C, Ulas S, Stelzer M, Grote A, Scheer M, Schomburg D (2013) BRENDA in 2013: integrated reactions, kinetic data, enzyme function data, improved disease classification: new options and contents in BRENDA. *Nucleic Acids Res* 41(Database issue):D764–D772. doi:[10.1093/nar/gks1049](https://doi.org/10.1093/nar/gks1049)
8. Aoki KF, Kanehisa M (2005) Using the KEGG database resource. *Curr Protoc Bioinformatics Chapter 1:Unit 1 12*. doi:[10.1002/0471250953.bi0112s11](https://doi.org/10.1002/0471250953.bi0112s11)
9. Punta M, Coggill PC, Eberhardt RY, Mistry J, Tate J, Boursnell C, Pang N, Forslund K, Ceric G, Clements J, Heger A, Holm L, Sonnhammer EL, Eddy SR, Bateman A, Finn RD (2012) The Pfam protein families database. *Nucleic Acids Res* 40(Database issue):D290–D301. doi:[10.1093/nar/gkr1065](https://doi.org/10.1093/nar/gkr1065)
10. Sigrist CJ, Cerutti L, Hulo N, Gattiker A, Falquet L, Pagni M, Bairoch A, Bucher P (2002) PROSITE: a documented database using patterns and profiles as motif descriptors. *Brief Bioinform* 3(3):265–274
11. Jones P, Binns D, Chang HY, Fraser M, Li W, McAnulla C, McWilliam H, Maslen J, Mitchell A, Nuka G, Pesseat S, Quinn AF, Sangrador-Vegas A, Scheremetjew M, Yong SY, Lopez R, Hunter S (2014) InterProScan 5: genome-scale protein function classification. *Bioinformatics (Oxford, England)* 30(9):1236–1240. doi:[10.1093/bioinformatics/btu031](https://doi.org/10.1093/bioinformatics/btu031)
12. Haft DH, Selengut JD, White O (2003) The TIGRFAMs database of protein families. *Nucleic Acids Res* 31(1):371–373
13. Berman HM, Westbrook J, Feng Z, Gilliland G, Bhat TN, Weissig H, Shindyalov IN, Bourne PE (2000) The protein data bank. *Nucleic Acids Res* 28(1):235–242
14. UniProt Consortium (2015) UniProt: a hub for protein information. *Nucleic Acids Res*

- 43(Database issue):D204–D212. doi:[10.1093/nar/gku989](https://doi.org/10.1093/nar/gku989)
15. Information NCBI (2016) <http://www.ncbi.nlm.nih.gov/>. Accessed 15 May 2016
 16. Mashima J, Kodama Y, Kosuge T, Fujisawa T, Katayama T, Nagasaki H, Okuda Y, Kaminuma E, Ogasawara O, Okubo K, Nakamura Y, Takagi T (2016) DNA data bank of Japan (DDBJ) progress report. *Nucleic Acids Res* 44(D1):D51–D57. doi:[10.1093/nar/gkv1105](https://doi.org/10.1093/nar/gkv1105)
 17. Nordberg H, Cantor M, Dusheyko S, Hua S, Poliakov A, Shabalov I, Smirnova T, Grigoriev IV, Dubchak I (2014) The genome portal of the department of energy joint genome institute: 2014 updates. *Nucleic Acids Res* 42(Database issue):D26–D31. doi:[10.1093/nar/gkt1069](https://doi.org/10.1093/nar/gkt1069)
 18. Institute TB (2016) <https://www.broadinstitute.org/>. Accessed 10 May 2016
 19. Aurrecochea C, Heiges M, Wang H, Wang Z, Fischer S, Rhodes P, Miller J, Kraemer E, Stoekert CJ Jr, Roos DS, Kissinger JC (2007) ApiDB: integrated resources for the apicomplexan bioinformatics resource center. *Nucleic Acids Res* 35(Database issue):D427–D430. doi:[10.1093/nar/gkl880](https://doi.org/10.1093/nar/gkl880)
 20. Institute WTS (2016) <http://www.sanger.ac.uk/>. Accessed 15 May 2016
 21. Institute JCV (2016) <http://www.jcvi.org/cms/home/>. Accessed 1 May 2016
 22. Finn RD, Clements J, Arndt W, Miller BL, Wheeler TJ, Schreiber F, Bateman A, Eddy SR (2015) HMMER web server: 2015 update. *Nucleic Acids Res* 43(W1):W30–W38. doi:[10.1093/nar/gkv397](https://doi.org/10.1093/nar/gkv397)
 23. Altschul SF, Gish W, Miller W, Myers EW, Lipman DJ (1990) Basic local alignment search tool. *J Mol Biol* 215(3):403–410. doi:[10.1016/s0022-2836\(05\)80360-2](https://doi.org/10.1016/s0022-2836(05)80360-2)
 24. Altschul SF, Madden TL, Schaffer AA, Zhang J, Zhang Z, Miller W, Lipman DJ (1997) Gapped BLAST and PSI-BLAST: a new generation of protein database search programs. *Nucleic Acids Res* 25(17):3389–3402
 25. Zhang Z, Schaffer AA, Miller W, Madden TL, Lipman DJ, Koonin EV, Altschul SF (1998) Protein sequence similarity searches using patterns as seeds. *Nucleic Acids Res* 26(17):3986–3990
 26. Fu L, Niu B, Zhu Z, Wu S, Li W (2012) CD-HIT: accelerated for clustering the next-generation sequencing data. *Bioinformatics* (Oxford, England) 28(23):3150–3152. doi:[10.1093/bioinformatics/bts565](https://doi.org/10.1093/bioinformatics/bts565)
 27. Notredame C, Higgins DG, Heringa J (2000) T-coffee: a novel method for fast and accurate multiple sequence alignment. *J Mol Biol* 302(1):205–217. doi:[10.1006/jmbi.2000.4042](https://doi.org/10.1006/jmbi.2000.4042)
 28. Katoh K, Misawa K, Kuma K, Miyata T (2002) MAFFT: a novel method for rapid multiple sequence alignment based on fast Fourier transform. *Nucleic Acids Res* 30(14):3059–3066
 29. Edgar RC (2004) MUSCLE: multiple sequence alignment with high accuracy and high throughput. *Nucleic Acids Res* 32(5):1792–1797. doi:[10.1093/nar/gkh340](https://doi.org/10.1093/nar/gkh340)
 30. Pei J, Kim BH, Grishin NV (2008) PROMALS3D: a tool for multiple protein sequence and structure alignments. *Nucleic Acids Res* 36(7):2295–2300. doi:[10.1093/nar/gkn072](https://doi.org/10.1093/nar/gkn072)
 31. Finn RD, Clements J, Eddy SR (2011) HMMER web server: interactive sequence similarity searching. *Nucleic Acids Res* 39(Web Server issue):W29–W37. doi:[10.1093/nar/gkr367](https://doi.org/10.1093/nar/gkr367)
 32. Nicholas KB, Nicholas HB, Deerfield D (1997) GeneDoc: analysis and visualisation of genetic variation. *EMBNet News* 4:14
 33. Larsson A (2014) AliView: a fast and lightweight alignment viewer and editor for large datasets. *Bioinformatics* (Oxford, England) 30(22):3276–3278. doi:[10.1093/bioinformatics/btu531](https://doi.org/10.1093/bioinformatics/btu531)
 34. Gouy M, Guindon S, Gascuel O (2010) SeaView version 4: a multiplatform graphical user interface for sequence alignment and phylogenetic tree building. *Mol Biol Evol* 27(2):221–224. doi:[10.1093/molbev/msp259](https://doi.org/10.1093/molbev/msp259)
 35. Criscuolo A, Gribaldo S (2010) BMGE (block mapping and gathering with entropy): a new software for selection of phylogenetic informative regions from multiple sequence alignments. *BMC Evol Biol* 10:210. doi:[10.1186/1471-2148-10-210](https://doi.org/10.1186/1471-2148-10-210)
 36. Thompson JD, Thierry JC, Poch O (2003) RASCAL: rapid scanning and correction of multiple sequence alignments. *Bioinformatics* (Oxford, England) 19(9):1155–1161
 37. Muller J, Creevey CJ, Thompson JD, Arendt D, Bork P (2010) AQUA: automated quality improvement for multiple sequence alignments. *Bioinformatics* (Oxford, England) 26(2):263–265. doi:[10.1093/bioinformatics/btp651](https://doi.org/10.1093/bioinformatics/btp651)
 38. Abascal F, Zardoya R, Posada D (2005) ProtTest: selection of best-fit models of protein evolution. *Bioinformatics* (Oxford, England) 21(9):2104–2105. doi:[10.1093/bioinformatics/bti263](https://doi.org/10.1093/bioinformatics/bti263)
 39. Stamatakis A (2014) RAxML version 8: a tool for phylogenetic analysis and post-analysis of

- large phylogenies. *Bioinformatics* (Oxford, England) 30(9):1312–1313. doi:[10.1093/bioinformatics/btu033](https://doi.org/10.1093/bioinformatics/btu033)
40. Guindon S, Dufayard JF, Lefort V, Anisimova M, Hordijk W, Gascuel O (2010) New algorithms and methods to estimate maximum-likelihood phylogenies: assessing the performance of PhyML 3.0. *Syst Biol* 59(3):307–321. doi:[10.1093/sysbio/syq010](https://doi.org/10.1093/sysbio/syq010)
 41. Trifinopoulos J, Nguyen LT, von Haeseler A, Minh BQ (2016) W-IQ-TREE: a fast online phylogenetic tool for maximum likelihood analysis. *Nucleic Acids Res* 44(W1):W232–W235. doi:[10.1093/nar/gkw256](https://doi.org/10.1093/nar/gkw256)
 42. Ronquist F, Teslenko M, van der Mark P, Ayres DL, Darling A, Höhna S, Larget B, Liu L, Suchard MA, Huelsenbeck JP (2012) MrBayes 3.2: efficient Bayesian phylogenetic inference and model choice across a large model space. *Syst Biol* 61(3):539–542. doi:[10.1093/sysbio/sys029](https://doi.org/10.1093/sysbio/sys029)
 43. Drummond AJ, Suchard MA, Xie D, Rambaut A (2012) Bayesian phylogenetics with BEAUti and the BEAST 1.7. *Mol Biol Evol* 29(8):1969–1973. doi:[10.1093/molbev/mss075](https://doi.org/10.1093/molbev/mss075)
 44. Kelley LA, Mezulis S, Yates CM, Wass MN, Sternberg MJ (2015) The Phyre2 web portal for protein modeling, prediction and analysis. *Nat Protoc* 10(6):845–858. doi:[10.1038/nprot.2015.053](https://doi.org/10.1038/nprot.2015.053)
 45. Yang J, Yan R, Roy A, Xu D, Poisson J, Zhang Y (2015) The I-TASSER suite: protein structure and function prediction. *Nat Methods* 12(1):7–8. doi:[10.1038/nmeth.3213](https://doi.org/10.1038/nmeth.3213)
 46. Emanuelsson O, Brunak S, von Heijne G, Nielsen H (2007) Locating proteins in the cell using TargetP, SignalP and related tools. *Nat Protoc* 2(4):953–971. doi:[10.1038/nprot.2007.131](https://doi.org/10.1038/nprot.2007.131)
 47. Horton P, Park KJ, Obayashi T, Fujita N, Harada H, Adams-Collier CJ, Nakai K (2007) WoLF PSORT: protein localization predictor. *Nucleic Acids Res* 35(Web Server issue):W585–W587. doi:[10.1093/nar/gkm259](https://doi.org/10.1093/nar/gkm259)
 48. Emanuelsson O, Nielsen H, von Heijne G (1999) ChloroP, a neural network-based method for predicting chloroplast transit peptides and their cleavage sites. *Protein Sci* 8(5):978–984. doi:[10.1110/ps.8.5.978](https://doi.org/10.1110/ps.8.5.978)
 49. Claros MG, Vincens P (1996) Computational method to predict mitochondrially imported proteins and their targeting sequences. *Eur J Biochem* 241(3):779–786
 50. Bendtsen JD, Jensen LJ, Blom N, Von Heijne G, Brunak S (2004) Feature-based prediction of non-classical and leaderless protein secretion. *Protein Eng Des Sel* 17(4):349–356. doi:[10.1093/protein/gzh037](https://doi.org/10.1093/protein/gzh037)
 51. Tardif M, Atteia A, Specht M, Cogne G, Rolland N, Brugiere S, Hippler M, Ferro M, Bruley C, Peltier G, Vallon O, Cournac L (2012) PredAlgo: a new subcellular localization prediction tool dedicated to green algae. *Mol Biol Evol* 29(12):3625–3639. doi:[10.1093/molbev/mss178](https://doi.org/10.1093/molbev/mss178)
 52. Gschloessl B, Guermeur Y, Cock JM (2008) HECTAR: a method to predict subcellular targeting in heterokonts. *BMC Bioinformatics* 9:393. doi:[10.1186/1471-2105-9-393](https://doi.org/10.1186/1471-2105-9-393)
 53. Zuegge J, Ralph S, Schmuker M, McFadden GI, Schneider G (2001) Deciphering apicoplast targeting signals—feature extraction from nuclear-encoded precursors of *Plasmodium falciparum* apicoplast proteins. *Gene* 280(1–2):19–26
 54. Gasteiger E, Hoogland C, Gattiker A, Se D, Wilkins MR, Appel RD, Bairoch A (2005) Protein identification and analysis tools on the ExPASy server. In: Walker JM (ed) *The proteomics protocols handbook*. Humana Press, Totowa, NJ, pp 571–607. doi:[10.1385/1-59259-890-0:571](https://doi.org/10.1385/1-59259-890-0:571)
 55. Krogh A, Larsson B, von Heijne G, Sonnhammer EL (2001) Predicting transmembrane protein topology with a hidden Markov model: application to complete genomes. *J Mol Biol* 305(3):567–580. doi:[10.1006/jmbi.2000.4315](https://doi.org/10.1006/jmbi.2000.4315)
 56. Tusnady GE, Simon I (2001) The HMMTOP transmembrane topology prediction server. *Bioinformatics* (Oxford, England) 17(9):849–850
 57. Dobson L, Remenyi I, Tusnady GE (2015) CCTOP: a consensus constrained TOPology prediction web server. *Nucleic Acids Res* 43(W1):W408–W412. doi:[10.1093/nar/gkv451](https://doi.org/10.1093/nar/gkv451)
 58. Kanz C, Aldebert P, Althorpe N, Baker W, Baldwin A, Bates K, Browne P, van den Broek A, Castro M, Cochrane G, Duggan K, Eberhardt R, Faruque N, Gamble J, Diez FG, Harte N, Kulikova T, Lin Q, Lombard V, Lopez R, Mancuso R, McHale M, Nardone F, Silventoinen V, Sobhany S, Stoehr P, Tuli MA, Tzouvara K, Vaughan R, Wu D, Zhu W, Apweiler R (2005) The EMBL nucleotide sequence database. *Nucleic Acids Res* 33(Database issue):D29–D33. doi:[10.1093/nar/gki098](https://doi.org/10.1093/nar/gki098)
 59. Thompson JD, Higgins DG, Gibson TJ (1994) CLUSTAL W: improving the sensitivity of progressive multiple sequence alignment through sequence weighting, position-specific gap penalties and weight matrix choice. *Nucleic Acids Res* 22(22):4673–4680

60. Kemena C, Notredame C (2009) Upcoming challenges for multiple sequence alignment methods in the high-throughput era. *Bioinformatics* (Oxford, England) 25(19):2455–2465. doi:[10.1093/bioinformatics/btp452](https://doi.org/10.1093/bioinformatics/btp452)
61. Thompson JD, Plewniak F, Ripp R, Thierry JC, Poch O (2001) Towards a reliable objective function for multiple sequence alignments. *J Mol Biol* 314(4):937–951. doi:[10.1006/jmbi.2001.5187](https://doi.org/10.1006/jmbi.2001.5187)
62. Anisimova M, Gascuel O (2006) Approximate likelihood-ratio test for branches: a fast, accurate, and powerful alternative. *Syst Biol* 55(4):539–552. doi:[10.1080/10635150600755453](https://doi.org/10.1080/10635150600755453)
63. Nylander JA, Wilgenbusch JC, Warren DL, Swofford DL (2008) AWTY (are we there yet?): a system for graphical exploration of MCMC convergence in Bayesian phylogenetics. *Bioinformatics* (Oxford, England) 24(4):581–583. doi:[10.1093/bioinformatics/btm388](https://doi.org/10.1093/bioinformatics/btm388)
64. Small I, Peeters N, Legeai F, Lurin C (2004) Predotar: a tool for rapidly screening proteomes for N-terminal targeting sequences. *Proteomics* 4(6):1581–1590. doi:[10.1002/pmic.200300776](https://doi.org/10.1002/pmic.200300776)
65. Jiroutova K, Horak A, Bowler C, Obornik M (2007) Tryptophan biosynthesis in stramenopiles: eukaryotic winners in the diatom complex chloroplast. *J Mol Evol* 65(5):496–511. doi:[10.1007/s00239-007-9022-z](https://doi.org/10.1007/s00239-007-9022-z)
66. Argos P, Rao JK, Hargrave PA (1982) Structural prediction of membrane-bound proteins. *Eur J Biochem* 128(2–3):565–575
67. Eisenberg D, Schwarz E, Komaromy M, Wall R (1984) Analysis of membrane and surface protein sequences with the hydrophobic moment plot. *J Mol Biol* 179(1):125–142
68. Kyte J, Doolittle RF (1982) A simple method for displaying the hydropathic character of a protein. *J Mol Biol* 157(1):105–132
69. Moller S, Croning MD, Apweiler R (2001) Evaluation of methods for the prediction of membrane spanning regions. *Bioinformatics* (Oxford, England) 17(7):646–653
70. Lewin TM, Wang P, Coleman RA (1999) Analysis of amino acid motifs diagnostic for the sn-glycerol-3-phosphate acyltransferase reaction. *Biochemistry* 38(18):5764–5771. doi:[10.1021/bi982805d](https://doi.org/10.1021/bi982805d)
71. Wendel AA LT, Coleman RA (2010) NIH public access 1791: pp 380–386
72. Zharkikh A, Li WH (1992) Statistical properties of bootstrap estimation of phylogenetic variability from nucleotide sequences: II. Four taxa without a molecular clock. *J Mol Evol* 35(4):356–366
73. Kall L, Krogh A, Sonnhammer EL (2004) A combined transmembrane topology and signal peptide prediction method. *J Mol Biol* 338(5):1027–1036. doi:[10.1016/j.jmb.2004.03.016](https://doi.org/10.1016/j.jmb.2004.03.016)

Isoprenylation of Monomeric GTPases in Human Trabecular Meshwork Cells

Evan B. Stubbs Jr.

Abstract

Small monomeric GTPases, including those belonging to the Rho family, regulate a diverse array of intracellular signaling pathways which affect vesicle transport/trafficking, endocytosis, cell cycle progression, cell contractility, and formation of stress fibers or focal adhesions. Functional activation of newly synthesized small monomeric GTPases is facilitated by a multistep post-translational process involving transferase-catalyzed addition of farnesyl or geranylgeranyl isoprenoids to conserved cysteine residues within a unique carboxy terminal CaaX motif. Here, using well-established and widely available contemporary methodologies, detailed protocols by which to semi-quantitatively evaluate the functional consequence of post-translational isoprenylation in human trabecular meshwork cells are described. We introduce the concept that isoprenylation alone is itself a key regulator of mammalian Rho GTPase expression and turnover.

Key words Farnesyl, Geranylgeranyl, Human, Trabecular meshwork, Monomeric GTPase

1 Introduction

Isoprenoids and their derivatives are a family of naturally occurring terpenoids. Synthesized as key constituents of membranes, isoprenoids also serve as metabolic building blocks of vitamins, pheromones, and reproductive hormones. Involved in oxidative phosphorylation and photosynthesis, and as integral components of signal transduction pathways, isoprenoids are found in a myriad of organisms as diverse as bacteria, fungi, insects, plants, and mammals [1]. In mammalian cells, sesquiterpene (farnesyl) and diterpene (geranylgeranyl) isoprenoids are synthesized as metabolic intermediates of the cholesterol biosynthetic pathway. Farnesyl and geranylgeranyl isoprenoids function as post-translational modifiers of a variety of intracellular proteins including nuclear lamins A and B, rhodopsin kinase, γ subunits of heterotrimeric GTP-binding proteins, as well as small monomeric Ras and Ras-related GTPases [2].

While the biochemical consequences of post-translational isoprenylation remains to be fully elucidated, one key biophysical

attribute is to enhance protein hydrophobicity thereby facilitating intracellular membrane localization and subsequent activation [3, 4]. An alternative role for isoprenoids within mammalian cells may involve regulation of gene expression or protein stability [5–7]. By limiting endogenous isoprenylation, monomeric GTPases were found to accumulate in the cytosol, in part, by enhancing expression of Rho GTPase isoforms [8]. These and other studies have generated considerable interest in evaluating the role of isoprenylation as a potential therapeutic target for the management of seemingly unrelated disorders involving dysregulation of monomeric GTPase signaling. Here, laboratory protocols using well-established and widely available contemporary methodologies to semi-quantitatively evaluate the functional consequences of post-translational isoprenylation in human trabecular meshwork cells are detailed.

2 Materials

Aqueous solutions should be prepared with ultrapure water exhibiting a resistivity of 18.2 M Ω .cm at 25 °C. Here, water is ultra-purified in a stepwise manner using a Milli-Q Advantage A10 system by first passing feed water through a carbon filter and subsequently subjecting the filtered water to reverse osmosis. Water is then passed through an Elix Advantage Progard T2 cartridge to a resistivity of 15 M Ω .cm and stored in a 100 L reservoir unit at 23 °C until needed. Ultra-purification is achieved on-demand by passing purified water through a Q-Gard T1 purification cartridge, a Quantum TIX polishing cartridge, and finally a BioPak polishing cartridge. Unless indicated otherwise, reagents used should be of electrophoresis grade purity. Materials used for cell culture should be either purchased sterile or filtered, as indicated, through a single-use Corning polystyrene filter unit with a 0.22 μ m cellulose acetate low-protein binding membrane. Cells should be cultured on RNase, DNase, and pyrogen-free noncytotoxic cell culture treated 100 \times 20 mm sterile polystyrene dishes and maintained at 37 °C under a humidified atmosphere of 5% CO₂ and 95% air.

2.1 Primary Human TM Cell Culture

1. Fresh cadaver corneoscleral rim.
2. One 100 \times 20 mm sterile polystyrene tissue culture dish and one 35 \times 10 mm sterile surface modified polystyrene *Primaria* tissue culture dish.
3. Complete MEM: Low glucose (1.0 g/L) Minimal Essential Medium (MEM) with 2 mM GlutaMaxTM-I plus Earle's salts and supplemented with 5% adult bovine serum, 10% fetal bovine serum, 1 \times concentration of nonessential and essential amino acids, 0.1% gentamycin, and 1% amphotericin B.

2.2 Transformed Human TM Cell Culture

1. Transformed human trabecular meshwork cell line (GTM3).
2. Pyrogen-free noncytotoxic cell culture treated 100 × 20 mm sterile polystyrene dishes.
3. Complete DMEM: High glucose (4.5 g/L) Dulbecco's Modified Eagle's Medium (DMEM) containing 4 mM GlutaMAX-I and supplemented with 10% fetal bovine serum, 100 U/mL penicillin, and 100 µg/mL streptomycin.
4. Trypsin-EDTA (0.05%) with phenol red.

2.3 Test Reagents

All test reagents used here are commercially available.

1. Lovastatin: This inactive lactone prodrug that must first be converted by alkaline hydrolysis to the active dihydroxy acid prior to use in cell culture. To prepare a 1000× (10 mM) concentrate, dissolve 4 mg of lovastatin in 0.1 mL absolute ethanol, add 0.15 mL of 0.1 N NaOH, and incubate for 2 h at 50 °C. Neutralize the resultant dihydroxy acid with 0.1 N HCl and bring to a final volume of 1 mL with sterile ultrapure water, aliquot, and store at -20 °C until use.
2. All other reagents (absolute ethanol, dimethyl sulfoxide, DL-mevalonolactone, farnesyl pyrophosphate (FPP), geranylgeranyl pyrophosphate (GGPP), farnesyl transferase inhibitor-277 (FTI-277), geranylgeranyl transferase inhibitor-298 (GGTI-298), actinomycin D, cycloheximide, epoxomicin, mouse anti-panRho (A, B, C) primary monoclonal antibody, mouse anti-RhoA primary monoclonal antibody, rabbit anti-RhoB primary polyclonal antibody, rabbit anti-GAPDH primary polyclonal antibody, horseradish peroxidase-conjugated goat anti-mouse secondary antibody, horseradish peroxidase-conjugated goat anti-rabbit secondary antibody) were prepared as specified in Subheading 3.

2.4 Electrophoresis and Electrotransfer

1. Precast Mini-PROTEAN Tris-glycine 4–20% polyacrylamide gels (10 or 15 well, 8.6 × 6.8 cm).
2. Gel running buffer (pH 8.3): 10× concentrate containing 1.92 M L-glycine, 1% sodium dodecyl sulfate (SDS), and 0.25 M Tris-base.
3. Laemmli sample buffer (2× concentrate) is commercially available.
4. 10× Cleland's Reagent (dithiothreitol, 0.5 M).
5. Prestained protein molecular weight standards (3.5–260 kDa range).
6. Electrotransfer buffer (pH 8.3): This 1× buffer contains 0.2 M L-glycine, 0.1% sodium dodecyl sulfate (SDS), 20% methanol, and 0.025 M Tris-base.

7. Nitrocellulose membranes (0.2 μm).
8. Mini trans-blot filter paper.
9. Ponceau S: 10 \times concentrate containing 2% Ponceau S, 1.2 M 5-sulfosalicylic acid dehydrate, and 1.8 M trichloroacetic acid.

2.5 Immunoblotting

1. Blocking buffer: 5% *Carnation* instant nonfat powdered milk suspended in 50 mM Tris-buffered isotonic saline (pH 7.4) supplemented with 0.05% Tween-20 (*see Note 1*).
2. Washing buffer: 50 mM Tris-buffered isotonic saline (pH 7.4) supplemented with 0.05% Tween-20.
3. Mouse anti-RhoA monoclonal (clone 26C4) & rabbit anti-RhoB polyclonal (Santa Cruz Biotechnology) and rabbit anti-GAPDH polyclonal (Trevigen) antibodies.
4. Goat anti-mouse IgG and goat anti-rabbit IgG horseradish peroxidase-conjugated secondary antibody (Jackson ImmunoResearch Laboratories).
5. SuperSignal West Pico Chemiluminescent Substrate.
6. High performance chemiluminescence film (Amersham HyperfilmTM ECL).

3 Methods

3.1 Preparation and Culture of Human Primary TM Cells

Human primary TM cells are prepared using a collagenase-free procedure as previously described [9]. Obtain approval for the use of human cadaver material from your local *Institutional Review Board* prior to tissue procurement. Advanced approval from your local *Institutional Biosafety Committee* as well as other required administrative committees is similarly recommended. The following tissue culture procedures should be conducted within a laminar flow hood using aseptic techniques.

1. In association with your Institutional Ophthalmology Department, establish a mechanism whereby whole or partial cadaver corneoscleral rims can be recovered as *discarded* material at time of corneal transplant. Once the corneal transplant button is excised, instruct the surgical team to return the unused *discarded* rim to the original corneal storage medium.
2. Prewarm complete MEM to 37 °C and transfer 10 mL to a 100 \times 20 mm sterile polystyrene tissue culture dish.
3. Gently transfer the corneoscleral rim to the culture dish and place cornea side down so as to expose the brown-colored remnant ciliary body and beige-colored TM (Fig. 1).
4. Under a well-illuminated dissecting microscope, identify the boundary between the clear/opaque cornea and the off-white

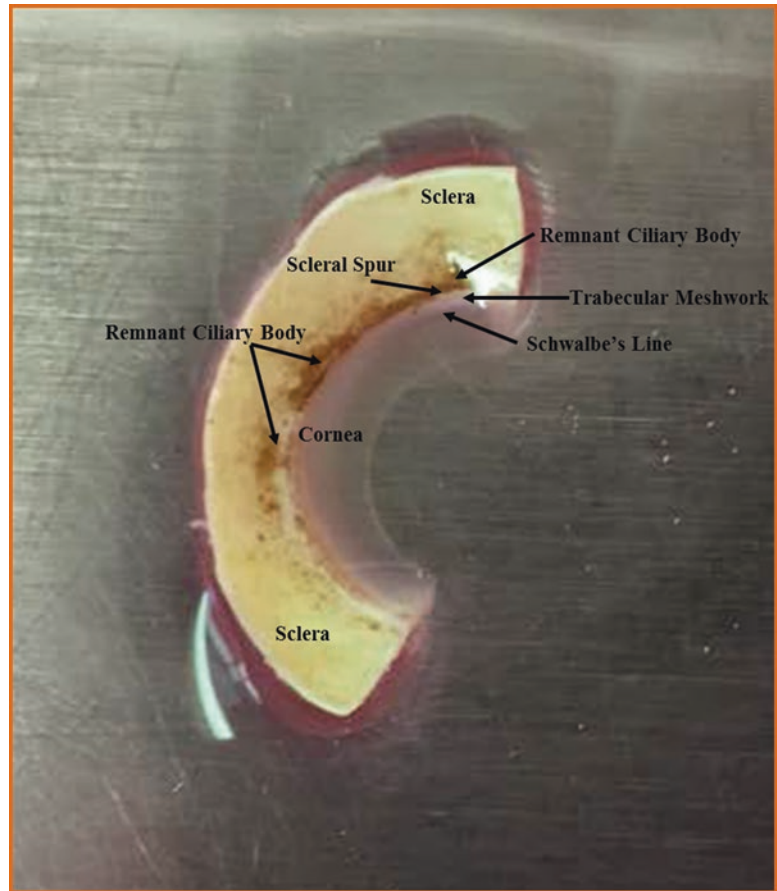


Fig. 1 One half of a discarded human corneoscleral rim immersed in prewarmed culture medium following removal of transplanted corneal button

sclera. The trabecular meshwork (TM) strip is nestled in a trough/valley adjacent to the cornea bordered by Schwalbe's line and the scleral spur.

5. Adjacent to the scleral spur, locate the remnants of the pigmented ciliary body band.
6. Use a pair of fine forceps to remove the remaining pigmented ciliary body band.
7. Once the remnant ciliary body band has been cleared, the beige-toned TM can be isolated by gently teasing one end out of the trough and lifting it away from the rim. With practice, one can remove the TM strip *en block* with one steady motion (*see Note 2*).
8. Transfer the isolated TM strip (explant) to a 35 × 10 mm sterile surface modified polystyrene *Primaria* tissue culture dish containing a button (200 μ L) of complete MEM media.

9. Using a sterile pipet, remove the media until the strip makes good contact with the surface of the *Primaria* tissue culture dish. Place the covered dish in the humidified 37 °C tissue culture incubator × 30 min.
10. Gently tilt the dish to confirm strip adherence and add 1 mL of complete MEM media without dislodging the explant (*see Note 3*).
11. Culture the TM explant *undisturbed* at 37 °C under a humidified atmosphere of 5% CO₂ and 95% air for 2 weeks (*see Note 4*).
12. After 3–4 weeks, cells from the explant will cover the bottom of the dish. At this time, primary TM cells can be passaged as needed using 0.05% Trypsin–EDTA. Cells can be passaged up to four times with good results (*see Note 5*).

3.2 Culture of Human Transformed TM Cells

Simian virus 40 (SV40)-transformed human TM cells used here are from a male glaucomatous patient (GTM3) and were a generous gift from A. F. Clark [10]. The following tissue culture procedures should be conducted within a laminar flow hood using aseptic techniques.

1. Prewarm complete DMEM to 37 °C and transfer 9.5 mL to each of several 100 × 20 mm sterile polystyrene tissue culture dishes (*see Note 6*).
2. Aspirate and discard the culture medium from a confluent flask of GTM3 cells.
3. Wash adherent cells with 10 mL of Hanks Balanced Salt solution to remove residual serum-containing media. Aspirate and discard the wash medium.
4. Add 1 mL of sterile 0.05% trypsin–EDTA to the washed cells. Gently rotate the flask to allow adherent cells to be coated with the trypsin–EDTA solution. Incubate × 3 min at 37 °C.
5. Confirm that the cells are beginning to dislodge from the flask bottom and add 9 mL of complete DMEM. Gently agitate the flask and transfer cell suspension to a sterile conical centrifuge tube.
6. Centrifuge suspended cells at 750 × *g* for 2 min. Resuspend by triturating the packed cell pellet in 5 mL of complete DMEM to a density of approximately 1 × 10⁶ cells per mL.
7. To make a 1:10 passage, transfer 0.5 mL (~500,000 cells) to one of the tissue culture dishes prepared in **step 1**. Swirl the dish to evenly distribute the cells.
8. Incubate the passaged cells at 37 °C under a humidified atmosphere of 5% CO₂ and 95% air.

3.3 Isoprenylation Alters GTPase Protein Expression

The effect of post-translational isoprenylation on GTPase protein expression in human TM cells is semi-quantitatively determined using cell-permeable inhibitors that either disrupt endogenous availability of isoprenoids or prevent the transfer of isoprenoids onto native GTPases.

1. To inhibit isoprenylation by limiting endogenous isoprenoid availability (Fig. 2), add to replicate flasks of semi-confluent (~70%) primary or transformed human TM cells 10 mL of fresh culture medium supplemented without or with DL-mevalonolactone (Mev, 5 mM) and treat with either 10 μ L of a 10% solution of absolute ethanol (Veh, 0.01% final concentration) or 10 μ L of a 10 mM working concentrate of activated lovastatin (Lov, 10 μ M final concentration) (*see Note 7*).
2. To identify which isoprenoid (15-carbon farnesyl or 20-carbon geranylgeranyl) may be selectively isoprenylating your protein of interest (Fig. 3), in a separate experiment add to replicate flasks of semi-confluent primary or transformed human TM cells 10 mL of fresh culture medium and treat with 10 μ L of a 10% solution of absolute ethanol (Veh, 0.01% final concentration), 10 μ L of a 10 mM working concentrate of activated lov-

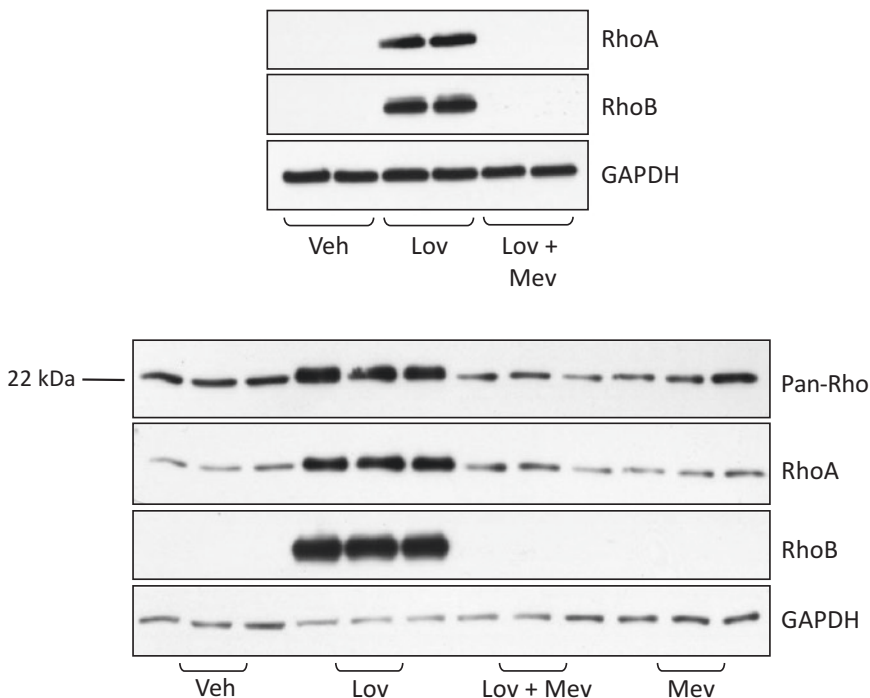


Fig. 2 Representative immunoblots of RhoA and RhoB GTPases present in lysates from primary (*top blot*) or transformed (*bottom blot*) human TM cells treated in the absence (vehicle, 0.01% ethanol) or presence of 10 μ M activated lovastatin (LOV), 5 mM mevalonolactone (Mev), or a combination of both (Lov + Mev), as indicated. Reproduced from [8] with permission from Springer

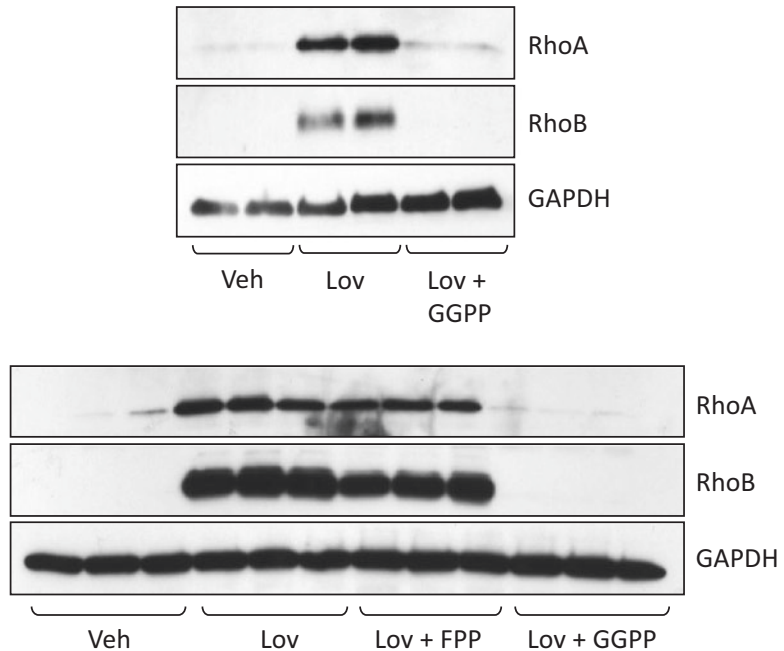


Fig. 3 Representative immunoblots of RhoA and RhoB GTPases present in lysates from primary (*top blot*) or transformed (*bottom blot*) human TM cells treated in the absence (vehicle, 0.01% ethanol) or presence of 10 μM activated lovastatin (LOV) without or with 10 μM farnesyl pyrophosphate (Lov + FPP) or 10 μM geranylgeranyl pyrophosphate (Lov + GGPP), as indicated. Reproduced from [8] with permission from Springer

astatin (Lov, 10 μM final concentration) in the absence or presence of 10 μM farnesyl pyrophosphate (FPP) or 10 μM geranylgeranyl pyrophosphate (GGPP) (*see Note 8*).

3. To confirm which isoprenoid (15-carbon farnesyl or 20-carbon geranylgeranyl) may be selectively isoprenylating your protein of interest (Fig. 4), in a separate experiment add to replicate flasks of semi-confluent primary or transformed human TM cells 10 mL of fresh culture medium and treat with 10 μL of DMSO (0.1%, final concentration), 10 μL of a 10 mM working concentrate of GGTI-298 in DMSO (10 μM final concentration), or 10 μL of a 10 mM working concentrate of FTI-277 in DMSO (10 μM final concentration) (*see Note 9*).
4. Additional experiments are recommended to determine whether observed changes in protein expression are transcriptional (actinomycin D, 1.0 $\mu\text{g}/\text{mL}$), translational (cycloheximide, 5 μM), or degradation by proteasome (epoxomicin, 10 μM) [8].
5. In each case, incubate primary human TM cells for 48 h or transformed human TM cells for 24 h at 37 $^{\circ}\text{C}$ under a humidified atmosphere of 5% CO_2 and 95% air.

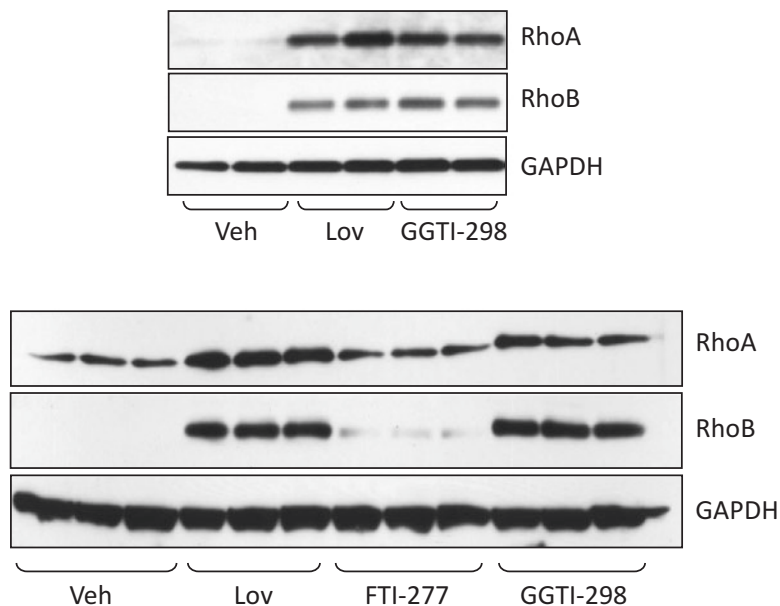


Fig. 4 Representative immunoblots of RhoA and RhoB GTPases present in lysates from primary (*top blot*) or transformed (*bottom blot*) human TM cells treated in the absence (vehicle, 0.1% DMSO or 0.01% ethanol) or presence of 10 μ M activated lovastatin (LOV), 10 μ M farnesyltransferase inhibitor (FTI-277), or 10 μ M geranylgeranyl transferase inhibitor-I (GGTI-298), as indicated. Reproduced from [8] with permission from Springer

6. Harvest treated cells with 0.05% trypsin–EDTA (*see* Subheading 3.2 above), wash the cell pellet once with fresh complete media. To determine the effect of added test agents on cell viability, treat an aliquot of harvested cells with 0.04% trypan blue dye for live-cell exclusion.
7. Prepare whole cell lysates by resuspending the washed cell pellet in 0.5 mL ultrapure water supplemented with a commercial cocktail of protease inhibitors. Store at -20°C until use.

3.4 SDS-PAGE and Electrotransfer

Prior to electrophoresis, protein concentrations in cell lysates are determined using a commercially available protein assay kit (bicinchoninic acid, BCA). Here, proteins in cell lysates were resolved on pre-cast 4–20% denaturing gels using a mini-PROTEAN apparatus.

1. Cell lysates are thawed, probe sonicated to homogeneity, and aliquots mixed with 20 μ L 2 \times Laemmli sample buffer, 4 μ L dithiothreitol, and balanced with ultrapure water in a total volume of 40 μ L. Samples are denatured by immersion in boiling water \times 3 min.
2. Remove the comb from the pre-cast gel, rinse wells thoroughly with ultrapure water, score and remove the strip at the bottom, and chamber the gel in the mini-PROTEAN apparatus. Fill the inner and outer chamber wells with running buffer (*see* Note 10).

3. Denatured cell lysates are carefully loaded (12 μL per well, 20 μg protein per lane) into the stacking gel wells using gel loading pipet tips. Proteins resolved at room temperature across a constant voltage (100 V) alongside prestained protein molecular weight standards.
4. When the dye front reaches the exposed strip at the bottom of the gel, the run is stopped and the plastic gel plates are carefully removed and the gel is rinsed with copious amounts of ultrapure water.
5. Slide the washed gel onto a glass support plate, cut away the stacking gel, and trim away unused side lanes and excess gel.
6. The trimmed gel is inverted (front side down) and placed on a filter pad premeasured (gel size) and presoaked in electrotransfer buffer.
7. A premeasured (gel size) and presoaked piece of nitrocellulose membrane is positioned onto the gel surface (*see Note 11*).
8. Place another premeasured (gel size) and presoaked filter pad onto the membrane. Remove any trapped air bubbles by rolling a clean test tube over the completed sandwich. Place the filter pad-gel-membrane-filter pad sandwich in an electrotransfer cassette and submerge in electrotransfer buffer (*see Note 12*).
9. Electrotransfer the resolved proteins overnight at room temperature using a low constant current of 30 mA (*see Note 13*).
10. Disassemble the electrotransfer apparatus and using fine forceps gently peel the membrane off the gel. Immerse the membrane, protein side up, in ultrapure water (*see Note 14*).
11. Validate the quality and the efficacy of the electrotransfer by immersing the washed membrane in a solution of 0.2% Ponceau S. Stain the membrane for no longer than 2 min.
12. Reduce background staining by dipping twice in ultrapure water and mark the lanes with a pencil.

3.5 Immunoblotting

1. Incubate the Ponceau S stained membrane protein side up in blocking buffer \times 1 h at 37 $^{\circ}\text{C}$ with gentle rocking (*see Note 15*).
2. Rinse the blocked membrane with washing buffer and immerse protein side up in 10 mL of fresh blocking buffer supplemented with primary antibody (1:1000 dilution of mouse anti-panRho (A, B, C) monoclonal (clone 55), or 1:200 dilution of mouse anti-RhoA monoclonal (clone 26C4), or 1:200 dilution of rabbit anti-RhoB polyclonal (119) all from Santa Cruz Biotechnology).
3. Incubate overnight at 4 $^{\circ}\text{C}$ with gentle rocking.
4. Rinse the immunostained membrane three times with 30 mL washing buffer for 5 min each and immerse membrane protein side up in 10 mL of fresh blocking buffer supplemented with

appropriate horseradish peroxidase-conjugated secondary antibody (1:2500 dilution of goat anti-mouse IgG or 1:10,000 dilution of goat anti-rabbit IgG, Jackson ImmunoResearch Labs) (*see Note 16*).

5. Incubate for 1 h at room temperature with gentle rocking.
6. Rinse the immunostained membrane three times with 30 mL washing buffer for 5 min each.
7. Remove the washed membrane and place protein side up on a Kim wipe tissue. Place the semi-dry membrane on a precut piece of Saran Wrap and coat with an appropriate amount of freshly premixed ECL reagent. Cover the membrane, place in an X-ray cassette.
8. In a dark room, place a piece of high performance chemiluminescence film over the Saran Wrap encased membrane, close the cassette to ensure good contact between film and membrane, and expose \times 2–5 min depending on desired results.
9. Develop film using an auto-processor and semi-quantify relative changes in GTPase band densities. Normalize to GAPDH band densities present in the same sample on the same blot [8].
10. To confirm equal protein loading on the same membrane, immerse the developed immunoblot in 10 mL of Restore Western Blot stripping buffer for 10 min at room temperature, rinse three times with 30 mL washing buffer for 5 min each, and repeat **steps 1–9** using a 1:10,000 dilution of rabbit anti-GAPDH as a primary antibody (Trevigen).

4 Notes

1. Increasing the percentage of Tween-20 (up to 0.2%) will reduce nonspecific background immunostaining, but at the costly expense of signal reduction as well.
2. Due to beige tone of the TM, it is very difficult to distinguish it from surrounding structures. Small stretches of the TM strip may break free and recoil around the tip of your forceps during the procedure. This is expected and is generally considered a good indicator that you are working with TM.
3. Adherence of the explant to the dish floor is critical for appropriate TM cell outgrowth spreading. If the strip dislodges, repeat Subheading 3.1, **step 9** until adherence is achieved.
4. Disrupting the flask at any time during the two week culture period risks dislodging the TM explant and will impede primary TM cell spreading. Do not change the media.
5. Explants can be relocated to a separate Primaria dish and the procedure repeated, if desired. Depending on the clinical history of the donor, not all explants produce viable TM cells.

6. If desired, sterile nonpyrogenic polystyrene T75 cell culture flasks with a 0.2 μm vented cap can be used in place of dishes.
7. To prepare DL-mevalonolactone, dissolve the appropriate amount to yield 5 mM final concentration in media containing antibiotics, sterile filter, and add FBS. Add 10 mL of this mevalonolactone supplemented media to cultured cells.
8. In our hands, farnesyl or geranylgeranyl pyrophosphates were readily taken up by cultured TM cells by a mechanism that remains unclear.
9. GGTI-298 and FTI-277 are cell permeant inhibitors of geranylgeranyl transferase-I and farnesyl transferase, respectively.
10. The gel should be immersed in running buffer up to, but not in communication with, the stacking gel.
11. Minimize moving the membrane once it is on the gel.
12. Care must be taken to be certain the membrane side of the sandwich is adjacent to the positive (red) pole and the gel side is adjacent to the negative (black) pole.
13. Proteins can be *hot*-transferred using a high current of 200 mA for 1 h if desired.
14. The orientation of the transfer should now be identical to the orientation used while loading the gel.
15. This will destain the membrane while blocking nonspecific binding sites.
16. Primary antibody solutions can be reused several times if desired. Add to the 10 mL of recovered solution 100 μL of a 2% sodium azide stock. Store the used solutions at 4 $^{\circ}\text{C}$.

Acknowledgements

The author thanks Mr. Jonathan Lautz for helpful comments and discussion. This work was supported, in part, by grants from the Department of Veterans Affairs, National Institutes of Health, the Midwest Eye-Banks (Eversight), the Illinois Society for the Prevention of Blindness, and the Richard A. Peritt Charitable Foundation.

References

1. Holstein SA, Hohl RJ (2004) Isoprenoids: remarkable diversity of form and function. *Lipids* 39(4):293–309
2. Zhang FL, Casey PJ (1996) Protein prenylation: molecular mechanisms and functional consequences. *Annu Rev Biochem* 65: 241–269
3. Gao J, Liao J, Yang GY (2009) CAAX-box protein, prenylation process and carcinogenesis. *Am J Transl Res* 1(3):312–325
4. Wright LP, Philips MR (2006) Thematic review series: lipid posttranslational modifications. CAAX modification and membrane targeting of Ras. *J Lipid Res* 47(5):883–891

5. Sever N, Song BL, Yabe D, Goldstein JL, Brown MS, DeBose-Boyd RA (2003) Insig-dependent ubiquitination and degradation of mammalian 3-hydroxy-3-methylglutaryl-CoA reductase stimulated by sterols and geranylgeraniol. *J Biol Chem* 278(52):52479–52490
6. Holstein SA, Wohlford-Lenane CL, Hohl RJ (2002) Isoprenoids influence expression of Ras and Ras-related proteins. *Biochemistry* 41(46):13698–13704
7. Holstein SA, Wohlford-Lenane CL, Hohl RJ (2002) Consequences of mevalonate depletion. Differential transcriptional, translational, and post-translational up-regulation of Ras, Rap1a, RhoA, and RhoB. *J Biol Chem* 277(12):10678–10682. doi:[10.1074/jbc.M111369200](https://doi.org/10.1074/jbc.M111369200)
8. Stubbs EB Jr, Von Zee CL (2012) Prenylation of Rho G-proteins: a novel mechanism regulating gene expression and protein stability in human trabecular meshwork cells. *Mol Neurobiol* 46(1):28–40. doi:[10.1007/s12035-012-8249-x](https://doi.org/10.1007/s12035-012-8249-x)
9. Yue BY, Higginbotham EJ, Chang IL (1990) Ascorbic acid modulates the production of fibronectin and laminin by cells from an eye tissue-trabecular meshwork. *Exp Cell Res* 187(1):65–68
10. Pang IH, Shade DL, Clark AF, Steely HT, DeSantis L (1994) Preliminary characterization of a transformed cell strain derived from human trabecular meshwork. *Curr Eye Res* 13(1):51–63

Chapter 19

Purification and Validation of Lipid Transfer Proteins

Matti A. Kjellberg, Anders P.E. Backman, Anna Möuts, and Peter Mattjus

Abstract

Understanding the holistic picture of lipid homeostasis not only involves the analysis of synthesis and breakdown of lipids but also requires a thorough understanding of their transport. The transport of lipid monomers in an aqueous environment is facilitated by different lipid transfer proteins. Their universal feature is the shielding or encapsulation of the hydrophobic part of the lipid, consequently overcoming the poor solubility of lipids in water. Here we describe a method to purify lipid transfer proteins using bacterial expression. We also present three methods to validate their transfer activity.

Key words Bacterial expression, Ni-sepharose, SDS-PAGE, Fluorescence, Lipid, Vesicle, Transfer protein, Surface plasmon resonance, Sensor chip

1 Introduction

Lipid transfer proteins play a key role in directing the right substrate to its right destination for further synthesis [1]. Lipid transfer and binding proteins also present specific lipids for the degradation machinery [2]. We will here describe methods for in vitro analysis of the lipid transfer protein activity, in particular a protein that works on glycosphingolipids, the glycolipid transfer protein, GLTP. It is clearly evident from work with GLTP that depending on the levels of the expression of GLTP the overall lipid profiles are affected, not only glycosphingolipids but also membrane phospholipids [3]. Changes in lipid levels also affect how the expression of GLTP is regulated [4], probably through regulation via mechanistic participation of Sp1/Sp3 transcription factors [5]. We present here a protocol for producing recombinant GLTP using bacterial expression. This protocol can be adapted for the production of other LTPs. We also introduce three different methods to measure the transfer activity of LTPs. Two are based on the use of fluorescently labeled lipids and one using a surface plasmon resonance approach.

2 Materials

2.1 Reagents for Bacterial Culture

Prepare all solutions using ultrapure water (18 M Ω -cm at 25 °C) and analytical grade reagents. Bacterial growth medium (LB medium) with ampicillin and kanamycin: 10 g/L tryptone, 5 g/L yeast extract, 10 g/L NaCl. All bacterial growth medium should be sterilized prior to use, e.g., by autoclaving at 121 °C for 20 min. 50 μ g/mL ampicillin and 25 μ g/mL kanamycin is added prior to inoculation with bacteria.

2.2 Buffers and Reagents for Protein Purification

The lysis, wash and elution buffers used in this protocol are imidazole containing phosphate buffered saline (PBS):

PBS: 140 mM NaCl, 2.7 mM KCl, 10 mM Na₂HPO₄, 1.8 mM KH₂PO₄, pH 7.40.

Lysis buffer: PBS with 10 mM imidazole, pH 7.4.

Wash buffer: PBS with 20 mM imidazole, pH 7.4.

Elution buffer: PBS with 250 mM imidazole, pH 7.4.

3 Methods

3.1 Expression and Purification of GLTP

In the protocol described below, polyhistidine tagged bovine GLTP is expressed in BL-21 *E. coli* and subsequently purified using affinity chromatography on a Ni-sepharose resin column. This particular protocol is the outcome of substantial method optimization, and consequently yields high amounts (>30 mg protein/L of bacterial culture) of highly purified, functional GLTP. The protocol can be adapted for the production of other LTPs; however alteration and additional optimization of the protocol may be required for similarly high-yield production, especially if other expression vectors are used. This protocol does not describe the cloning and verification processes used to produce the bacterial expression vector.

The gene for the bovine GLTP was cloned into the bacterial expression vector pQE-9 and transformed into the *E. coli* strain BL-21(M15). Bacterial cultures were prepared from successfully transformed colonies and frozen and stored in 20% glycerol as several aliquots in -80 °C.

Day 1—Pre culture

All bacterial solutions should be handled under sterile conditions until *Day 3*.

1. Inoculate 10–50 mL of LB medium, supplemented with ampicillin (50 μ g/mL) and kanamycin (25 μ g/mL), with the pQE-9-bGLTP BL-21(M15) bacterial glycerol stock solution (*see above*) and grow overnight (<18 h) in a bacterial incubator shaker (37 °C, 180 RPM), *see Note 1*.

Day 2—Culture and induction of protein expression

1. Transfer the overnight grown culture to a 2 L culture flask containing 1 L of LB medium, supplemented with 50 µg/mL ampicillin and 25 µg/mL kanamycin. This volume is generally enough to produce >30 mg of GLTP; however, the protocol can be scaled up if needed.
2. Culture under agitation at 37 °C (180 RPM) until OD₆₀₀ reaches >0.8. Add isopropyl-β-D-thiogalactoside (IPTG) to a final concentration of 0.5 mM. Culture overnight (<18 h) at 15 °C under agitation at 180 RPM, *see Note 2*.

Day 3—Lysis and purification

From here on, solutions should be kept cold or on ice and all work should preferably be performed in a cold room, if possible.

1. Dispense the culture in suitable centrifuge bottles (500 mL) and centrifuge at 3500 × *g* at 4 °C for 10 min. Discard the supernatant and place the centrifuge bottles with the bacterial pellet(s) on ice.
2. Resuspend the pellet(s) in lysis buffer (20 mL/L of bacterial culture); transfer to smaller centrifuge tubes (50 mL) and add lysosome to a final concentration of 1 mg/mL. Shake the cells (on ice) for 30 min and sonicate for six short 10 s intervals for a total of 60 s with probe sonifier. Keep the tubes on ice to ensure that the suspension does not warm up.
3. Transfer the bacterial lysate to centrifuge tubes and centrifuge at 12,000 × *g* in 4 °C for 30 min to pellet the bacterial debris.
4. Transfer the clear supernatant to a clean tube and mix with Ni-sepharose beads. (1 mL of a 50% bead slurry in lysis buffer/1 L of bacterial culture). Rotate the tube end-over-end for 15 min and pour the supernatant/bead slurry in a plastic chromatography column, pipetting by hand or by using a peristaltic pump. Do not allow the beads to dry.
5. Once all the supernatant has run through the column, wash the Ni-sepharose beads with the bound protein with wash buffer (by hand or by using a peristaltic pump), until the OD₂₈₀ value of the flow-through is 0.02 or lower.
6. Elute the bound protein by adding elution buffer (250 mM imidazole) in 10–15, 0.5 mL fractions. Each eluted fraction should immediately be placed on ice.

Analysis and storage

1. The protein concentration in each tube should be determined with standard methods. Each fraction should be analyzed for purity on SDS-PAGE, using Coomassie staining. The most pure and concentrated samples can be pooled and the protein concentration re-determined.

2. For storage, adding glycerol up to 20% prior to freezing the aliquots is recommended. Addition of dithiothreitol (DTT) to a concentration of 1 mM can be useful for inhibiting protein aggregation due to disulfide bond formation. For GLTP, a 20% glycerol buffer with 1 mM DTT is essential for long-term stable storage, and these aliquots can be kept at $-20\text{ }^{\circ}\text{C}$ for up to a year. If necessary, the buffer can be exchanged using dialysis or diafiltration, *see* **Note 3**.
3. The transfer protein should next be analyzed for lipid transfer activity.

3.2 Fluorescence Dequenching Assay

We present three different approaches that can be used to determine lipid transfer protein activity. GLTP serves as an example; however other lipid transfer proteins can also be assayed for transfer activity by changing the lipid that will be transferred.

A typical fluorescence dequenching lipid transfer assay uses two different populations of vesicles. The donor vesicle population contains the transferrable lipid of interest, fluorescently labeled and the acceptor vesicle population, which receives the lipids from the transfer protein. The emission of the transferrable energy donor lipid is quenched by the second nontransferrable fluorophore, the energy acceptor, also present in the donor vesicle population. When the lipid transfer protein moves the lipids to the acceptor vesicle population the emission increases as a function of time, and describes the transfer rate (Fig. 1). The ratio between the donor and acceptor population varies; however mostly the acceptors are in five to tenfold excess. The fluorophore pairs commonly used are BODIPY and DiO-C16, anthrylvinyl and perylenoyl [6], NBD and rhodamine [7].

Determination of lipid transfer rates

The half-time ($t_{1/2}$) for the equilibrium of the transfer process can be determined as illustrated in panel (c) in Fig. 1. The first-order rate constant, k_{obs} , and the half-time for the transfer rate can be determined from the semilogarithmic plot of [8] shown in (c) inset:

$$\ln \frac{F_{\infty}}{F_{\infty} - F_{rec}}$$

versus time from the relationships:

$$k_{obs} = -slope$$

$$t_{1/2} = \frac{\ln 2}{k_{obs}}$$

The transfer rate can also be determined by comparing the levels of the fluorescence intensity without LTP and 1 min after LTP was added, with the value for the fluorescence intensity after the

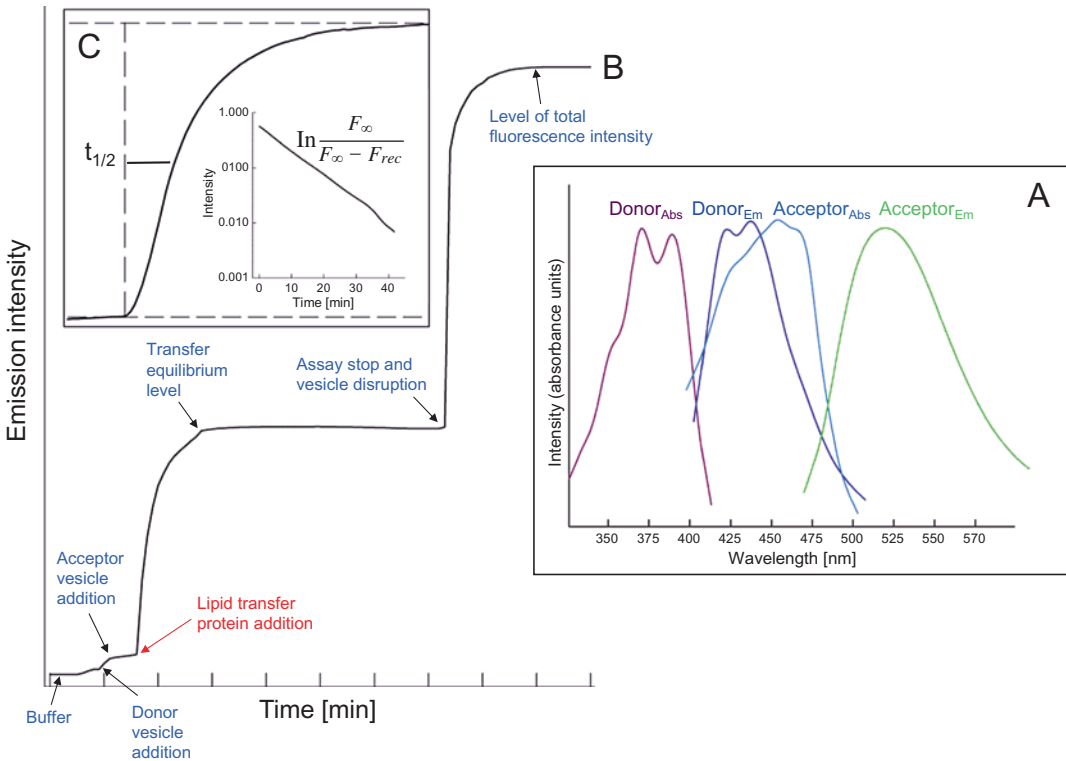


Fig. 1 Fluorescence dequenching lipid transfer protein activity measurement. (a) Normalized spectra of a typical fluorophore pair with overlapping excitation and emission spectra. (b) Schematic presentation of a typical transfer protein assay monitoring real-time lipid transfer kinetics. The kinetics of fluorescently labeled lipid intermembrane transfer can be determined by continuously monitoring the increase in fluorescence at a constant wavelength as a function of time. Donor vesicles are added to a buffer solution followed by the addition of acceptor vesicles. The assay is started with the addition of a lipid transfer protein (LTP). The rapid dequenching of the fluorescence (donor fluorescence emission increase) represents LTP-mediated transfer of the labeled lipid to the acceptor vesicle population. The transfer levels out and reaches equilibrium. This level represents the final amount of lipid transferred. Disruption of the vesicles (with detergents) stops the assay and gives the total intensity values for each experiment, needed for calculation of the transfer rate. (c) Half-time for the transfer reaction in schematic description, as well as a semilogarithmic plot versus time for the trace shown in panel (b). The slope of this plot can also be used to calculate the transfer half-time

addition of detergent. To calculate the transfer rates one needs to correct for the potential quenching by the added detergent of the labeled fluorescent lipid. Calculating the initial transfer rates at 1 min allows for a much faster collection of data, and a better reproducibility than the use of transfer rates at the half-time of the transfer reaction [9].

3.3 Assay for Nonfluorescent Glycolipids

An approach called fluorescence competition assay can be useful if there is a limited availability of fluorescently labeled lipids that you want to analyze for transfer (Fig. 2). A fluorescently labeled lipid

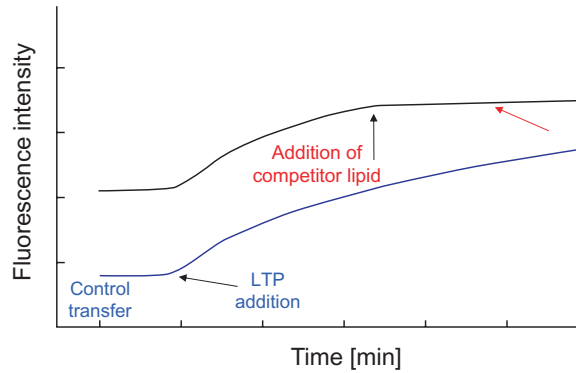


Fig. 2 Lipid transfer protein competition assay. A schematic illustration of BODIPY-phosphatidylcholine transfer mediated by sterol carrier protein-2, SCP-2, without (*blue trace*) and with the addition of phosphatidylinositol containing vesicles (*black trace*). The deviation in the slope of the transfer rate of BODIPY-PC is marked with the *red arrow*. The decline in the transfer rate for BODIPY-PC is a result of SCP-2 transfer of unlabeled phosphatidylinositol

that is a substrate for the assayed transfer protein is needed. After a steady transfer rate has been reached, of for instance BODIPY-PC in sphingomyelin vesicles by sterol carrier protein-2 (SCP-2) using a fluorescence assay described above, unlabeled lipids (phosphatidylinositol) incorporated in vesicles are added to the transfer reaction mixture. This would result in a decrease in the transfer rate of the fluorescently labeled lipid, if the added lipids were competing with the labeled lipid. If the added lipids were not substrates for the transfer protein, no deviation in the slope of the transfer rate would occur [10]. This approach can also be used for many types of lipids, inhibitors, or activators that can be screened in automated lipid transfer assay setups. The rates are analyzed as described above for the fluorescence dequenching assay.

3.4 Assay for Lipid Binding and Transfer Using Surface Plasmon Resonance (SPR)

SPR is a sensitive method for studying molecular interactions and has proven to be useful in studying transfer protein and lipid interactions as well [11, 12]. It is an optical method that measures the changes in the refractive index upon increase or decrease in mass on the sensor surface of the instrument. In our approach of studying the interactions of GLTP and various vesicle formulations it has to be emphasized that the protein preparations need to be of high quality and purity. In addition to regular purification of the protein it is important to both dialyze and filter the protein solution (filter pore size 0.2 μm). The response in the SPR is sensitive to changes in buffer conditions; therefore the running buffer used in the experiments is the same as in which the protein has previously been dialyzed. Prior to use, however, it has to be filtered and properly degassed.

1. The sensor chip for capturing lipid vesicles is a functionalized dextran gel that is attached to the gold surface of the sensor via a self-assembled monolayer of hydroxyalkyl thiols, using a method based on the work by Löfås [13]. The dextran forms a flexible hydrogel matrix that is further carboxymethylated and through EDC-NHS coupling is activated to bind the amine group of decylamine. The resulting long alkyl chains bind the vesicles by inserting into the hydrophobic part of the lipid bilayer and thus anchoring them onto the surface of the sensor chip.
2. The setup of the experiments for determining transfer activity of GLTP is based on the protocol used by Ohvo-Rekilä, Fig. 3 [11]. We used a flow rate of 10 $\mu\text{L}/\text{min}$ and a temperature set point of 23 $^{\circ}\text{C}$. Before vesicles are loaded onto the sensor chip it is washed twice with CHAPS detergent to establish a stable baseline.

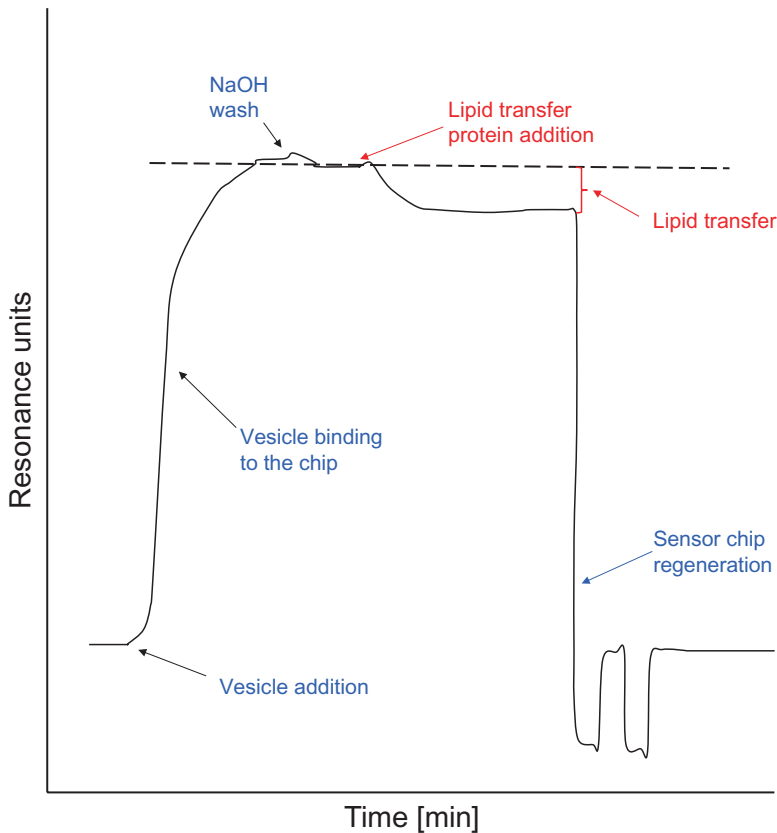


Fig. 3 Lipid transfer protein activity using surface plasmon resonance. Vesicles are allowed to bind to the chip, then the baseline is stabilized, and unbound vesicles eluted with NaOH. The extraction of lipids is started with the addition of transfer protein, a protein binding is observed, response units increase, followed by a decrease in the response units as a function of decrease in the mass of the vesicles bound to the chip. The chip is regenerated after a detergent wash that releases the bound vesicles and the response unit returns to the starting level

3. To load the sensor with vesicles, a buffer (the same as the running buffer) solution with a 0.5 mM concentration of lipids is injected for 10 min. To remove unbound vesicles, the sensor is washed with a 50 mM solution of NaOH in buffer.
4. After the baseline is stabilized, the LTP sample can be injected and run for 10 min, where after injecting running buffer stops the run. At this point it is important to keep the duration of each LTP injection as similar as possible for good comparison of different sets of data.
5. To start a new cycle CHAPS is injected twice to strip the remaining vesicles from the chip and to reach the original baseline established in the beginning. If detergent is not sufficient to remove a particular kind of vesicle, a 2:3 mixture of 50 mM NaOH and isopropanol can be tried instead.

4 Notes

1. Plasmid description. The BL-21(M15) strain contains the pREP4 repressor plasmid that expresses the lac repressor protein and subsequently represses the *E. coli* T5 promoter on the pQE-9 vector. This allows for tight regulation of recombinant protein expression, where the pQE-9 vector can be rapidly induced by the addition of isopropyl- β -D-thiogalactoside (IPTG), which binds to the lac repressor protein and inactivates it.
2. Producing high-expressing bacterial colonies. Several (10–20) colonies should be picked and separately placed in L-broth with ampicillin (50 μ g/mL) and kanamycin (25 μ g/mL). The bacterial cultures are grown at 37 °C under vigorous shaking (180 RPM) and the growth curves of each culture should be plotted by measuring the absorbance of the bacterial culture at 600 nm at 30 min intervals, until all cultures have reached an OD₆₀₀ value of 0.8. At this point, the bacterial solutions are normalized to an OD₆₀₀ value of 0.5 by dilution using LB media. Protein expression is then induced by the addition of IPTG and protein expression levels are assayed by SDS-PAGE and Coomassie staining. Colonies that demonstrate rapid growth as well as high production of target protein should be chosen for future experiments.
3. Buffer exchange. Depending on what the end purpose of the purified protein is, the buffer may have to be exchanged. Various methods can be employed for exchanging the buffer, including size exclusion spin columns and dialysis membranes. It should be noted that buffer exchange generally results in loss of material. Therefore a determination of the protein concentration after buffer exchange is important.

Acknowledgements

This work was supported by Sigríd Jusélius Foundation, Magnus Ehrnrooth Foundation, Medicinska Understödsföreningen Liv och Hälsa, Svensk Österbottniska Samfundet.

References

1. Tuuf J, Mattjus P (2014) Membranes and mammalian glycolipid transferring proteins. *Chem Phys Lipids* 178:27–37. doi:[10.1016/j.chemphyslip.2013.10.013](https://doi.org/10.1016/j.chemphyslip.2013.10.013)
2. Sandhoff K (2012) My journey into the world of sphingolipids and sphingolipidoses. *Proc Jpn Acad Ser B Phys Biol Sci* 88(10):554–582
3. Kjellberg MA, Backman AP, Ohvo-Rekilä H, Mattjus P (2014) Alternation in the glycolipid transfer protein expression causes changes in the cellular lipidome. *PLoS One* 9(5):e97263. doi:[10.1371/journal.pone.0097263](https://doi.org/10.1371/journal.pone.0097263)
4. Kjellberg MA, Mattjus P (2013) Glycolipid transfer protein expression is affected by glycosphingolipid synthesis. *PLoS One* 8(7):e70283. doi:[10.1371/journal.pone.0070283](https://doi.org/10.1371/journal.pone.0070283)
5. Zou X, Gao Y, Ruvolo VR, Gardner TL, Ruvolo PP, Brown RE (2010) Human glycolipid transfer protein gene (GLTP) expression is regulated by Sp1 and Sp3: involvement of the bioactive sphingolipid ceramide. *J Biol Chem* 286:1301–1311. doi:[10.1074/jbc.M110.127837](https://doi.org/10.1074/jbc.M110.127837). [pii]:M110.127837
6. Mattjus P, Molotkovsky JG, Smaby JM, Brown RE (1999) A fluorescence resonance energy transfer approach for monitoring protein-mediated glycolipid transfer between vesicle membranes. *Anal Biochem* 268(2):297–304. doi:[10.1006/abio.1998.3065](https://doi.org/10.1006/abio.1998.3065)
7. Nichols JW, Pagano RE (1983) Resonance energy transfer assay of protein-mediated lipid transfer between vesicles. *J Biol Chem* 258(9):5368–5371
8. Mattjus P, Pike HM, Molotkovsky JG, Brown RE (2000) Charged membrane surfaces impede the protein-mediated transfer of glycosphingolipids between phospholipid bilayers. *Biochemistry* 39(5):1067–1075. doi:[10.1021/bi991810u](https://doi.org/10.1021/bi991810u)
9. Nylund M, Mattjus P (2005) Protein mediated glycolipid transfer is inhibited FROM sphingomyelin membranes but enhanced TO sphingomyelin containing raft like membranes. *Biochim Biophys Acta* 1669(2):87–94. doi:[10.1016/j.bbamem.2004.12.014](https://doi.org/10.1016/j.bbamem.2004.12.014)
10. Viitanen L, Nylund M, Eklund DM, Alm C, Eriksson AK, Tuuf J, Salminen TA, Mattjus P, Edqvist J (2006) Characterization of SCP-2 from *Euphorbia lagascae* reveals that a single Leu/Met exchange enhances sterol transfer activity. *FEBS J* 273(24):5641–5655. doi:[10.1111/j.1742-4658.2006.05553.x](https://doi.org/10.1111/j.1742-4658.2006.05553.x)
11. Ohvo-Rekilä H, Mattjus P (2011) Monitoring glycolipid transfer protein activity and membrane interaction with the surface plasmon resonance technique. *Biochim Biophys Acta* 1808(1):47–54. doi:[10.1016/j.bbamem.2010.08.018](https://doi.org/10.1016/j.bbamem.2010.08.018)
12. Alm I, Garcia-Linares S, Gavilanes JG, Martinez-Del-Pozo A, Slotte JP (2015) Cholesterol stimulates and ceramide inhibits Sticholysin II-induced pore formation in complex bilayer membranes. *Biochim Biophys Acta* 1848(4):925–931. doi:[10.1016/j.bbamem.2014.12.017](https://doi.org/10.1016/j.bbamem.2014.12.017)
13. Löfås S, Johnsson B (1990) A novel hydrogel matrix on gold surfaces in surface plasmon resonance sensors for fast and efficient covalent immobilization of ligands. *J Chem Soc Chem Commun* 21:1526–1528. doi:[10.1039/c39900001526](https://doi.org/10.1039/c39900001526)

Incorporation of Artificial Lipid-Anchored Proteins into Cultured Mammalian Cells

Rania Leventis and John R. Silvius

Abstract

Exogenous lipid-anchored proteins can be incorporated into the plasma membranes of living mammalian cells, allowing the chemical structure of the incorporated protein and its lipid anchor to be controlled (and varied) to a much greater degree than is possible for proteins expressed by the cells themselves. This technology offers a variety of potential applications, including incorporating novel and complex protein constructs into cell surfaces and exploring structure-function relationships for biologically important lipid-anchored proteins such as glycosylphosphatidylinositol-anchored proteins. Here we describe detailed methods for stable incorporation of artificial lipid-anchored proteins into cultured mammalian cells under mild, nonperturbing conditions.

Key words Polyethyleneglycol-lipids, Membrane traffic, Glycosylphosphatidylinositol-anchored proteins, Fluorescence microscopy, Endocytosis

1 Introduction

Incorporation of exogenous lipid-anchored proteins into mammalian cells offers a useful alternative to conventional transfection-based methods to introduce novel protein species stably into cellular membranes and to observe their physical and biological properties. Lipid-anchored proteins can be inserted into the plasma membrane under mild, nontoxic conditions and can then be trafficked to other cellular compartments along the endosomal pathway [1, 2]. With a better understanding of the relevant targeting signals, it may also become possible to deliver these species to other intracellular membranes (e.g., Golgi or ER) through retrograde trafficking pathways [3–5]. To date, artificial lipid-anchored proteins and polypeptides have been incorporated into mammalian cells to modulate immune cell function [6, 7] and to investigate the physical bases of signaling and trafficking of endogenous glycosylphosphatidylinositol proteins (GPI-proteins) [1, 2, 8]. Additional applications can readily be envisioned to exploit the

unique advantages of this technology, including the complete control that it allows over the chemical structures of both the incorporated protein and the lipid *anchor*.

Proteins modified with a single long-chain acyl or alkyl group can associate with membrane bilayers, but in most cases this association is rapidly reversible [9, 10]. By contrast, proteins linked to long-chain diacyl phospholipids (or cholesterol) show long-lived association with membranes [10, 11]. Unfortunately, proteins modified with these more hydrophobic lipid anchors are prone to aggregation and consequently are difficult to incorporate into living cells without introducing cell- or membrane-perturbing agents such as detergents [12, 13]. An alternative strategy to incorporate lipid-anchored proteins stably into cell membranes is to incorporate first into the cells a suitably functionalized lipid-polyethylene glycol (lipid-PEG), then to bind an exogenous soluble protein to this anchor to form a stable lipid-PEG-protein conjugate. Cholesterol and phospholipids modified with long-chain PEGs can be inserted into cell membranes under mild, nonperturbing conditions [14–17], and several types of functionalized phosphatidylethanolamine-PEGs (PE-PEGs) have been utilized to anchor exogenous proteins to membranes in a highly specific manner [1, 2, 8, 18–20].

We have examined the membrane incorporation and biological behavior of a variety of conjugates formed by functionalized PE-PEGs and proteins that bind to them either covalently, via bioorthogonal reactions, or by formation of noncovalent but high-affinity complexes. In this chapter we describe protocols to insert functionalized PE-PEGs into cultured mammalian cells and subsequently to bind appropriate protein partners to them, forming stably membrane-anchored lipid-protein conjugates.

2 Materials

Prepare all solutions using distilled water. All reagents should be reagent grade where not otherwise specified.

2.1 *Fluorescent Labeling of Anti-dinitrophenyl Antibody*

1. Streptavidin (lyophilized powder).
2. Phosphate-buffered saline without calcium or magnesium (PBS(-)).
3. 1 M NaHCO₃: Just before use, dissolve 84 mg NaHCO₃ in 1 mL distilled water.
4. Alexa Fluor®-488 or -555 NHS ester: obtained from Invitrogen/Molecular Probes, individually aliquoted as portions of ester sufficient to label 1 mg protein.
5. Anhydrous dimethyl sulfoxide (DMSO).

6. BioGel P-6 column in PBS(-), packed to a bed height of 25 cm in a 1 cm (ID) × 30 cm column and washed with two volumes of PBS(-).
7. Centrifugal filter unit (4 mL capacity, 10 kDa cutoff).
8. 20 mM sodium azide solution: dissolve 1.3 mg of sodium azide (**toxic reagent**) in 10 mL distilled water; store in a capped tube at 4 °C.

2.2 Preparation of Acid-Treated Cover Slips

1. Concentrated hydrochloric acid (12–13 M).
2. Concentrated nitric acid (68–70%).
3. Glass cover slips, 22 × 22 × 1.5 mm.
4. Two 400 mL glass beakers, one with a watch glass to cover.
5. Distilled water.
6. Four sterilized 150 mm glass culture dishes.
7. Sterile distilled water.
8. Sterile forceps.
9. Sterile 250 mL beaker and sterilized 4 × 4" aluminum foil sheets (wrapped in a larger piece of foil and autoclaved) to cover it.
10. 70% ethanol: mix 110 mL redistilled 95% ethanol with 40 mL distilled water.

2.3 Preparation of PE-PEG-Ligand Conjugate/BSA Complexes

1. Dipalmitoylphosphatidylethanolamine-polyethyleneglycol 1500-biotin (DPPE-PEG-biotin): prepared as described in [8]; store as a 5 mg/mL solution in CH₂Cl₂ at -20 °C in a glass tube with a PTFE-lined cap.
2. 50 or 100 μL Hamilton syringe.
3. 13 × 100 mm disposable borosilicate glass tubes.
4. 400 mL beaker partly filled with hot water (45 °C).
5. Nitrogen gas cylinder with regulator, connected by a length of Tygon tubing to a 5-3/4" Pasteur pipet.
6. Vacuum dessicator connected to a high-vacuum oil pump.
7. 95% ethanol.
8. Phosphate-buffered saline without calcium or magnesium (PBS(-)).
9. BSA/PBS solution: Dissolve 0.68 g of defatted bovine serum albumin (BSA) in 10 mL of PBS(-); adjust pH to 7.4 with 10 M NaOH; dialyze solution overnight against 1 L of PBS(-); store at 4 °C no longer than 1 month.
10. Dialysis tubing (10 mm diameter, molecular weight cutoff 12–14 kDa).
11. 1.5 mL Eppendorf tubes.

2.4 Collagen Coating of Acid-Treated Cover Slips

1. Acid-treated cover slips: *see* Subheading 2.2.
2. Sterile six-well plastic tissue culture plates.
3. 70% ethanol:mix 110 mL redistilled ethanol with 40 mL distilled water.
4. Sterile phosphate-buffered saline solution, without calcium and magnesium (PBS(-)).
5. Sterile 10 mL pipets.
6. Rat tail collagen, sterile solution: dilute sterile collagen solution (Invitrogen, 3 mg/mL) into sterile PBS (without calcium/magnesium) to a final concentration of 50 µg collagen/mL; prepare just before use.

2.5 Incorporation of Lipid-PEG-TNP Conjugates into BHK Cells

1. Collagen-treated cover slips in six-well dishes: *see* Subheading 2.4.
2. Sterile 10 mL pipets.
3. Sterile serum-free Ham's F12 medium.
4. Fetal bovine serum.
5. BSA/DPPE-PEG-biotin complex: *see* Subheading 2.3.
6. Alexa488- or Alexa555-labeled streptavidin.

2.6 Cell Fixation and Mounting

1. Hanks' buffered saline solution plus HEPES (HBSS/HEPES): Add 12.5 mL 1 M HEPES to 500 mL of HBSS; check pH and adjust to 7.2 if necessary.
2. 4% paraformaldehyde (PFA) in phosphate-buffered saline (4% PFA/PBS): In a fume hood weigh out 0.8 g of PFA (**toxic reagent**) into a 50 mL capped disposable plastic tube; add 18 mL distilled water and 20 µL of 1 M NaOH; tightly cap tube and transfer the capped tube to a beaker partly filled with 80–90 °C water, placed in a covered ice bucket also partly filled with 80–90 °C water; swirl the tube occasionally until the PFA is completely dissolved, then cool to room temperature and add 20 µL 1 M HCl followed by 2 mL of 10× PBS(-).
3. 5–3/4" Pasteur pipets.
4. Ice bucket filled with wet ice.

Items 5–9 below are required only if the cells are also to be immunolabeled using an antibody against an intracellular marker protein.

5. Methanol chilled to –20 °C: Incubate methanol (20 mL per 6 cover slips) in a tightly capped bottle at –20 °C (freezer) for at least 1 h prior to fixation; remove from freezer immediately before the indicated step in the protocol.
6. Blocking solution: 10 mg/mL BSA in PBS(-).
7. Rocking platform.

8. Primary antibody solution: appropriate dilution of primary antibody in PBS(-) containing 10 mg/mL BSA.
9. Phosphate-buffered saline with calcium or magnesium (PBS(-)).
10. Secondary antibody solution: appropriate dilution of fluorescent-labeled secondary antibody in PBS(-) containing 10 mg/mL BSA.
11. Scalpel blade.
12. Kimwipes.
13. Mounting solution: In 50 mL glass beaker combine 2.4 g of Mowiol 4-88, 6 g of glycerol, and 6 mL of distilled water; mix well with a stir bar (the Mowiol will not entirely dissolve at this stage) and leave at room temperature for at least 6 h; add 12 mL of 0.2 M Tris, pH 8.5 and heat to 50 °C for 10 min with occasional stirring; centrifuge for 15 min at 5000 × *g* in a 50 mL plastic tube, then remove roughly 95% of the supernatant, taking care not to disturb the pellet; add 0.55 g 1,4-diazabicyclo[2.2.2] octane (DABCO) to the recovered supernatant, stir to dissolve and degas briefly under vacuum; aliquot 1 mL portions into 1.5 mL Eppendorf tubes and store at -20 °C.
14. Colorless nail polish.

3 Methods

3.1 *Fluorescent Labeling of Streptavidin (See Note 1)*

1. Dissolve 1 mg of streptavidin in 0.5 mL of PBS(-); add 20 μL of freshly prepared 1 M NaHCO₃.
2. To a pre-aliquoted vial of Alexa488- or Alexa555-NHS (*see* Subheading 2.1) add 5 μL dry DMSO and a 1.5 × 7 mm magnetic spinbar. Gently rotate the vial to dissolve the labeling reagent completely, then rapidly add the protein/NaHCO₃ solution to the vial while stirring.
3. Cover the vial with aluminum foil to protect from light and continue stirring for 1 h, then apply the sample to a BioGel P6 column and elute with degassed PBS(-). Collect the faster-eluting peak, corresponding to labeled protein, and concentrate to <1 mL using an Amicon filter.
4. Measure the volume of concentrated solution, add sodium azide solution to 0.5 mM and store at 4 °C. The protein concentration can be estimated from the measured final volume, assuming essentially quantitative protein recovery.

3.2 *Preparation of Acid-Washed Cover Slips (See Notes 2-4)*

Steps 1-3 should be carried out in a fume hood and using suitable protective clothing and eyewear; Steps 4 and 5 should be carried out in a tissue culture cabinet.

1. Mix 100 mL nitric acid and 50 mL hydrochloric acid in a 400 mL glass beaker with a stir bar or by gentle swirling. The solution will turn orange and evolve gas bubbles.
2. Carefully drop cover slips individually into the acid mixture, ensuring that the entire surface of each becomes wetted with the reagent. After all cover slips have been added, cover the beaker with a watch glass; after 30 min swirl gently, then leave overnight in the fume hood.
3. Next day, decant the acid into a second 400 mL glass beaker, then rinse the cover slips with six changes of 300 mL distilled water, swirling after each change of water to ensure efficient acid removal.
4. Fill each of four sterilized 150 mm glass culture dishes with 20 mL sterile distilled water and a 250 mL sterilized glass beaker with 150 mL 70% ethanol. With sterile forceps transfer cover slips successively through the four dishes, in groups of roughly six at a time, each time swirling the dish before transferring the cover slips to the next, then transfer the cover slips into the beaker containing 70% ethanol. Cover the beaker with aluminum foil and leave overnight.
5. Using sterile forceps, transfer cover slips into a 250 mL beaker containing sterile distilled water, and cover with sterile aluminum foil; cover slips can be stored indefinitely at this point.

3.3 Preparation of PE-PEG-Ligand/BSA Conjugates (See Notes 5–7)

1. With a Hamilton syringe dispense 200 nmol of PE-PEG-ligand conjugate into a disposable glass tube. Place the tube in a beaker of warm water and dry off excess solvent under a stream of nitrogen. Pump down the dried sample for ≥ 2 h in a vacuum dessicator.
2. To the dried conjugate add 200 μ L of 95% ethanol and briefly warm to 40 °C to dissolve the conjugate. Into a second glass tube aliquot 400 μ L of BSA/PBS solution; vortex the BSA/PBS while adding the ethanolic conjugate solution dropwise over roughly 15 s. Add 400 μ L of PBS (without calcium and magnesium).
3. Transfer the BSA/conjugate mixture into a dialysis bag and dialyze overnight at 4 °C against 500 mL of PBS. Centrifuge for 1 h at $80,000 \times g$ and carefully remove the supernatant. Measure the volume of the recovered supernatant and store at 4 °C in 1.5 mL Eppendorf tubes. For storage for more than 1 week, add sodium azide solution to 0.5 mM NaN_3 .

3.4 Collagen Coating of Acid-Washed Cover Slips

All steps should be carried out in a tissue culture cabinet under sterile conditions. Collagen-treated cover slips should be used within 2 days of preparation.

1. Place cover slips in the wells of six-well dishes. To each well add 2 mL 70% ethanol and let stand for 5 min.

2. Remove the ethanol from each well, and wash the cover slips once with sterile PBS (-).
3. Add 1 mL of collagen solution to each well and incubate for 2 h at 37 °C or overnight at 4 °C.
4. Remove collagen solution and replace with sterile PBS(-).

3.5 Cell Incubation to Incorporate Conjugates (See Notes 8 and 9)

Cell incubations at 37 °C should be carried out in a tissue culture incubator.

1. Remove PBS(-) from the wells of six-well plates containing collagen-treated cover slips and seed wells with BHK cells at 30% confluency; culture for 2 days.
2. Wash cells twice with 1 mL sterile serum-free medium (SFM), finally leaving the cells in 1 mL of SFM.
3. Add PE-PEG-biotin/BSA conjugate to the cells to a final concentration of 10 µM and incubate at 37 °C for 30 min.
4. Wash the cells four times with 1 mL SFM equilibrated to 37 °C.
5. Incubate the cells for 1 h at 37 °C.
6. To the cell medium add 5 µg of Alexa488- or Alexa555-labeled streptavidin and incubate for 1 h at 37 °C.
7. Remove medium from cells and wash four times with 1.5 mL SFM.
8. Cells can be further incubated in SFM at 37 °C for up to at least 8 h to examine the time-dependent intracellular trafficking of the inserted lipid-protein conjugates or to allow the distribution of the conjugates between compartments to approach steady state.

3.6 Cell Fixation and Mounting (See Note 10)

Steps 1–5 should be carried out in a fume hood.

1. Prechill 4% PFA/PBS and HBSS/HEPES to 0 °C; also have available HBSS/HEPES at room temperature.
2. Remove the medium from the cover slips in the six-well dishes and gently wash four times with 1.5 mL room temperature HBSS/HEPES. Add 1.5 mL HBSS/HEPES to each well and incubate the dishes on ice for 5 min.
3. Remove HBSS/HEPES, add 1 mL ice-cold 4% PFA/PBS, and incubate for 10 min on ice.
4. Wash cells twice with 1.5 mL ice-cold HBSS/HEPES.

Steps 5–8 are necessary if the cells are to be immunofluorescence-labeled using an antibody directed against an intracellular marker protein.

5. Remove HBSS/HEPES and add 1.5 mL of -20°C methanol. Incubate for 5 min at 0°C , then wash the cells four times with 1.5 mL ice-cold HBSS/HEPES.
6. To the washed cells add blocking solution and incubate with gentle rocking for 1 h at room temperature.
7. Remove blocking solution and replace with primary antibody solution. Incubate with gentle rocking for 2 h at room temperature or overnight at 4°C .
8. Wash cells four times with 1.5 mL PBS, then incubate with gentle rocking for 2 h at room temperature with fluorescent-labeled secondary antibody solution, covering the 6-well dishes with tinfoil to exclude light.
9. Wash cover slips four times with HBSS/HEPES.
10. Prepare one appropriately labeled microscope slide for mounting each cover slip; in the center of each slide dispense $40\ \mu\text{L}$ of Mowiol and allow the liquid to spread.
11. For each washed cover slip in turn, gently lift one edge with the aid of a scalpel blade, remove from the liquid, and allow the liquid to drain off for a few seconds. Gently grasping the cover slip by the edges, carefully blot one edge and the *cell-free* face of the cover slip with a Kimwipe to remove any remaining liquid. Gently lower the cover slip, at a slight angle to the horizontal and with the cell-bearing side facing downward, over the spread drop of Mowiol on a microscope slide until one edge of the cover slip touches the slide, then release the cover slip; the Mowiol solution should spread to fill the entire space between slide and cover slip without entrapping bubbles.
12. Place the mounted cover slips at 4°C overnight with exclusion of light to allow the mounting medium to set, then store the samples at 4°C , protected from light, until ready for examination. If samples are to be stored for more than 1–2 days, after initial overnight incubation the cover slips should be sealed to the slide by applying a thin layer of colorless nail polish around the entire perimeter of the cover slip.
13. Preliminarily examine cells under a wide-field fluorescence microscope using a $40\times$ objective, to verify that the cell plasma membranes appear uniformly labeled and that large, bright aggregates are not found on the cell surfaces (*see Note 9*). Examples of confocal images of BHK fibroblasts and polarized HepG2 hepatocytes incorporating different PE-PEG-protein conjugates are shown in Fig. 1.

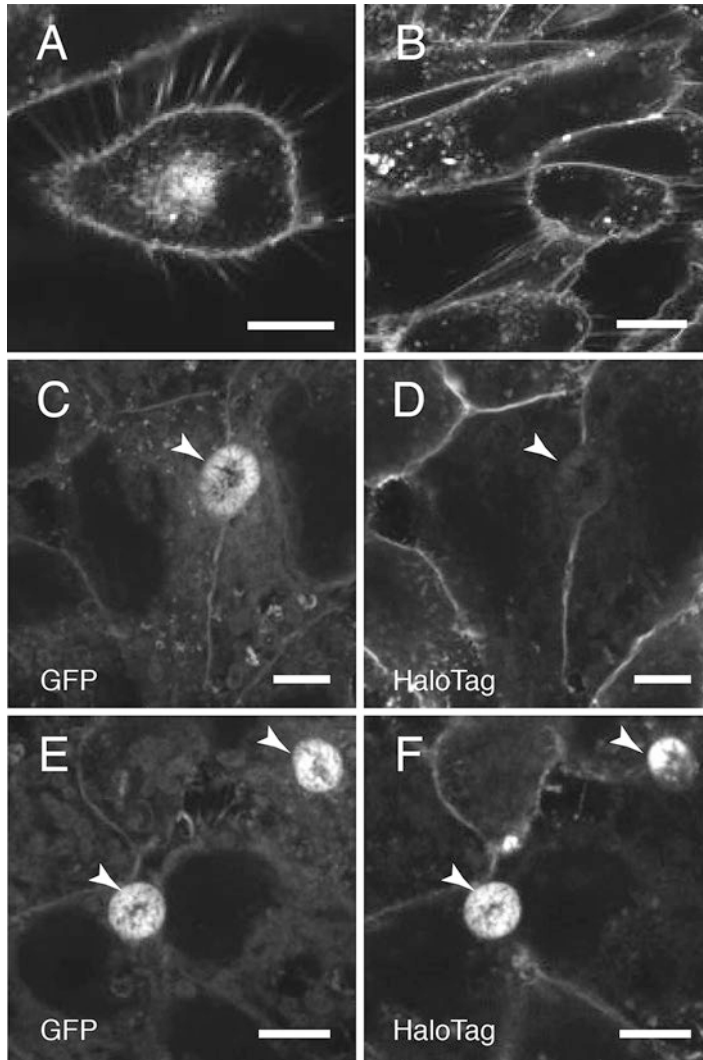


Fig. 1 Confocal micrographs of cultured mammalian cells incorporating PE-PEG-protein conjugates. *Top panels*--BHK cells treated with (a) dioleoyl-PE-PEG1500-biotin followed by Alexa555-labeled streptavidin or (b) dihexadecyl-PE-PEG1500-methotrexate conjugate followed by Alexa555-labeled *E. coli* dihydrofolate reductase, in both cases postincubating for 2 h at 37 °C before fixing and imaging. In both images fluorescence is observed in endosomal subcompartments as well as on the plasma membrane, reflecting uptake of a portion of each lipid-anchored protein to subcompartments of the endosomal system (identified using known markers for these subcompartments [2]). *Middle panels (c) and (d)*--HepG2 cells stably expressing glycosylphosphatidylinositol-anchored green fluorescent protein (GPI-GFP), treated successively with dipalmitoyl-PE-PEG1500-Halo-ligand and with Alexa555-labeled HaloTag protein [21], then fixed and imaged. *Bottom panels (e) and (f)*--As for panels (c) and (d), but the cells were additionally postincubated for 6 h at 37 °C before fixing and imaging. As illustrated by panels (d) and (f), the lipid-anchored HaloTag protein rapidly labels the basolateral plasma membrane domains of the cells, but it requires longer times to be trafficked to the apical plasma membrane domains found in intercellular lumens (indicated by arrowheads). Space bars =10 μm

4 Notes

1. The labeling protocol described can be applied to a variety of proteins. The reaction medium should contain no components other than the protein itself that incorporate amino groups, such as Tris buffer or free amino acids. If such components are present, they should be removed before labeling by concentrating the protein solution in a centrifugal filter unit, repeatedly diluting with a buffer free of amine components and reconcentrating.
2. Cover slips must be rigorously cleaned, using procedures like that described here, in order for cells to adhere efficiently to them. We have observed that cover slips cleaned using milder procedures appear more prone to adsorb lipid conjugates, giving higher background fluorescence, which can sometimes appear granular, in cell-free areas.
3. The nitric/hydrochloric acid mixture is highly corrosive and should be handled with caution. After use the recovered acid mixture should be allowed to stand in a fume hood until it decolorizes, then disposed of appropriately.
4. Subheading 2.2, **item 4** serves to remove residual traces of acid; sterile water and dishes are used at this stage simply to minimize the amount of nonsterile material introduced into the tissue culture cabinet.
5. Diverse functionalized PE-PEGs can be prepared as BSA complexes using the procedure described. Detailed procedures for synthesis of PE-PEGs, including DPPE-PEG-biotin, are described in [1] and [8]. Several functionalized derivatives of distearoylphosphatidylethanolamine-PEG2000 (DSPE-PEG2000), including DSPE-PEG2000-biotin, are commercially available from Avanti Polar Lipids (Alabaster, AL), although we have found that analogous derivatives of DSPE-PEG1500 are more difficult to incorporate homogeneously into cell membranes than the corresponding derivatives of dipalmitoyl- or dioleoyl-PE-PEG1500. Heterobifunctional PEG derivatives suitable as precursors for synthesis of functionalized PE-PEG [1, 22, 23] can be obtained from Sigma (www.sigmaaldrich.com), JenKem Technology USA (www.jenkemusa.com/products), or Nektar Therapeutics (www.nektar.com/peg).
6. Glass tubes and glass/metal syringes must be used to handle lipid stocks; organic solvents can leach contaminants from plastics, and the high vapor pressures of lipid solvents can cause substantial volume errors if air-displacement pipettors are used.

7. Loss of BSA/lipid complexes during dialysis and centrifugation is typically slight (<10%). It is somewhat tedious, and typically unnecessary, to assay the concentration of PE-PEG conjugate in each preparation of complexes; we normally estimate the concentration of lipid conjugate from the measured final volume and the original amount of conjugate dispensed, assuming near-quantitative recovery.
8. In order to minimize the risk of cell detachment and loss during repeated washings and other manipulations, during washing steps we add solutions to six-well culture plates by tilting the dish and dispensing the liquid slowly down the lower edge of each well, then gently returning the dish to a level position to immerse the cover slips. The importance of this precaution depends on the cell line used.
9. Using certain combinations of cell types and PE-PEG conjugates, in addition to the expected uniform staining of the plasma membrane we have also observed aggregates of the lipid-protein conjugate on cell surfaces, apparently formed through aggregation of the functionalized PE-PEG during incubation with the cells (Subheading 2.5, **item 3** in the described protocol). In our experience, when this problem is encountered it can usually be resolved by testing an alternative protein/PE-PEG combination with the cell line of interest. In cases where this is not feasible, the problem may be mitigated if the conjugates are dispersed and loaded into cells from an isotonic sucrose-based medium as described in [1]. However, for some cell lines this latter method can cause cell rounding or other transient morphological perturbations during conjugate treatment. In some cases, addition of β -cyclodextrin (10–30 mM) to cell/conjugate incubation mixtures (Subheading 2.5, **item 3**) can markedly enhance conjugate incorporation into cells.
10. It is important to use paraformaldehyde (PFA) for fixation of lipid-anchored proteins, even if the cells will subsequently be treated with cold methanol to permeabilize them for immunofluorescence labeling. Lipid-anchored glycosylphosphatidylinositol-anchored proteins can redistribute within cells during treatment with cold methanol if not first fixed with PFA, suggesting that PE-PEG-anchored proteins could behave similarly during methanol fixation. We have also observed that for some cell lines (e.g., HepG2 hepatocytes), cells treated with PFA alone show morphological perturbations that can be mitigated when the cells are treated with cold methanol after PFA fixation.

References

- Bhagatji P, Leventis R, Comeau J, Refaei M, Silvius JR (2009) Steric and not structure-specific factors dictate the endocytic mechanism of glycosylphosphatidylinositol-anchored proteins. *J Cell Biol* 186(4):615–628. doi:10.1083/jcb.200903102. jcb.200903102 [pii]
- Refaei M, Leventis R, Silvius JR (2011) Assessment of the roles of ordered lipid microdomains in post-endocytic trafficking of glycosylphosphatidylinositol-anchored proteins in mammalian fibroblasts. *Traffic* 12(8):1012–1024. doi:10.1111/j.1600-0854.2011.01206.x
- Johannes L, Popoff V (2008) Tracing the retrograde route in protein trafficking. *Cell* 135(7):1175–1187. doi:10.1016/j.cell.2008.12.009. S0092-8674(08)01570-5 [pii]
- Johannes L, Wunder C (2011) Retrograde transport: two (or more) roads diverged in an endosomal tree? *Traffic* 12(8):956–962. doi:10.1111/j.1600-0854.2011.01200.x
- Geiger R, Luisoni S, Johnsson K, Greber UF, Helenius A (2013) Investigating endocytic pathways to the endoplasmic reticulum and to the cytosol using SNAP-trap. *Traffic* 14(1):36–46. doi:10.1111/tra.12018
- Chung HA, Tajima K, Kato K, Matsumoto N, Yamamoto K, Nagamune T (2005) Modulating the actions of NK cell-mediated cytotoxicity using lipid-PEG (n) and inhibitory receptor-specific antagonistic peptide conjugates. *Biotechnol Prog* 21(4):1226–1230. doi:10.1021/bp049646b
- Tomita U, Yamaguchi S, Sugimoto Y, Takamori S, Nagamune T (2012) Poly(ethylene glycol)-lipid-conjugated antibodies enhance dendritic cell phagocytosis of apoptotic cancer cells. *Pharmaceuticals (Basel)* 5(5):405–416. doi:10.3390/ph5050405
- Wang TY, Leventis R, Silvius JR (2005) Artificially lipid-anchored proteins can elicit clustering-induced intracellular signaling events in Jurkat T-lymphocytes independent of lipid raft association. *J Biol Chem* 280(24):22839–22846. doi:10.1074/jbc.M502920200
- Silvius JR, l'Heureux F (1994) Fluorimetric evaluation of the affinities of isoprenylated peptides for lipid bilayers. *Biochemistry* 33(10):3014–3022
- Shahinian S, Silvius JR (1995) Doubly-lipid-modified protein sequence motifs exhibit long-lived anchorage to lipid bilayer membranes. *Biochemistry* 34(11):3813–3822
- Peters C, Wolf A, Wagner M, Kuhlmann J, Waldmann H (2004) The cholesterol membrane anchor of the hedgehog protein confers stable membrane association to lipid-modified proteins. *Proc Natl Acad Sci U S A* 101(23):8531–8536
- van den Berg CW, Cinek T, Hallett MB, Horejsi V, Morgan BP (1995) Exogenous glycosyl phosphatidylinositol-anchored CD59 associates with kinases in membrane clusters on U937 cells and becomes Ca(2+)-signaling competent. *J Cell Biol* 131(3):669–677
- Premkumar DR, Fukuoka Y, Sevlever D, Brunschwig E, Rosenberry TL, Tykocinski ML, Medof ME (2001) Properties of exogenously added GPI-anchored proteins following their incorporation into cells. *J Cell Biochem* 82(2):234–245
- Baba T, Rauch C, Xue M, Terada N, Fujii Y, Ueda H, Takayama I, Ohno S, Farge E, Sato SB (2001) Clathrin-dependent and clathrin-independent endocytosis are differentially sensitive to insertion of poly (ethylene glycol)-derivatized cholesterol in the plasma membrane. *Traffic* 2(7):501–512
- Ishiwata H, Sato SB, Vertut-Doi A, Hamashima Y, Miyajima K (1997) Cholesterol derivative of poly(ethylene glycol) inhibits clathrin-independent, but not clathrin-dependent endocytosis. *Biochim Biophys Acta* 1359(2):123–135
- Sato SB, Ishii K, Makino A, Iwabuchi K, Yamaji-Hasegawa A, Senoh Y, Nagaoka I, Sakuraba H, Kobayashi T (2004) Distribution and transport of cholesterol-rich membrane domains monitored by a membrane-impermeant fluorescent polyethylene glycol-derivatized cholesterol. *J Biol Chem* 279(22):23790–23796
- Chung HA, Kato K, Itoh C, Ohhashi S, Nagamune T (2004) Casual cell surface remodeling using biocompatible lipid-poly(ethylene glycol)(n): development of stealth cells and monitoring of cell membrane behavior in serum-supplemented conditions. *J Biomed Mater Res A* 70(2):179–185. doi:10.1002/jbm.a.20117
- Kato K, Itoh C, Yasukouchi T, Nagamune T (2004) Rapid protein anchoring into the membranes of mammalian cells using oleyl chain and poly(ethylene glycol) derivatives. *Biotechnol Prog* 20(3):897–904. doi:10.1021/bp0342093
- Totani T, Teramura Y, Iwata H (2008) Immobilization of urokinase on the islet surface by amphiphilic poly(vinyl alcohol) that carries alkyl side chains. *Biomaterials*

- 29(19):2878–2883. doi:[10.1016/j.biomaterials.2008.03.024](https://doi.org/10.1016/j.biomaterials.2008.03.024)
20. Tomita U, Yamaguchi S, Maeda Y, Chujo K, Minamihata K, Nagamune T (2013) Protein cell-surface display through in situ enzymatic modification of proteins with a poly(ethylene glycol)-lipid. *Biotechnol Bioeng* 110(10): 2785–2789. doi:[10.1002/bit.24933](https://doi.org/10.1002/bit.24933)
21. England CG, Luo H, Cai W (2015) HaloTag technology: a versatile platform for biomedical applications. *Bioconjug Chem* 26(6):975–986. doi:[10.1021/acs.bioconjchem.5b00191](https://doi.org/10.1021/acs.bioconjchem.5b00191)
22. Zalipsky S (1995) Functionalized poly(ethylene glycol) for preparation of biologically relevant conjugates. *Bioconjug Chem* 6(2):150–165
23. Zalipsky S, Brandeis E, Newman MS, Woodle MC (1994) Long circulating, cationic liposomes containing amino-PEG-phosphatidylethanolamine. *FEBS Lett* 353(1):71–74

Chapter 21

Sonication-Based Basic Protocol for Liposome Synthesis

Roberto Mendez and Santanu Banerjee

Abstract

Liposomes are spherical vesicles with a wide range of sizes from nano- to micrometer scale. For the past 7–8 decades, these vesicles have occupied the interest of a variety of scientists due to its physical, chemical, and mathematical properties and, to say the least, for its immense utility and potential as delivery vehicles for toxic and nontoxic excipients into biological tissues. Methods related to selection of reagents for creation of specific liposomes of certain properties are beyond the scope of this chapter, but here, we would outline a simplistic protocol to prepare and qualify an uniform batch of simple liposome with basic cargo. This chapter will attempt to provide the reader with a starting point for this immensely potent tool to build upon the right kind of liposome, appropriate for their studies.

Key words Liposome, Sonication, Vesicle, Lipid, Drug delivery, SUV, LUV, Phospholipids, Lipid bilayer

1 Introduction

The etymology of liposomes originates from very early work of Gerald Weissmann, where he renamed the hitherto known *artificial spherules* and described their properties. He recognized that these vesicles are very similar to natural membrane bound structures and capable of mimicking behavior of erythrocytes, lysosomes, and mitochondria, when exposed to similar physical or chemical stimuli in a biological system [1]. At this time, as acknowledged by Weissmann, the basic structure and composition of natural membranes was not well known and this knowledge would come several years later with the seminal work of Singer and Nicolson with their report of *Fluid Mosaic Model* of membrane structure [2]. Before the advent of our understanding of the nature of biological membranes, it was clear that its biological properties could be described by the chemistry and physics of constituent lipids, which was vindicated by the fluid mosaic model. Further work on biological membranes has improved upon *fluid mosaic* but fundamentally remained faithful to the basic arrangement of

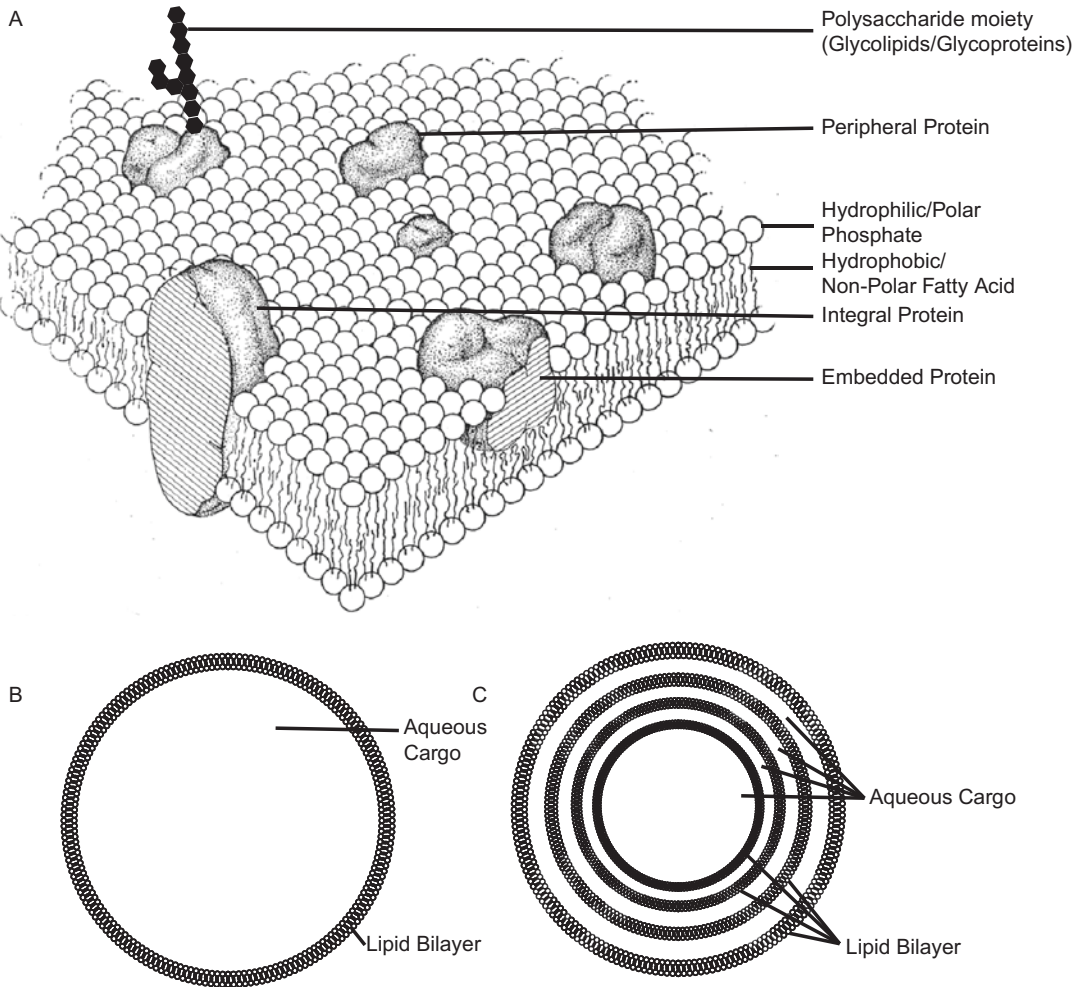


Fig. 1 (a) Fluid Mosaic Model of biological membranes as adapted from Singer and Nicolson's 1972 paper [2], depicting a phospholipid bilayer with proteins embedded to various degrees in the bilayer. (b) Unilamellar Vesicle with single spherical phospholipid bilayer membrane and (c) Multilamellar vesicle with multiple layers of lipid bilayer, interspersed with aqueous cargo

lipid bilayer postulated by Singer and Nicolson's original work (Fig. 1a). As we know today, this is the most thermodynamically stable configuration of phospholipids constituting plasma membrane, membranes of the organelles, and natural extracellular vesicles and exosomes [3–5]. Synthesis and usage of liposomes mimic the horizontal transfer of information already existing in biological system, while expanding on the flexibility and latitude of going a step further to modulate diseased cells and tissues by delivering drugs and excipients without incurring off target effects [6].

Liposomes are synthetic self-assembled vesicles, which can be prepared from natural phospholipids and cholesterol, which encapsulate a cargo of choice, appropriate for the goal of the experiment. Since

natural constituents are used for the membrane, which are more often than not, extracted from biological tissues (both plant and animal origin) and brought to extreme purity, liposomes tend to be relatively less toxic for biological applications, including tissue-specific, toxic, and nontoxic drug delivery for various diseases including cancer [6–12]. By altering the lipid composition and engineering proteins and other macromolecules into lipid bilayer of liposomes, significant changes in the properties (tissue-specificity, bioavailability, escape from gastric acid/professional antigen-presenting cells, longevity, etc.) have been achieved [7, 13]. Fundamentally, liposomes are classified based on their constitution and size. Depending on the presence of single or multiple lipid bilayer(s), they could be classified as unilamellar vesicles (Fig. 1b) or multilamellar vesicles (MLV; Fig. 1c). Depending on size, the unilamellar vesicles are further classified into Small Unilamellar Vesicles (SUVs) and Large Unilamellar Vesicles (LUVs). In all cases, liposomes are either a single, or an onion-like multilayered spherical lipid bilayer, enclosing an aqueous cargo, both of which (liposome size/layers and constitution of cargo) can be modified based on the target of the experiment.

In this chapter, a very simplistic protocol is being presented for the preparation of basic SUVs. This is a widely used method for the preparation of liposomes with the cargo of choice, which in this case will be presented as HEPES Buffered Saline (HBS), but may be substituted with excipients of experimenter's choice.

2 Materials

1. Phospholipids— α -Phosphatidylcholine from Chicken egg, L- α -Phosphatidylserine (Bovine brain), and L- α -Phosphatidylethanolamine (Bovine liver) (*see Note 1*).
2. Vacuum Evaporator—Eppendorf 5301 or Labonco Rapidvap vacuum system.
3. Water bath sonicator—Branson 2510 or 5510 (*see Note 2*).
4. Hepes Buffered Saline—100 mM NaCl, 20 mM HEPES, adjust to pH 7.5 using NaOH (*see Note 3*).
5. Gas phase: Nitrogen or Argon.
6. Fume hood.
7. Vortex mixer.

3 Methods

1. Inside the fume hood, mix L- α -Phosphatidylcholine, L- α -Phosphatidylserine, and L- α -Phosphatidylethanolamine in a 2:2:1 molar ratio in a glass tube (*see Note 4*).

2. Still inside the fume hood, dry down the mixture of phospholipids, preferably under a very gentle stream of Nitrogen or Argon gas (*see Note 5*).
3. Dry the residual chloroform in a vacuum evaporator (*see Note 6*).
4. Resuspend dried phospholipids in HBS. Let it stand at room temperature for an hour to overnight. Cover the tube with Parafilm (*see Note 7*).
5. Vortex the tube three to four times for 30 s each. This should result in a milky suspension. Vortex more if clumps remain. Gently pipette up and down with a Pasteur pipette if vortex mixing does not disperse clumps (*see Note 8*).
6. Set the tube with O-rings provided with the bath sonicator and set up sonication at medium level till the solution turns almost clear (from milky). Check every 15–20 min (*see Notes 9 and 10*).

4 Notes

1. Best to purchase these phospholipids already dissolved in chloroform. Both Sigma-Aldrich and Avanti Polar Lipids supply this in >99% pure form, dissolved in chloroform.
2. For the purposes of liposome preparation, a probe sonicator may also be used. However, water bath sonicators are sufficient, inexpensive and do not require protective earphones. Another advantage to bath sonicators is that probe sonicators tend to heat up and cause decomposition of phospholipids at the surface of the probe and sometimes leach metal into the solution.
3. Mix NaCl and HEPES at room temperature. Titrate to pH 7.5 gently by adding 0.5–1 M NaOH solution. Bring it close to pH 7.5. If the solution becomes more alkaline, do not add acid to bring the pH down. Instead, double the volume with 100 mM NaCl and 20 mM HEPES and titrate again. Use freshly mixed and titrated solution for each liposome preparation.
4. Specific volume and concentration will depend on the vendor from where the phospholipids are purchased and the original concentration. Ratio based on molar concentration will equalize the final ratio of the components. Glass tube is preferred over plastic or polycarbonate tubes. Tube size is not critical, but the starting liquid volume should not exceed 5% of tube length. Popular choice is 13 × 100 mm tubes (low surface tension) with maximum 250 μ L liquid volume.
5. Argon is preferred, but Nitrogen works too. Attach a Pasteur pipette to the outlet tube from the appropriate gas cylinder. Adjust gas to a very gentle flow, so as not to agitate the phospholipid mixture inside the tube. Insert the tube so as to rest the tip of the Pasteur pipette an inch above the liquid interface.

Do not insert the pipette tip into the phospholipid mixture. With 13 × 100 mm tube and 200 μL phospholipid mixture, it would take between 1 and 2 h for the mixture to dry.

6. For this step, do not exceed 40 °C temperature. Room temperature is preferred. Vacuum evaporation between 45 and 60 min should be sufficient. This is the **first stop-point** in this protocol. At this point, the tube with dried phospholipid may be covered with parafilm and refrigerated at 4 °C. Please get the tube to room temperature with the parafilm on, to prevent hydration of the phospholipids at this stage. Usually, 20–30 min at room temperature is enough.
7. The optimal ratio for resuspension is 1 mL per total μM concentration of phospholipids in the original mixture. If a total of 2 μM phospholipid mix was taken, resuspend in 2 mL HBS. If left for overnight incubation, consider leaving it at the lowest shelf of refrigerator (10–15 °C). Another option is to leave it at room temperature with 0.02% Na-Azide solution. Bring to room temperature before the next step as described in **Note 6**. This is the **second stop-point** in this protocol.
8. Never use polycarbonate tips with auto-pipettes. Always use glass Pasteur pipettes. At this stage, we have obtained MLVs. If some clumps prove to be resistant to dispersion, selectively pick them up with Pasteur pipette and reject them.
9. At this stage, we are sonicating to convert MLVs to SUVs. It is a good idea to have a thermometer in the water bath sonicator and not allow the temperature to exceed 40 °C. Adding ice cubes within nylon mesh, away from the tube to maintain room temperature works nicely. For scaleup, it is preferred to have multiple tubes, rather than higher volume in a single tube.
10. At **step 6** in the protocol above, gentle sonication was used to disperse the MLVs to generate SUVs encapsulating the added HBS. These SUVs can be stored at 4 °C for 5–7 days before downstream use. For generating LUVs, with higher retention volumes, SUVs from **step 6** can be subjected to repeated freeze-thaw, followed by mild sonication. Altering the phospholipid composition for specific experimental needs and other methods for generating special liposomes are also available in the literature [6–8, 10, 12–22].

References

1. Sessa G, Weissmann G (1968) Phospholipid spherules (liposomes) as a model for biological membranes. *J Lipid Res* 9(3):310–318
2. Singer SJ, Nicolson GL (1972) The fluid mosaic model of the structure of cell membranes. *Science (New York, NY)* 175(4023):720–731. doi:10.1126/science.175.4023.720
3. Chahar HS, Bao X, Casola A (2015) Exosomes and their role in the life cycle and pathogenesis of RNA viruses. *Viruses* 7(6):3204–3225. doi:10.3390/v7062770
4. Madison MN, Okeoma CM (2015) Exosomes: implications in HIV-1 pathogenesis. *Viruses* 7(7):4093–4118. doi:10.3390/v7072810

5. Mu J, Zhuang X, Wang Q, Jiang H, Deng ZB, Wang B, Zhang L, Kakar S, Jun Y, Miller D, Zhang HG (2014) Interspecies communication between plant and mouse gut host cells through edible plant derived exosome-like nanoparticles. *Mol Nutr Food Res* 58(7):1561–1573. doi:[10.1002/mnfr.201300729](https://doi.org/10.1002/mnfr.201300729)
6. Akbarzadeh A, Rezaei-sadabady R, Davaran S, Joo SW, Zarghami N, Hanifehpour Y, Samiei M, Kouhi M, Nejati-Koshki K (2013) Liposome: classification, preparation, and applications. *Nanoscale Res Lett* 8(102):1–9. doi:[10.1002/asia.201500957](https://doi.org/10.1002/asia.201500957)
7. Monteiro N, Martins A, Reis RL, Neves NM (2014) Liposomes in tissue engineering and regenerative medicine. *J R Soc Interface* 11(101):20140459–20140459. doi:[10.1098/rsif.2014.0459](https://doi.org/10.1098/rsif.2014.0459)
8. Abbasi E, Aval SF, Akbarzadeh A, Milani M, Nasrabadi HT, Joo SW, Hanifehpour Y, Nejati-Koshki K, Pashaei-Asl R (2014) Dendrimers: synthesis, applications, and properties. *Nanoscale Res Lett* 9(1):247–247. doi:[10.1186/1556-276X-9-247](https://doi.org/10.1186/1556-276X-9-247)
9. Huang H, Cruz W, Chen J, Zheng G (2015) Learning from biology: synthetic lipoproteins for drug delivery. *Wiley Interdiscip Rev Nanomed Nanobiotechnol* 7(3):298–314. doi:[10.1002/wnan.1308](https://doi.org/10.1002/wnan.1308)
10. Shahzad MMK, Mangala LS, Han HD, Lu C, Bottsford-Miller J, Nishimura M, Mora EM, Lee J-W, Stone RL, Pecot CV, Thanappapasr D, Roh J-W, Gaur P, Nair MP, Park Y-Y, Sabnis N, Deavers MT, Lee J-S, Ellis LM, Lopez-Berestein G, McConathy WJ, Prokai L, Lacko AG, Sood AK (2011) Targeted delivery of small interfering RNA using reconstituted high-density lipoprotein nanoparticles. *Neoplasia (New York, NY)* 13(4):309–319. doi:[10.1593/neo.101372](https://doi.org/10.1593/neo.101372)
11. McConathy WJ, Nair MP, Paranjape S, Mooberry L, Lacko AG (2008) Evaluation of synthetic/reconstituted high-density lipoproteins as delivery vehicles for paclitaxel. *Anti-Cancer Drugs* 19:183–188. doi:[10.1097/CAD.0b013e3282f1da86](https://doi.org/10.1097/CAD.0b013e3282f1da86)
12. Skalickova S, Nejdil L, Kudr J, Ruttkay-Nedecky B, Jimenez AMJ, Kopel P, Kremplova M, Masarik M, Stiborova M, Eckschlager T, Adam V, Kizek R (2016) Fluorescence characterization of gold modified liposomes with antisense N-myc dna bound to the magnetisable particles with encapsulated anticancer drugs (doxorubicin, ellipticine and etoposide). *Sensors (Switzerland)* 16(3):1–11. doi:[10.3390/s16030290](https://doi.org/10.3390/s16030290)
13. Immordino ML, Dosio F, Cattel L (2006) Stealth liposomes: Review of the basic science, rationale, and clinical applications, existing and potential. *Int J Nanomedicine* 1(3):297–315. doi:[10.1023/A:1020134521778](https://doi.org/10.1023/A:1020134521778)
14. Baillie G, Owens MD, Halbert GW (2002) A synthetic low density lipoprotein particle capable of supporting U937 proliferation in vitro. *J Lipid Res* 43(1):69–73
15. Batzri S, Korn ED (1973) Single bilayer liposomes prepared without sonication. *Biochim Biophys Acta* 298(4):1015–1019. doi:[10.1016/0005-2736\(73\)90408-2](https://doi.org/10.1016/0005-2736(73)90408-2)
16. Luna AC, Saraiva GK, Filho OM, Chierice GO, Neto SC, Cuccovia IM, Maria DA (2016) Potential antitumor activity of novel DODAC/PHO-S liposomes. *Int J Nanomedicine* 11:1577–1591. doi:[10.2147/IJN.S90850](https://doi.org/10.2147/IJN.S90850)
17. Huang HC, Mallidi S, Liu J, Chiang CT, Mai Z, Goldschmidt R, Ebrahim-Zadeh N, Rizvi I, Hasan T (2016) Photodynamic therapy synergizes with irinotecan to overcome compensatory mechanisms and improve treatment outcomes in pancreatic cancer. *Cancer Res* 76(5):1066–1077. doi:[10.1158/0008-5472.CAN-15-0391](https://doi.org/10.1158/0008-5472.CAN-15-0391)
18. Liu D, He C, Wang AZ, Lin W (2013) Application of liposomal technologies for delivery of platinum analogs in oncology. *Int J Nanomedicine* 8:3309–3319. doi:[10.2147/IJN.S38354](https://doi.org/10.2147/IJN.S38354)
19. Silva RGD, Huang R, Morris J, Fang J, Gracheva EO, Ren G, Kontush A, Jerome WG, Rye K-A, Davidson WS (2008) Structure of apolipoprotein A-I in spherical high density lipoproteins of different sizes. *Proc Natl Acad Sci U S A* 105(34):12176–12181. doi:[10.1073/pnas.0803626105](https://doi.org/10.1073/pnas.0803626105)
20. Tasaniyananda N, Chairri U, Tungtrongchitr A, Chaicumpa W, Sookrung N (2016) Mouse model of cat allergic rhinitis and intranasal liposome-adjuvanted refined Fel d 1 vaccine. *PLoS One* 11(3):e0150463. doi:[10.1371/journal.pone.0150463](https://doi.org/10.1371/journal.pone.0150463)
21. Wagner A, Vorauer-Uhl K (2011) Liposome technology for industrial purposes. *J Drug Deliv* 2011:1–9. doi:[10.1155/2011/591325](https://doi.org/10.1155/2011/591325)
22. Yoon YI, Kwon YS, Cho HS, Heo SH, Park KS, Park SG, Lee SH, Hwang SI, Kim YI, Jae HJ, Ahn GJ, Cho YS, Lee H, Lee HJ, Yoon TJ (2014) Ultrasound-mediated gene and drug delivery using a microbubble-liposome particle system. *Theranostics* 4(11):1133–1144. doi:[10.7150/thno.9945](https://doi.org/10.7150/thno.9945)

On Electrochemical Methods for Determination of Protein-Lipid Interaction

Zhiping Hu and Yanli Mao

Abstract

Amyloid- β ($A\beta$) peptides are important and reliable molecular biomarkers for the diagnosis and prognosis of Alzheimer's disease. Aggregation and fibrillization of $A\beta$ peptides on ganglioside GM1 (GM1)-containing lipid membranes is considered a cause of neurodegenerative disease. Because GM1 is abundant in the central nervous system and plays a key role in the aggregation of $A\beta$, the interaction of $A\beta$ with supported planar lipid bilayers (SPBs) containing GM1 is of great significance. We have prepared SPBs containing GM1 in order to study the electrochemical characteristics of GM1/sphingomyelin/cholesterol SPBs and their interaction with $A\beta(1-40)$ by cyclic voltammetry and electrochemical impedance spectroscopy (EIS), which proves that electrochemical is a promising method for analyzing the interaction between peptides and lipid membranes.

Key words Protein-lipid interaction, Electrochemical, Alzheimer's disease, Amyloid- β , Ganglioside GM1, Lipid bilayer

1 Introduction

Alzheimer's disease (AD) is a very common neurodegenerative disorder characterized by memory loss, disorientation, and difficulty performing daily tasks, among other issues. Many studies have shown that one of the primary pathological hallmarks of AD is the presence of insoluble neuritic plaques composed primarily of amyloid- β peptides ($A\beta$) [1, 2]. $A\beta$ peptides are important and reliable molecular biomarkers for the diagnosis and prognosis of Alzheimer's disease. $A\beta$ peptides, mainly containing $A\beta(1-40)$ and $A\beta(1-42)$, are generated by normal cleavage of membrane-anchored amyloid precursor protein by β - and γ -secretases.

Many reports have suggested that aggregation of toxic $A\beta$ peptides occurs on lipid membranes which contain ganglioside GM1 (GM1) [3, 4]. GM1 is abundant in the central nervous system and plays a key role in the aggregation of $A\beta$ [5, 6]. A specific form of $A\beta$ bound to GM1 has been identified in early pathological changes

associated with AD, and the GM1-bound form of A β may serve as a seed for the formation of A β aggregates [7]. In particular, GM1, sphingomyelin (SM), and cholesterol (Chol) are crucial components of membrane rafts which play an important role in signal transduction, cellular transport, and lipid sorting. Previous studies have used nuclear magnetic resonance to study the interaction of A β (1–40) with GM1 using GM1/SM/Chol micelles as model systems [8]. It has also been reported that A β is bound by a cluster of liposome composed of GM1/SM/Chol [9, 10]. Furthermore, structural changes in A β -bound membranes composed of GM1/SM/Chol have been studied using circular dichroism [10].

Due to the complexity of biomembranes, artificial lipid bilayers have been widely used to study the interaction between proteins and biomembranes. In particular, supported planar lipid bilayers (SPBs) have been used as *in vitro* cell membrane systems for studying lipid-protein and cell-cell interactions. A variety of different approaches have been utilized to study these interactions, such as dual polarization interferometry [11], multiple molecular dynamics simulations [12, 13], optical methods [14], and electrochemistry [15, 16]. Among them, the electrochemical methods are easy, cost-effective, and based on attachment of lipid membrane preparations on the electrode [15–17]. For instance, the interaction between daunomycin with peptide-1 and U937 cells, a human histiocyte-related lymphoma cell line, has been monitored by voltammetry [18], and the interaction of baicalin with lipid membranes by cyclic voltammetry (CV) [19].

Some previous reports have probed A β aggregation and its interaction with biomolecules, drugs, and metal using electrochemical techniques [20, 21]. To the best of our knowledge, no reports have used electrochemical methods to investigate interactions between A β and SPBs containing GM1 yet. In the present work, we have fabricated SPBs composed of GM1/SM/Chol on an Au electrode, then investigated A β (1–40) aggregation and its effect on GM1/SM/Chol SPBs using CV and electrochemical impedance spectroscopy (EIS). The results are further confirmed by fluorescence microscopy and atomic force microscopy (AFM) methods.

2 Materials

Ganglioside-GM1 (bovine brain), Cholesterol and Amyloid beta(1–40), and Thioflavin T (ThT) are purchased from Sigma-Aldrich (Shanghai, China); Sphingomyelin (brain) and C6-NBD-Sphingomyelin (NBD-SM) are purchased from Avanti (Alabaster, Alabama). Aluminum oxide powders (0.05 μm , 0.1 μm) are purchased from Aidahengsheng Technology Co., Ltd. (Tianjin, China). CV and EIS measurements were carried out using a CHI660A electrochemical work station (Chenhua Instrument

Co. Ltd., Shanghai, China). A three-electrode electrochemical system was used for CV and EIS experiments, where an Au electrode, Pt plate, and saturated Ag/AgCl (KCl-saturated) electrode served as working, counter, and reference electrodes, respectively. CV was conducted in a potential range of -0.1 to 0.6 V. The formal potential of the 0.05 M $\text{K}_3\text{Fe}(\text{CN})_6/0.05$ M $\text{K}_4\text{Fe}(\text{CN})_6$ probe solution was 0.23 V, which was also adopted for impedance measurements, and EIS was measured from 0.5 to 10^5 Hz with an amplitude of 5 mV. CV and EIS measurements were carried out using a CHI660A electrochemical work station (Chenhua Instrument Co. Ltd., Shanghai, China). A three-electrode electrochemical system was used for CV and EIS experiments, where an Au electrode, Pt plate, and saturated Ag/AgCl (KCl-saturated) electrode served as working, counter, and reference electrodes, respectively. CV was conducted in a potential range of -0.1 to 0.6 V. The formal potential of the 0.05 M $\text{K}_3\text{Fe}(\text{CN})_6/0.05$ M $\text{K}_4\text{Fe}(\text{CN})_6$ probe solution was 0.23 V (*see Note 1*), which was also adopted for impedance measurements, and EIS was measured from 0.5 to 10^5 Hz with an amplitude of 5 mV. Fluorescence images were collected with a fluorescence microscope (Nikon Ti-E, Tokyo, Japan) equipped with a EMCCD camera (Evolve 512 Delta, Photometrics, Tokyo, Japan).

2.1 Preparation of Vesicles

SPBs are composed of GM1, SM, and Chol in a 20:40:40 molar ratio. Appropriate amounts of all lipids are dissolved in a 1:1 (v/v) chloroform: methanol solvent (*see Notes 2 and 3*). Dry lipid films are formed by evaporation under a stream of nitrogen and then stored in a vacuum overnight (*see Note 4*). The lipid film is rehydrated to a final concentration of 0.12 mg/mL using a buffer solution (150 mM NaCl, 10 mM 4-(2-Hydroxyethyl)piperazine-1-ethanesulfonic acid (HEPES), 2 mM CaCl_2 ; pH 7.4), freeze-thawed three times, and then sonicated at 70 °C to obtain small unilamellar vesicles (*see Note 5*). The concentration of NBD-SM is 1% (mol/mol).

2.2 Preparation of A β (1–40) Solution

A β (1–40) is first dissolved in a 0.02% ammonia solution and then centrifuged at $21700 \times g$ at 4 °C for 3 h to remove insoluble aggregates. The final concentration of A β (1–40) peptide in solution is 600 μM , and this solution is stored at -20 °C until use. The A β (1–40) monomer solution is diluted to a concentration of 100 μM with Milli-Q water at the time of assay (*see Note 6*).

3 Method

3.1 Preparation of Au Electrode

Prior to SPBs formation, the Au electrode (diameter is 2 mm) is polished with alumina slurry (0.05 μm , 0.1 μm) on polishing cloth then washed in an ultrasonic bath with ionized water, acetone, and pure water for 5 min each, respectively, to remove any adhesive particles. In order to polarize the electrode, it is electrochemically



Fig. 1 The water contact angle (WCA) of Au substrate is 27° , which shows the surface of Au has a good hydrophilicity, so the lipid vesicles can form planar bilayers on the surface

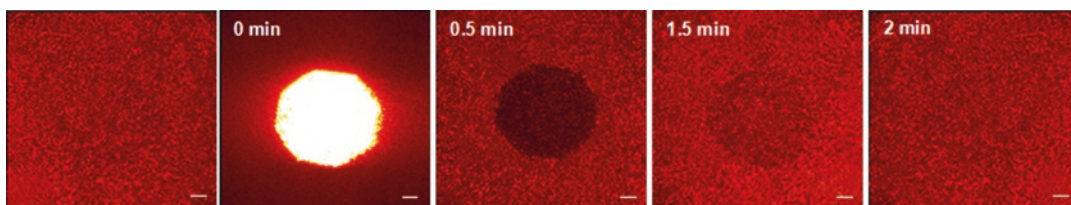


Fig. 2 Sequential fluorescence images after photobleaching of GM1/SM/Chol SPBs formed on the Au electrode surface. The observed times are before and after photobleaching (0, 0.5, 1.5, and 2.0 min) from left to right. The scale bar is $0.05 \mu\text{m}$

polished by scanning from -0.3 to 1.6 V (versus Ag/AgCl) in a 0.5 M H_2SO_4 solution for 15 min. The water contact angle of the electrode just after the electrochemical polishing is 27° (Fig. 1), which shows the hydrophilicity of the electrode surface.

3.2 Preparation of SPBs on the Au Electrode

After polarization, the Au electrode is immersed in the small unilamellar vesicle solution for 12 h at 70°C (see Note 7) then immediately transferred into 0.05 M $\text{K}_3\text{Fe}(\text{CN})_6/0.05$ M $\text{K}_4\text{Fe}(\text{CN})_6$ containing 0.5 M NaCl (see Notes 8, 9 and 1). The SPBs on Au electrode are formed, which can be observed by fluorescence microscope (Fig. 2).

3.3 Electrochemistry

CV and EIS measurements are carried out using a electrochemical work station. A three-electrode electrochemical system is used for CV and EIS experiments, where an Au electrode, Pt plate, and saturated Ag/AgCl (KCl-saturated) electrode served as working, counter, and reference electrodes, respectively. CV is conducted in

a potential range of -0.1 to 0.6 V. The formal potential of the 0.05 M $\text{K}_3\text{Fe}(\text{CN})_6/0.05$ M $\text{K}_4\text{Fe}(\text{CN})_6$ probe solution is 0.23 V, which is also adopted for impedance measurements, and EIS is measured from 0.5 to 10^5 Hz with an amplitude of 5 mV.

3.4 Fluorescence Microscope

Fluorescence images are collected with a fluorescence microscope equipped with a EMCCD camera. The ThT is added after $\text{A}\beta(1-40)$ interacting with SPBs; the final concentration of ThT is 5 μM .

3.5 AFM (Atomic Force Microscope)

The samples are kept in fluid environment. AFM is performed in the buffer solution using a scanning probe microscopy system using a Si_3N_4 cantilever. The spring constant and the resonance frequency of the cantilevers were 1.6 N/m and 26 kHz.

4 Notes

1. Filter the electrolyte containing $\text{K}_3\text{Fe}(\text{CN})_6/\text{K}_4\text{Fe}(\text{CN})_6$ and NaCl before using.
2. Prepare the precursor solution include GM1, SM, and Chol by vibrating for at least 1 ht.
3. The precursor solution containing GM1, SM, and Chol should be stored under -20 $^\circ\text{C}$.
4. Dry lipid films are formed by evaporation under a stream of nitrogen and then stored in a vacuum oven overnight.
5. The solution containing small unilamellar vesicles should be store at $0-4$ $^\circ\text{C}$.
6. Store the $\text{A}\beta(1-40)$ solution under -20 $^\circ\text{C}$. The peptides would degenerate easily at room temperature.
7. Immerse the polished Au electrode in the small unilamellar vesicle solution for at least 12 h at 70 $^\circ\text{C}$.
8. Sonicate the lipid mixture solution for 10 min to disperse lipids vesicles before using.
9. The Au electrode should be used after polarization immediately.

Acknowledgements

This work was supported by National Natural Science Foundation of China (Grant No. 21103043), the Science and technology research project of Henan province (No. 142102210389), the National Science Foundation of China (No. 21173068), and the Program for Innovative Research Team (in Science and Technology) in the University of Henan Province (No. 13IRTSTHN01).

References

1. Harper JD, Lansbury PT Jr (1997) Models of amyloid seeding in Alzheimer's disease and scrapie: mechanistic truths and physiological consequences of the time-dependent solubility of amyloid proteins. *Annu Rev Biochem* 66(1):385–407
2. Lansbury PT (1997) Structural neurology: are seeds at the root of neuronal degeneration? *Neuron* 19(6):1151–1154
3. Matsuzaki K (2007) Physicochemical interactions of amyloid β -peptide with lipid bilayers. *Biochim Biophys Acta* 1768(8):1935–1942
4. Matsuzaki K, Kato K, Yanagisawa K (2010) A β polymerization through interaction with membrane gangliosides. *Biochim Biophys Acta* 1801(8):868–877
5. Oikawa N, Yamaguchi H, Ogino K, Taki T, Yuyama K, Yamamoto N, Shin R-W, Furukawa K, Yanagisawa K (2009) Gangliosides determine the amyloid pathology of Alzheimer's disease. *Neuroreport* 20(12):1043–1046
6. Okada T, Ikeda K, Wakabayashi M, Ogawa M, Matsuzaki K (2008) Formation of toxic A β (1–40) fibrils on GM1 ganglioside-containing membranes mimicking lipid rafts: polymorphisms in A β (1–40) fibrils. *J Mol Biol* 382(4):1066–1074
7. Yanagisawa K, Odaka A, Suzuki N, Ihara Y (1995) GM1 ganglioside-bound amyloid beta-protein (a beta): a possible form of preamyloid in Alzheimer's disease. *Nat Med* 1(10):1062–1066
8. Brambilla D, Le Droumaguet B, Nicolas J, Hashemi SH, Wu L-P, Moghimi SM, Couvreur P, Andrieux K (2011) Nanotechnologies for Alzheimer's disease: diagnosis, therapy, and safety issues. *Nanomedicine* 7(5):521–540
9. Kakio A, S-I N, Yanagisawa K, Kozutsumi Y, Matsuzaki K (2001) Cholesterol-dependent formation of GM1 ganglioside-bound amyloid β -protein, an endogenous seed for Alzheimer amyloid. *J Biol Chem* 276(27):24985–24990
10. Ikeda K, Yamaguchi T, Fukunaga S, Hoshino M, Matsuzaki K (2011) Mechanism of amyloid β -protein aggregation mediated by GM1 ganglioside clusters. *Biochemistry* 50(29):6433–6440
11. Sanghera N, Swann MJ, Ronan G, Pinheiro TJ (2009) Insight into early events in the aggregation of the prion protein on lipid membranes. *Biochim Biophys Acta* 1788(10):2245–2251
12. Mori K, Mahmood MI, Neya S, Matsuzaki K, Hoshino T (2012) Formation of GM1 ganglioside clusters on the lipid membrane containing sphingomyelin and cholesterol. *J Phys Chem B* 116(17):5111–5121
13. Yahi N, Aulas A, Fantini J (2010) How cholesterol constrains glycolipid conformation for optimal recognition of Alzheimer's β amyloid peptide (A β 1–40). *PLoS One* 5(2):e9079
14. Wang J, Wang L, Liu S, Han X, Huang W, Wang E (2003) Interaction of K₇Fe₃P₂W₁₇O₆₂H₂ with supported bilayer lipid membranes on platinum electrode. *Biophys Chem* 106(1):31–38
15. Han X, Tong Y, Huang W, Wang E (2002) Study of the interaction between lanthanide ions and a supported bilayer lipid membrane by cyclic voltammetry and ac impedance. *J Electroanal Chem* 523(1):136–141
16. Liu X, Huang W, Wang E (2005) An electrochemical study on the interaction of surfactin with a supported bilayer lipid membrane on a glassy carbon electrode. *J Electroanal Chem* 577(2):349–354
17. Ho Y-F, Wu M-H, Cheng B-H, Chen Y-W, Shih M-C (2009) Lipid-mediated preferential localization of hypericin in lipid membranes. *Biochim Biophys Acta* 1788(6):1287–1295
18. Sugawara K, Kadoya T, Kuramitz H (2015) Monitoring of the interaction between U937 cells and electroactive daunomycin with an arginine-rich peptide. *Bioelectrochemistry* 105:95–102
19. Zhang Y, Wang X, Wang L, Yu M, Han X (2014) Interactions of the baicalin and baicalein with bilayer lipid membranes investigated by cyclic voltammetry and UV-Vis spectroscopy. *Bioelectrochemistry* 95:29–33
20. Chikae M, Fukuda T, Kerman K, Idegami K, Miura Y, Tamiya E (2008) Amyloid- β detection with saccharide immobilized gold nanoparticle on carbon electrode. *Bioelectrochemistry* 74(1):118–123
21. Islam K, Jang Y-C, Chand R, Jha SK, Lee HH, Kim Y-S (2011) Microfluidic biosensor for β -amyloid (1–42) detection using cyclic voltammetry. *J Nanosci Nanotechnol* 11(7):5657–5662

Angiogenesis Model of Cornea to Understand the Role of Sphingosine 1-Phosphate

Joseph L. Wilkerson and Nawajes A. Mandal

Abstract

The role of sphingolipids, mainly sphingosine 1-phosphate (S1P) and the receptors for which it serves as a ligand, is an interesting and promising area in both sphingolipid and vascular biology. S1P is crucial for establishing blood flow competent blood vessels (Jung et al. *Dev Cell* 23(3):600–610, 2012). The role of S1P in neovascular pathology is of great interest and promising as a target for treatment. Here we describe an easy and affordable in vivo model of neovascularization by an alkali chemical burn to the cornea. This gives a consistent and easy way to quantitate methods for neovascularization.

Key words Angiogenesis, Neovascularization, Cornea, Sphingosine 1-phosphate

1 Introduction

Determining the role of sphingolipids, specifically sphingosine 1-phosphate and its receptors (S1P1-5), has been a major focus in various fields, one of which is angiogenesis and the maintenance of blood vessels [1]. It is known that S1P, working through S1P1, is responsible for establishing and maintaining an interplay between angiogenic signals and VE-cadherins establishing adherens junctions responsible for flow competent blood vessels [2, 3]. In contrast, S1P2 signaling has been shown to play a role in enhancing pathological angiogenic events [4]. Neovascular pathologies play a significant role in a wide range of diseases from tumor biology to complications with diabetic retinopathies that can lead to blindness [1, 5]. It is critical to understand the interaction of sphingolipids in this process by using animal model systems. Here we describe a method to study neovascularization in an adult mouse without the need for specialized equipment necessary as in other models of in vivo neovascularization. The cornea provides an excellent model for neovascularization because the tissue is avascular (Fig. 1a). A 30 s alkali burn to the center of the cornea by sodium hydroxide induces a strong response and blood vessels grow into the center

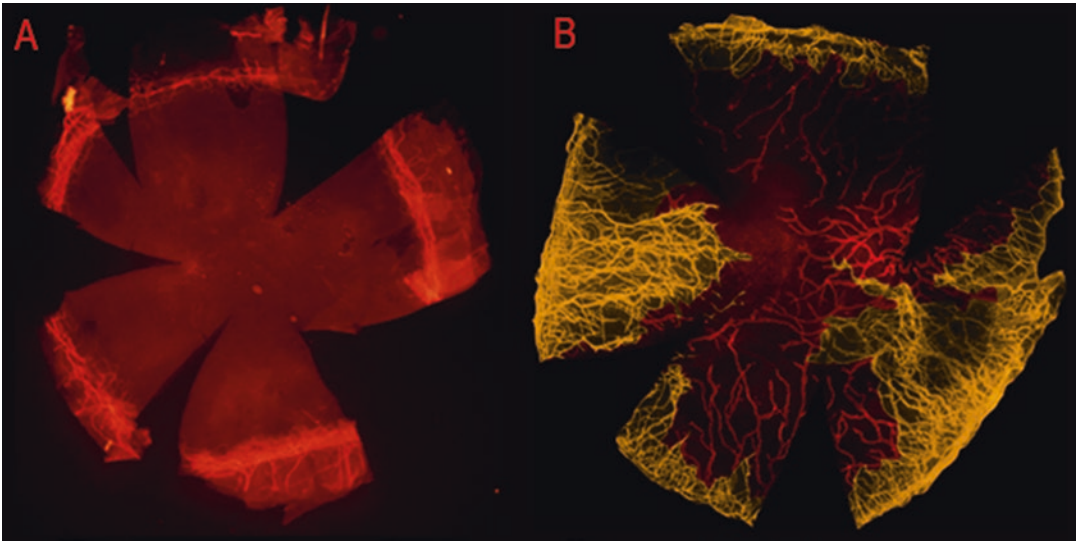


Fig. 1 Cornea from an alkali unburned and burned cornea from the same animal, stained with CD31 to label blood vessels. **(a)** An unburned normal cornea. The *center* is avascular, surrounded by the limbal vessels. **(b)** A burned cornea 10 days post-burn. The areas of neovascularization are highlighted in *yellow*. Lymphatic vessels can also be seen growing into the cornea (*red*)

of the tissue (Fig. 1b). The alkali burn model is well established and produces reproducible results equal to other classic methods of cornea models that require specialized surgical skills [6]. While many cornea models require a rating system similar to clinical systems, scored by the investigator, we will explain how to determine the full degree of neovascularization that occurs [7]. Easy access to the cornea also provides a convenient *in vivo* model for drug delivery by either a systemic approach or direct application via eye drops.

2 Materials

2.1 Corneal Wounding

1. Ketamine/xylazine.
2. 0.5% proparacaine hydroxide.
3. 2 mm round punches of Whatman No.1 filter paper. These are done by using a hole punch specific to the size; these can be obtained at any major craft store or online retailer.
4. 1 M sodium hydroxide is made with ultrapure water and NaOH pellets. The solution is stored at room temperature for up to 6 months.
5. 0.9% sterile saline.
6. 0.5% erythromycin ophthalmic ointment.

2.2 Cornea Harvest and Immunohistochemistry

1. 4% paraformaldehyde: 100 mL of a 20% solution is first made from powder in ultrapure water. The solution is heated to 60 °C while constantly being stirred. (Do not go over 60 °C as the solution will become highly acidic.) As it stirs measure 4 g of NaOH pellets and dissolve in 10 mL of ultrapure water. Add six drops of this solution to the heated PFA. The solution should turn clear in a few seconds. Filter through Whatman No.1 filter paper. Dilute this 20% solution to 4% in ultrapure water and 2× PBS so that the final solution is 4% PFA in 1× PBS.
2. Triton X-100 from VWR. Diluted to 10% in 1× PBS is a good stock solution to make the 1% Triton, 0.1% Triton, and block buffer.
3. Block buffer: horse serum aliquoted and stored at –20 °C. This is used to make 10% solution of horse serum in 1% Triton and 1× PBS.
4. Antibodies: monoclonal mouse anti-Armenian hamster CD-31 (PECAM-1) concentrate from DSHB. Mouse anti-rat Lyve-1 from eBioscience.
5. 50% glycerol diluted in 1× PBS.

3 Methods

3.1 Corneal Wounding

All of the of procedures, the dose and route of anesthetic drugs, and postprocedure care should be approved by the appropriate authority such as the Institutional Animal Care and Use Committee (IACUC) from your institute before starting the experiment. A single eye undergoes the chemical burn, leaving the second eye as a non-burn control (Fig. 1). We have observed that if the non-burned control eye has neovascularization then the burned eye will be extremely severe. These cases are not quantified. Neovascularization is also highly variable from mouse to mouse. It is recommended to use at least an *n* of 10 for a given experiment.

1. Anesthetize mice with an intraperitoneal injection of ketamine (100 mg/kg) and xylazine (10 mg/kg). Allow the anesthetic to completely incapacitate the animal.
2. Trim whiskers and eyelashes with small dissection scissors (*see Note 1*).
3. Apply 0.5% proparacaine hydroxide to the eye to further numb the tissue then wick dry (*see Note 2*).
4. Apply a 2 mm round piece of Whatman No.1 filter paper, soaked in 1 M NaOH to the central cornea for 30 s. This is best done under a surgical or dissection microscope (*see Note 3*).
5. Quickly remove the filter paper pad and immediately wash the eye with 20 mL of 0.9% sterile saline solution.

6. Apply a topical antibiotic, erythromycin ophthalmic ointment 0.5%.
7. Mice should be observed to make sure they awake from anesthetic.
8. Ten days postinjury the mice can be euthanized and corneal tissue harvested.

3.2 Cornea Harvest and Immuno-histochemistry

1. Enucleate the eye with a pair of fine tip forceps. Clean off excess tissue with a pair of micro-scissors (*see Note 4*).
2. Using micro-scissors make an incision posterior to the limbus and cut around the eye to remove the anterior portion containing the cornea, iris, and limbus (*see Note 5*).
3. Using a pair of fine tip curved forceps remove the iris (*see Note 6*).
4. Use 4% paraformaldehyde made in 1× PBS to fix the tissue for 10 min.
5. Move the cornea into 1% Triton made in 1× PBS to permeabilize the tissue. Leave overnight at 4 °C.
6. Block samples with 10% horse serum/1% Triton in 1× PBS for 1 h at room temperature.
7. Add primary antibodies, CD31 for vasculature and/or Lyve1 for lymphatics in a 1:100 dilution made in the block buffer. Incubate for 24 h at 4 °C (*see Note 7*).
8. Wash the tissues three times for 30 min in 0.1% Triton made in 1× PBS.
9. Add secondary antibodies made in block buffer and incubate overnight at 4 °C.
10. Wash the tissues three times for 30 min in 0.1% Triton made in 1× PBS.
11. Mount the cornea onto a microscope slide by making four to five cuts in the tissue to resemble a four leaf clover and flatten onto the slide.
12. Coverslip in 50% glycerol and 1× PBS, be careful that there are no air bubbles around the tissue. Seal the coverslip with clear nail polish.

3.3 Imaging

This step could be considered variable depending on your needs and the equipment available. We find it is best to obtain images with a 10× objective or equivalent and then merge the images to make a whole picture of the flat-mounted cornea. Some systems have a mosaic mode that allows this to be done in an automated manner. However, it can also be done manually in Photoshop.

1. With a 10× objective, begin imaging the flat mount with a suitable exposure time. Some background of the cornea is actually helpful, so it is best if you do not completely background subtract the tissue background.

2. Image the corneas in a grid like fashion. Each image should have about a 20–30% overlap so that if you are manually stitching the images together it is easy to find landmarks.
3. Images can be saved as .tiff or .jpeg for invasion quantification.

3.4 Invasion Percent Quantification

These instructions are for Photoshop CC on a Windows platform. There may be minor differences in other versions of Photoshop.

1. To merge multiple images in Photoshop CC choose the File drop-down menu and then *Automate*. This will open a pop out menu and select *Photomerge*.
2. In the Photomerge window under layout choose *Reposition* and uncheck the *Blend Images Together* box. Then select the files that need to be merged under source files and click OK. This will assemble the chosen files into a larger mosaic of the whole cornea (*see Note 8*).
3. Select the *layer* drop-down menu and then select *flatten image*.
4. From the toolbar on the left of the screen choose *Magnetic Lasso Tool* and trace the outline of the entire cornea. Only the leading edge of the neovascularization is included, not the entire limbus (*Fig. 2A*) (*see Note 9*).
5. Copy the selected area.

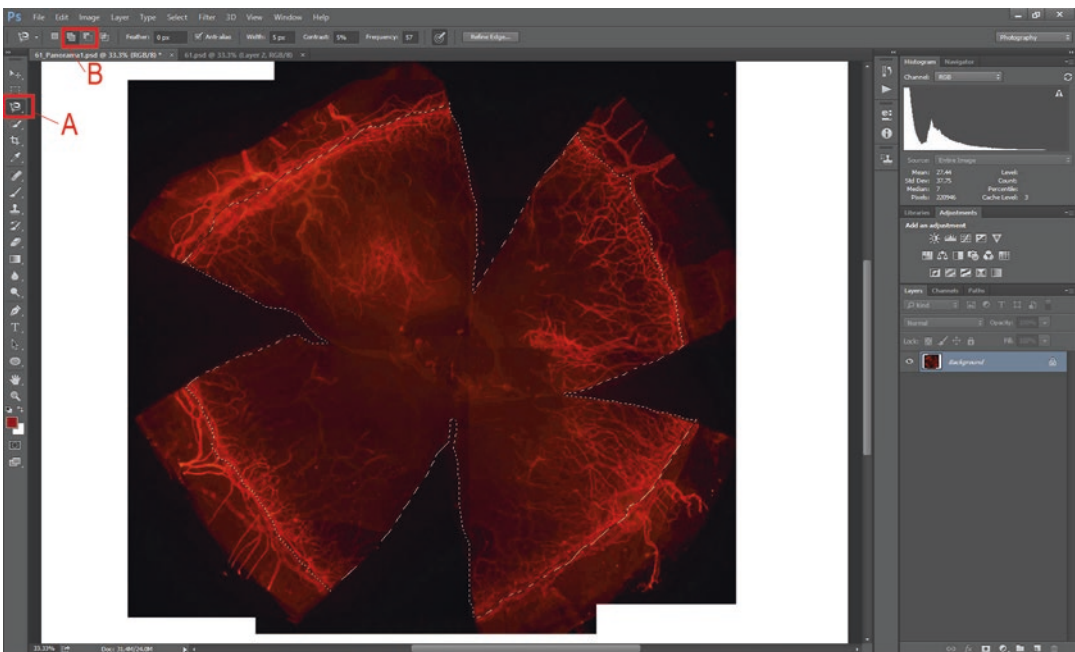


Fig. 2 A flat-mounted cornea stained with CD31 after the individual images have been pieced together to form the whole cornea. **(A)** The Magnetic Lasso Tool, used to select the area of the entire cornea from the leading edge of the neovascularization. This is seen by the *white dots* surrounding the cornea. **(B)** The Add or Subtract from Selection options, these can be used to help tailor the full area of the selection

6. Under the drop-down menu *File*, select *New*. In the New window select the document type as Clipboard. Width and Height of the new background can be set if you would like all of your new images to have the same consistent size (e.g., 3000 × 3000 pixels). The background color is a personal preference but black is the standard color (*see Note 10*).
7. Paste the selection from **step 5** onto the new background.
8. Select the layer that was just pasted under the Layers panel.
9. In the histogram select the source as the *Selected Layer* (Fig. 3A). A small error sign will appear in the upper right corner. Click the symbol with the mouse and it will reset the readings for the histogram to only measure the selected layer (this can be seen in Fig. 4B).
10. Record the Pixels value. This is the number of pixels that your layer contains, or the total area of the cornea you selected (Fig. 3B).
11. Again select the *Magic Lasso Tool* from the left toolbar. From the upper toolbar select *Add to selection* (Fig. 4A).
12. Trace the areas of angiogenesis/neovascularization (Fig. 4).
13. Copy the selection and paste it onto the background as a new layer.
14. Select the new layer.

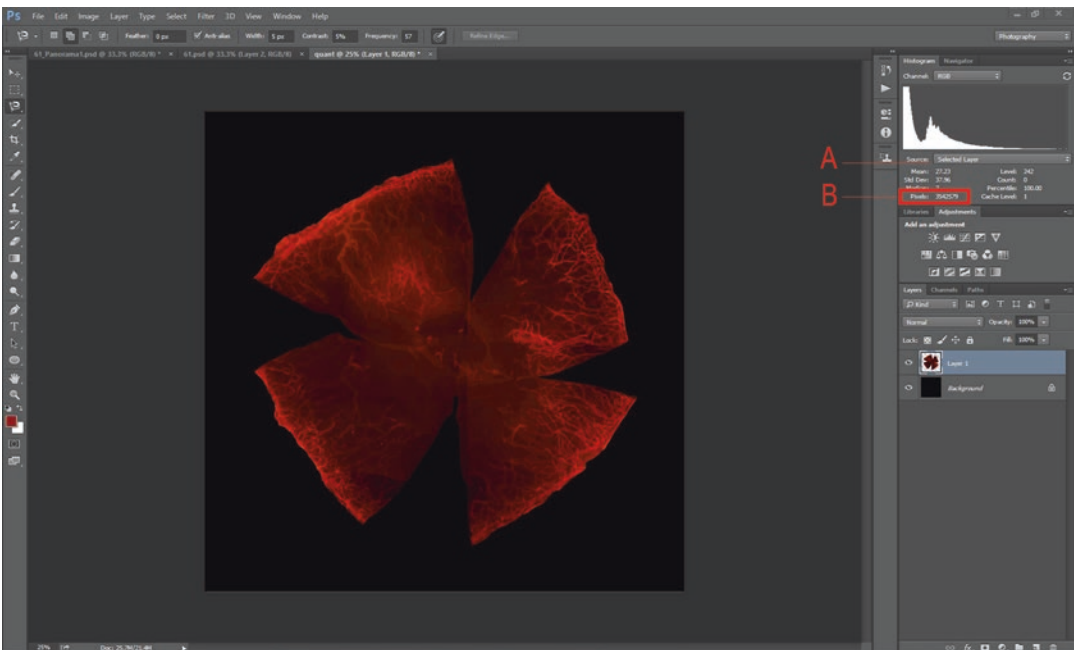


Fig. 3 The entire cornea selected has been pasted onto a new black background. (A) Source and the dropdown menu should be Selected Layer. (B) Pixels, this is the number of pixels in the selected layer, which is the area of the whole cornea selected

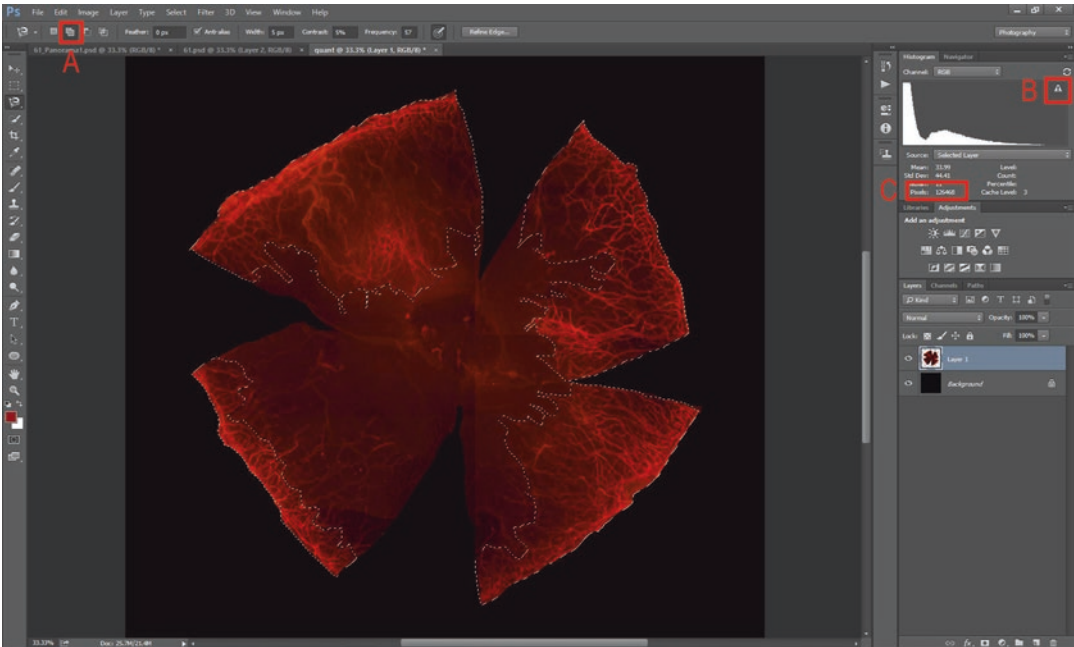


Fig. 4 Selection of neovascularized areas. **(A)** Add to selection option must be toggled to select all of the areas of neovascularization. This area is seen surrounded by *white dots*. **(B)** The error given when you first select the layer from Source. Click the error with the mouse to read the new settings. **(C)** Pixels, this is the number of pixels selected, or the area of neovascularization

15. In the histogram from source select the *Selected Layer* and click on the error triangle symbol to reset the values.
16. Record the pixels value. This value is the area of neovascularization (Fig. 4C).
17. Area of Neovascularization divided by area of the cornea will give the invasion fraction. This multiplied by 100 gives the Invasion Percent of the cornea.
18. For aesthetic purposes it is valuable to highlight the area of neovascularization. Each of the layers in the Photoshop image can be adjusted using Hue/Saturation under the Adjustments tab under the histogram (Fig. 5).

4 Notes

1. Once the numbing eye drops have been applied, the eyelashes will stick to the eye. It is best to trim them so that they do not wick NaOH to the sclera.
2. Leave the eye drop on the eye for about 15 s but more is fine. Completely wick all of the moisture off of the eye before applying the NaOH filter pad. Excess fluid will cause the NaOH in the filter pad to diffuse across the sclera and into the membranes around the eyelid causing excess inflammation for the animal.

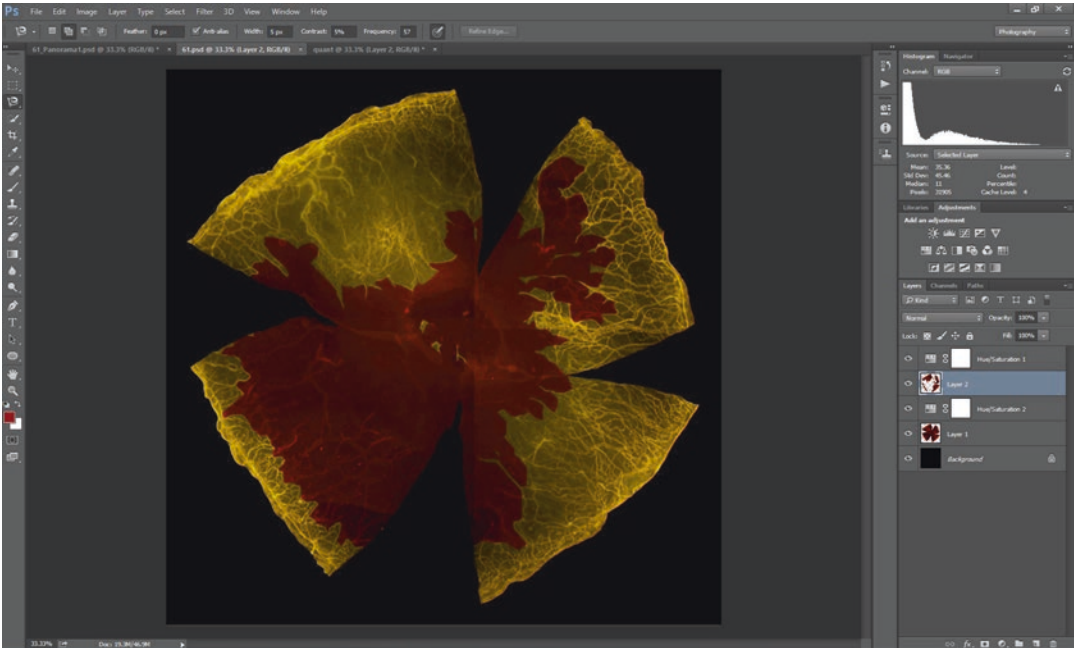


Fig. 5 Using Hue/Saturation the area of neovascularization can be highlighted to very quickly visualize the extent of invasion by the blood vessels

3. This is best done with fine tip forceps. Immediately before applying the filter pad to the eye it is best to wick any excess liquid out of your forceps so that you do not flood the eye with NaOH. It is also important to center the filter paper on the cornea as best as possible. If it lays to one side or the other there will be significantly more neovascularization to that side, instead of an even vascularization across the whole cornea.
4. This is easily done by using a pair of straight fine tip forceps. Apply pressure to the area around the eye making it bulge from the socket. Close the forceps and use a quick straight pulling motion to pull the eye away from the socket.
5. In a black mouse the limbus will appear as a milky white line at the base of the cornea. It is best to cut well below this line to keep the integrity of all of the tissue. In white mice this line is seen as slightly reddish or darker in color due to the high concentration of blood vessels.
6. The iris can be very *sticky*, but it is very important to remove all of it. If you are only interested in imaging the neovascularization, then use a cotton tipped swab in a pool of 1× PBS to scrape the iris off of the cornea and limbus area. This will result in the loss of some endothelial cells on the posterior of the cornea so this is not recommended if you are doing lipidomics. In black mice the iris is black and will block any light during imaging. In white mice the iris is clear; however, it will be

heavily vascularized and stain along with the corneal vascularization resulting in very poor images.

7. Other vascular specific markers can be used, such as isolectin.
8. It is important to use *Reposition* as many of the other settings will alter the images in a way that they should not be quantified. While this automated way of merging images works well most of the time, it is not always able to reconstruct a full image. If it cannot, then using the *Reposition* and the unchecked *blend images together* box still inserts all of the selected images onto a background layer and allows the user to easily reconstruct the full corneal image by manually placing the images.
9. Once the Magnetic Lasso Tool is selected the tool bar at the top of the Photoshop window will change to give you access to its settings. Width and contrast can be easily changed to help select the areas of interest. It is very easy to miss areas or get areas you are not interested in; this does not mean you have to start over. Finish the selection then use either the *Add to selection* or *Subtract from selection settings* to outline the full cornea. It is also much easier to trace the outline of the cornea and the neovascularization if you have zoomed into the image, then hold the spacebar down to move the image and start tracing again.
10. It is not necessary to copy the selected area into a new background layer. All quantification can occur in the full image. However, we have found that it is much easier to eliminate mistakes and easier to quickly do quantifications by creating the new image. It also allows making a more aesthetic image for publication and presentations in which the invasion area is highlighted.

Acknowledgements

NAM: NIH grants EY022071, EY025256, EY021725. Foundation Fighting Blindness and Research to Prevent Blindness, USA.
JLW: T32EY023202

References

1. Kunkel GT, Maceyka M, Milstien S, Spiegel S (2013) Targeting the sphingosine-1-phosphate axis in cancer, inflammation and beyond. *Nat Rev Drug Discov* 12(9):688–702. doi:[10.1038/nrd4099](https://doi.org/10.1038/nrd4099)
2. Jung B, Obinata H, Galvani S, Mendelson K, Ding BS, Skoura A, Kinzel B, Brinkmann V, Rafii S, Evans T, Hla T (2012) Flow-regulated endothelial S1P receptor-1 signaling sustains vascular development. *Dev Cell* 23(3):600–610. doi:[10.1016/j.devcel.2012.07.015](https://doi.org/10.1016/j.devcel.2012.07.015)
3. Gaengel K, Niaudet C, Hagikura K, Lavina B, Muhl L, Hofmann JJ, Ebarasi L, Nystrom S, Rymo S, Chen LL, Pang MF, Jin Y, Raschperger E, Roswall P, Schulte D, Benedito R, Larsson J, Hellstrom M, Fuxe J, Uhlen P, Adams R, Jakobsson L, Majumdar A, Vestweber D, Uv A, Betsholtz C (2012) The sphingosine-1-phosphate receptor S1PR1 restricts sprouting angiogenesis by regulating the interplay between VE-cadherin and VEGFR2. *Dev Cell* 23(3):587–599. doi:[10.1016/j.devcel.2012.08.005](https://doi.org/10.1016/j.devcel.2012.08.005)

4. Skoura A, Sanchez T, Claffey K, Mandala SM, Proia RL, Hla T (2007) Essential role of sphingosine 1-phosphate receptor 2 in pathological angiogenesis of the mouse retina. *J Clin Invest* 117(9):2506–2516. doi:[10.1172/JCI31123](https://doi.org/10.1172/JCI31123)
5. Bachmann B, Taylor RS, Cursiefen C (2013) The association between corneal neovascularization and visual acuity: a systematic review. *Acta Ophthalmol* 91(1):12–19. doi:[10.1111/j.1755-3768.2011.02312.x](https://doi.org/10.1111/j.1755-3768.2011.02312.x)
6. Giacomini C, Ferrari G, Bignami F, Rama P (2014) Alkali burn versus suture-induced corneal neovascularization in C57BL/6 mice: an overview of two common animal models of corneal neovascularization. *Exp Eye Res* 121:1–4. doi:[10.1016/j.exer.2014.02.005](https://doi.org/10.1016/j.exer.2014.02.005)
7. Cheng SF, Dastjerdi MH, Ferrari G, Okanobo A, Bower KS, Ryan DS, Amparo F, Stevenson W, Hamrah P, Nallasamy N, Dana R (2012) Short-term topical bevacizumab in the treatment of stable corneal neovascularization. *Am J Ophthalmol* 154(6):940–948.e1. doi:[10.1016/j.ajo.2012.06.007](https://doi.org/10.1016/j.ajo.2012.06.007)

INDEX

A

- Accurate mass 69, 151
 Acylglycerol-3-phosphate acyltransferase
 (AGPAT).....208–210
 Acyltransferase family
 Acyltransferases 196, 208–210
 Alignment 97, 102, 196, 200, 201, 203–204
 AliView 200
 9-Aminoacridine (9-AA) 111, 112, 115–117
 Annotation of algal lipid proteins
 Anthrylvinyl 234
 Approximate likelihood ratio test (aLRT)..... 204, 212
 Are we there yet? (Awty)..... 205
 Artificial spherules..... 255
 Automated quality improvement for MSAs
 (AQUA) 201, 204

B

- Bacterial culture..... 174–175, 232, 233, 238
 Bacterial expression 231, 232
 Bayesian-based methods..... 205
 Bayesian Evolutionary Analysis Sampling Trees
 (BEAST)..... 201
 Bioavailability 257
 Biological..... 5, 6, 38, 39, 43, 65, 66, 83, 91, 93, 99,
 108, 111, 114, 120, 123, 124, 127, 137, 141–147, 150,
 175, 241, 242, 255–257
 Biosequence analysis using profile hidden Markov models
 (HMMER)..... 198, 200, 203, 208, 211
 Bipartite signals 206
 BL-21 232, 238
 Block Mapping and Gathering with Entropy
 (BMGE)..... 200, 204, 208, 211
 BODIPY 234, 236
 Bootstrap analysis 198, 204, 212
 Brenda 199
 Broad Institute 199
 Buffers 3–5, 27, 29, 35–38, 40, 52, 53, 55,
 66, 67, 93, 98, 99, 109, 111, 174, 175, 186–189, 193,
 219, 220, 225–228, 232–236, 238, 244, 249, 257,
 263, 264, 269, 270

C

- Cancer stem cells 25, 26, 28–30
 CD133..... 25, 26, 28–30

- CD-HIT 200, 208
 Centrifuge 3–5, 7, 11, 16, 27, 28, 33, 35–40,
 53, 54, 67, 94, 95, 98, 111, 130–132, 136, 150, 153,
 174, 175, 182, 186, 188, 189, 191–193, 222, 233,
 245, 246, 251, 263
 Ceramides..... 59, 79, 98, 130, 152, 154, 161, 162
 Cerebrosides 57–62
 Chemical shift 118
 Chloroform-methanol 2, 3, 10–12, 15, 16,
 20, 22, 58, 60, 62, 66, 93–95, 99, 111, 119, 125, 127,
 130–132, 136, 263
 ChloroP 202, 205
 Chloroplast target peptide (cTP) detection 212
 Chloroplast transit peptide (cTP)..... 205
 Cholesterol 25, 26, 45, 47–49, 51–55, 66, 126, 130,
 134, 137, 185–193, 196, 209, 210, 217, 242, 256, 262
 Cholesteryl esters (CholE) 66, 79, 130, 152, 154, 161
 Chromatogram 61, 67–71, 87, 90, 97, 101,
 102, 142–144, 146, 153, 154, 165
 Chromatography 57–62, 65, 67–80, 91–104,
 108, 109, 124, 146, 150, 152, 173, 190, 191, 232, 233
 Clustal 203
 Clustering..... 103, 200, 204, 208
 Constrained Consensus Topology Prediction
 (CCTOP)..... 202
 Construction..... 211
 Conventional outflow pathway
 Convergence of runs 205
 Coomassie staining..... 233, 238

D

- DAGAT family 209
 Data-mining 200, 202–203, 208, 211
 Dataset definition..... 197–202, 210
 Dendroscope
 Density gradient centrifugation..... 182, 186, 192
 Desorption electrospray ionization (DESI)..... 57
 Detergent extraction 188
 Diacylglycerol acyltransferase 1 (DGAT1)..... 206,
 209, 210
 Diacylglycerol acyltransferase 2 (DGAT2)..... 209, 210
 Diafiltration..... 234
 Dialysis 234, 238, 243, 246, 251
 2,5-Dihydroxybenzoic acid (DHB) 45–47, 111, 112,
 114–117, 119, 120, 175, 177
 DiO 234

Dithiothreitol (DTT).....234
 3D modeling201
 DNA Data Bank of Japan (DDBJ)199
 Drug.....172, 173, 219, 256, 257, 262, 268, 269

E

Ecological applications10
 Ecophysiology9
 Egg yolk 111–113, 116–118
 Electrophoresis218–220, 225
 Electrospray ionization (ESI)59, 85, 86, 89, 92,
 98, 108, 109, 114, 142, 153–156, 159, 160
 Electrotransfer 193, 219–220, 225–226
 Elution buffer232, 233
 Energy acceptor234
 Energy donor.....234
 Enhanced chemiluminescence.....220, 227
 Epithelial mesenchymal transition (EMT).....26
 Eukaryotic Pathogen Database Resources
 (EuPathDB)199
 Evolutionary model selection201
 Excipient256, 257
 Exosome182, 256
 Expiry tools.....199, 206
 Extracellular 26, 171, 197, 256

F

Fatty acids..... 26, 34, 79, 86, 91, 92, 100–102,
 109, 128, 129, 149, 172, 173, 185–193, 196, 208
 File conversion.....26, 156–157
 Flow rate89, 96, 155, 175, 237
 Fluid mosaic model 185, 255, 256
 Fluorescence 55, 142, 234–236, 248–250, 262–265
 Fluorescence dequenching.....234–236
 Functionalized dextran gel.....237

G

Galactosylceramide.....60
 Gas chromatography (GC)..... 58, 109, 124, 191
 GeneDoc200
 General databases199
 General software.....76, 80
 Glaucoma
 closed-angle glaucoma
 congenital glaucoma
 glaucoma suspect
 normal-tension glaucoma
 open-angle glaucoma
 secondary glaucoma
 Glucosylceramide60
 Glycerol-3-phosphate acyltransferase (GPAT)208–210
 Glycerolipid synthesis pathway.....208–210
 Glycolipids57, 66, 231, 235–236
 Glycosphingolipids 58, 79, 231

Gold surface237
 Group-specific software202, 208

H

Half-time.....234, 235
 Hallmarks/proteins.....199
 Hectar.....202, 206
 Hidden Markov Model Topology Prediction
 (HMMTOP).....202, 207
 High-performance liquid chromatography
 (HPLC).....3–5, 57, 58, 67, 108–110, 190
 High-performance thin-layer chromatography
 (HPTLC).....57–61
 HKD motif.....207–208
 HMMALIGN200, 208
 Human trabecular meshwork cell culture217–228
 Hydrophobic indexes.....206
 Hydrophobicity analysis196, 206

I

Imidazole.....232, 233
 Immunoblotting192, 220, 226–227
 Injection conditions
 Inoculate232
 Interpro199
 Ion suppression.....92, 109, 110, 174
 IPTG.....238
 IQ-Tree.....201
 I-Tasser201
 iTOL

J

John Craig Venter Institute (JCVI).....199, 200

K

Kyoto Encyclopedia of Genes and Genomes
 (KEGG)199

L

Labelled lipids231, 235
 Large unilamellar vesicles (LUVs).....257
 LCAT family209, 210
 Lipid bilayer26, 123, 206, 237, 256, 257, 262
 Lipid extraction.....1–4, 6, 9–22, 52, 53, 58,
 62, 66–67, 90, 92, 94, 95, 124, 125, 127, 131–132, 136,
 142, 166, 186
 Lipid raft25, 26, 28–30, 172, 185, 192
 Lipid transfer protein (LTP)231–238
 LipidBlast library.....149–169
 Lipidomic.....26, 39, 58, 65, 66, 83, 85, 86, 91–104, 108,
 110, 123–137, 141, 142, 146, 149–169, 186, 190, 274
 Lipids1, 10, 26, 33, 44, 52, 57, 65, 83, 91, 107,
 123, 141, 149, 172, 185, 196, 231, 241, 256, 261

Liposome.....255–259, 262
Liquid-chromatography (LC) 65, 67–80,
91–103, 124, 142, 146, 150, 152, 173, 191
Location-specific software.....202
Lysis buffer29, 35, 52, 53, 232, 233
Lyosphosphatidylcholines (LPC) 78, 93, 107,
118, 152, 154, 161

M

MAFFT200, 204, 208
Manual method47, 80, 102, 113, 211
Markov Chain Monte Carlo (MCMC)205, 212
Mass by charge ratios (m/z)..... 44, 48, 124
Mass spectrometry (MS) 43–49, 51, 57, 58, 62, 65,
67–80, 83–88, 90–104, 107–120, 124, 127, 131–135,
142, 145, 149, 150, 152, 153, 173, 174, 176, 180
Matrix-assisted laser desorption/ionization
(MALDI) 44, 45, 47, 57, 107–120, 173–175
Maximum likelihood (ML)-based methods204
Membrane Bound O-Acyltransferase family209
Membrane microdomains..... 26, 185–193
Membrane organization25, 185
Membrane proteins25, 33, 172, 206–207, 226
Membranes..... 3, 11, 25, 33, 123, 141, 171,
185, 196, 217, 226, 231, 241, 255, 261, 273
Metastasis26
Mist sprayer 59, 61
Mitochondria transit peptide (mTP).....205
MitoProt.....202
Mobility..... 57, 110
MS PepSearch158
Multilamellar256, 257
Multiple sequence alignment (MSA)196–198,
200, 201, 203–204, 206, 208, 211, 212
MUSCLE200, 204

N

National Center for Biotechnology Information
(NCBI)199
NBD..... 234, 262, 263
NCBI Genomes 199, 200, 202, 210
Ni-sepharose.....232, 233
NIST MS/MS..... 152, 166, 167
Non-polar solvents 10, 11, 15
Nuclear magnetic resonance (NMR) spectroscopy.....58,
59, 107–120, 142, 262

O

Ocular hypertension 1, 4–6, 186
Optiprep 27, 29, 30,
187–189, 192
Orcinol reagent..... 57, 60, 61
Organelle..... 172, 197, 205, 256
Organelle dual targeting.....212

P

Pancreatic cancer25–27
Pattern Hit Initiated Blast (Phi-BLAST) 198, 200,
203, 207
Peroxidase-conjugated secondary antibodies219,
220, 227
Perylenoyl.....234
Petroleum ether 10–12, 14, 15, 22
Pfam 199, 208–211
Phosphatidylcholine (PC) 45, 47–49, 78, 93, 108,
111, 115, 130, 151, 152, 154, 161, 162, 168, 236, 257
Phosphatidylethanolamine (PE) 78, 93, 115,
152, 154, 161, 162, 242, 257
Phosphatidylglycerol (PG)78, 93, 94, 104,
114, 115, 125, 130, 162
Phosphatidylinositol (PI)78, 86–88, 117, 129,
130, 144, 154, 162, 236
Phospholipase D superfamily annotation 196, 207–208
Phospholipid (PL)..... 10, 11, 15, 26, 66, 83, 84,
107–120, 172, 207, 208, 210, 231, 242, 256–259
Phospholipid:diacylglycerol acyltransferase
(PDAT) 209, 210
Phylogenetic analysis208
Phylogenetic tree reconstruction 198, 204–205
Phylogeny..... 198, 201, 204, 212
PhyML..... 201, 204, 208
Phyre201
Plasma12, 25, 26, 58, 91–104, 150, 152–154,
168, 172, 185, 186, 188, 205, 241, 248, 250, 251, 256
Polar solvent 10, 11, 15, 22
Polyhistidine232
Position-Specific Iterated BLAST
(PSI-BLAST)..... 198, 200, 211
pQE-9 232, 238
PredAlgo 202, 206
Prediction of Apicomplast Targeted Sequences
(PATS).....202
Predotar201, 205
Primary19, 27, 137, 142, 205, 218–225, 227, 245, 261
Primary antibodies.....226–228, 245, 248, 270
Primuline62
Prosit 199, 203
Prostaglandin F₂α
Protein 2, 10, 25, 52, 90, 93, 107, 124,
142, 172, 185, 195, 217, 226, 231, 241, 257, 261
Protein activity 231, 234, 235, 237
Protein Data Bank (PDB)199
Protein expression..... 223–225, 233, 238
Protein hydrophobicity206, 218
Protein modification
acetylation
carbonylation224
farnesylation 217, 223, 224
geranylgeranylation..... 217, 223, 224

Protein modification (<i>cont.</i>)	
glycosylation	124
glypiation	
isoprenylation	217, 223–225
lipidation	90, 261–265
lipoylation	
myristolation	
palmitoylation	
phosphorylation	217
post-translational	217, 223
serine/threonine	78
SUMOylation	
tyrosine	35
ubiquitination	91
Protein-protein Blast (BLASTp)	200
Protein purification	232
ProteoWizard	96, 156–158
ProtScale	202, 206, 212
Protest	201, 204
PSI-predictor	198
Q	
Quenching	235
R	
RASCAL	201, 204
RAxML	201, 204
Resin	232
Reversed phase columns	108, 109
Rhodamine	234
S	
Saponification	52
SDS-PAGE	193, 225–226, 233, 238
SeaView	200
Secondary endosymbiosis	206
SecretomeP	202, 205, 212
Secretory signal peptide (SP) detection	205
Selection and refinement	204
Self-assembled	256
Self-assembled monolayer	237
Sensor	236–238
Sequence Clustering and Comparison	200
SignalP	201, 213
Single cell suspension	27–28
Small monomeric GTPases	
Arf	
CDC42	
KRas, NRas, HRas	27
Rab	
Rac1	
Ran	
Ras	217
Ras superfamily	217
Rho	218
RhoA, RhoB, RhoC	219, 220, 223–226
Small unilamellar vesicles (SUV)	257, 259, 263, 264
Software	45, 47, 69, 87, 92, 93, 96, 97, 101–103, 135, 137, 142, 144, 146, 150, 156, 158, 168, 191, 203, 204, 206
Sonicate	168, 188, 190, 191, 225, 233, 263
Sonication	192, 255–259
Soxhlet apparatus	11, 14–16
SP cleavage	206
Specific genomes	199
Sphingolipids	26, 59, 66, 79, 83, 123, 141, 185–186, 267
Sphingomyelin (SM)	79, 98, 118, 130, 152, 154, 161, 236, 262
Stable isotope analysis (SIA)	9–22
Standard deviation analysis	205
Statistical branch support	204
Subcellular localization prediction	205–206
Superfamily	195, 196, 198, 199, 202–204, 207–208, 210, 211
Supernatant	5, 6, 28, 34, 37, 38, 53, 54, 131, 172, 175, 177, 180, 188, 189, 193, 233, 245, 246
Surface plasmon resonance (SPR)	231, 236–238
Swissprot	197, 208, 210, 211
Synthesis	208–210, 231, 249, 255–259
Synthetic	1, 6, 80, 91, 176, 256
T	
Tandem mass spectrometry	65, 67–80, 84, 91–104, 124, 149, 179, 180
TargetP	201, 205, 206
T-COFFEE	200, 204
The European Bioinformatics Institute (Uniprot)	199
The Joint Genome Institute (JGI)	199, 211
Thin-layer chromatography (TLC)	51–55, 57–62, 108, 109, 173, 190
TIGRFAM	199
Time-of-flight (TOF)	44, 45, 47, 49, 107–120, 150, 153, 174, 176
Time-of-flight mass spectrometry	107–120, 152, 176
TLC developing tank	59
Trabecular meshwork (TM)	4, 217–228
Transfer assay	234, 236
Transformed	219, 222–225, 232
Transitive Consistency Score (TCS)	201, 204, 211
Transmembrane Hidden Markov Model (TM-HMM)	202, 207
Transmembrane segment (TMS) analysis	206, 207
Transport	141, 262
Tree visualization and editing	
Triacylglycerols (TG)	66, 116, 130, 152, 154, 161, 164, 168

U

Uniprot.....199, 210
 Uveoscleral outflow pathway

V

Vacuum evaporator.....257, 258
 Vapor phase62
 Vehicle.....223–225

Vesicle.....34, 38, 171–182, 234–238, 255–257, 263, 264
 Visualization/editing55, 61, 62, 167, 200

W

Water bath sonicator257–259
 Wellcome Trust Sanger Institute200
 Window size selection206
 WoLF PSORT201, 205